SHRP-C-343

# Eliminating or Minimizing Alkali-Silica Reactivity

David Stark
Bruce Morgan
Paul Okamoto

Construction Technology Laboratories, Inc.
5420 Old Orchard Road
Skokie, IL 60077

Sidney Diamond

Purdue University
West Lafayette, Indiana


**Strategic Highway Research Program**
National Research Council
Washington, DC 1993

SHRP-C-343
Contract SHRP-87-C202
ISBN 0-309-05603-9

Program Manager: *Don M. Harriott*
Project Manager: *Inam Jawed*
Program Area Secretary: *Carina Hreib*
Copyeditor: *Katharyn L. Bine Brosseau*

May 1993

key words:
aggregate
alkali-silica reactivity
cracking
expansion
fly ash
distress mechanisms
lithium
nondestructive testing
portland cement concrete

Strategic Highway Research Program
2101 Constitution Avenue N.W.
Washington, DC 20418

(202) 334-3774

The publication of this report does not necessarily indicate approval or endorsement by the National Academy of Sciences, the United States Government, or the American Association of State Highway and Transportation Officials or its member states of the findings, opinions, conclusions, or recommendations either inferred or specifically expressed herein.

©1993 National Academy of Sciences

1.5M/NAP/593

# Acknowledgments

The research described in this report was sponsored by the Strategic Highway Research Program (SHRP). SHRP is a unit of the National Research Council that was authorized by section 128 of the Surface Transportation and Uniform Relocation Assistance Act of 1987.

Many workers participated in the research and preparation of reports completed under this project. The authors extend special thanks to Dr. Richard Helmuth, Mr. John Gajda, and Mrs. Virginia Nicodemus at Construction Technology Laboratories, and Dr. Micheline Moranville-Regourd, formerly of Centre Experimental de Recherches et D'Etudes du Batiment et des Travaux Publics and Ecole Normale Superieure de Cachan, France.

Work in this project could not have been carried out without the cooperation of numerous state transportation agencies. Particular thanks are extended to Messrs. James Stokes and Joseph Barela of the New Mexico State Highway Department for their major contributions throughout this project. Also, special thanks are extended to Mr. Richard Moore and Mrs. Sohila Bemanian of the State of Nevada Department of Transportation for their participation in the project.

# Contents

# List of Figures

# List of Tables

# Abstract

This report describes investigations into various aspects of alkali silica reactivity (ASR) as it affects performance of highway structures. Emphasis was placed on practical needs of the concrete engineer, primarily with respect to improving means to evaluate the potential of aggregate for expansive ASR in new concrete, procedures to evaluate material for safe use in new concrete, and means to mitigate ASR and associated adverse effects in existing concrete.

A rapid test method, based on immersion of mortar bars in sodium hydroxide solution, as originally developed at the National Building Research Institute in South Africa, was further evaluated and extended to identify cement alkali levels and pozzolan proportions required to prevent deleterious ASR with a particular aggregate.

Extensive research was carried out on the efficacy of using lithium salts in concrete to suppress expansion due to ASR. Reaction chemistry was investigated, together with dosage requirements to prevent expansion. Results were extremely favorable and the approach is highly recommended.

Means to mitigate ASR and its effects on concrete also were investigated. It was found that restraint to expansion and application of lithium hydroxide solutions are possible means to control expansion due to ASR.

Work in this project was oriented to educating highway engineers in identifying ASR in concrete, primarily through seminars and publications.

# Executive Summary

The purpose of this report is to present findings and conclusions of investigations concerning alkali-silica reactivity (ASR) in highway concrete. Three tasks as originally defined in the project were as follows:

Task A: Investigate fundamental aspects of ASR mechanisms.
Task B: Develop rapid and reliable test methods to identify potential for deleterious ASR of aggregates and cement-aggregate combinations
Task C: Develop means to mitigate expansive ASR in existing concrete.

As the investigations progressed, it was agreed that greater emphasis should be placed on the more practical aspects of ASR and that fundamental studies in Task A should be reoriented, as needed, to support the activities in Tasks B and C. Thus, most of the investigations reported herein were carried out to meet the revised objectives of these tasks.

To serve as background information for this investigation, a virtually complete annotated bibliography, current through 1991 (Diamond 1992), and a synthesis of published literature, including identification of gaps in our knowledge of ASR (Helmuth 1993), were developed and published. Areas of investigation conducted in this project were based on information in these sources and are described below.

The synthesis of literature indicates that the Powers and Steinour model for safe and unsafe reactions is generally supported by recent research. In this model, alkali and lime first react with silica at the surface of an aggregate particle to form a relatively high lime non-expansive gel reaction product. As reactivity proceeds into the particle, the greater diffusivity of alkali ions (potassium and sodium) may result in a lower lime-alkali ratio gel reaction product. Although the reaction itself results in a chemical shrinkage, the gel product may have a great capacity to swell upon absorption of moisture. Swelling due to uptake of moisture apparently can develop when the relative humidity exceeds about 80 percent referenced to 70 to 75°F (21 to 24°C). To prevent expansion of the concrete, excessive volume of gel reaction product must diffuse out of the reacted particle. If higher lime-alkali gel formed earlier in the process prevents diffusion, expansion with associated cracking can occur. Higher cement alkali contents result in increased alkali and hydroxyl ion, and decreased lime, concentration in pore solutions, and therefore gel reaction products with greater capacity to swell. Conversely, low alkali cements result in higher lime, lower alkali reaction products that may have little or no capacity to swell. The eventual manifestations of ASR in a particular concrete depend on hydroxyl ion concentration in the pore solution, permeability of the cement paste (water-cement ratio), composition and permeability of the reactive aggregate particle, moisture availability, and restraint to expansion.

Responses to a questionnaire sent to all state transportation departments revealed a wide range of knowledge of ASR within their respective states. Test methods used to identify potentially deleteriously reactive aggregates, and specifications in force to control the

reaction varied accordingly. Western states that use the 0.60 percent ASTM limit for low alkali cement have experienced severe cracking due to ASR in highway structures. Other states vary the permissible cement alkali level, depending on composition of the aggregate. In other states, it is uncertain whether ASR is a problem.

It was also evident from the questionnaire that nearly all states depend on ASTM C 289 or C 227 tests to identify potentially deleteriously reactive aggregates and cement-aggregate combinations. Both tests are known to be unreliable, particularly in identifying slowly reacting aggregates such as granite gneiss and quartzite. From knowledge of the geographical distribution of rock types, it is concluded that potential for deleterious ASR in highway concrete exists in every state in the United States.

Given this situation, numerous field inspection and sampling trips were taken to obtain information on ASR-induced distress patterns and relative humidity (RH) values in concrete structures. Samples of a wide range of known reactive aggregates were collected, especially slowly reactive aggregates and those that react deleteriously with low alkali cements, for laboratory tests. Innocuous aggregates were also included. Photographs included in a handbook for identifying ASR were obtained during these field investigations (Stark 1991a).

During the field studies, RH values were obtained to determine the availability of moisture for expansive ASR in pavements and bridge structures in different climates. From results of these determinations, it is concluded that highway concrete is sufficiently damp in all natural climates in the United States to support expansive ASR. However, RH levels in elevated concrete members, such as bridge decks, may reach the threshold 80 percent level only on a diurnal or seasonal cyclic basis in hot desert regions. Pavement concrete in all climates likely will be sufficiently damp to continuously support expansive ASR. This condition is maintained by direct rainfall and by diffusion of moisture from the base upward into the slab. Thus, climatic environment as well as the geographic distribution of aggregate materials creates a potential for deleterious ASR in highway concrete in the United States.

A rapid and reliable test method to identify potentially deleteriously reactive aggregates is perhaps the most badly needed technology concerned with ASR. Evaluation of possible methods indicated that a procedure developed at the National Building Research Institute (NBRI) in South Africa was the most promising. Furthermore, this method appeared to be sufficiently adaptable to resolve the important question of determining safe cement alkali levels and quantity of pozzolan required to control expansions due to ASR. This test consists of calculating expansions of mortar bars, made in general accordance with C 227 but stored in 1N NaOH for 14 days after one day of storage in water, both at approximately 176°F (80°C). A major difference from C 227 is that mortar bars are made using a fixed water-cement ratio of 0.50 instead of gauging water content according to workability. This difference is necessary because, in the test, ASR is dependent on diffusion of alkali solution into the mortar bar, so permeability must be held as constant as possible.

Results for innocuous and deleterious aggregates in this project indicate the procedure properly classifies aggregates according to service record at a test criterion of 0.08 percent expansion at 14 days. This is slightly less than the 0.10 percent criterion previously established, and also does not incorporate the 0.10 percent to 0.20 percent expansion range to denote uncertainty of potential for deleterious ASR. The result also revealed that aggregates arbitrarily classified as slowly reactive produced less expansion than those considered as highly reactive. The use of concrete prisms in the test did not appear to produce satisfactorily consistent results, although further testing adjustments may avoid this problem.

As developed by NBRI, a 1N NaOH solution was used initially for immersion of test specimens. However, it was reasoned that NaOH might be changed to correspond to different specific cement alkali levels and water-cement ratios. The objective in this case would be determining cement alkali levels below which excessive expansion due to ASR does not develop at different water-cement ratios. The synthesis of literature in this project permitted development of a linear regression equation that relates solution normality to equivalent $Na_2O$ of the cement at given water-cement ratio, as follows:

$$\text{Normality} = 0.339 \frac{Na_2O}{w/c} + 0.022 \pm 0.06 \text{ moles/L}$$

A graph relating these parameters was drawn, and testing using the different solution normalities was carried out. As expected, 14-day expansions decreased progressively as concentration (normality) decreased. It was also apparent that a different test criterion would be necessary for the different solutions. Accordingly, innocuous as well as deleterious aggregates were tested in different solutions and a curve developed that relates safe expansion levels to solution concentration and therefore to cement alkali level.

It appeared also that the test could be extended to evaluate the effectiveness of pozzolans in preventing excessive expansions due to ASR, again at various alkali levels in the cement-pozzolan system. From 14-day results for several fly ashes and a blast furnace slag, it was concluded that the capability of pozzolans to prevent abnormal expansion due to ASR, and required proportions for prevention, can be determined using this method. These results approximate those obtained for samples of the same pozzolans and aggregate in evaluated C 227 mortar bar tests.

Investigations in this project thus suggest that this single rapid procedure with appropriate adjustments for alkali levels, etc., can be used to determine not only whether an aggregate is potentially deleteriously reactive, but also safe cement alkali levels and pozzolan requirements for preventing deleterious ASR.

Extensive research also was carried out to evaluate the effectiveness of lithium salts to prevent excessive expansion due to ASR, as first suggested by McCoy and Caldwell in work using a highly reactive Pyrex glass aggregate. Reaction chemistry was investigated using $Li_2CO_3$, LiF, and LiOH salts, the former two being nearly insoluble in ordinary water. However, it was found that all three dissolve in the high pH solution in fresh concrete, with precipitation of $CaCO_3$ and CaF with use of $Li_2CO_3$ and LiF. To avoid possible set retardation effects with these two salts, efforts were centered on LiOH additions. The studies indicate that a lithium-alkali silicate gel forms in the reaction and possesses little or no capability of subsequent swelling.

Test results using this salt indicate a threshold molar ratio of Na:Li exists at about 1:0.67 to 1:1 at which expansion due to ASR is reduced to safe levels. Lower concentrations of lithium ion become less effective. Additional testing indicated that lithium ion also is effective in mitigating expansion due to ASR when used with pozzolans in the concrete mixture and, further, that it is able to control expansions in the presence of NaCl solutions such as would be present with the application of deicer salts.

Subsequently, experimental sections of pavement concrete containing added LiOH or fly ashes, and control sections, were installed on State Route 352 near I-40 in Albuquerque, New Mexico in June 1992. Rapid immersion tests on samples of aggregate and fly ash used in the road indicated the ASTM Class F ash adequately controlled expansion while the Class F-C mixture and the straight Class C ash failed to do so. Previous testing with lithium

hydroxide additions in the same proportion to cement alkali as used in the experimental pavement confirmed its mitigative capabilities with aggregate from the same source.

It also was felt that LiOH may be capable of preventing continued expansion due to ASR in existing hardened concrete. Tests in which expanded mortar bar specimens were soaked in LiOH confirmed its mitigative capability. Accordingly, test sections on I-80 near Winnemucca, Nevada, in which cracking due to ASR had already developed, were treated with LiOH. Existing cracks, in this case were depended on to carry LiOH solution into the concrete. Other test sections, in which high molecular weight methacrylate or silane was used, also were included in this study. Falling weight deflectometer measurements are being used to monitor performance. Thus far, the methacrylate treatment, which is intended to fill and cement cracks, has shown some tendency to decrease deflections due to load. Monitoring should continue on these test sections.

Drying the hardened concrete also appeared to provide some beneficial effect in combating ASR. In addition to simply removing moisture that would otherwise be available for absorption by ASR gel, drying apparently results in alkali fixation by cement hydration products. Alkali fixation appears to persist for prolonged periods of time but the alkali is slowly released, even though the concrete had been rewetted long before the release of alkalies. Drying may be a feasible approach to mitigating expansive ASR in some concrete members, such as bridge columns, but repeat drying probably would be necessary.

Limited field evaluation of silane/siloxane surface treatments also was carried out. Since their role in ASR would appear to involve controlling moisture diffusion into the concrete, RH determinations were made on treated and untreated pavement and bridge deck concrete in Wyoming. Results for the bridge deck concrete indicated the treatments had little effect on RH values except, perhaps, within the upper 2 in. (51 mm) of the wearing surface. In the treated pavement slabs, RH values were still sufficiently high to support expansive ASR. Thus, the efficacy of using surface treatments to prevent expansion due to ASR, but permit vapor diffusion, is questionable.

Restraint to expansion also was investigated as a means of minimizing expansion due to ASR. Triaxial restraint of concrete cylinders made with high alkali cement and highly reactive coarse and fine aggregates was found to prevent expansion with restraint stresses in the range of 200 to 300 psi (1.38 to 2.07 MPa). To simulate highway pavement, a miniature pavement 12 ft (3.658 m) long was built in the laboratory and placed under varying levels of restraint depending on expansions developed due to ASR. As demonstrated by companion unrestrained slabs made with reactive aggregate, ASR and strain gradient effects, if left unchecked, lead to severe three-dimensional cracking. Low levels of restraint, of the order of tens of psi (several hundreds of kPa), has a positive effect on controlling microcracking. Application of uniaxial restraint of the order of hundreds of psi (several MPa) may actually aggravate developing conditions. In addition, distress patterns that developed due to ASR under uniaxial restraint occurred as generally horizontal cracking. Concrete slabs containing innocuous aggregates did not develop such crack patterns. It appeared that application of moderate, one-dimensional restraint can control expansion in the direction of restraint and significantly reduce the rate of expansion in other directions.

Several areas of investigation with regard to ASR are still in need of further work. These include:

1) Further validation of the rapid immersion test method including determining safe cement alkali and pozzolan levels.

2) The use of concrete prisms to evaluate cementitious material and aggregates in the rapid immersion test.

3) Field evaluation of LiOH used to combat expansion due to ASR, both as an admixture and as an application to hardened concrete.

4) Text methods to determine remaining potential for expansive ASR in existing concrete.

# 1.0 Introduction

Alkali-silica reactivity (ASR) has been known since the late 1930s to be a potential source of distress in highway and other portland cement concrete structures (Stanton 1940). ASR by itself seldom results in the need to rebuild the structure but, rather, it may weaken or degrade the condition of the structure to the extent that other factors, such as traffic loading, cause premature failure. Since its initial discovery, voluminous literature has developed (Diamond 1992) that reports results of research efforts to resolve various aspects of the problem. A synthesis of findings, together with gaps currently existing in our knowledge of ASR, has been developed by Helmuth (1993) under this SHRP project.

Even with the benefit of more than 50 years' research, major problems still exist in avoiding deleterious ASR in field concrete. This deficiency is attributed primarily to three factors:

1) Improper use of existing knowledge of ASR in field applications.
2) Inadequate research on certain aspects of ASR as they affect the course of the reaction.
3) Deficiencies in existing test methods.

It was the purpose of this research to resolve, as far as possible, various aspects of ASR so that reliable guidance can be provided to eliminate or mitigate deleterious ASR in new and existing highway structures. As such, three tasks were formulated under which research in this project was conducted. These are as follows:

Task A: Conduct fundamental studies on chemical reactions and mechanisms associated with ASR;

Task B: Identify cement-aggregate-environmental interactions, and develop test methods that reliably indicate susceptibility of concrete materials to deleterious ASR;

Task C: Devise means of mitigating expansion due to ASR in existing structures.

During the early stages of this project, it became evident the most fruitful activities would be those most directly related to practical field applications (Tasks B and C). Accordingly, the scope of the fundamental studies (Task A) was revised to the more immediate needs of the highway engineer.

Salient features of work in this project are presented in this final report. Alkali-carbonate rock reaction was not included in the scope of this project.

# 2.0 Nature and Extent of ASR

ASR has caused abnormal expansion and cracking in highway structures throughout the United States and other areas of the world. Three basic requirements exist which are necessary for this reaction to occur:

1) Reactive silica or siliceous components in the aggregate.
2) Sufficiently high hydroxyl ion concentration in the pore solution in the concrete.
3) Sufficiently available moisture in the concrete.

Various external factors affect the rate and extent to which the reaction proceeds. These include temperature, restraint, and external sources of alkali that increase the hydroxyl ion concentration in solution in the concrete.

This section of the report provides further information on the occurrences of ASR reported by state transportation departments and descriptions of mechanisms that result in safe and unsafe ASR.

## 2.1 Extent of the Problem

Potentially deleteriously reactive rock types exist in every state in the United States. However, ASR-induced distress is not reported in numerous areas for several reasons. These include: the use of cements with sufficiently low alkali contents to preclude ASR development; use of pozzolans that are effective in suppressing ASR; lack of familiarization by highway personnel with symptoms of ASR; and overdependence on inadequate laboratory test methods, thereby leading to the false conclusions that the problem does not exist. In addition, what may be a deleterious type of reaction in one application may not be so in another. This complicates a nationwide assessment of the impact of ASR on the serviceability and maintenance requirements of highway structures.

To obtain a better understanding of the extent of ASR in the United States, a questionnaire was distributed to state transportation departments in 1988. The objectives were to identify, for possible further investigation, structures affected by ASR, to obtain reactive and non-reactive aggregates for laboratory evaluation, and to identify existing means of preventing or mitigating expansive ASR. Responses to the questionnaire were received from 44 states and the District of Columbia. Of the 44 states, 23 stated they had no ASR-associated problems while 19 stated that they are experiencing problems. Occurrence of ASR was uncertain in two states. The map in Figure 2.1 summarizes responses to the questionnaire with respect to whether ASR has been identified as a current problem in highway structures in the respective states. Two states, Maine and Pennsylvania, which previously were known to have ASR problems in highway structures, reported that they had no ASR-related problems.

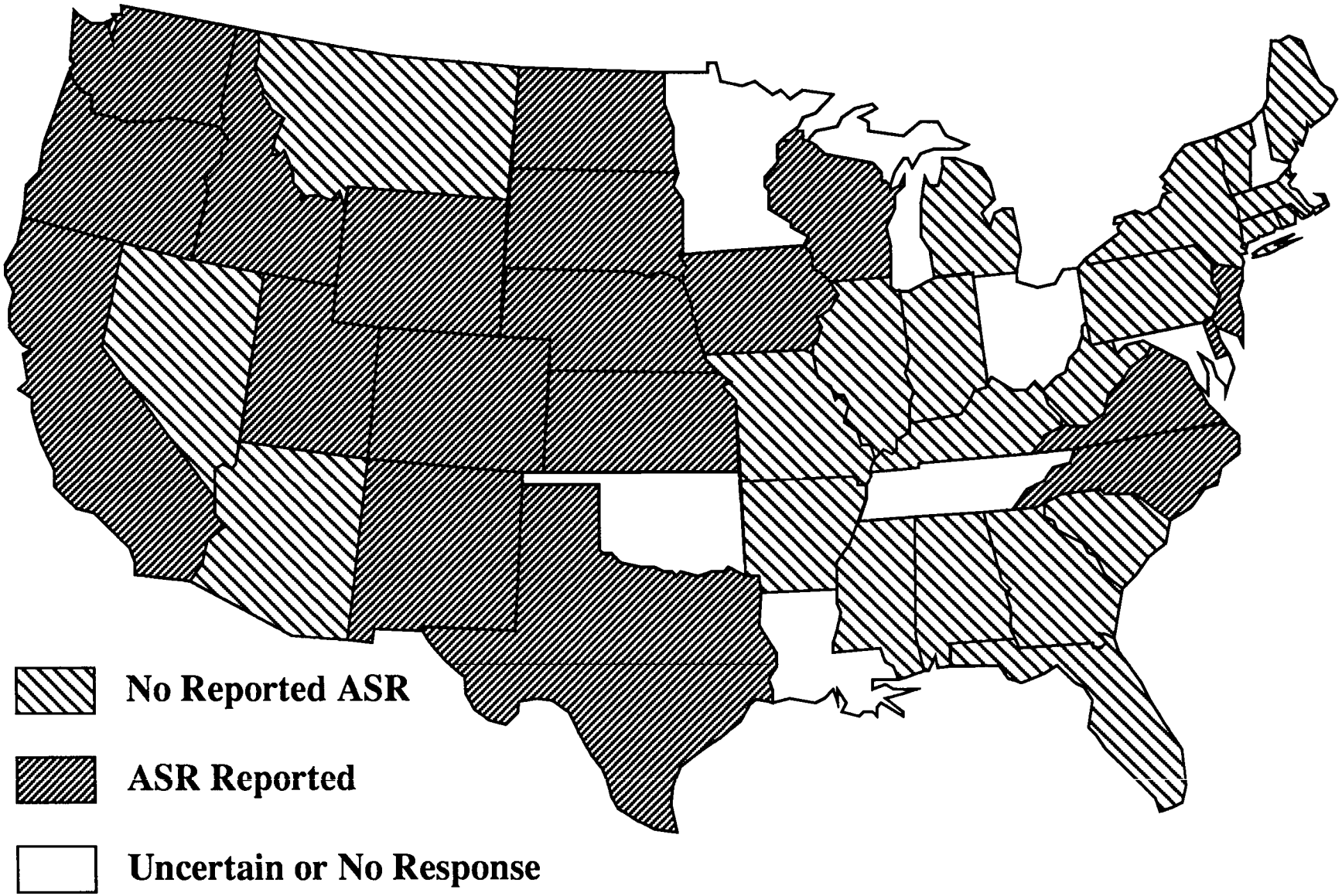


Figure 2.1. Occurrence of ASR reported by states in C-202 questionnaire.

It should not be inferred from the questionnaire results that the potential for ASR does not exist in states that reported no problems. For example, Alabama is known to have had ASR problems in highway structures built in the 1940s, but has successfully prevented deleterious ASR with the use of low alkali cement and Class F fly ash. Also, it is probable that potentially reactive aggregates exist in Montana and South Carolina, but the use of cements with extremely low alkali levels preclude deleterious ASR in those states. The point is that, although deleterious ASR is not reported, the known geological distribution of potentially reactive rock types in the United States virtually ensures that expansive ASR could develop anywhere, provided other requirements such as sufficiently available alkali and moisture also are present.

The questionnaire also provided information on other aspects of ASR in the various states. The level and range of cement alkali limits imposed to prevent expansive ASR varies from state to state. As might be expected, most transportation departments use the traditional 0.6 percent (equivalent $Na_2O$) limitation on cement. Of the 23 states reporting no ASR problems, six impose a 0.5 percent limit on cement alkali, while 11 of 19 that reported ASR problems also impose the 0.6 percent limit. Seven of these 11 states are located in the western United States where volcanic materials are known to be the reactive components of the aggregate.

Questionnaire responses also indicated cement alkali limitations range from 0.4 percent to 0.90 percent. The 0.4 percent limit was reported by North Carolina only for argillite aggregate. New York imposes a 0.7 percent limit if the aggregate has been determined to be deleteriously reactive or consists of at least 5 percent chert. The state of Washington uses a 0.75 percent limit on cement alkali levels except "in critical applications" where 0.60 percent is imposed. The highest limit was 0.90 percent alkali in Iowa when ASTM Types I or III cement are used.

## 2.2 Field Manifestations of ASR

Adverse effects due to ASR result from the expansive nature of the reaction. If sufficient expansion develops, cracking occurs. The orientation of the cracks depends on the internal or external restraint to such expansion.

Rate of development and severity of distress depend on a number of factors, primarily the nature and quantity of reactive aggregate, cement alkali level, ambient temperature, moisture availability, and restraint. Commonly, ASR by itself does not necessitate repair of the concrete. Rather, it weakens concrete to the extent that other factors, such as traffic loading, lead to failure. Numerous instances also exist in highway structures where expansive ASR has not necessitated repair measures even after more than 50 years of service. Characteristic manifestations of ASR-induced distress in highway structures are illustrated in a handbook produced under this project (Stark 1991a). Photographs in this publication illustrate predominant trends in distress patterns and displacement due primarily to ASR. These are summarized below.

1) Map cracking and longitudinal cracking are the predominant manifestations of distress due to ASR in highway pavement. This reflects degree of longitudinal restraint to movement by abutting pavement slabs, thus greatest expansion develops primarily in transverse and vertical directions. This tendency is characteristic of both jointed and continuously reinforced concrete (CRC)

pavement. In jointed pavement, only random or map-cracking may develop in transverse joint areas due to lack of restraint (presence of open joint) in upper levels of the pavement slab.

2) ASR-induced distress develops full depth in pavement slabs, but usually progresses more rapidly in upper and middle levels of the slab. Traffic loading, freezing and thawing, and drying shrinkage can exacerbate cracking.

3) Distress due to ASR in bridge decks may be manifested also as longitudinal and map cracking, again depending on restraint. In bridge decks, embedded reinforcing steel, as well as supporting girders and other substructure components, provide restraint which influences crack patterns. Generally, random cracking through the full depth of the slab with no strongly preferred orientation develops due to ASR.

4) The predominant orientation of cracking induced by ASR in bridge columns is usually longitudinal, with finer random cracks interconnecting the longitudinal cracks. Individual longitudinal cracks usually do not extend the full length of the column and may be confined to either or both the top end and bottom end of the column.

5) Parapet walls and other non-load bearing components of highway structures generally exhibit map cracking and the earliest signs of distress due to ASR probably because of less restraint to movement. However, resulting cracking can be mistakenly attributed to other possible causes of distress, such as freezing and thawing or corrosion of reinforcing steel. As much evidence as possible should be obtained in field inspections and laboratory examinations before conclusions are reached regarding the source(s) of distress.

6) Relative displacement of concrete members, such as revealed by closed joints, or misalignment of concrete units and equipment anchored to the units, may be early indications of expansion due to ASR.

In addition to distress patterns, ASR also can be identified by a characteristic gel reaction product. Traditionally, this gel has been recognized as a glassy-clear or white powdery deposit that occurs within reacted aggregate particles and as linings or fillings in air voids and cracks. Examination using the petrographic microscope is needed to confirm the presence of ASR gel.

A staining procedure developed at Cornell University (Natesaiyer and Hover 1988) has proven to be very useful by more rapidly identifying possible deposits of ASR gel. This technique involves treating freshly fractured concrete surfaces with uranyl acetate solution, then examining the treated surface, under ultraviolet light, for deposits that display characteristic yellow-green fluorescence. This procedure requires discrimination between broad, faint areas of fluorescence which reflect, for example, pretreatment locations of alkali absorbed on cement hydration products, and ASR gel deposits, which usually occur within the periphery of reacted aggregate particles. This procedure can be used on freshly fractured surfaces at field sites as well as on samples in the laboratory. Further guidance and details are given in the handbook (Stark 1991a) mentioned above.

## 2.3 Reaction Chemistry

The chemical reaction aspects of the overall ASR problem may not be readily understood by engineers faced with preventing or dealing with ASR manifestations over the years. In part, this is due to lack of a chemical background on the part of conventionally-trained civil engineers. The problems involved are sufficiently complex that even well-trained chemists familiar with cement chemistry may have difficulties with them. Accordingly, the treatment provided here is slightly oversimplified in places. For further information and detail, refer to the overview of research written under this project (Helmuth 1993).

ASR involves chemical reactions between dissolved substances in concrete pore solutions, and certain reactive siliceous aggregate components. These reactions take place locally, to different extents in different areas within the same concrete structure, depending on local composition of the pore solution and on local occurrence of reactive components. Furthermore, the affected concrete is normally exposed to field conditions involving wetting, drying, freezing, thawing, and occasional exposure to fairly high temperatures. This exposure is not only variable with time, but is often different from place to place within the concrete structure. Accordingly, the progress of alkali-silica reactions in a given structure cannot be quantified.

Nevertheless, enough research has been done that the main outlines of the chemical reaction can be specified and easily understood by interested engineers. The following sections are an attempt to provide this outline.

### *2.3.1 Alkalies and Concrete Pore Solutions*

It is not universally appreciated that even "dry" appearing field concretes contain significant amounts of aqueous liquid pore solution. Depending on mix design and previous drying exposure, this solution might amount to 3 or 4 percent of the overall mass of the concrete. Concrete exposed to prolonged rainfall or positioned so that it is exposed under water will approach a saturated condition and may contain 5 percent or more by weight of this pore solution.

For concretes made with aggregates of low absorption, the solution is confined to pores in the paste portion of the concrete. Entrained air voids are not usually invaded. To the extent that porous aggregates are used, pore solution may be found in the pores of the aggregates as well. Such solution may or may not be identical in composition to that found in the paste pores, but because of the usual easy diffusion of ions in coarse pores, it is unlikely to be very different. If the aggregate is cracked, and cracks are open to the outside of the aggregate particles, pore solution will invade the cracks and ASR may occur in the interior of the aggregate as well as at its outer periphery where it is in contact with the cement paste.

Studies have shown that the zones of cement paste near the aggregate surfaces constitute a special so-called "transition zone," characterized by a higher porosity than the cement paste further away from aggregate surfaces. This more porous zone probably promotes the alkali-silica reaction, since it permits alkali-rich pore solutions to move more easily to reacting aggregate surfaces.

The compositions of concrete pore solutions depend primarily on the nature and chemistry of the cement used. However, they are also influenced by the water-cement ratio, the influences of any mineral or chemical admixtures used, the nature of soluble substances that may have infiltrated the concrete from outside (such as salt, sulfates, etc.), the effects of leaching that may have taken place, and the extent to which prior alkali-silica reactions have tied up some of the alkalies.

For many years it has been possible to study the actual compositions of pore solutions mechanically separated from cement pastes and concretes in the laboratory, and to a limited extent from field concretes as well. The separation can be carried out by pressure filtration before set, and by use of special high pressure dies for hardened cement pastes and concretes (Barneyback and Diamond 1981).

For the general range of portland cements, it has been established that before set, the solutions separated from fresh cement paste or concrete contain appreciable concentrations (about 0.10 to 0.40 moles) of alkali ions (i.e., $K^+$ and $Na^+$), of sulfate ($SO_4^{2-}$) ions, and of hydroxyl ($OH^-$) ions. While $Ca^{2+}$ ions are inevitably present, their concentration rarely exceeds 0.005 moles. Such solutions are much more alkaline than saturated calcium hydroxide in that the pH is substantially higher, typically around 13.2. It is also alkaline in the sense that it contains appreciable concentrations of alkali ions (sodium or potassium or both).

All of the substances dissolved in these solutions are derived from the portland cement. The alkalies and calcium are derived from the clinker minerals; the sulfate is derived primarily from interground gypsum; and the hydroxyl ions are produced by the reaction of the clinker constituents with water. Generally speaking, the higher the alkali content of the cement as equivalent $Na_2O$, the higher the alkali concentration in the pore solution, even at this stage.

Aluminum, iron, and silica-bearing ions are not usually detected in the solution in appreciable concentrations, even in the early stages. This is true even though the early cement hydration reactions involve both tricalcium aluminate ($C_3A$) which in cement contains both aluminum and iron, and tricalcium silicate ($C_3S$).

The occurrence of setting is not marked by any particular change in the composition of the solution, but major changes normally start to occur a few hours after setting and are completed within the first 24 hours. During this period the concentration of sulfate ions typically decreases to negligible amounts, and the sulfate is replaced by an equivalent increase in the concentration of hydroxyl ions. At the same time the already low concentration of $Ca^{2+}$ ions is further reduced since the presence of sodium or potassium, or both, in the solution greatly reduces the solubility of $Ca(OH)_2$.

The results of these changes are of profound importance for the possibility of ASR. The typical pore solution at the end of the first day, even though saturated with respect to $Ca^{2+}$, consists almost entirely of potassium hydroxide (KOH) and sodium hydroxide (NaOH), the concentrations of which are much higher than were previously present. These concentrations may be on the order of 0.50 to 0.90 moles, for cements of the normal range of alkali contents. The corresponding pH values may approach 14.0 for very high alkali cements hydrated at low water-cement ratios.

Further changes in pore solution composition with time are much more restricted. For pastes or concretes sealed in containers and isolated from external influences, there is a further slow

increase in alkali hydroxide concentration as solvent water is progressively reduced through its reaction with cement constituents in late hydration. This process generally slows and has negligible effect on pore solution concentrations after a few weeks. For concretes exposed to natural conditions, partial drying may increase concentrations but reduce the amount and availability of the pore solution. On the other hand, thin concrete sections exposed to flowing water may experience slow reductions due to leaching of the alkalies.

Since alkali-silica reactions usually take place over a prolonged time period, it is the steady state concentration of alkalies in solution (and the equal concentration of hydroxyl ions) that are of most concern. For a given water-cement ratio, experience indicates that these concentrations are a linearly related function of the alkali content of the specific cement that was used. Figure 2.2 shows data compiled from the published work of a number of researchers in the United States, England, and France. The data fit a common trend. The $OH^-$ concentrations of pore solutions for 0.5 water-cement ratio paste or mortar is found to be 0.7 moles per percent equivalent $Na_2O$ of the cement (Diamond 1989). The fragmentary data available indicate that, as expected, lower water-cement ratios lead to roughly proportionally higher alkali concentrations for a given cement.

Thus, if one considers a 1 percent equivalent $Na_2O$ cement batched at a water-cement ratio of 0.5 as roughly typical of concrete affected by ASR, the starting concentration of alkalies and of $OH^-$ in the pore solution of that concrete is expected to be at least 0.7 moles, or higher if some evaporative drying has taken place. Such a solution is extremely alkaline and aggressive. It is very different from the kinds of solutions that aggregate rock components normally encounter in the natural course of geological exposure. It is thus not surprising that some components of some aggregates are subject to chemical reactions when kept in prolonged contact with such solutions inside concrete.

Concretes batched with chemical or mineral admixtures may generate pore solutions affected by these components. For example, Na-neutralized naphthalene sulfonate high-range water reducing admixtures (HRWR) have been found to leave the $Na^+$ ions behind when the dissolved HRWR polymers are absorbed by the hydrating cement components. The $Na^+$ ions remaining in solution are then balanced by an equal concentration of newly-liberated $OH^-$ ions, leading to increases in both alkali and hydroxide ion concentrations proportional to the dosage of HRWR used. Alkali-bearing admixtures of other kinds may produce the same effect.

On the other hand, fly ash and silica fume incorporated as mineral admixtures usually reduce the steady state concentration of alkali and $OH^-$ ions that the concrete would otherwise have. This is true even though fly ash, in particular, may contain a relatively high concentration of alkali ions within the structure of the glass making up most of the fly ash. For silica fume, rapid reaction liberates most of the relatively small contents of alkali within the glass, but subsequent reaction of the remaining silica fume with the cement removes most of the alkali ions (and $OH^-$ ions) from solution, leading to a net decrease in the concentrations available for later ASR reaction.

The alkali contents of pore solutions may be modified as a result of field exposure to deicer salts (NaCl) or other alkali-bearing compounds. Deicing salt applied to concrete bridge decks (and subsequently washed onto other concrete structural components) provides a notorious example, as does salt spray in locations near ocean or brackish water. A major proportion of the chloride ion is absorbed or removed from solution by reaction: the sodium ions left are then balanced by newly-liberated $OH^-$ ions, and the pH and alkalinity of the pore solution increase. This increase promotes ASR. In addition, any residual chloride ions

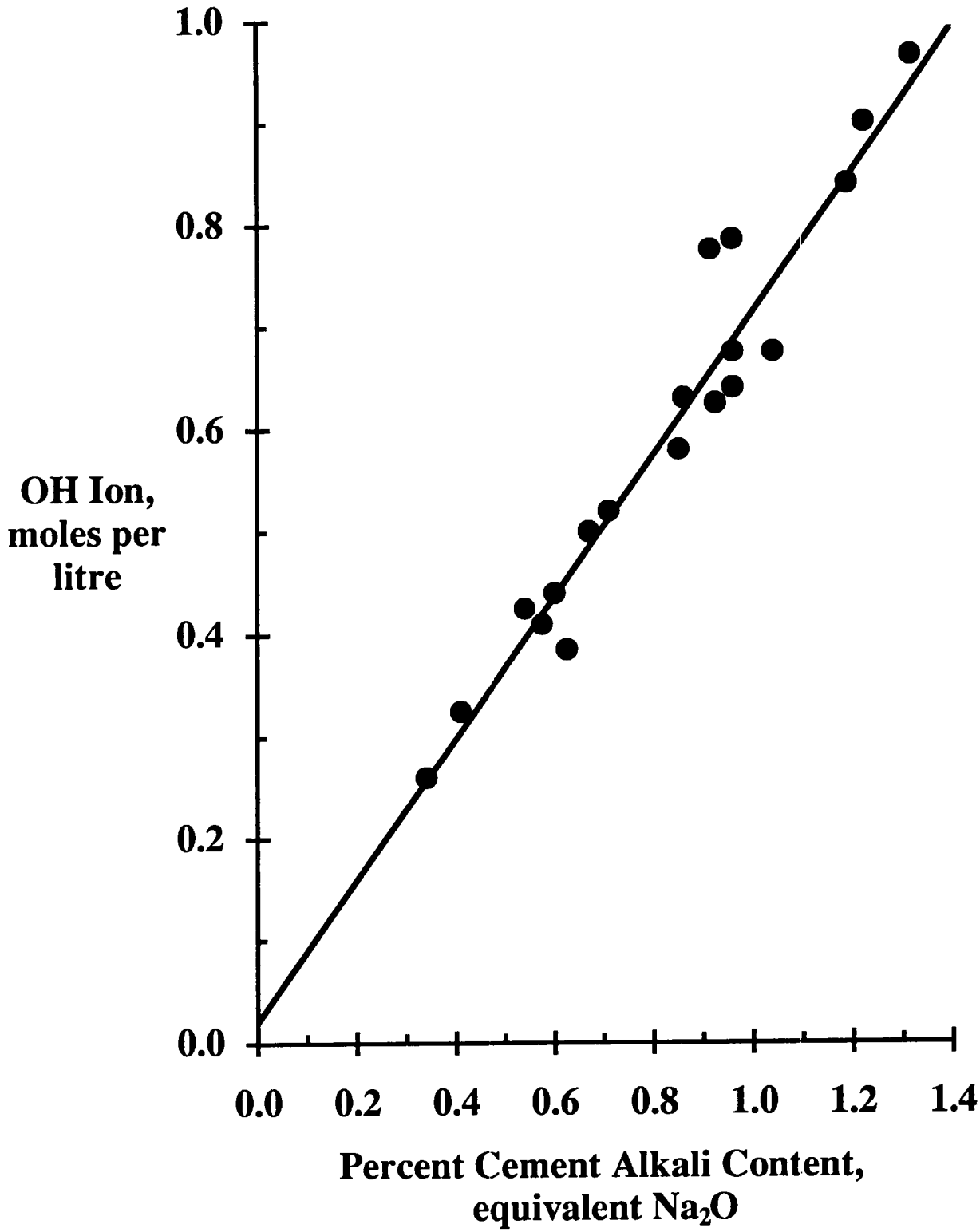


Figure 2.2. Relation between equilibrium OH ion concentrations of pore solution and an alkaline content of the cement, for pastes and mortars of w/c=0.5.

also may play a role in promoting ASR by a different mechanism. Finally, to the extent that prior ASR has taken place and the alkali and $OH^-$ ions have been incorporated in reaction products, the residual concentrations of these ions are reduced.

To sum up, concrete pore solutions are primarily alkali hydroxide solutions of high concentration. The actual concentrations strongly reflect the original alkali content of the cement, but may be modified by other factors.

### *2.3.2 Reactive Aggregates*

The kinds of aggregate component known to be involved in ASR to a sufficient degree to create a problem in concrete are numerous. By the definition of ASR, all of these are composed of, or contain, major percentages of $SiO_2$. Some are crystalline, such as tridymite, cristobalite, strained quartz, etc., while many are glassy or only partly crystalline, such as opal, some chert, and glassy volcanic materials. Others are exceedingly complex rocks that may contain both crystalline and glassy components, including graywackes and phyllites.

The size of the aggregate particle and the nature of the environmental exposure of the concrete influence the rate of ASR reaction that may take place with a given alkali concentration in the pore solution. But, irrespective of these effects, different aggregates react at very different rates. The reactions may go to completion in a matter of weeks with some aggregates while others may require many years to produce noticeable effects (Helmuth 1992).

### *2.3.3 Reaction Products*

It is generally agreed that the reaction products are initially amorphous siliceous gels containing alkalies (usually more $K^+$ than $Na^+$), $Ca^{2+}$, and often some $Al^{3+}$. The incorporation of hydroxyl ions is inferred from the reduction in OH ion concentration that accompanies the reaction. The composition is quite variable from place to place within a given concrete. In some cases some of the gel appears to subsequently crystallize into secondary crystalline reaction products.

Swelling of the gel by absorption of moisture is usually considered to be the main source of expansion and cracking produced by ASR.

### *2.3.4 Sites of the Chemical Reaction*

Regardless of the specific character of the rock component involved, one would expect that the reaction takes place initially at the contact between the rock surface and the hardened cement paste. This may not always be true, however, since in some cases the solution is able to enter existing cracks or channels in potentially reactive aggregate and carry on sufficient reaction to cause extensive deterioration and local expansion within the boundaries of the aggregate particle. Comparatively little is known about the details of how the reaction site may shift from place to place as ASR proceeds. It appears that while some of the

reaction involves in situ conversion of solid aggregate component to reaction product, some of it may involve removal of some of the rock material and deposition elsewhere in the concrete.

Two standard reactive aggregates have been studied around the world. One of these materials is derived from calcining flint commonly found in southern England. It is known either as calcined flint or, in terms of its crystal structure, cristobalite. The other is known as Beltane opal, and is a naturally occurring opaline rock mined in Sonoma County, CA.

Of the two, the calcined flint is usually the more moderate reactor and requires a much higher proportion in the aggregate for maximum response. This pessimum proportion is about 30 percent Beltane opal is a well-known rapid reactor and provides a maximum response at a proportion of only 4 to 5 percent of the total aggregate.

Figures 2.3 and 2.4 represent the appearance of reactive mortars containing pessimum proportions of calcined flint and Beltane opal, respectively, after 90 days' exposure at 100°F (38°C) and 100 percent RH. The mortar was encapsulated in epoxy resin, a fresh surface was sawn across it and then polished, and the surface examined in a scanning electron microscope using the backscatter detector system. The chemical composition of various points on the surface was determined using energy-dispersive X-ray analysis (EDAX).

In Figure 2.3, the obvious cracks present in the calcined flint sand grain have been produced by the calcining process, not by ASR reaction. Similar cracks exist in calcined flint grains that have not been exposed to cement paste. ASR reaction products (as indicated by chemical composition) are present as solid-looking material within the wide horizontal crack, and elsewhere within other cracks. They are slightly lighter in color, but otherwise not much different in appearance than the unaltered calcined flint. The bulk of the grain is completely unaltered $SiO_2$, including the periphery of the grain that has been in close contact with the cement paste surrounding it.

It does not appear at first glance that the limited amount of reaction product visible in the cracks in Figure 2.3 could have done much damage. However, the sand used in preparing this mortar contains 30 percent by mass of such particles and all of them seem to have reacted, at least within the pre-existing cracks. The combined effect of these reactions has been the development of 0.4 percent expansion in 90 days.

Figure 2.4 shows a much different situation. Here the reaction is much more localized within the mortar, since only 4.5 percent by mass of the sand grains is composed of the Beltane opal material. However, all of the opal grains have reacted extensively, generating a very large and visible amount of reaction product. Indeed, all of the visible residual material in the altered opal grain in the center of Figure 2.4 has reacted; all parts of it contain significant amounts of alkalies. In the process, much of the original opal material has been dissolved. The reaction product so produced has been translated to other locations, primarily pockets within the cement paste. Large vacant areas exist within the original boundary of the opal grain.

Commercially used reactive aggregates probably would show different patterns of reaction. Very little research has been done along these lines.

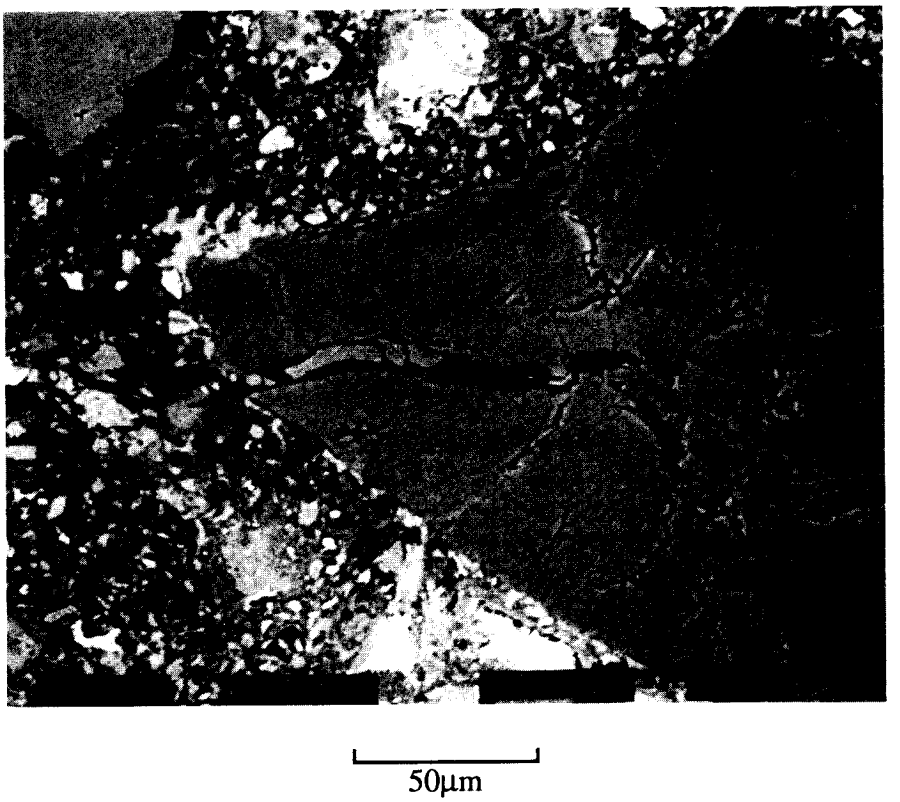


Figure 2.3. Backscatter scanning electron micrograph of reacted calcined flint in ASR reacted mortar, showing that reaction is confined to the areas of cracks.


Figure 2.4. Backscatter scanning electron micrograph showing reacted Beltane opal particle in ASR reacted mortar.

### *2.3.5 Possible Self-Limitation of the ASR Reaction*

One consequence of ASR is that the alkali and hydroxyl ions in the pore solution that take part in the reaction are incorporated in the reaction product gel, which typically has alkali contents exceeding 10 percent. These alkali and $OH^-$ ions are lost to the pore solution (unless recycled by subsequent reaction of the gel with other components). Accordingly, as the ASR reaction proceeds, the pore solution grows progressively less concentrated in alkali and hydroxyl ion, leading to a progressively weaker attacking solution. Thus, ASR reactions are at least partly self-limiting. If and when the hydroxyl ion concentration falls below some limiting value, the reaction should slow down and eventually stop, regardless of how much reactive aggregate remains. This has probably already happened with the calcined flint of Figure 2.3. The $OH^-$ ion concentration at 90 days has dropped to 0.28 moles (from a peak value of about 0.63 moles at one day). While most of the calcined flint remained unreacted at 90 days, little further reaction took place. Essentially no additional expansion was recorded even though measurements were continued for an additional 180 days.

Some researchers have suggested that in certain cases a recycling of the alkalies can take place, in that calcium may exchange for potassium or sodium or both, returning these alkalies to the pore solution for additional reaction. No later-stage increase in the alkali concentration of the pore solution (as envisaged by such a process) is ordinarily recorded in research studies.

## 2.4 Moisture Availability

Absorption of moisture by gel reaction products is the fundamental step causing expansion of concrete due to ASR. If moisture in the concrete is too tightly held by cement hydration products, expansion will not occur even if the reaction between the alkaline pore solution and siliceous aggregate has occurred. A convenient measure of indicating moisture availability for absorption by ASR gel is relative humidity (RH). Previous work (Stark 1991b) has determined that RH values greater than 80 percent, referenced to 70 to 75°F (21 to 24°C), indicates moisture is sufficiently available for absorption by ASR gel and, under this circumstance, expansion can occur. In general, the higher the RH above 80 percent, the greater the possible level of expansion in a given concrete. At 100 percent RH, the amount of moisture, thus the volume increase of the gel, can vary significantly, depending on the water-cement ratio and porosity of the aggregate. Consequently, RH values, which reflect thermodynamic free energy levels of the moisture, are most convenient for indicating moisture availability for expansive ASR.

A technique has been developed (Stark 1991b) by which RH gradients in concrete can be determined. This consists of drilling to obtain powder samples which are then transferred to small bottles into which a probe is inserted through a tightly fitting hole in the cap. The RH of the air in the space above the powder is then measured.

In this project, RH measurements were obtained on concrete in numerous pavements and bridge structures to indicate availability for ASR. This work was carried out in a range of climatic conditions and structure components at the time concrete cores were obtained from the respective structures. Data obtained are extensive, therefore only those representative for conditions having major effects on RH are presented below.

Climate would be expected to exert a major influence on the RH of concrete, particularly in hot arid desert regions where extreme drying is possible. Figure 2.5 compares summertime RH gradients, referenced to 70° to 75°F (21° to 24°C), for highway pavements in California, Georgia, New Mexico, and South Dakota, representing major differences in climate in the United States. These data indicate that, regardless of climate, the only major differences in RH in the pavements occurred within the top approximately 2 in. (51 mm) of concrete. Below this level, RH values were very similar and all above the 80 percent RH threshold level required to support expansive ASR. As expected, the most severe drying occurred in the arid desert region of California, while an intermediate degree of drying occurred in the semi-arid, cooler desert region in New Mexico. Lesser severity of near-surface drying occurred in the warm, relatively humid region in Georgia and the cooler, somewhat drier area in South Dakota.

Figure 2.6 compares typical summertime RH values for bridge decks located in the same areas as the pavements for which RH data are presented in Figure 2.5. These data show the same general order of severity of drying as indicated for the pavements. That is, the most severe near-surface drying occurred in the hot arid climate of California and the least severe in South Dakota. In contrast to the pavements, the bridge decks in California, Georgia, and New Mexico showed sufficient drying through the full thickness of the slab to prevent expansion due to ASR. In these structures, drying occurred from the bottom as well as the top surface, as would be expected. For the bridge deck in South Dakota, degree of drying was relatively uniform top to bottom, but RH values remained slightly above the level required for expansive ASR.

Seasonal climatic changes also would be expected to influence RH levels in concrete, with the greatest changes expected in hot desert areas. Figure 2.7 compares seasonal effects on pavement and nearby bridge parapet concrete in the California desert region. These data indicate that seasonal climatic changes had a pronounced effect on RH through the full 12 in. (305 mm) thickness of the parapet concrete, which is exposed directly to the climate on two faces, with no direct access to groundwater. For the pavement concrete, severe drying occurred near the wearing surface in the direct access to groundwater. For the pavement concrete, severe drying occurred near the wearing surface in the summer season, but diffusion of condensed water upward through the slab in the cooler, wetter, winter season prevented all but minor drying. More importantly, RH values were above the 80 percent threshold level for expansive ASR through the full thickness of the pavement slab in the winter season.

Several conclusions can be drawn from the RH data presented in Figures 2.5, 2.6, and 2.7.

1) Pavement concrete (on grade) is sufficiently damp year around in the United States to support expansive ASR through most of the pavement thickness, regardless of prevailing climatic condition. Diffusion of condensed water on the under surface upward through pavement slabs is sufficient to maintain greater than 80 percent RH continuously through all but the upper 2 in. (51 mm), or so, of the concrete. Surface regions experience cyclic wetting and drying which may intermittently reduce RH values in the near-surface region to less than 80 percent.

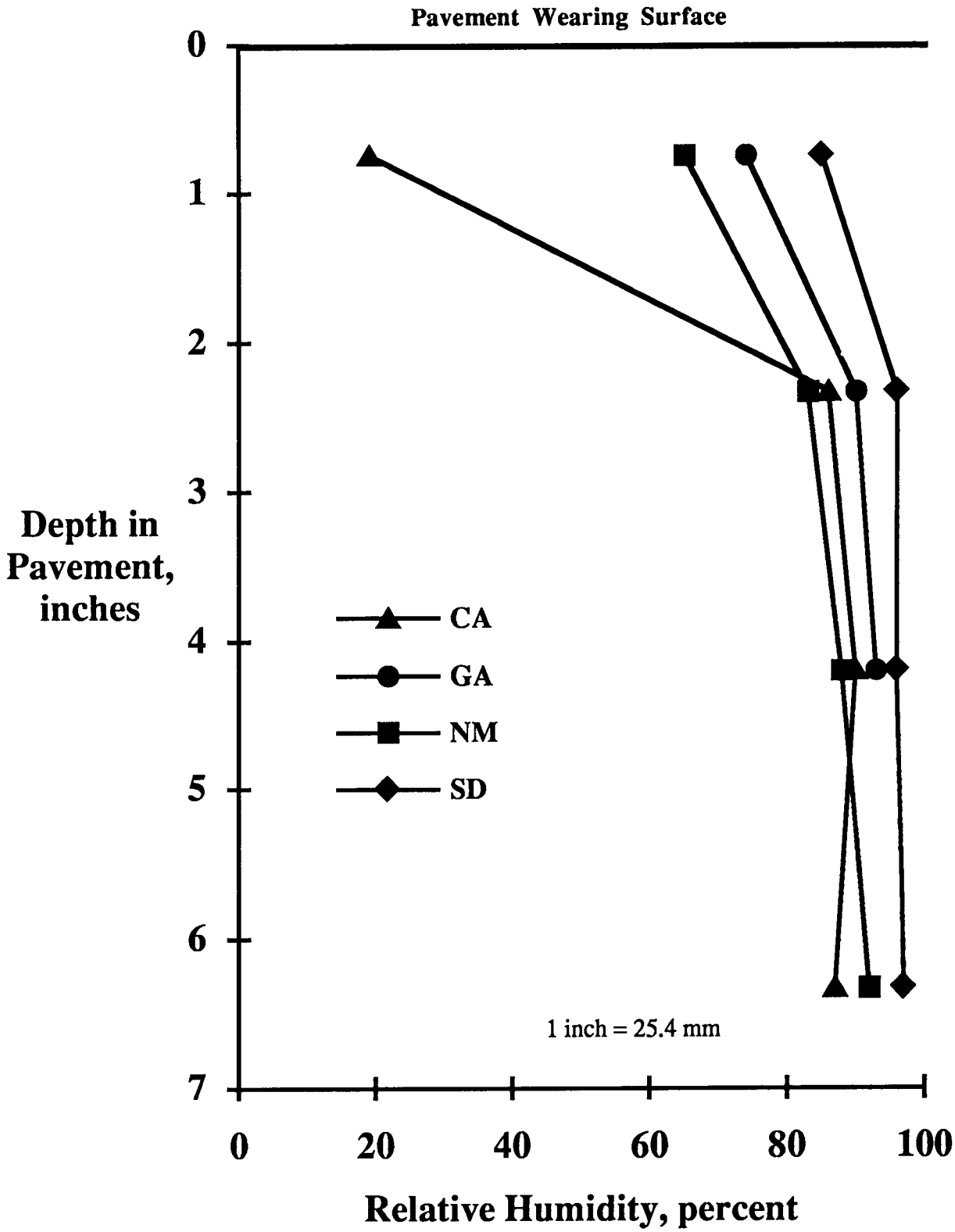


Figure 2.5. Comparison of RH levels in pavement slabs in California, Georgia, New Mexico, and South Dakota.

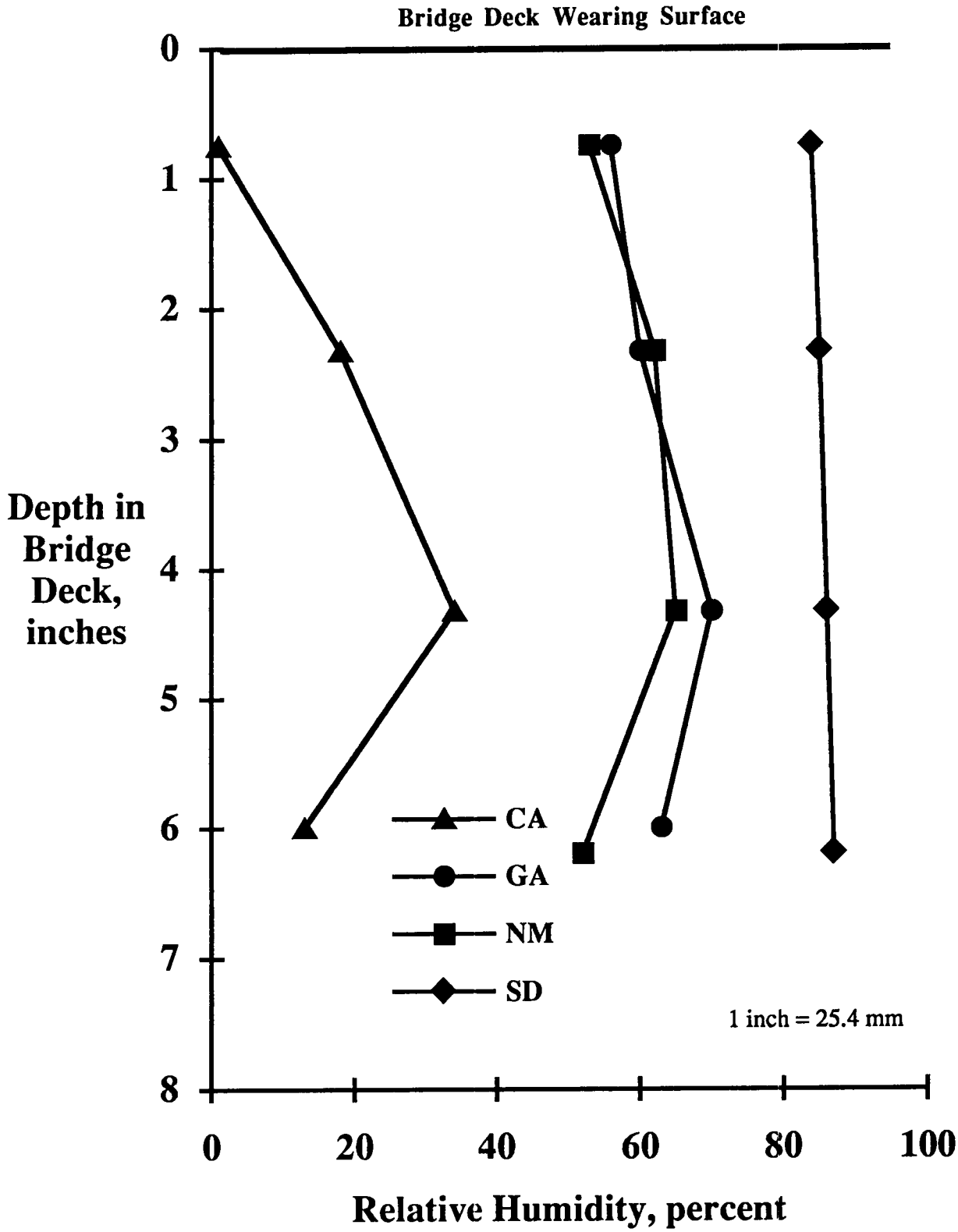


Figure 2.6. Comparison of RH values in bridge decks in California, Georgia, New Mexico, and South Dakota.

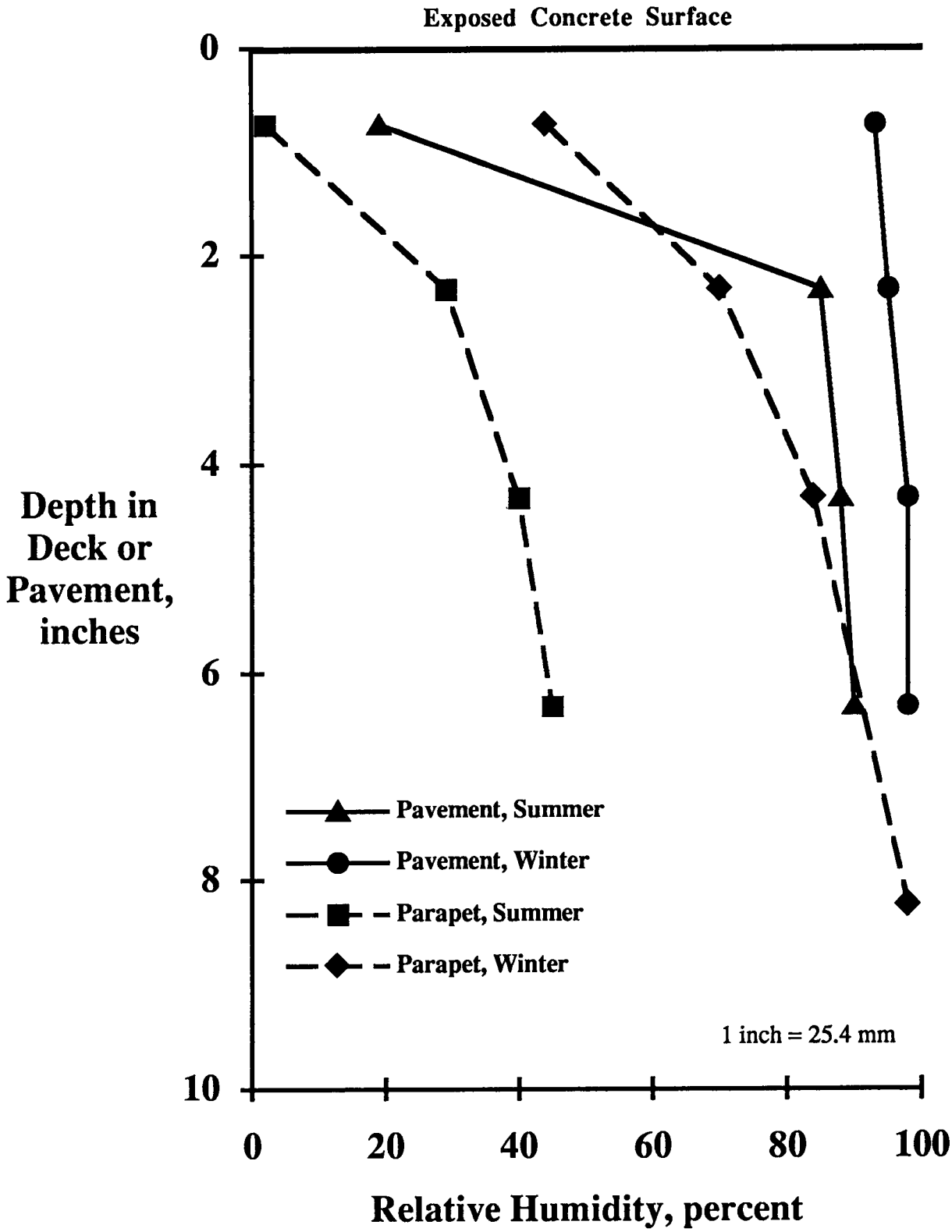


Figure 2.7. Comparison of RH values in pavement slab and bridge abutment wall in California in winter and summer seasons.

2) Climatic drying can be sufficiently intense to reduce RH values below the 80 percent threshold level through the full depth of bridge deck slabs and other thin concrete members above grade, particularly in warm temperate or hot arid climates where the concrete is exposed to direct sunlight.

Prevailing climatic temperature and moisture conditions undoubtedly operate at cross purposes in exacerbating or mitigating expansion due to ASR. High temperatures accelerate reactions between alkalies and silica, but they also commonly intensify drying which reduces the RH and removes moisture necessary for absorption by, and expansion of, ASR gel reaction products. Cooler climates reduce rates of alkali-silica reactions but result in less severe drying, so more moisture is available in the concrete for absorption by, and swelling of, ASR gel. Cyclic wetting and drying, which occurs in virtually all highway concrete, would appear to represent conditions most favorable to expansive ASR. Drying would increase the hydroxyl ion concentration in pore solutions in the concrete, thereby accelerating or intensifying attack on potentially reactive aggregate. Subsequent wetting introduces more moisture into the concrete which then becomes available for absorption by gel reaction products formed under the warmer, drier conditions. Drying further increases distress by increasing widths of cracks initiated by ASR. Furthermore, differential stresses that simultaneously develop due to expansive ASR and drying shrinkage would accentuate cracking.

## 2.5 External Sources of Alkali

In almost all cases of ASR the primary source of reactive alkalies (and the $OH^-$ ions that accompany them in solution) is the portland cement used in making the concrete. In some cases, however, alkalies are introduced from sources outside the concrete. In others, alkalies may be fed into the pore solution as a result of partial decomposition of alkali-bearing rock components of the aggregates resulting from ongoing ASR. In either case, the potentially self-limiting effect that would otherwise arise as the cement-derived alkalies are removed from solution and tied up within ASR gel cannot be relied on, and ASR reactions and the resulting damage may continue indefinitely.

### *2.5.1 Alkalies From Sources Outside the Concrete*

The usual source of external alkalies is salt (NaCl), either applied deliberately to the concrete as a deicer, or derived from ingress of salt water or salt spray.

Distress associated with ASR induced or accelerated by deicer salts is not confined to pavement or bridge deck surfaces. Deicing salts are commonly washed off of bridge decks and onto other structural members where their effects may be severe.

Highway and bridge engineers have become accustomed to thinking of the deleterious effects of such exposures in terms of accelerated steel corrosion in reinforced concrete members. Certainly such effects can be more severe than acceleration of potential ASR damage. The latter requires the presence of reactive aggregates in the concrete, and this is often absent.

ASR effects in salt exposures appear to be very complex and may involve several different mechanisms. Dissolved NaCl in concrete usually undergoes a partial conversion to NaOH, as some of the chloride ions are taken up from solution as Friedel's salt, the chloride-bearing equivalent of the monosulfoaluminate hydration product found in most concretes. In extreme cases a chloride-bearing ettringite also can be formed within the paste. In either case the formation of these chloride-bearing compounds and the consequent removal of chloride ions from the pore solution implies a one-to-one increase in the hydroxyl ion concentration of the solution. This in turn causes the pH to rise, accelerating any ASR reaction that may be taking place. On the other hand, at least some of the dissolved NaCl remains as $Cl^-$ ions in the pore solution. It is this part that causes the onset or acceleration of steel corrosion. There are strong indications in the literature that some of this residual chloride may also accelerate ASR, by a mechanism involving uptake of chloride into the early-stage ASR reaction product (Helmuth 1992). Details of this phenomenon are not understood.

Figure 2.8 is a scanning electron micrograph of a triangular-shaped reacted opal aggregate grain in a mortar undergoing ASR. After several months of exposure to 100 percent RH and after considerable expansion and cracking occurred, the mortar was immersed in a warm NaCl solution. Much additional expansion then occurred. The grain shows extensive dissolution and cracking characteristic of ASR. Analysis of various spots within the grain indicated reveals that about 4 percent of $Cl^-$ ions have been quite uniformly incorporated, along with similar amounts of $Na^+$ ions. Figure 2.9 is a scanning electron micrograph of a similar sample showing the deposition of pockets of Friedel's salt (indicated by arrows) within the hardened cement paste.

Reports of other sources of external alkalies are uncommon. However, one unusual possible future source of difficulty from external sources should be mentioned. This arises from experimental electrochemical procedures to remove chloride from salt-affected concrete structures threatened with steel corrosion problems. The electrochemical process by which the chloride is removed. at the same time, causes increases in hydroxyl ion concentrations (and in pH) of the pore solution from which the chloride is being removed. This might induce or accelerate subsequent ASR.

### *2.5.2 Alkalies From Decomposing Aggregates*

It has been known for some years that some of the more complex reactive aggregates may contain components that slowly decompose during the course of ASR so as to liberate new alkali ions into the pore solution. To the extent that these ions are balanced by hydroxyl ions, they increase the capacity for ASR to continue beyond the point where the reduced concentration of cement-derived alkalis would force the reaction to slow down and stop. The alkali-releasing component may or may not be the primary ASR-active component in the reactive aggregate. In some aggregates it is clear that strained quartz (or the microcrystalline quartz that accompanies it) is the primary reactor, but that feldspars accompanying the quartz may decompose as well, releasing sodium or potassium to the pore solution in concrete.

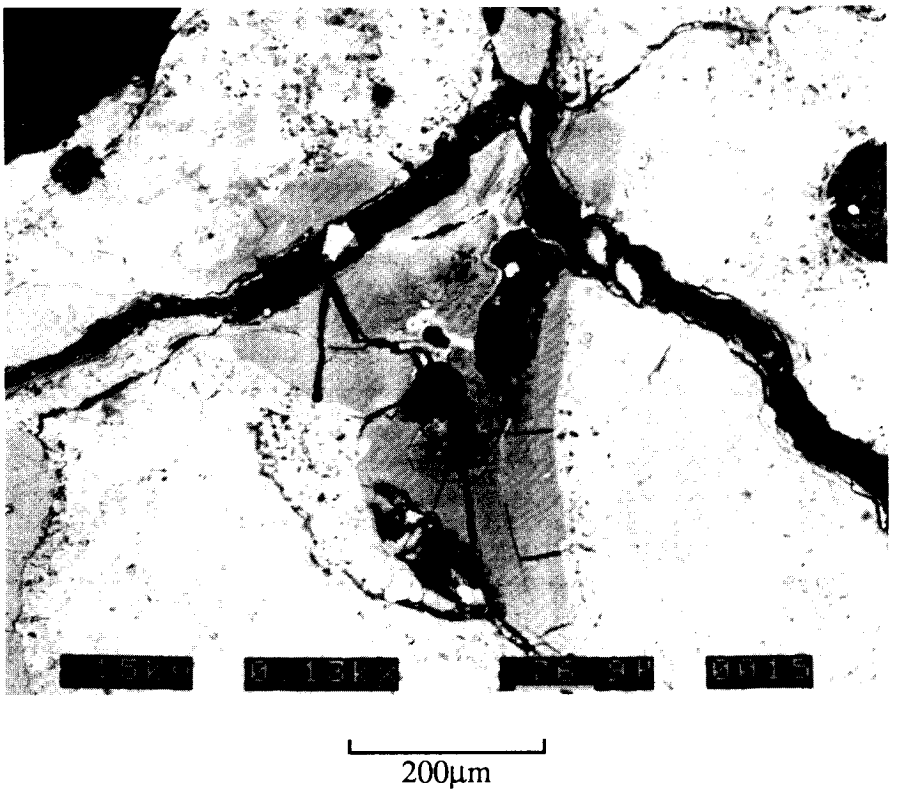


Figure 2.8. Backscatter scanning electron micrograph of reacted opal grain in mortar undergoing ASR which has been immersed in salt solution.

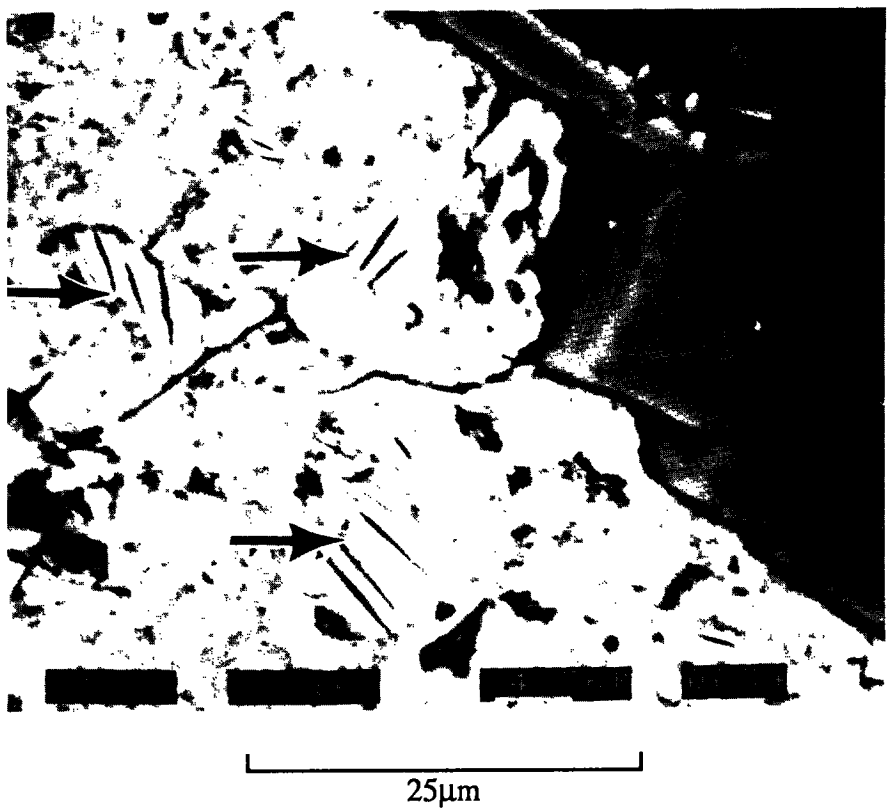


Figure 2.9. Backscatter scanning electron micrograph showing deposition of Friedel's Salt in ASR-reacting mortar immersed in salt solution.

## 2.6 *Conclusions*

State transportation department personnel appear not to be adequately familiar with the symptoms, nature, and extent of ASR in highway structures in their respective states. This is reflected in the development of expansive ASR in states where, for example, use of low alkali cement contributed to the formation of deleterious ASR or where aggregates associated with ASR-induced distress were used without precautions being taken to avoid this problem.

This situation appears to stem partially from the lack of training and understanding of the complex chemical reactions that occur in concrete that can result in expansive ASR. The highly alkaline solutions in concrete result in natural siliceous aggregate suddenly being subjected to an environment totally different from that in which it evolved over geologic time. If cement alkali levels are sufficiently high (pH of 13 to 14), certain components of the aggregate may chemically react with the solutions to produce a gel reaction product that can absorb water and swell, possibly resulting in abnormal expansion of the concrete.

It appears that sufficient moisture is available in concrete to support expansive ASR, regardless of climatic environment. In hot, arid, desert regions, such as in southern California, sufficient moisture is available at least on a cyclic basis. Elsewhere in the United States, sufficient moisture appears always to be available in some part of the structure to support expansive ASR.

Sources other than cementitious components of the concrete, such as NaCl deicer salts, salt spray in ocean environments, and alkalies in certain aggregate in the concrete, appear to have potential to exacerbate expansive ASR.

# 3.0 Rapid Test to Evaluate Potential of Aggregate for ASR

A major reason why ASR is a problem in highway structures is the use of test procedures for screening aggregates that do not properly identify the aggregates that may react deleteriously in concrete. In particular, slowly reacting aggregates often pass existing tests but cause failures due to ASR in field structures. Also, low alkali cement (equivalent $Na_2O$ less than 0.60 percent) is often specified to prevent abnormal expansion due to ASR when, in fact, deleterious ASR is widespread where such cements have been used. In addition, fly ash is often recommended for use to avoid deleterious ASR although, in some cases, it is found to have no mitigative value and, in other cases, actually increases the expansion due to ASR. This may be related partially to the ratio of cement to fly ash in the concrete mixture (Stark 1993).

Clearly, a need exists to improve testing techniques, not only to identify the potential reactivity of an aggregate, but to reliably indicate precautions or mitigative measures than can be taken to safely use the aggregate in question. A major phase of this project was to develop rapid testing procedures that meet these objectives. This section of the report describes the procedures and findings of this phase of the investigation.

## 3.1 Suite of Test Aggregates

Aggregates with known service records were obtained from various locations in the United States to develop a rapid and reliable ASR test procedure. The selection primarily included so-called slowly reactive aggregates, which pass existing tests but fail in field structures. These included quartzites, gneisses, and schists. Innocuous and rapidly reacting aggregates also were included. In addition, it included aggregates used in different climatic and geographic areas of the United States.

Table 3.1 lists the aggregate types and areas from which they were obtained. Selection was based partly on responses to the questionnaire sent to state transportation departments, on discussions with transportation personnel, and on first-hand observation of field performance. In most cases, the aggregates were collected during sampling for RH measurements and field procurement of concrete cores.

Review of the table indicates that 8 of the 12 sources of deleterious aggregate are located in the mid-Atlantic states. This is the area where susceptible aggregates are widespread and react slowly with alkalies in concrete. Two sources containing highly reactive volcanic aggregate were obtained in the dry, southwestern region of the United States. The source in New Mexico was used most extensively in this project because, due to its highly reactive nature, mitigative procedures developed using this material more certainly would apply to other aggregates.

Table 3.1 Aggregate sources in test program

| Source Identity | Source Area | Aggregate Type | Field Performance |
|---|---|---|---|
| | | **Deleterious** | |
| AL | Albuquerque, NM | Mixed sand and gravel, reactive rhyolite to andesite | Rapidly reactive with low alkali cement |
| BK | Bennettsville, SC | Quartz, quartzite gravel, reactive quartzite | Slowly reactive with high alkali cement |
| GH | Salisbury, NC | Quarried argillite | Slowly reactive with high alkali cement |
| GR | Charlottesville, VA | Quarried metabasalt | Slowly reactive with high alkali cement |
| OR | Barstow, CA | Mixed sand and gravel, reactive rhyolite to andesite | Rapidly reactive with low alkali cement |
| PR | Princeton, NC | Quarried granite to granite gneiss | Slowly reactive with high alkali cement |
| RH | Charlottesville, NC | Quarried granite-granite gneiss | Slowly reactive with high alkali cement |
| RQ | Montgomery, AL | Mixed sand and gravel, reactive chert and quartzite | Reactive with high alkali cement |
| SF | Wilmington, DE | Quarried granite-gneiss to amphibolite | Slowly reactive with high alkali cement |

| | | | |
|---|---|---|---|
| SX | Sioux Falls, SD | Quarried quartzite | Slowly reactive with high alkali cement |
| TM | Petersburg, VA | Mixed sand and gravel, reactive chert and quartzite | Slowly reactive with high alkali cement |
| WR | Trenton, NJ | Mixed sand and gravel, reactive chert, quartzite, granite gneiss | Slowly reactive with high alkali cement |

## Innocuous

| | | | |
|---|---|---|---|
| DR | St. Paul, MN | Quarried gabbro-diabase | Non-reactive with high alkali cement |
| EC | Eau Claire, WI | Mixed siliceous sand and gravel | Non-reactive with high alkali cement |
| EL | Chicago, IL | Mixed carbonate and siliceous sand and gravel | Non-reactive with high alkali cement |
| ML | Rock Island, IL | Quarried limestone | Non-reactive with high alkali cement |
| TH | Chicago, IL | Quarried dolomite | Non-reactive with high alkali cement |
| TR | Central New Jersey | Quarried gabbro-diabase | Non-reactive with high alkali cement |

A variety of innocuous aggregates also was selected for this project. Quarried sources of virtually pure limestone and dolomite were included because of the absence of siliceous components, including clays. Two basic igneous rocks with excellent service records also were included. These were very dense, uniform gabbros and diabases which are commonly referred to as traprock. The fifth source is a mixed siliceous gravel that includes primarily granite, quartzite, and dense metavolcanics.

## 3.2 Need for Improved Test to Evaluate Aggregates

The need for reliable and rapid tests to evaluate aggregates for ASR potential can be seen in results obtained using two ASTM standards, C 289 and C 227, both of which have been widely used for more than 40 years.

Figure 3.1 presents results of tests made in accordance with ASTM C 289-87, "Standard Test Method for Potential Reactivity of Aggregates (Chemical Method)," commonly referred to as the "Quick Chemical Test." Most of the aggregates from sources associated with deleterious ASR, when used with high alkali cements in highway structures, are indicated to be innocuous. These materials, BK, GR, PR, RH, RQ, SF, and WR, are classified as slowly reacting aggregates and consist primarily of granite gneisses and quartzites. Aggregates from three sources (BK, GH, and TM) were confirmed as deleterious and consist of argillite and quartzite. Of the two sources associated with deleterious ASR with low as well as high alkali cement, one (AL) was found to be innocuous while the other (OR) was found to be deleterious. Reactive components in both aggregates are glassy to cryptocrystalline volcanics of rhyolitic to andesitic composition. All innocuous sources tested were confirmed as such by the test .

From these results it is evident that ASTM C 289 is too lenient in its identification of "deleterious" or "potentially deleterious" aggregates. That is, aggregates that may be deleteriously reactive in highway structures are liable to be identified as innocuous in the test. This deficiency relates primarily to the slowly reactive rock types such as granite gneiss and some quartzites. In addition, the test was not reliable in identifying materials which, in this investigation, were known to be deleteriously reactive with low as well as with high alkali cements.

Tests run in accordance with ASTM C 227, "Standard Test Method for Potential Alkali Reactivity of Cement-Aggregate Combinations (Mortar Bar Method)," resulted in similar findings. Seventeen of the aggregates in this investigation were evaluated by this procedure, using Cement A with 1.00 percent alkali as equivalent $Na_2O$ (Table 3.2) and extending the test period to 31 months. Results for these cement-aggregate combinations are given in Table 3.3. Results for selected aggregates are given in Figures 3.2 and 3.3. Only the two combinations with highly reactive volcanic materials, AL and OR, and the one containing argillite, GH, exceeded the expansion criteria of 0.05 percent and 0.10 percent at 6 and 12 months, respectively which are suggested in the Appendix of ASTM C 33. Expansions for all other combinations containing known deleterious materials did not exceed 0.04 percent at 12 months and 0.07 percent at 31 months. Those containing known innocuous aggregates reached the range of 0.03 percent to 0.05 percent at 31 months. Collectively, these results fail to reliably distinguish between known slowly reactive and innocuous aggregates, but they do properly identify materials classified as rapidly reactive. This deficiency is basically the same as that found for results of C 289 tests.

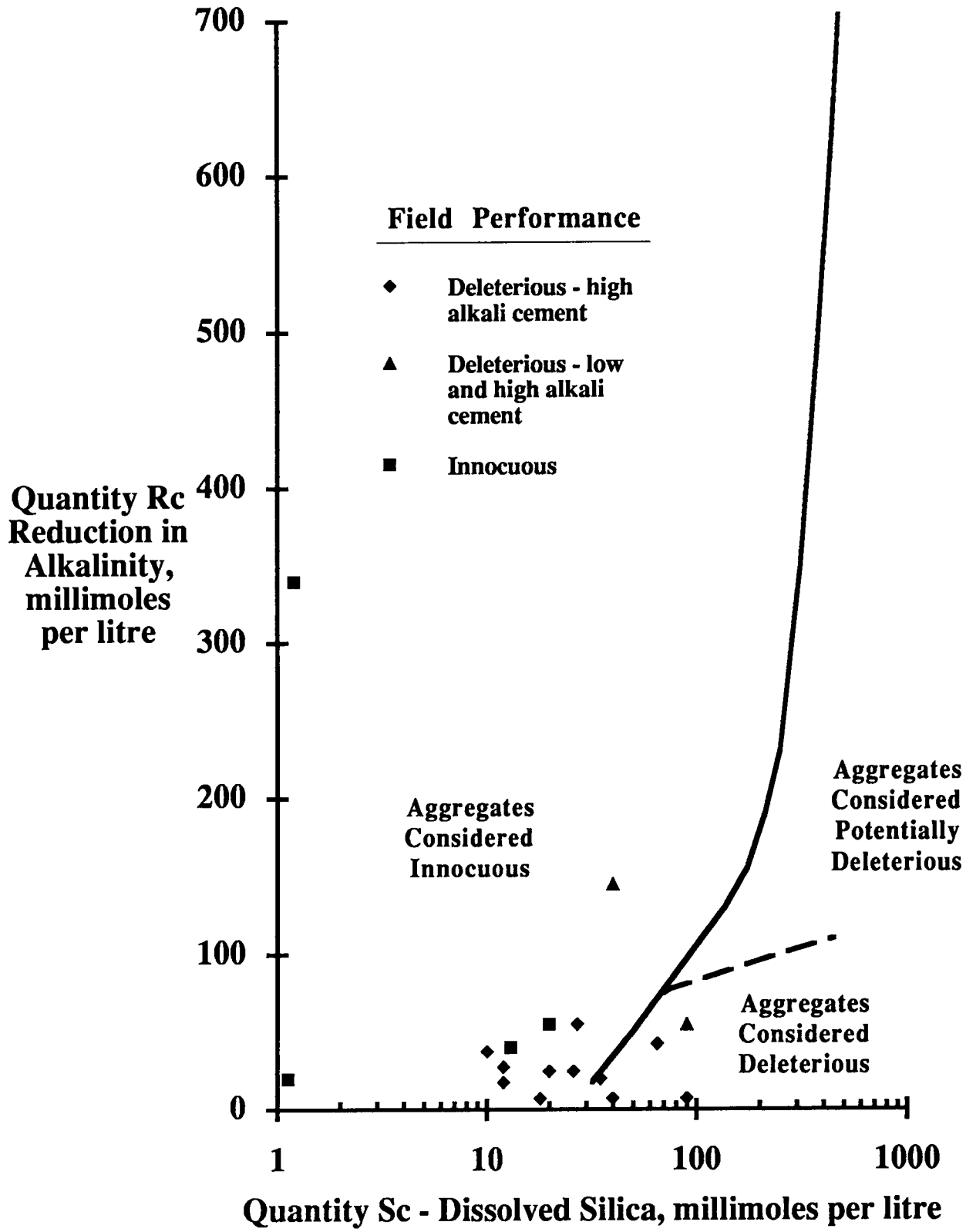


Figure 3.1. Results of ASTM C 289 tests on aggregates in this investigation.

Table 3.2 Compositions of the cements used in this project

| Analyte | Percent A | B | C |
|---|---|---|---|
| CaO | 62.20 | 65.25 | 64.03 |
| $SiO_2$ | 20.37 | 21.22 | 20.88 |
| $Al_2O_3$ | 4.49 | 4.86 | 4.71 |
| $Fe_2O_3$ | 3.32 | 3.39 | 3.36 |
| $M_gO$ | 3.88 | 0.52 | 1.87 |
| $SO_3$ | 2.76 | 2.38 | 2.53 |
| L.O.I | 1.18 | 1.13 | 1.15 |
| I.R. | 0.12 | 0.19 | 0.79 |
| $Na_2O$ | 0.41 | 0.02 | 0.16 |
| $K_2O$ | 0.90 | 0.25 | 0.52 |
| Total alkalies as equivalent $Na_2O$ | 1.00 | 0.18 | 0.50 |
| Calculated per ASTM 150 | | | |
| $C_3S$ | 55 | 57 | 56 |
| $C_2S$ | 18 | 18 | 18 |
| $C_3A$ | 7 | 8 | 8 |
| $C_4AF$ | 10 | 10 | 10 |

Note: All analyses performed in accordance with requirements of ASTM C 150.

Table 3.3 Expansions of mortar bars in ASTM C227 tests

| Identity | Aggregate Type | Reactive Component | Expansion, percent 6M | 12M | 24M | 30M |
|---|---|---|---|---|---|---|
| **Deleterious in Field Peformance** | | | | | | |
| AL | Mixed Siliceous Gravel | Volcanics | .64 | .83 | .92 | .93 |
| BK | Mixed Siliceous Gravel | Quartzite | .03 | .03 | .04 | .04 |
| GH | Quarried Stone | Argillite | .10 | .15 | .20 | .21 |
| GR | Quarried Stone | Metabasalt | .03 | .03 | .04 | .04 |
| OR | Mixed Siliceous Gravel | Volcanics | .05 | .11 | .14 | .14 |
| PR | Quarried Stone | Granite Gneiss | .04 | .04 | .06 | .06 |
| RH | Quarried Stone | Granite Gneiss | .03 | .04 | .05 | .06 |
| RQ | Mixed Siliceous Gravel | Chert, Quartzite | .03 | .04 | .06 | .06 |
| SF | Mixed Quarried Stone | Granite Gneiss | .03 | .03 | .04 | .04 |
| SX | Quarried Stone | Quartzite | .03 | .04 | .06 | .07 |
| TM | Siliceous Gravel | Quartzite, Chert | .03 | .04 | .04 | .05 |
| WR | Mixed Siliceous Gravel | Quartzite, Chert | .04 | .04 | .05 | .05 |
| **Innocuous in Field Performance** | | | | | | |
| DR | Quarried Gabbro | -- | .02 | .02 | .03 | .03 |
| EC | Mixed Siliceous Gravel | -- | .02 | .04 | .05 | .05 |
| ML | Quarried Limestone | -- | .03 | .03 | .04 | .04 |
| TH | Quarried Dolomite | -- | .02 | .03 | .04 | .04 |
| TR | Quarried Gabbro | -- | .03 | .03 | .04 | .04 |

Note: M = months.

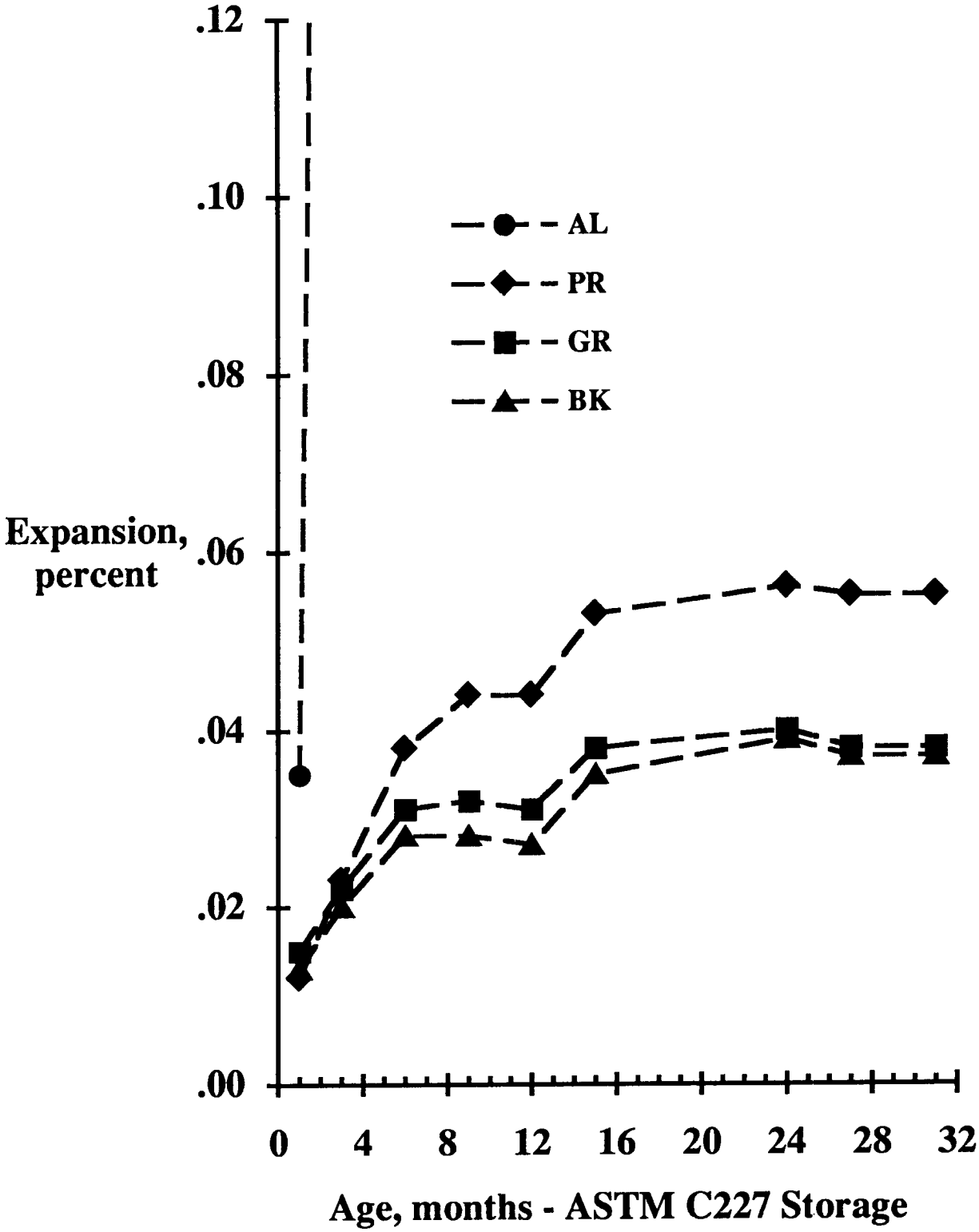


Figure 3.2. ASTM C227 mortar bar test results for deleterious aggregates AL, PR, GR, and BK.

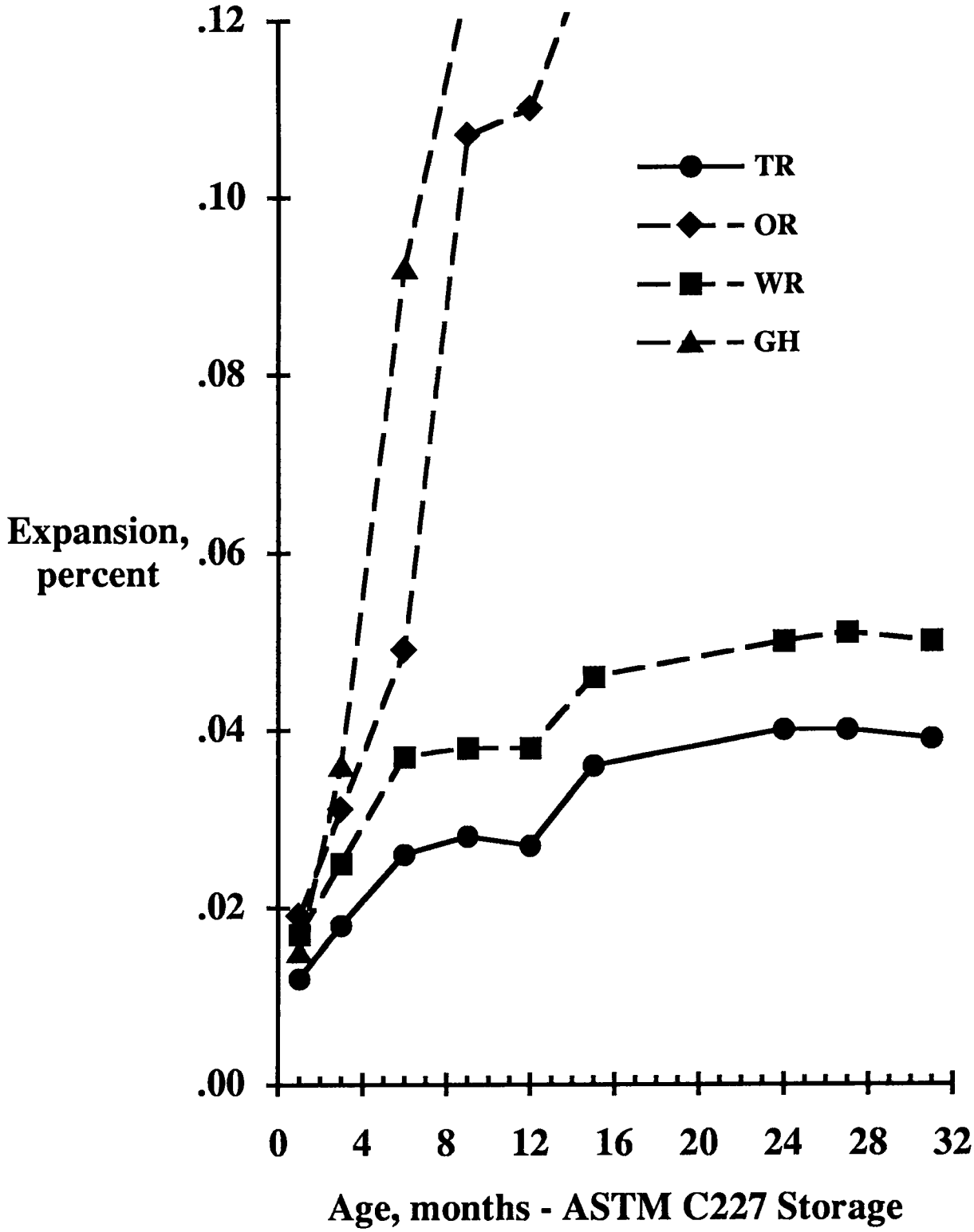


Figure 3.3. ASTM C227 mortar bar tests results for deleterious aggregates OR, WR, and GH, and innocuous aggregate TR.

## 3.3 Development of Test Procedure

The C 289 and C 227 data clearly demonstrate the need for improved test methods to identify aggregates susceptible to causing expansive ASR. It was reasoned early in this investigation that any new test method should have the following characteristics:

1) The procedure should be rapid, requiring preferably not more than 28 days.
2) The procedure should reliably discriminate between innocuous and slowly reactive as well as highly reactive aggregates.
3) The procedure should have the capability of identifying means to safely use cement-aggregate combinations susceptible to deleterious ASR.

The latter requirement is very significant and carries current aggregate or cement-aggregate evaluation beyond simply indicating whether they are potentially deleteriously reactive. To obtain this additional information, existing procedures generally require more than one test method, which then must rely on questionable relationships among those tests as well as correlations with field performance. The more such relationships that are required, the more uncertain becomes an economical and feasible final solution. The present investigation was undertaken with the belief that existing ASTM procedures do not satisfy all of the three requirements.

### *3.3.1 Selection of Candidate Procedure*

Review of published literature and discussion among researchers in this investigation indicated a method developed at the National Building Research Institute (NBRI) in South Africa (Oberholster and Davies 1986) which, with certain modifications, could meet the three requirements set forth above. Briefly, this procedure consists of preparing, in accordance with ASTM C 227, four companion mortar bars, removing the bars from the molds at one day and immersing them in water at 176°F (80°C) for one day, then immersing them in one normal sodium hydroxide (1N NaOH) solution at that temperature for 14 days. Comparator readings are made periodically through the 14-day test period, with the initial reading being obtained just after removal of the bars from water and before initial storage in the NaOH solution.

Based on this procedure, ASTM Committee C-9 proposed a standard, P 214, in which the following criteria for classifying the test aggregate were stated:

1) "When the mean expansion of the test specimens exceeds 0.20 percent at 16 days from casting (14 days from zero reading), it is indicative of potentially deleterious expansion."

2) "When the mean expansion of the test specimens is less than 0.10 percent at 16 days after casting, it is indicative of innocuous behavior."

3) "When the mean expansion of the test specimens is above 0.10 percent and less than 0.20 percent at 16 days from casting, the results are not as yet conclusive."

As stated in these three criteria, the test method is considered a means of determining whether the aggregate is innocuous or potentially deleteriously reactive. It does not indicate

whether the aggregate can be used safely in concrete if, for example, low alkali cement is used in the highway structure. This aspect of the evaluation might be determined by using different solution concentrations of NaOH if normality of the solution can be related to cement alkali level. A further limitation in these three criteria is the inconclusive nature of the results when expansions are in the range of 0.10 percent to 0.20 percent. If this can be clarified by further testing, utility of the test could be increased.

Investigations in South Africa also were carried out to determine whether pozzolans could be evaluated in this procedure. It was concluded from that work that the test could be used to screen different mineral admixtures for their effectiveness in preventing deleterious expansion due to ASR. It was further noted that, because the test apparently represents a "worst case, the amounts of mineral admixture required to prevent deleterious expansion in this test should represent the maximum required in practice, for a particular aggregate." (Davies and Oberholster 1987) Thus, it appeared possible that this procedure also could be used to determine the quantity and source of mineral admixture needed to prevent expansive ASR for different aggregates and cement alkali levels. Overall, this procedure, with certain modifications, appeared capable of serving as the single method possessing all three characteristics stated earlier. Development and refinement of this procedure thus was undertaken as described below.

### *3.3.2 Materials*

The initial tests using this rapid immersion method were conducted on 11 aggregates found to be associated with deleterious ASR in highway structures, and on five known innocuous aggregates, all of which are listed in Table 3.1. ASTM Type I cement, with 1.0 percent equivalent $Na_2O$, (Table 3.2) was used for all mixes. The characteristics of the aggregates are given in Table 3.1. Coarse aggregates were crushed, sieved, and washed to meet the C 227 grading. Except for crushing, natural sands that were tested were similarly processed. An aggregate to cement ratio of 2.25:1.00 and a water-cement ratio of 0.50 were used for all mixtures. A fixed water-cement ratio is essential because ASR in this test depends on diffusion of NaOH solution into the test specimens, and permeability of the mortar bar specimens under this test condition is strongly dependent on water-cement ratio.

All mortar mixtures were prepared in accordance with C 227. One batch of mortar was used for each set of four companion specimens. Following casting, the specimens were stored per the NBRI procedure, in this case, to a test age of 28 days. Longer test periods were considered to extend beyond the understanding of "rapid" as a required characteristic.

### *3.3.3 Results for Mortar Bars Immersed in 1N NaOH Solution*

Results of the tests are summarized in Table 3.4. Curves representing results for several deleteriously reactive and innocuous aggregates are plotted in Figures 3.4 to 3.6. These data indicate that 14-day expansions for all deleterious aggregates were greater than for all innocuous aggregates except EC. That is, the least expansions were greater for the deleterious aggregates than the greatest expansions for all innocuous aggregates except EC. The data also indicate that the greatest expansions developed for aggregates AL and OR, both of which are deleteriously reactive with low as well as high alkali cement in field structures. Also, aggregates classed as slowly reactive, such as BK, RN, SF, and GR, produced the

Table 3.4 Results of initial rapid immersion tests

| Source | Composition | Expansion, Percent 4D | 7D | 10D | 14D | 21D | 28D |
|---|---|---|---|---|---|---|---|
| | | **Deleterious in Field Performance** | | | | | |
| AL | Granitic Volcanic | .190 | .483 | .713 | .867 | 1.035 | 1.098 |
| OR | Granitic Volcanic | .205 | .296 | .375 | .424 | .500 | .541 |
| GH | Argillite | .080 | .252 | .354 | .418 | .511 | .566 |
| RQ | Chert, Quartzite | .070 | .212 | .328 | .409 | .515 | .574 |
| WR | Quartzite, Chert | .073 | .160 | .246 | .314 | .416 | .487 |
| PR | Granitic Gneiss | .108 | .189 | .239 | .309 | .385 | .422 |
| SX | Quartzite | .069 | .122 | .170 | .225 | .312 | .389 |
| TM | Quartzite, Chert | .032 | .066 | .116 | .177 | .270 | .309 |
| BK | Quartzite, Chert | .042 | .063 | .073 | .106 | .142 | .196 |
| RH | Granitic Gneiss | .013 | .032 | .065 | .096 | .132 | .164 |
| SF | Granitic Gneiss | .044 | .038 | .064 | .086 | .124 | .146 |
| GR | Metavolcanics | .026 | .040 | .052 | .082 | .115 | .146 |
| | | **Innocuous in Field Peformance** | | | | | |
| ML | Limestone | .025 | .024 | .029 | .026 | .035 | .024 |
| TH | Dolomite | .028 | .047 | .066 | .066 | .077 | .078 |
| TR | Gabbro | .014 | .022 | .029 | .044 | .066 | .102 |
| EC | Mixed Siliceous | .055 | .076 | .181 | .278 | .329 | .388 |
| DR | Gabbro | .032 | 0.27 | .061 | .075 | .157 | .263 |

Notes: D = days
All results are the averages for four companion specimens.

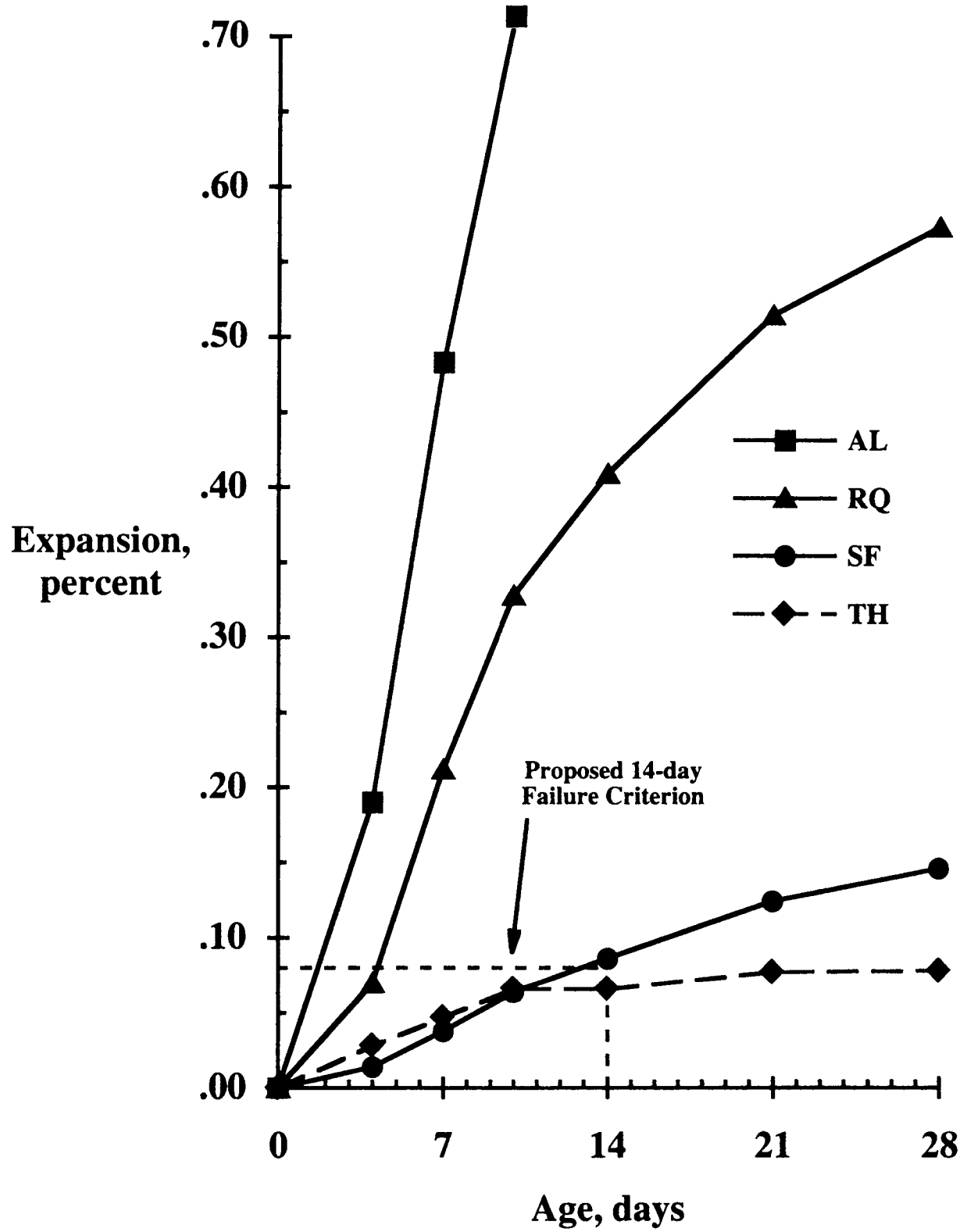


Figure 3.4 Results of rapid immersion test for deleterious aggregates AL, RQ, and SF, and innocuous aggregate TH.

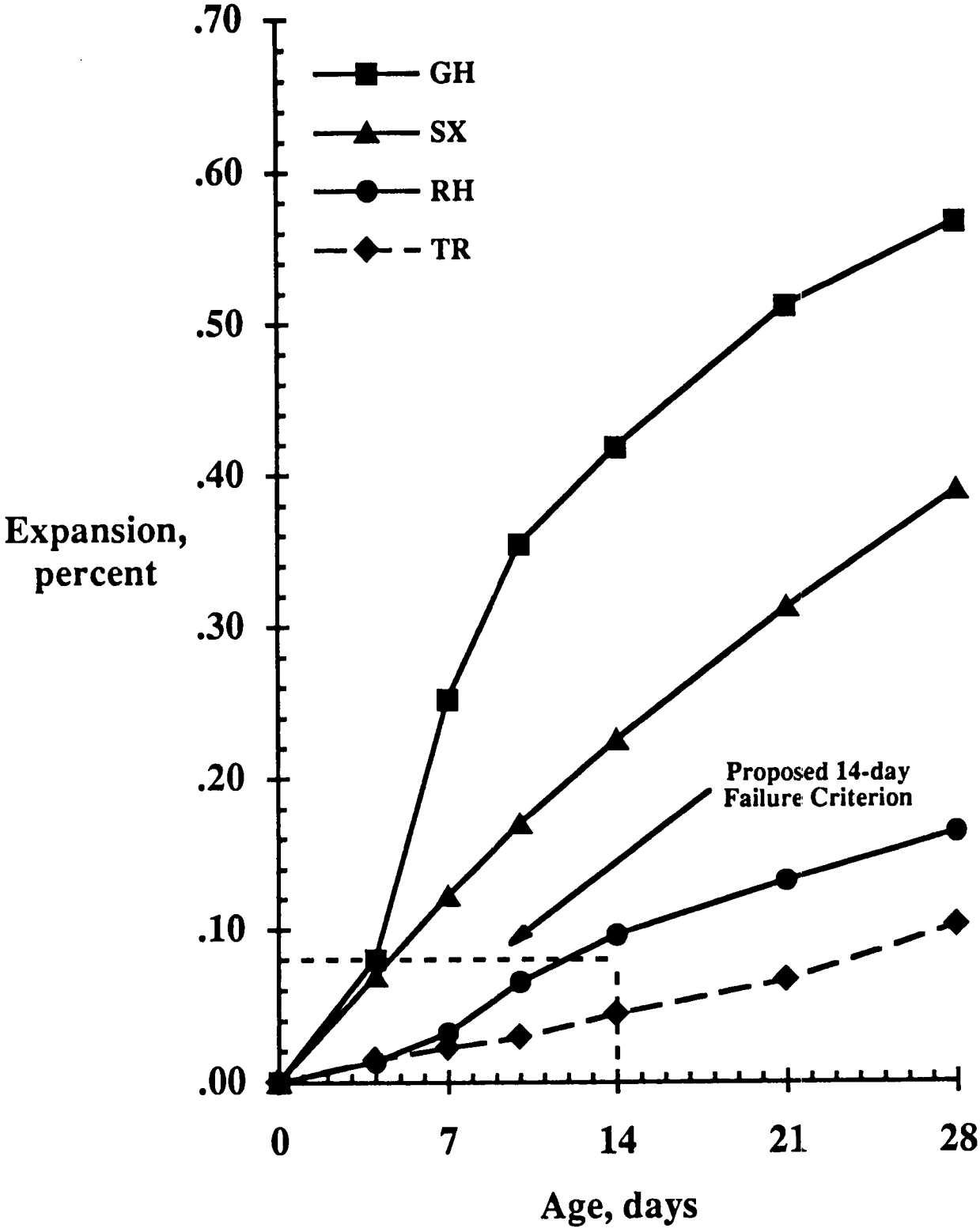


Figure 3.5 Results of rapid immersion test for deleterious aggregates GH, RH, and SX, and innocuous aggregate TR.

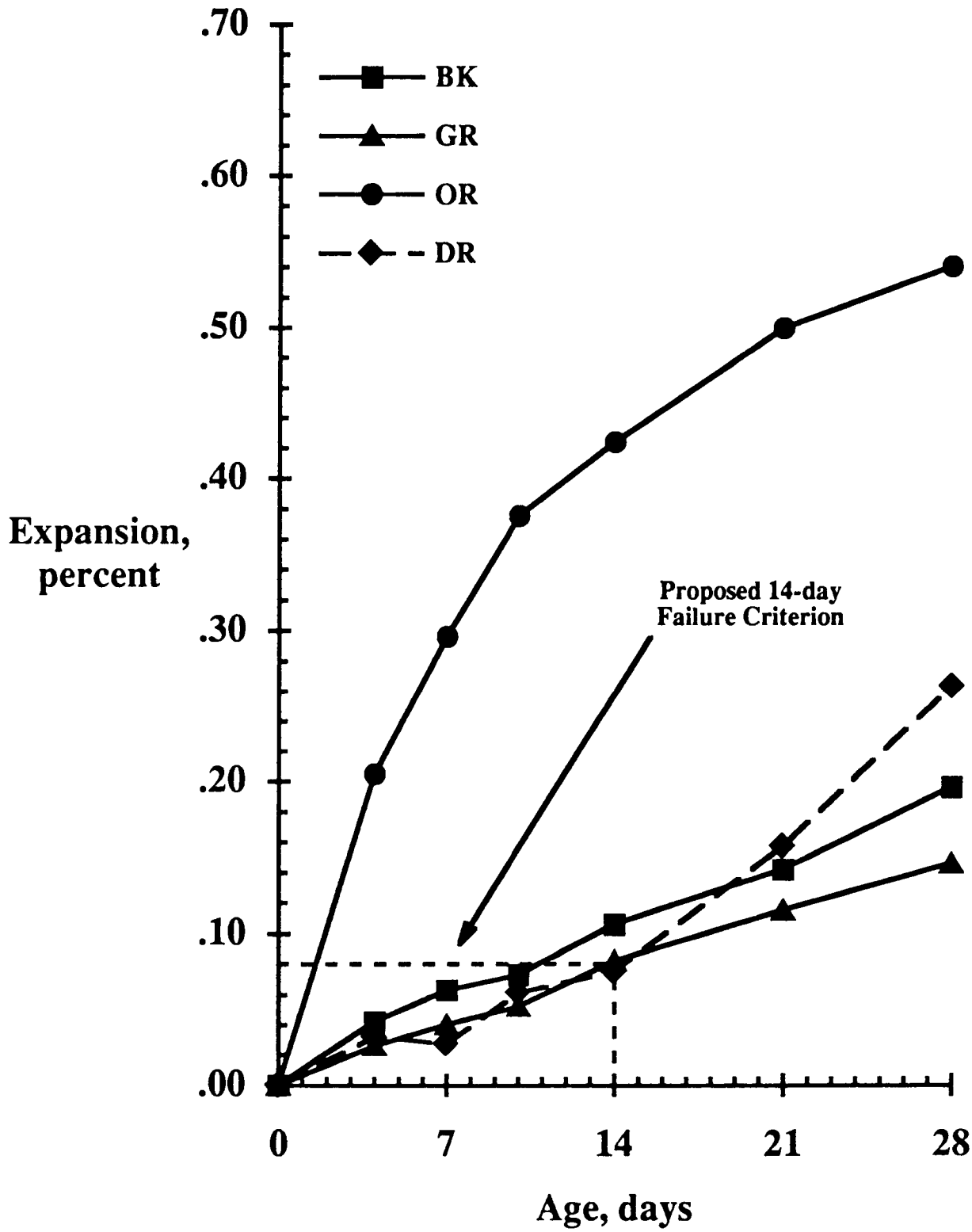


Figure 3.6 Results of rapid immersion test for deleterious aggregates BK, GR, and OR, and innocuous aggregate DR.

lowest expansions. Thus, there appears to be a generally consistent relationship between observed performance in field structures with respect to ASR and level of expansion in the test. Based on these results, the failure criterion selected is 0.08 percent at 14 days. This is the level at which expansions of slowly reactive and innocuous aggregates are nearly the same.

As stated above, a notable exception to the apparent relationship between field performance and 14-day expansion level in the test is aggregate EC. This exception underscores the severity of the test and reflects the fact that observed satisfactory field performance was based on use with high alkali cements that produce pore solutions in concrete less alkaline than the 1N solution used in the test. The same is probably true to varying degrees for all of the test aggregates. But, for aggregate EC, much greater expansions developed with increase in solution normality above that likely present in the highway structure. A similar situation is seen for innocuous aggregate DR, for which relatively high expansion levels developed after the 14-day test period.

The situation for aggregates EC and DR is opposite that which exists for ASTM C 227 and C 289, as both of these tests are too lenient. It also points out the fact that classification as deleterious in the test does not mean the aggregate necessarily will react deleteriously in highway structures. This again suggests this test might be used to determine safe cement alkali levels by adjusting normalities of immersion solutions to correspond to given cement alkali levels. This concept is investigated in the next section of this report.

Results developed in this series of tests thus appear to agree with results reported at NBRI. These researchers also report that this test procedure can identify slowly reacting aggregates, such as granite gneisses. However, where they recognized an intermediate expansion range of 0.10 percent to 0.20 percent as uncertain, testing in this project indicated, with the aforementioned exception of aggregate EC, that expansions greater then 0.08 percent indicate potential for deleterious ASR.

### *3.3.4 Determining Safe Cement Alkali Levels*

Existing ASTM and other specified tests do not address the important issue of how to safely use potentially deleteriously reactive aggregate. Consideration suggests the rapid immersion method lends itself to determining safe cement alkali levels with modifications that appear to relate directly to avoiding expansive ASR in the field. The approach used in this procedure to meet this objective is described below.

Expansions developed in the rapid immersion method depend on diffusion of the immersion solution into the test specimen and on alkali and ($OH^-$) concentration of that solution. The solution used in tests reported above is 1N NaOH which, at 176°F (80°C), greatly increases the rate of expansion. It follows that reducing the alkalinity of the solution, for example, to 0.50N NaOH should reduce expansions. It appears that systematically reducing normality should result in progressively reduced expansions at, say, 14 days, perhaps to a level that does not exceed that of innocuous aggregates in the same solutions. Based on this premise, tests were run to determine safe cement alkali levels for otherwise potentially deleteriously reactive aggregates.

To determine the maximum safe cement alkali level, a relationship must first be developed between normality of the test solution and alkali content of the cement. In a report

developed as part of this project, (Helmuth 1992) a linear regression equation, (2.2.1) is presented, based on published data, that relates cement alkali level to solution normality in a hydrated cement paste of given water-cement ratio. This equation is as follows:

$$[OH^-] = 0.339 \frac{Na_2O}{w/c} + 0.022 \pm 0.06 \text{ moles/L}$$

Where: $[OH^-]$ corresponds to NaOH normality

$Na_2O$ = equivalent percent $Na_2O$ of the cement

and w/c = water-cement ratio

Using this equation, relationships among $OH^-$ concentration (normality), cement alkali level, and water-cement ratio are given in Table 3.5 and shown graphically in Figure 3.7. Examples using this equation and Figure 3.7 are given in Appendix A. Normality values shown in the table and plotted in Figure 3.7 were calculated using the scatter in data on the high side (+0.06 moles/L in the equation) of the average. This provides somewhat conservative (low) maximum cement alkali contents that would be required for safe levels of expansion.

Determining the safe cement alkali level with a particular aggregate would appear to require a different failure criterion than 0.08 percent. According to the data in Table 3.5, normality of the immersion solution (1N) would correspond to a cement alkali level of about 1.39 percent equivalent $Na_2O$ for a 0.50 water-cement ratio. This is much higher than those of cements used in highway structures where deleterious ASR has developed. For example, a deleterious aggregate such as SF falls only very slightly above the 0.08 percent, 14-day test criterion. Reducing solution normality to, say 0.90N, would result in a corresponding cement alkali level of about 1.2 percent at 0.50 water-cement ratio, yet that aggregate caused expansion and cracking with cement levels reported to be in the range of 0.85 percent to 0.95 percent. It thus appears that cement alkali level at which deleterious ASR developed in highway structures must be factored in to identifying the test failure criterion to identify safe cement alkali levels.

To obtain this information, several series of rapid immersion tests were run using NaOH solution normalities of 0.70N, 0.52N, 0.35N, and 0.18N in addition to the standard 1N concentration. Innocuous aggregates TH and TR, and deleterious aggregates SF and GR, all falling close to the 0.08 percent criterion for 1N NaOH, and more highly reactive aggregate WR, were included in these series.

Results given in Table 3.6 do indicate that expansions decrease progressively as solution normality decreases. Obviously, the decrease can be greater for aggregates such as WR that develop high expansion in the standard 1N solution. Plots of these data, together with a projected failure criterion for the various solution normalities (cement alkali levels) are shown in Figure 3.8. The data point for innocuous aggregate ML, evaluated in 1N solution, is plotted as a boundary condition for the criterion at that normality. The projected failure criterion (dashed line) is shown as 0.08 percent at 1N concentration. The criterion is then shown to decrease at a rate dictated by the coincidence of the curves for SF and TR and TH and the fact that the line falls below the field failure indicated for SF. This convergence point should insure lack of ASR because TR and TH have known satisfactory service records.

Table 3.5 NaOH solution normalities for different cement akali levels and water-cement ratios

| Cement Alkali Level | Water-Cement Ratio 0.60 | 0.50 | 0.40 | 0.30 |
|---|---|---|---|---|
| 1.40 | .87 | 1.03 | 1.27 | 1.66 |
| 1.20 | .76 | .90 | 1.10 | 1.44 |
| 1.10 | .70 | .83 | .1.01 | 1.32 |
| 1.00 | .65 | .76 | .93 | 1.21 |
| .90 | .59 | .69 | .84 | 1.10 |
| .80 | .53 | .62 | .76 | .99 |
| .70 | .48 | .56 | .68 | .87 |
| .60 | .42 | .49 | .59 | .76 |
| .50 | .36 | .42 | .51 | .65 |
| .40 | .31 | .35 | .42 | .53 |
| .30 | .25 | .28 | .34 | .42 |
| .20 | .20 | .22 | .25 | .31 |

Note: Calculated normalities based on worst case (+0.082 moles/L)

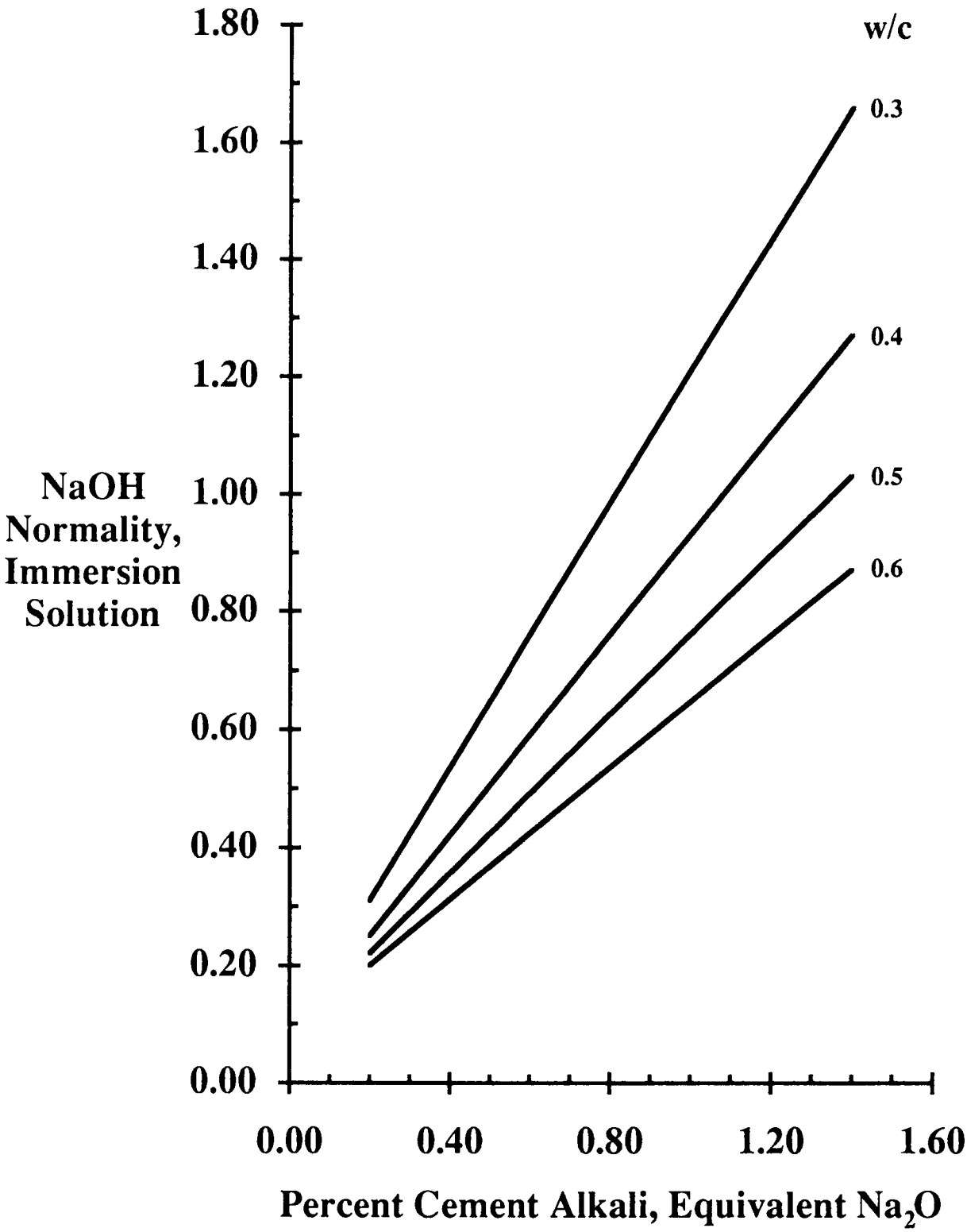


Figure 3.7 Relationship between cement alkali level and NaOH concentration of immersion solution for different water-cement ratios.

Table 3.6 Rapid immersion test results for mortar bars immersed in solutions of different NaOH concentrations.

| Aggregate Source | Estimated Cement Alkali Level for ASR in Concrete | NaOH Solution Normality | 14 Day Expansion Percent |
|---|---|---|---|
| TR | No ASR | 1.00 | .026 |
| Innocuous | | 0.75 | .014 |
| | | 0.52 | .011 |
| | | 0.35 | .002 |
| | | 0.18 | .002 |
| TH | No ASR | 1.00 | .023 |
| Innocuous | | 0.75 | .014 |
| | | 0.52 | .011 |
| | | 0.35 | .002 |
| | | 0.18 | .006 |
| SF | 0.85% | 1.00 | .086 |
| Deleterious | to | 0.70 | .042 |
| | 0.95% | 0.52 | .009 |
| | | 0.35 | .004 |
| | | 0.18 | .006 |
| GR | 0.75% | 1.00 | .096 |
| Deleterious | to | 0.70 | .060 |
| | 0.85% | 0.52 | .032 |
| | | 0.35 | .016 |
| | | 0.18 | .010 |
| WR | 0.70% | 1.00 | .272 |
| Deleterious | to | 0.70 | .214 |
| | 0.80% | 0.52 | .040 |
| | | 0.35 | .004 |
| | | 0.18 | .005 |

Notes: 1. Estimated cement alkali levels were reported by state transportation personnel
2. All results are the averages for three companion mortar bars

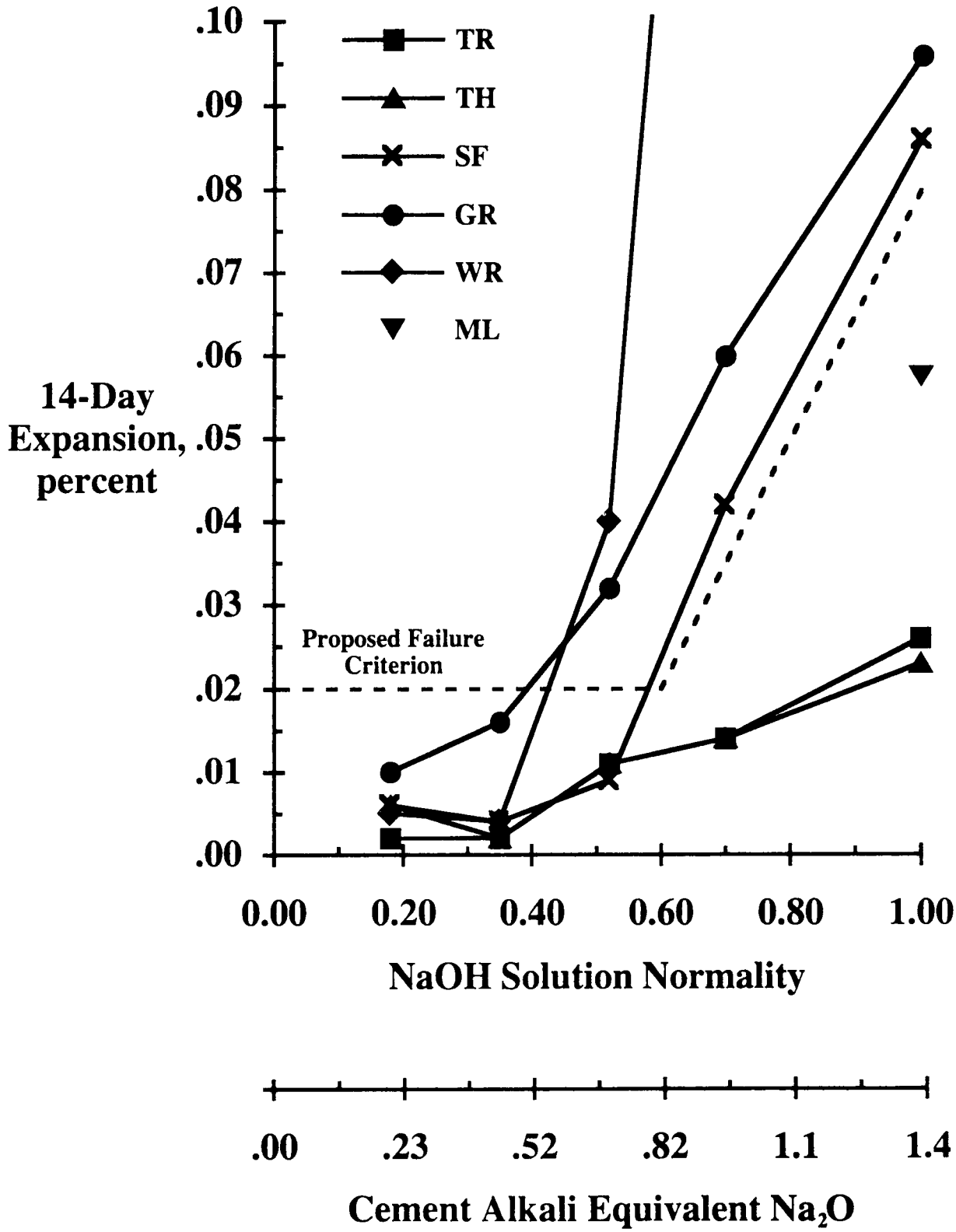


Figure 3.8 Projected failure criterion to determine safe cement alkali level for deleterious aggregates.

The point (about 0.60N) at which the criterion extends parallel to the abscissa was determined by the location of failure levels for the deleterious aggregates and an expansion level as close as possible to that for the innocuous aggregates TR and TH when tested in 1N NaOH solution. This level thus occurs at 0.02 percent expansion for solution normalities less than about 0.60N, which corresponds to a cement alkali level of about 0.82 percent equivalent $Na_2O$ at a water-cement ratio of 0.50.

This criterion admittedly is based on very limited data. Performance data on concrete containing potentially deleteriously reactive aggregate from these sources, where long-term satisfactory performance exists with the use of cements with lower alkali levels, would be particularly useful. Such data, for example, might require the failure criterion to slope downward for normalities less than 0.60N. Another factor in establishing this portion of the criterion curve is the intrinsic behavior of the cement itself in this test. From these series of tests, it is evident that virtually no expansion would develop that is independent of solution normality, as evidenced by the data for the 0.35N and 0.18N solutions.

Selection of the failure criterion is felt to represent reasonable, or slightly conservative values. At the present time additional data are desirable to more precisely define the criterion. The alternative is to use the 0.08 percent criterion for the 1N NaOH solution and, based on that result, conduct further testing, if necessary, using pozzolanic materials, or simply to use lithium hydroxide as an admixture in fresh concrete. These alternatives are described in subsequent sections of this report.

### *3.3.5 Evaluation of Pozzolans*

The usual methods of evaluating mineral admixtures to combat ASR in concrete are based on ASTM standards. Fly ash, for example, would be evaluated in accordance with C 311, C 441, and C 618 (AASHTO M 295). However, C 618 requirements are optional when pertaining to ASR. The intent of the requirements of C 618 regarding ASR is that they are to be invoked only when the aggregate to be used in the concrete has been declared "reactive" and no other precautions regarded as sufficient have been taken to preclude excessive expansion. Ignoring ASR-related testing does not appear always to be advisable since the fly ash itself could introduce significant quantities of alkali into the mixture, thereby converting an otherwise innocuous cement-aggregate combination into a deleterious cement-fly ash-aggregate combination. It thus appears prudent to evaluate a mineral admixture for its effect on ASR regardless of the assumed lack of history of development of ASR-induced distress.

Current ASTM standards for assessing the potential of mineral admixtures to prevent expansive ASR can be questioned. For example, ASTM C 441 specifies tests for comparing the expansions of mortar bars containing portland cement and highly reactive Pyrex glass with mortar bars containing the same materials but with a 25 percent replacement of the cement with an amount of fly ash equal to the volume of cement replaced. Neither the C 441 test procedure nor the C 618 specification provides a comparative criterion for acceptance. Instead, C 618 lists a 0.020 percent expansion maximum at 14 days for acceptance of the test mixture. This criterion has been almost impossible to meet for fly ashes, primarily because the Pyrex glass is more highly reactive than the fly ash and therefore the fly ash can not provide any beneficial effect. This situation is the reverse of that encountered with commercially used aggregate. ASTM C 618 also provides a supplementary optional requirement on "available" alkalies determined in accordance with

C 311. Exactly how this relates to field performances is not clear. Furthermore, guidance for determining the amount of fly ash required to prevent deleterious ASR in highway concrete is somewhat uncertain in the ASTM standards.

The rapid immersion procedure appears to be a viable alternative to current specified procedures. The possibility of reliably evaluating mineral admixtures using this test method was first reported by NBRI (Davies and Oberholster 1987). They included fly ash, ground granulated blast furnace slag, and silica fume in their studies, and concluded the procedure represented a "worst case" situation indicating the maximum amount of admixture needed to suppress ASR for a given aggregate.

Several series of tests were run in this project to evaluate the potential of the rapid immersion method to identify the quantity of mineral admixture necessary to prevent deleterious ASR. Three fly ashes and one ground granulated blast furnace slag were included, the compositions of which are given in Table 3.7. Three aggregates were used with various proportions of these admixtures: AL (reactive volcanics), RQ (quartz, chert), and PR (granite gneiss). The slag admixture was used only with aggregate AL. Cement B, with an alkali content of 0.18 percent as equivalent $Na_2O$, and a 1N NaOH immersion solution, were used for all tests. In addition to these combinations, each fly ash also was evaluated at the 20 percent cement replacement level using innocuous limestone aggregate ML.

Results of these tests are given in Tables 3.8 through 3.10. Fourteen-day results for each fly ash are plotted in Figures 3.9 through 3.11. These plots indicate, with one minor exception, a progressive reduction in expansion with increase in proportion of fly ash in the mixture. This follows general expectations for fly ash use in concrete. More important is the proportion of fly ash required to meet the 0.08 percent failure criterion proposed for this procedure, using the 1N solution. The results indicate that different minimum cement replacement levels are required for the various aggregate-fly ash combinations, as would be expected. These levels are tabulated below for each fly ash-aggregate combination.

| Aggregate Source | Approximate Minimum Fly Ash* | | |
|---|---|---|---|
| | B | J | L |
| AL | 20 | 23 | >60 |
| PR | 20 | 25 | >60 |
| RQ | 15 | 18 | >60 |

* Percent replacement of cement, extrapolated from data plotted in Figures 3.9 to 3.11.

The required minimum percentages for fly ashes B and J, both of which are ASTM Class F ashes, fall in the range of 15 to 25 percent, which range is commonly used in practice. Results for fly ash L, which is an ASTM Class C ash, indicate greater than 60 percent cement replacement with no evidence that greater levels of that ash would prevent deleterious ASR. This follows expectations for fly ashes, with such high lime (27 percent) contents, low

Table 3.7 Composition of mineral admixtures used in this project

| Analyte | Percent Fly Ash B | Fly Ash J | Fly Ash L | Blast Furnace Slag |
|---|---|---|---|---|
| $SiO_2$ | 51.40 | 48.71 | 33.00 | 35.60 |
| $Al_2O_3$ | 18.50 | 19.98 | 18.90 | 9.40 |
| $Fe_2O_3$ | 16.10 | 15.26 | 5.97 | 0.80 |
| Total | 86.00 | 83.95 | 57.87 | |
| | | | | |
| CaO | 4.49 | 5.67 | 27.00 | 46.90 |
| MgO | 1.06 | 1.31 | 5.28 | 10.90 |
| S (sulfide) | 1.43 | 0.67 | 2.60 | 1.40($SO_3$) |
| Total $Na_2O$ | 0.84 | 0.73 | 1.98 | - |
| Total $K_2O$ | 2.34 | 2.53 | 0.39 | - |
| Total Equivalent as $Na_2O$ | 2.38 | 2.39 | 2.25 | - |
| Density | 2.42 | 2.45 | 2.76 | 2.96 |

Note: All analyses performed in accordance with requirements of ASTM C 618.

Table 3.8 Rapid immersion test results for mineral admixtures with aggregate AL

| Admixture Source | % Cement Replacement | Percent Expansion 1D | 7D | 14D | 28D |
|---|---|---|---|---|---|
| None | 0 | -- | .483 | .867 | 1.098 |
| Fly Ash B | 10 | .044 | .319 | .489 | .696 |
| (Class F) | 10 | .005 | -.009 | .054 | .139 |
| | 30 | .002 | -.012 | -.001 | .034 |
| Fly Ash J | 10 | .098 | .420 | .623 | .853 |
| (Class F) | 20 | .031 | .044 | .102 | .246 |
| Fly Ash L | 30 | .019 | .020 | .023 | .105 |
| (Class C) | 45 | .207 | .429 | .510 | .585 |
| | 60 | .226 | .368 | .535 | .585 |
| Blast | | | | | |
| Furnace | 40 | .001 | .075 | .172 | .342 |
| Slag | 65 | .000 | .007 | -.011 | .010 |

Note: All results are the average of four companion mortar bars.

Table 3.9 Rapid immersion test results for mineral admixtures with aggregate PR

| Admixture Source | % Cement Replacement | Percent Expansion 1D | 7D | 14D | 28D |
|---|---|---|---|---|---|
| None | 0 | - | .189 | .309 | .422 |
| Fly Ash B | 10 | .018 | .099 | .231 | .346 |
| (Class F) | 20 | .007 | .003 | .064 | .114 |
| | 30 | .004 | -.018 | .008 | .031 |
| Fly Ash J | 10 | .046 | .178 | .247 | .480 |
| (Class F) | 20 | .031 | .054 | .111 | .210 |
| | 30 | .024 | .024 | .040 | .087 |
| Fly Ash L | 30 | .029 | .119 | .231 | .357 |
| (Class C) | 45 | .041 | .108 | .178 | .249 |
| | 60 | .044 | .106 | .170 | .215 |

Note: All results are the average of four companion mortar bars.

Table 3.10 Rapid immersion test results for mineral admixtures with aggregate RQ

| Admixture Source | % Cement Replacement | Percent Expansion 1D | 7D | 14D | 28D |
|---|---|---|---|---|---|
| None | 0 | - | .212 | .409 | .574 |
| Fly Ash B | 10 | .023 | .067 | .146 | .235 |
| (Class F) | 20 | .008 | -.005 | .000 | .022 |
| | 30 | .004 | -.009 | -.006 | .013 |
| Fly Ash J | 10 | .041 | .131 | .232 | .425 |
| (Class F) | 20 | .027 | .021 | .028 | .050 |
| | 30 | .019 | .011 | .014 | .032 |
| Fly Ash L | 30 | .060 | .194 | .310 | .410 |
| (Class C) | 45 | .052 | .154 | .230 | .294 |
| | 60 | .040 | .090 | .125 | .150 |

Note: All results are the average of four companion mortar bars.

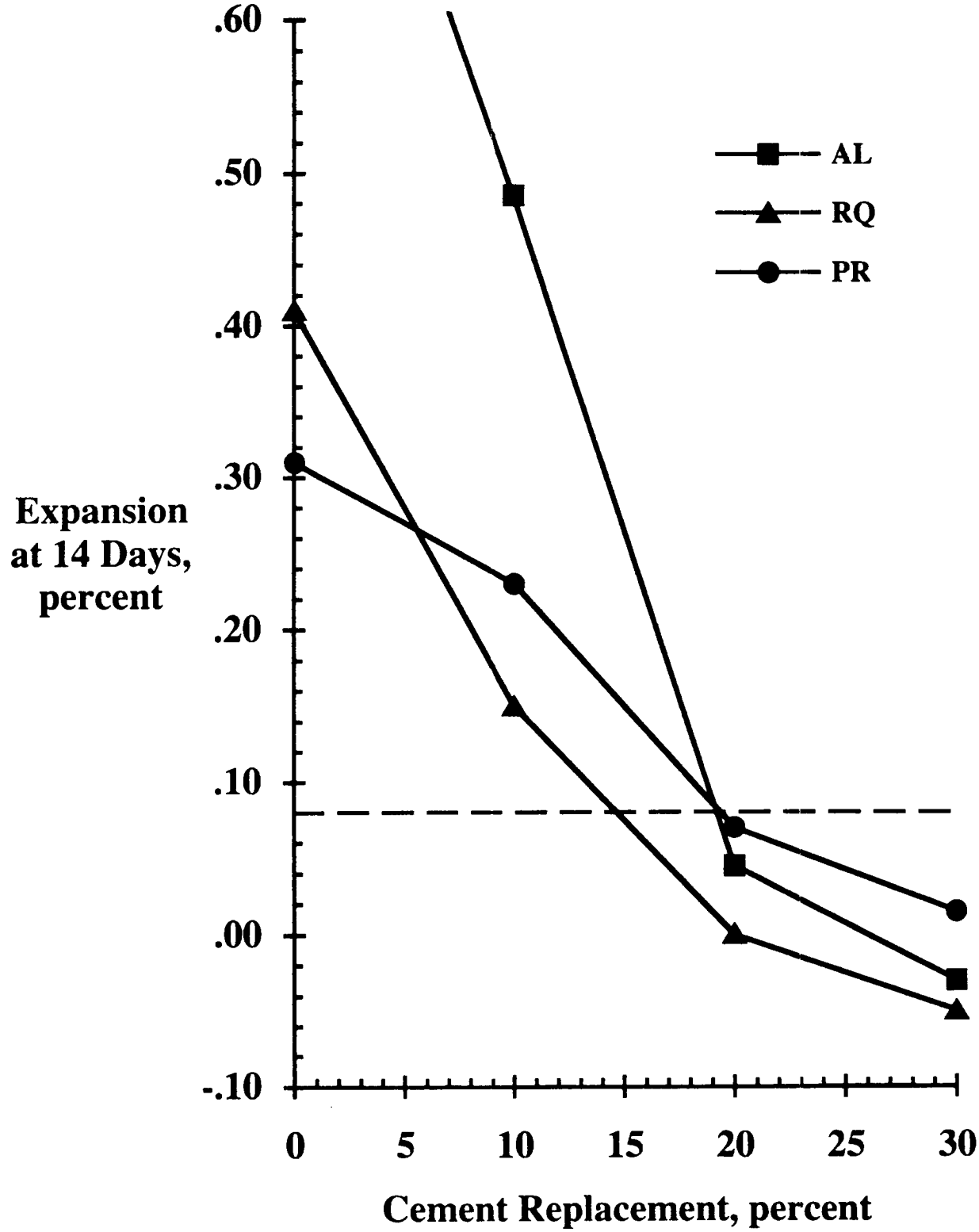


Figure 3.9 14-day rapid immersion test results for Fly Ash B used with different reactive aggregates.

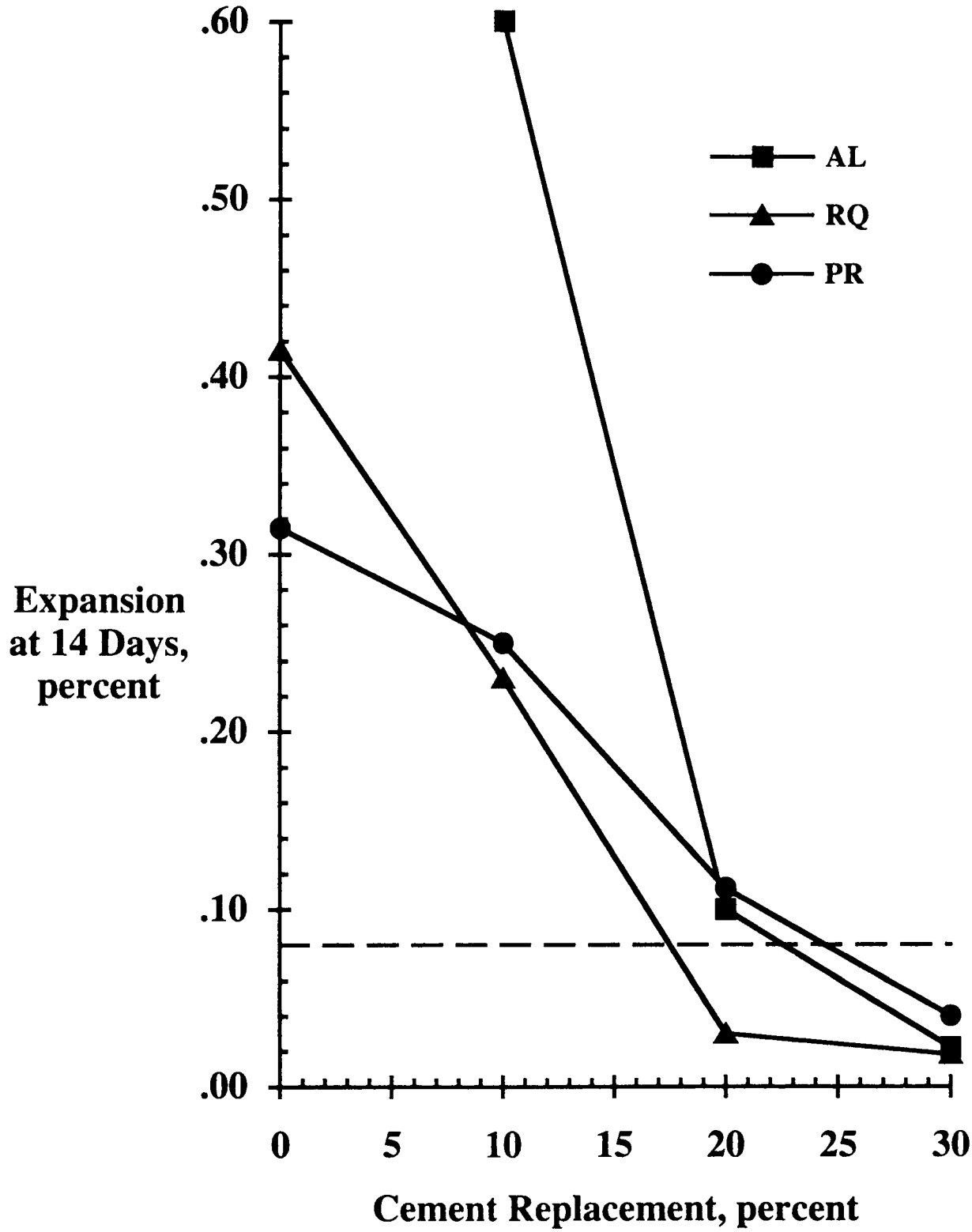


Figure 3.10 14-day rapid immersion test results for Fly Ash J used with different reactive aggregates.

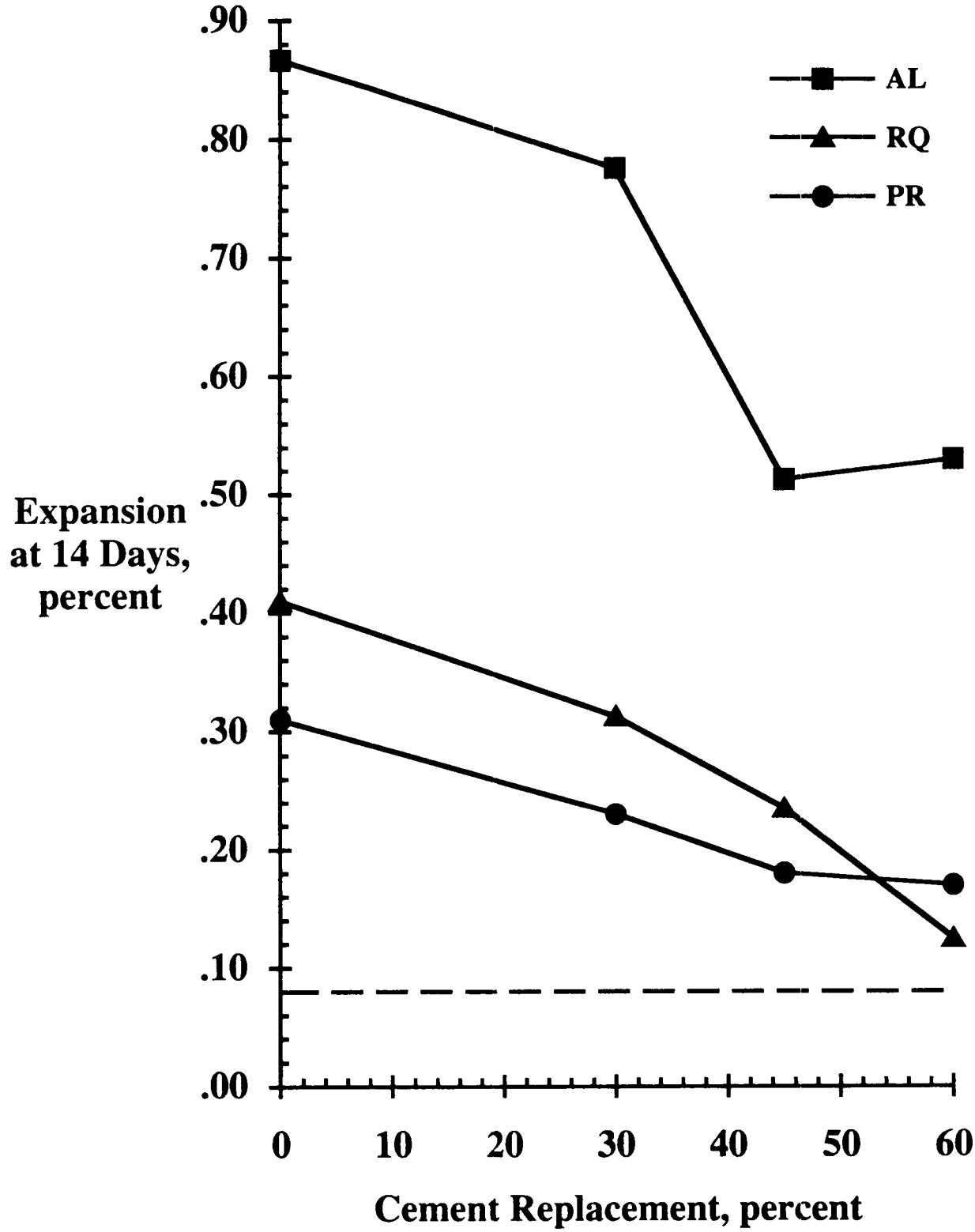


Figure 3.11 14-day rapid immersion test results for Fly Ash L used with different reactive aggregates.

(58 percent) $SiO_2$ + $Al_2O_3$ + $Fe_2O_3$ contents, and relatively high total equivalent $Na_2O$ levels. The results thus obtained appear to support those obtained at NBRI and also suggest the procedure can identify minimum cement replacement levels required to prevent deleterious ASR. In addition, it would appear that required cement replacement levels could be determined for lower cement alkali levels using this test procedure. Further work is needed in this determination.

Table 3.8 also presents results for the ground granulated blast-furnace slag used in mortar bars made with highly reactive aggregate AL. Fourteen-day data for the 40 percent and 65 percent.

In summary, the rapid immersion procedure appears to show promise as a means of rapidly identifying mineral admixture requirements for preventing deleterious ASR in highway structures. Both the source of aggregate and proportion of mineral admixture, probably together with different cement alkali levels, can be identified. Major advantages of this approach are the rapidity with which results are obtained and determination of the required parameters with the use of a single test method. Procedural examples are given in Appendix A.

## 3.4 Testing of Concrete Prisms

All rapid immersion test results reported thus far have been obtained on 1 x 1 x 11 1/4-in. (25 x 25 x 286 mm) mortar bars made with a fixed water-cement ratio of 0.50 and washed aggregates processed in accordance with ASTM C 227. More realistic test specimens would be larger prisms that could accommodate aggregate gradations and concrete mixture proportions actually used in highway construction. This, however, might introduce more uncertainties into test results because, in the test, expansion due to ASR depends on diffusion of NaOH immersion solution through the cross section of the test specimen. Larger prisms, for example, 3 x 3 x 11 1/4-in. (76 x 76 x 286 mm), probably would reduce the uniformity with which the test solution diffuses into the specimen, and the much coarser aggregate gradings undoubtedly would reduce expansions within the prescribed 14-day test period because of reduced surface area to volume ratios of potentially reactive aggregate particles. Also, different cement factors and water-cement ratios would affect diffusion rates of immersion solution into the concrete prism.

To determine whether meaningful results can be obtained, two series of tests were run on 3 x 3 x 11 1/4-in. (76 x 76 x 286 mm) prisms made with concrete mixture proportions approximating those used in highway construction. Both deleterious and innocuous aggregates were evaluated using Cement B with an alkali content of 0.18 percent equivalent $Na_2O$. A fixed water-cement ratio of 0.50, which is used in the mortar bar tests, was used for the concrete mixtures. The following proportions and aggregate gradings were used:

| | | |
|---|---|---|
| Coarse aggregate SSD | 1866 lb/yd$^3$ | (1107 kg/m$^3$) |
| Fine aggregate SSD | 1260 lb/yd$^3$ | (748 kg/m$^3$) |
| Cement | 564 lb/yd$^3$ | (335 kg/m$^3$) |
| Net water | 282 lb/yd$^3$ | (167 kg/m$^3$) |

| | | | |
|---|---|---|---|
| Coarse aggregate | 1 in. to 3/4 in. (25.0 mm to 19.0 mm) | 342 lb/yd$^3$ | (203 kg/m$^3$) |
| | 3/4 in. to 3/8 in. (19.0 mm to 9.5 mm) | 1140 lb/yd$^3$ | (676 kg/m$^3$) |
| | 3/8 in. to No. 4 (9.5 mm to 4.75 mm) | 384 lb/yd$^3$ | (228 kg/m$^3$) |
| Fine aggregate | ASTM C 227 grading | | |

In one series, ten deleterious and four innocuous coarse aggregates were combined with an innocuous dolomite fine aggregate from source TH in individual sets of three companion concrete prisms in the proportions listed above. After curing in the molds for one day at 73 $\pm$ 2°F (23 $\pm$ 1°C), comparator readings were taken and the prisms then immersed in 1N NaOH solution and brought to 176°F (80°C). Readings also were taken the following day, which served as the initial reading. The prisms were then returned to the solution for storage and periodic readings to a test age of 42 days.

In the first series, only the 1N NaOH immersion solution was used. Three additional mixtures were made using coarse and fine aggregate AL in concrete prisms, which then were stored in 1.0N, 0.70N, and 0.35N NaOH solution under the same test conditions. These conditions were intended to simulate 0.50 water-cement ratio concrete with cement alkali levels of approximately 1.40 percent, 1.00 percent, and 0.50 percent. In the second series of tests on concrete prisms, NaOH was introduced into the mixing water in proportion to that corresponding to 1.0N, 0.70N, or 0.35N NaOH solutions. Three deleterious coarse aggregates, AL, GH, and PR, and one innocuous aggregate, ML, were included in this series. After removal from the molds at one day, comparator readings were taken and the prisms then immersed in NaOH solution concentrations corresponding to that in the mixing water. Readings were made at one day, which served as the reference, then at 7, 14, 28, and 42 days.

Results for these two series of tests are summarized in Tables 3.11 and 3.12. Data in Table 3.11 show no consistent clear distinction in expansions, up to 42 days, for innocuous and deleterious aggregates. The maximum expansion reached for innocuous aggregates was 0.026 percent while minimum expansions for deleterious aggregates ranged down to 0.010 percent. Of the ten deleterious coarse aggregates tested, 42-day expansions fell below the greatest expansion for the innocuous aggregates. Only one coarse aggregate, RH, which is a granite gneiss, clearly expanded more than the innocuous aggregates. The very low 42-day expansion for source GH was surprising since, in mortar bar tests, it developed relatively high expansions. Overall, these results indicate the test procedure used did not reliably identify potentially deleterious or innocuous coarse aggregates.

Table 3.11 also presents results for concrete prisms containing both fine and coarse aggregate from source AL and immersed in NaOH solutions of 1.0N, 0.70N, or 0.35N concentration. Data for these prisms indicate progressively less expansion at 42 days as NaOH concentration is reduced. In this case, there is little difference in results for the 1.00N and 0.70N concentrations as expansions reached 0.21 to 0.24 percent at 42 days. However, when NaOH concentration was decreased to 0.35N, there was a major reduction in expansion -- to 0.036 percent. Extrapolating these results to cement alkali level, this larger reduction occurred at a corresponding cement alkali level of 0.50 percent. However, expansion at this

Table 3.11 Expansions of concrete prisms in the rapid immersion test method

| Coarse Aggregate | Composition | NaOH Test Solution | Percent Expansion 7D | 14D | 28D | 42D |
|---|---|---|---|---|---|---|
| | | **Innocuous Aggregate** | | | | |
| ML | Limestone | 1.0N | .004 | .010 | .018 | .024 |
| EL | Carbonate and Siliceous sand and gravel | 1.0N | .003 | .009 | .012 | .019 |
| TR | Gabbro | 1.0N | .006 | .010 | .012 | .018 |
| TH | Dolomite | 1.0N | .005 | .009 | .007 | .026 |
| | | **Deleterious Aggregates** | | | | |
| GH | Argillite | 1.0N | .007 | .007 | .005 | .010 |
| RH | Granite Gneiss | 1.0N | .011 | .018 | .025 | .044 |
| GR | Metabasalt | 1.0N | .009 | .013 | .017 | .031 |
| SF | Granite Gneiss | 1.0N | .005 | .013 | .020 | .031 |
| TM | Chert, Quartzite | 1.0N | .007 | .010 | .015 | .020 |
| OR | Mixed sand and gravel | 1.0N | .013 | .015 | .015 | .028 |
| SX | Quartzite | 1.0N | .007 | .012 | .012 | .024 |
| WR | Metasilicates, Quartzite | 1.0N | .010 | .013 | .012 | .020 |
| BK | Quartz, Quartzite | 1.0N | .012 | .017 | .020 | .031 |
| AL | Mixed Siliceous coarse | 1.0N | .005 | .010 | .017 | .027 |
| AL | Mixed Siliceous coarse and fine | 1.0N | .037 | .098 | .181 | .235 |
| AL | Mixed Siliceous coarse and fine | .70N | .021 | .087 | .157 | .208 |
| AL | Mixed Siliceous coarse and fine | .35N | .006 | .011 | .019 | .036 |

Notes: 1. All results are the averages for three companion prisms.
2. Innocuous fine aggregate, TH, was used in all mixtures except as noted.
3. D = days.

reduced cement alkali level still exceeds the maximum for the innocuous aggregate, and aggregate from this source is known to have performed deleteriously in highway structures when used with cements in the alkali range of 0.50 to 0.55 percent. Thus, in this respect, field performance correlated with relative expansion level in the test.

In view of the relatively low expansions for some concrete prisms containing deleterious aggregate, it was felt these inconsistencies might be related to reduced diffusion of the NaOH immersion solution into the concrete prisms because of the larger cross section of the prism compared with the mortar bar. To investigate this possibility, several concrete prisms containing deleterious aggregate were broken open and examined by UV light after treatment with uranyl acetate solution. These examinations revealed the presence of ASR gel in the outer 3/4 to 1 in. (19 to 25 mm) of the 3 x 3 in. (76 x 76 m) cross section, with virtually no gel present in the central 1 in.$^2$ (645 mm$^2$) cross section. Thus it indeed appeared that the NaOH solution did not penetrate the full cross section of these prisms, thereby possibly contributing to the inconsistency of the results.

The second series of concrete prisms was tested in which NaOH solution was added to the mixing water prior to batching to minimize this problem. Results for this series, presented in Table 3.12 and Figure 3.12, reveal generally greater expansions than those produced for prisms in which no NaOH was added to the mixing water. This appears to support the observation that reduced diffusion of NaOH into the prisms when alkali is not added to the mixing water is a factor in limiting expansions in the test. The results do indicate, as expected, generally progressively less expansion as NaOH concentration is decreased. However, the level of expansion for deleterious coarse aggregate GH was less than those for innocuous aggregate ML at the 1.0N and 0.70N concentrations. This is a major inconsistency since GH (argillite) is one of the more highly reactive aggregates in this investigation.

Review of all results for concrete prisms indicates lack of consistency in properly identifying deleterious and innocuous coarse aggregates. This occurs regardless of whether NaOH is added to the mixing water. Considering the desirability of using concrete prisms for this test, further work may be warranted but is beyond the scope of this project.

## 3.5 Effect of Steam Curing on Expansion Due to ASR

Steam curing is a procedure routinely used across the United States to produce precast concrete components for highway structures. Probably the most widespread use of such concrete is for bridge girders. Even though these bridge members commonly contain aggregates from sources associated with deleterious ASR in pavement concrete, reports of suspected ASR are seldom received. This may be due to the uniformly drier exposure conditions of the covered, elevated beams or girders in the bridge, to some intrinsic property of steam-cured concrete that tends to mitigate expansive ASR, or to lack of familiarity by inspection teams of manifestations of ASR-induced distress.

Cast-in-place mass concrete, such as that in large abutments and piers, also can experience temperatures in the range used in steam-curing. Thus, the same uncertainty with regard to ASR applies to these types of highway construction as well.

To help clarify this situation, several series of mortar bars were fabricated in which two potentially reactive aggregates, AL (volcanics), and PR (granite gneiss), and one innocuous

Table 3.12 Expansions of concrete prisms with NaOH added to the mix water

| Coarse Aggregate | Composition | NaOH Test Solution | Percent Expansion 7D | 14D | 28D | 42D |
|---|---|---|---|---|---|---|
| | | **Innocuous Aggregate** | | | | |
| ML | Limestone | 1.0N | .008 | .010 | .030 | .049 |
| | | .70N | .000 | .002 | .013 | .038 |
| | | .35N | .000 | .001 | .003 | .010 |
| | | **Deleterious Aggregates** | | | | |
| PR | Granite Gineiss | 1.0N | .025 | .029 | .053 | .071 |
| | | .70N | .013 | .016 | .032 | .051 |
| | | .35N | .005 | .006 | .022 | .032 |
| AL | Sil. (Volcanic) | 1.0N | .029 | .041 | .065 | .098 |
| | | .70N | .019 | .020 | .042 | .060 |
| | | .25N | .000 | .001 | .010 | .011 |
| GH | Argillite | 1.0N | .014 | .006 | .015 | .028 |
| | | .70N | -.005 | .002 | .017 | .022 |
| | | .35N | .000 | .001 | .007 | .022 |

Notes: 1. All results are the averages for three companion prisms.
2. Innocuous fine aggregate, TH, was used in all mixtures.

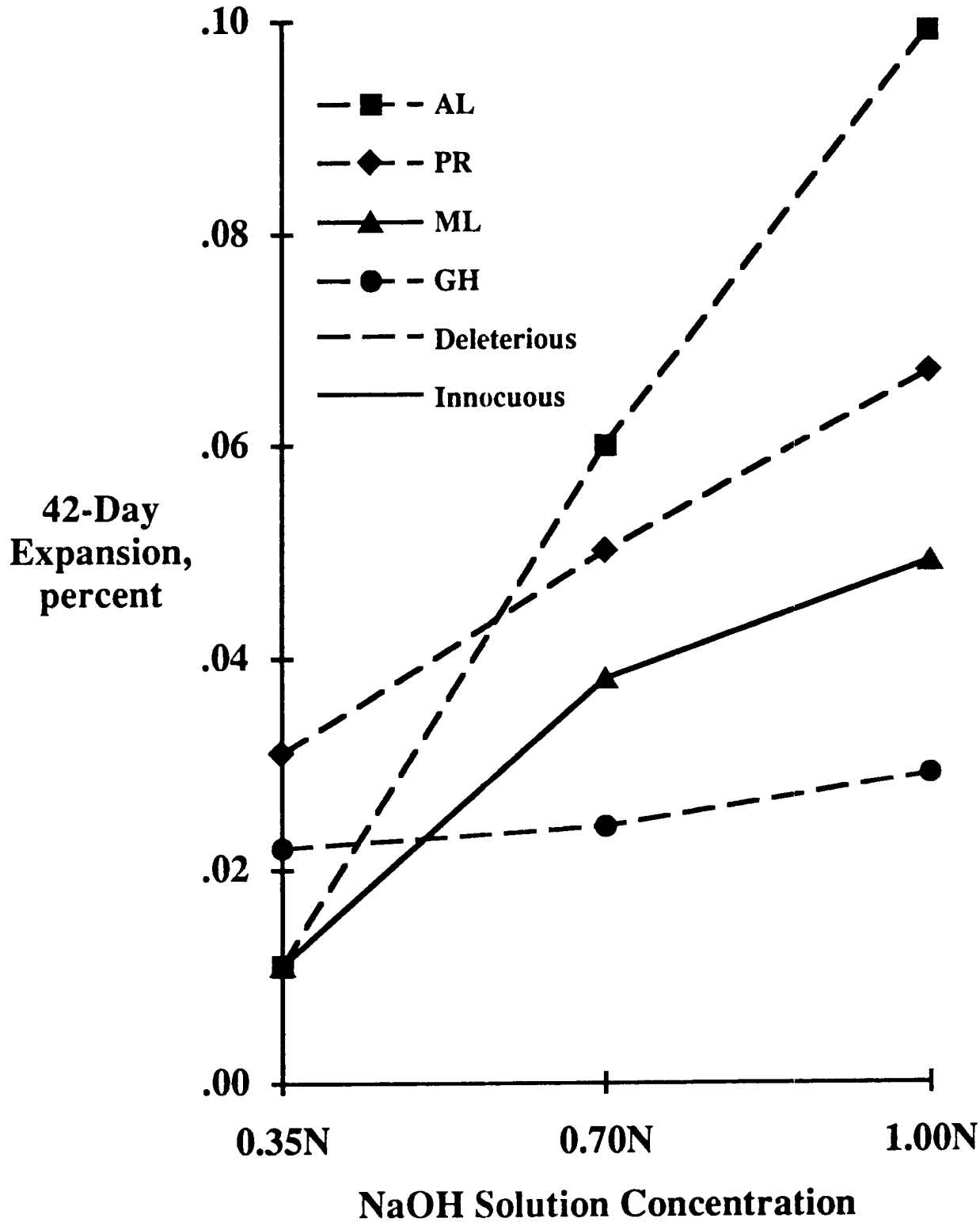


Figure 3.12 Forty-two day results for rapid immersion method for concrete prisms containing mix water with added NaOH.

aggregate, ML (limestone), were used with portland cements A and C (Table 3.2), with 1.00 percent or 0.50 percent equivalent $Na_2O$, in mortar bars proportioned in accordance with C 227. The following three curing regimes were used in this investigation:

Regime A - 1. Remain in molds for 24 hours in a moist room at 73±2°F (23±1°C).
2. Remove from the molds at 24 hours, take comparator reading, and transfer to storage over water in sealed containers held at 100±2°F (38±1°C).

Regime B - 1. Remain in molds for 3-1/2 hours at 73±2°F (23±1°C).
2. Transfer to steam curing and heat to specimen temperature of 140±2°F (60±1°C) at rate of 28°F (15°C) per hour.
3. Hold at 140±2°F (60±1°C) for 10 hrs.
4. Turn off heat and allow to cool overnight to 73±2°F (23±1°C).
5. Take comparator reading and transfer to storage over water in sealed containers held at 100±2°F (38±1°C).

Regime C - 1. Remain in molds for 3-1/2 hours at 73±2°F (23±1°C).
2. Transfer to steam curing and heat to specimen temperature of 180±2°F (82±1°C) at rate of 28°F (15.6°C) per hour.
3. Hold at 180±2°F (82±1°C) for 10 hrs.
4. Turn off heat and allow to cool overnight to 73±2°F (23±1°C).
5. Take comparator reading and transfer to storage over water in sealed containers held at 100±2°F (38±1°C) .

Comparator readings were then made periodically over a test period of 12 months.

Results of these tests are summarized in Table 3.13. Data for deleterious aggregates AL and PR are plotted in Figure 3.13. Results for innocuous limestone aggregate ML are not plotted, but expansions for specimens made with 0.50 percent or 1.00 percent cement alkali levels were in the ranges of 0.008 percent to 0.011 percent and 0.022 percent to 0.028 percent, respectively.

For deleterious aggregate AL (volcanics), expansions at all temperatures were much greater where cement with 1.00 percent alkali was used than where the 0.50 percent alkali cement was used, as might have been expected. More significant is the fact that expansions increased progressively with increase in first-day curing temperature, particularly between 140°F (60°C) and 180°F (82°C). Smaller increases developed over the temperature range of 73°F (23°C) to 140°F (60°C), with the greater increase in this range developing with the 0.50 percent cement alkali level.

Results for slowly reacting aggregate PR (granite gneiss) show greater expansions for the higher cement alkali level at all first-day curing temperatures compared with results for the low-alkali cement, again as would be expected. Also, expansions increased progressively with increase in first-day curing temperature for specimens made with the 0.50 percent alkali cement, although the expansion level reached was only 0.028 percent at 12 months. For the high alkali cement, the greater expansion (0.074 percent) developed for specimens cured at 140°F (60°C) while the lowest expansion (0.055 percent) developed for the 180°F (82°C) cure. Overall, results for aggregate PR indicate no well-defined trends in expansion for first-day curing temperature. This is not surprising since this aggregate earlier produced only small expansions under C 227 test conditions.

Table 3.13 Effect of steam curing on expansion due to ASR

| Aggregate Source | Cement Alkali, Percent | Curing Temp. °F | Percent Expansion 1M | 2M | 3M | 6M. | 9M | 12M |
|---|---|---|---|---|---|---|---|---|
| ML | 0.50 | 73 | .004 | .003 | .003 | .013 | .008 | .008 |
| (Limestone) | | 140 | .004 | .003 | .004 | .012 | .009 | .008 |
| | | 180 | .011 | .011 | .011 | .029 | .015 | .011 |
| | 1.00 | 73 | .008 | .011 | .011 | .023 | .019 | .028 |
| | | 140 | .013 | .016 | .016 | .031 | .025 | .025 |
| | | 180 | .012 | .013 | .015 | .027 | .022 | .022 |
| AL | 0.50 | 73 | .005 | .005 | .011 | .053 | .218 | .273 |
| (Mixed Siliceous) | | 140 | .011 | .014 | .026 | .194 | .346 | .413 |
| | | 180 | .016 | .040 | .076 | .291 | .434 | .559 |
| | 1.00 | 73 | .090 | .257 | .340 | .518 | .696 | .763 |
| | | 140 | .180 | .324 | .387 | .565 | .701 | .795 |
| | | 180 | .125 | .329 | .446 | .681 | .747 | .990 |
| PR | 0.50 | 73 | .002 | .003 | .004 | .012 | .009 | .010 |
| (Granite Gneiss) | | 140 | .010 | .011 | .012 | .026 | .021 | .021 |
| | | 180 | .009 | .010 | .014 | .029 | .026 | .028 |
| | 1.00 | 73 | .013 | .022 | .027 | .054 | .058 | .062 |
| | | 140 | .018 | .027 | .038 | .068 | .067 | .074 |
| | | 180 | .015 | .020 | .029 | .047 | .048 | .055 |

Notes: 1. All results are the average of three or four companion specimens.
2. Six months' results for ML and PR include what appears to be a small systematic error.
3. 73°F ≈ 23°C, 140°F ≈ 60°C, and 180°F ≈ 82°C.
4. M = month(s).

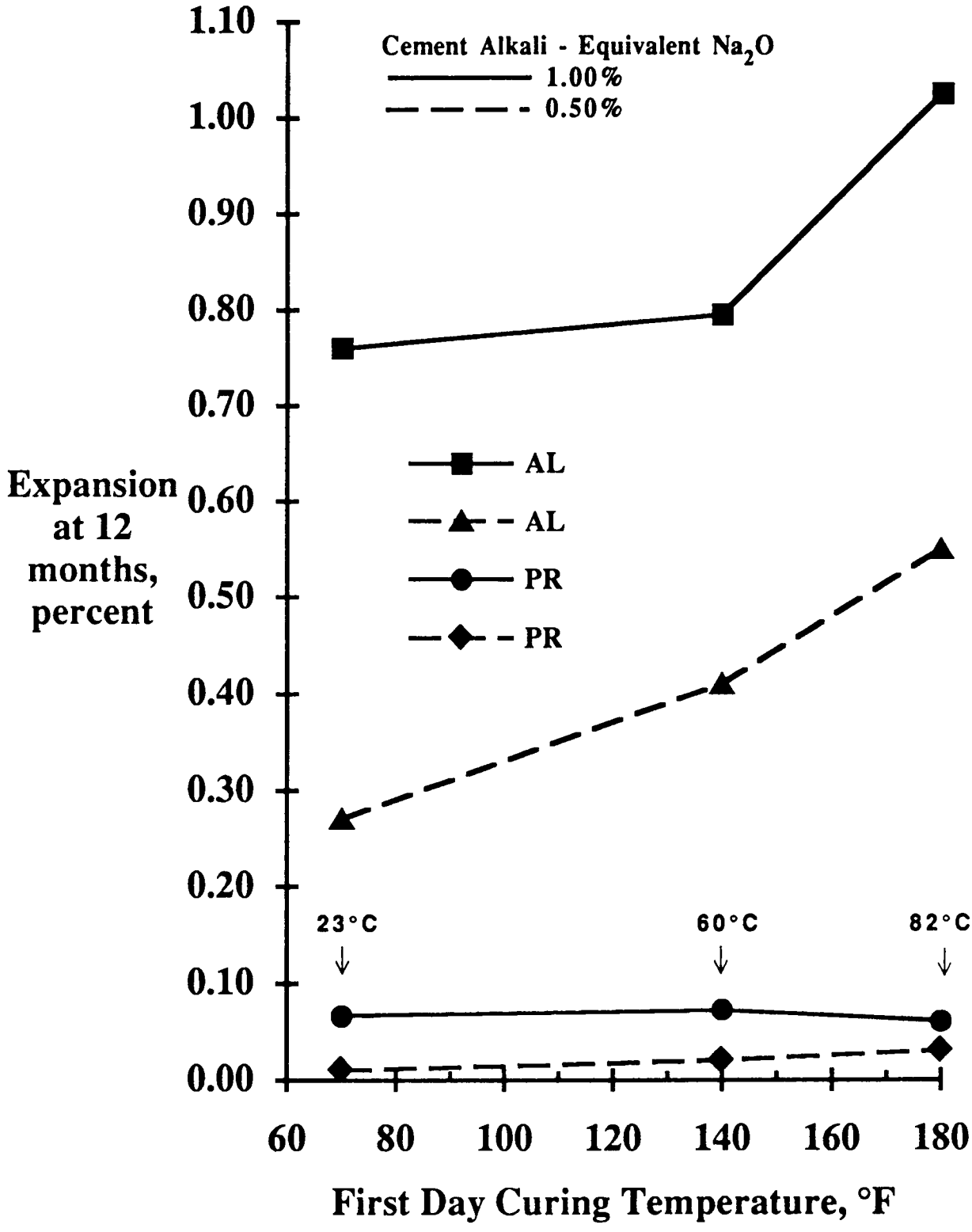


Figure 3.13 Effect of first day curing temperature on expansion due to ASR.

From this limited investigation, it is concluded that this concrete, steam-cured at elevated temperatures, was more vulnerable to expansion due to ASR than concrete maintained at near ambient conditions regardless of cement alkali level and that, in general, the higher the first-day steam curing temperature the greater the potential for expansion. Thus, more rigid precautions to avoid expansive ASR in steam-cured concrete appear to be necessary than for concrete in which curing temperatures are maintained at near-ambient conditions. These more rigid precautions also should be considered for cast-in-place mass concrete in which temperatures may reach, for example, more than 140°F (60°C).

## 3.6 Conclusions

From work in this project, it is concluded that ASTM standards C 227 and C 289, which are heavily relied on to properly classify deleterious and innocuous aggregates, fail particularly to identify slowly reacting aggregates that cause abnormal expansion in highway structures. Review of published literature has indicated that a rapid immersion test developed at NBRI in South Africa showed the greatest promise of identifying aggregates as deleterious or innocuous with respect to ASR. In this procedure, mortar bars containing the test aggregate are immersed in 1N NaOH solution with expansions calculated at 14 days. Numerous series of tests were run in this project to further evaluate this general procedure and, with certain modifications, extend it to predict safe cement alkali levels and identify the capability of mineral admixtures to prevent deleterious ASR.

From results of these tests, the following conclusions were drawn.

1) The rapid immersion test properly classifies innocuous and potentially deleterious aggregates, including slowly reactive aggregates, when the failure criterion is set at 0.08 percent expansion at 14 days.

2) The rapid immersion test also is capable of estimating maximum cement alkali levels that can be tolerated with little or no risk of deleterious ASR. This is done by using a linear regression equation that relates immersion solution normality to cement alkali level for given water-cement ratios, then adjusting the solution to the appropriate NaOH normality.

3) When determining the safe cement alkali level, the test criterion must be adjusted progressively downward to a minimum of about 0.02 percent as solution normality decreases to about 0.60N.

4) Mineral admixture requirements to prevent abnormal expansion due to ASR can be determined by the rapid immersion method, using 1N NaOH immersion solution and the 14-day test criterion of 0.08 percent expansion. Although not researched, it appears the requirement could be determined for different cement alkali levels by appropriately adjusting immersion solution normality.

5) Testing indicated that concrete prisms containing aggregate gradings in the range used in highway structures are not suitable replacements for smaller cross section mortar bars in the rapid immersion test. This appears to be due primarily to non-uniform diffusion of NaOH solution into the concrete prism and comparatively low surface area to volume ratios of potentially reactive aggregate particles. Further work is needed in this area of research.

6) For a given aggregate, steaming curing tends to exacerbate expansive ASR, particularly in the steam curing temperature range of 140°F (60°C) to 180°F (82°C).

# 4.0 Effects of Lithium Salts on ASR

The three traditional methods used to avoid expansive ASR have had varying degrees of long-term success. Reducing cement alkali levels to less than 0.60 percent often has been found only to delay development of deleterious expansion. Mineral admixtures, such as fly ash, have been successful in many cases but, in others, appear to have exacerbated ASR. Finally, innocuous aggregates may not be locally available to avoid deleterious ASR.

A fourth alternative is the introduction of lithium salts into portland-cement mortars to prevent deleterious ASR. This was first revealed in published results (McCoy and Caldwell 1951) for mortar bars made with high alkali cement and highly reactive Pyrex glass aggregate in which small dosages of $Li_2CO_3$, LiF, or LiCl, as admixtures, prevented abnormal expansions due to ASR. It was clearly evident from these tests that the lithium ion, per se, was the component preventing abnormal expansion due to ASR.

Considering their potential to prevent abnormal expansion, the feasibility of using lithium salts to mitigate deleterious ASR in both new and existing highway concrete was investigated in this project. Chemical interactions with components of the cement-aggregate system were investigated, and tests were run on series of mortar bars containing reactive aggregate. Treatment of expanded laboratory test specimens with lithium solutions also was investigated. Knowledge developed in the laboratory studies was applied to new and existing concrete in highway structures. Results of this work are presented below.

## 4.1 Reaction Chemistry

As indicated previously, the possibility of using lithium salts to prevent future ASR damage in new concrete has been known for more than 40 years. This section summarizes the results of extensive research carried out to determine the reaction chemistry involved in such mitigation or prevention of future damage.

### *4.1.1. Conversion of Lithium Salts to Lithium Hydroxide in Concrete*

In laboratory experiments lithium salts usually have been added as part of the mixing water at dosages on the order of 1 percent by mass of cement. For these salts, this amount was required at reasonable water-cement ratios. One of the first problems was to understand the effectiveness of these lithium salts when added in excess of what could be dissolved.

The salts investigated were lithium fluoride (LiF) and lithium carbonate ($Li_2CO_3$), both of which had been found effective at 1 percent dosages in early laboratory studies by McCoy and Caldwell.

For concrete with a water-cement ratio of 0.48, a dosage of $Li_2CO_3$ equal to 1 percent by weight of cement, if completely dissolved in the mix water, would yield a mix solution of 0.56N in both $Li^+$ and $CO_3^{2-}$ ions. The corresponding ion concentration for a 1 percent treatment using LiF is 0.80N.

Data provided in the *Handbook of Chemistry and Physics* (1987-88) suggested that the saturation concentration of $Li_2CO_3$ at room temperature should be 0.41N; that is, 73 percent of the specified dose should be dissolved, leaving 27 percent undissolved. The corresponding value for LiF is only 0.10N; in this case only 13 percent should be dissolved, leaving 87 percent undissolved.

Actual tests indicated that these values were overly optimistic. Trials were carried out to see how much of each salt could actually be dissolved in deionized water. It was found that the concentration actually brought into solution after prolonged, continuous, rapid stirring for 14 hours was only 50 percent (instead of 73 percent) of the projected $Li_2CO_3$ dose. Only 4 percent (instead of 13 percent) of the projected LiF dose could be dissolved. Presumably, the amount dissolved would be even less in a concrete mixer.

It is well understood that the mixing water in fresh concrete is highly alkaline; $OH^-$ ion concentrations approaching 0.5N and pH values often exceeding 13 are rapidly generated. Accordingly, whether significantly more of the lithium salt could be dissolved in water brought to higher $OH^-$ ion concentrations was investigated. Alkaline mixing waters with $OH^-$ ion concentrations of 0.2N, 0.4N, 0.6N, 0.8N, and 1N were prepared by prior dissolution of the appropriate amounts of potassium hydroxide, and dissolution of $Li_2CO_3$ and LiF was checked. Again, continuous rapid stirring for 14 hours was employed.

Results for $Li_2CO_3$ indicated a small progressive increase in the percentage dissolved with increasing alkalinity of the mixing water. Increasing its $OH^-$ ion concentration to 1N increased the percentage of $Li_2CO_3$ dissolved from 50 percent of the dose to 67 percent of the dose, with proportional increases for intermediate $OH^-$ ion concentrations. The effect on LiF dissolution was similar, but the percentage dissolved increased only from 4 percent to 6 percent with the highest $OH^-$ ion concentration.

Accordingly, it is evident that at the dosages contemplated for concrete, much of the lithium salt would remain undissolved even in highly alkaline mixing water. If as much as 94 percent of the added LiF remains undissolved in the concrete mixing water, and the LiF treatment still works, the dissolved part of the LiF must be extraordinarily effective. Alternatively, another phenomenon must occur to produce the observed effectiveness in concrete in spite of the insolubility of the salt. Further studies were therefore carried out to determine on what the chemistry of the response was based.

Portland cement pastes were prepared at a water-cement ratio 0.48 using a normal Type I cement of relatively low alkali content (0.18 percent $Na_2O$ equivalent). Pastes were prepared with 1 percent $Li_2CO_3$ and with 1 percent LiF, but with only normal mixing, as specified in ASTM C 305. Similar control pastes with no lithium treatment were also prepared. For each paste the resulting solution was separated at intervals from the solid by pressure filtration before setting, and after setting by high pressure expression using the pore solution

expression die. Sampling times ranged from 10 minutes to one week after mixing. The solutions recovered were analyzed for $Li^+$ and for the corresponding anion. For $Li_2CO_3$ pastes, the $CO_3^{2-}$ ion concentrations found were on the order of 0.05N. This amounts to about 10 percent of the added dose. For the LiF pastes, the $F^-$ ion concentration was effectively zero. Thus only little carbonate and no fluoride at all was dissolved in the solutions separated from pastes made with the corresponding lithium salts.

However, substantial and increasing concentrations of lithium ion were recorded in the solutions of both kinds of paste. The concentrations of $Li^+$ ion in the two systems are given in Figure 4.1 as functions of time. While the earliest concentrations (10 minutes) are somewhat different, the patterns of change with time are almost identical. $Li^+$ ion concentrations in both systems increase to about 0.42N by 10 hours, then reduce to a steady state of about 0.37N thereafter. Thus the added lithium is finding its way into both kinds of pore solution in substantial amounts, and neither anion ($CO_3^{2-}$ or $F^-$) is accompanying the $Li^+$ to an appreciable extent. The fluoride ion from LiF treatment was completely absent from the solution and the $CO_3^{2-}$ ions from $Li_2CO_3$ was almost completely absent.

The corresponding $OH^-$ ion concentrations for the two lithium-treated paste pore solutions, and for the control paste without treatment are plotted in Figure 4.2. The $OH^-$ ion concentration of the control paste of this relatively low alkali cement reaches a steady state value of about 0. 38N. In contrast, for the $Li_2CO_3$ and LiF treated pastes, the $OH^-$ ion concentration is much enhanced, reaching about 0.60N and 0.70N, respectively. It is evident that lithium in the pore solution is not present as dissolved lithium carbonate or dissolved lithium fluoride, but rather as what would be considered dissolved lithium hydroxide.

The mechanism suggested for the overall response is (a) dissolution of some $Li_2CO_3$ (or LiF), followed by (b) almost immediate precipitation of the $CO_3^{2-}$ or $F^-$ ions as $CaCO_3$ or $CaF_2$, followed by (c) further dissolution of additional $Li_2CO_3$ or LiF, etc. Precipitation as $CaCO_3$ (or $CaF_2$) is necessarily accompanied by the generation of an equivalent amount of $OH^-$ ion according to the following equations:

$$Li_2CO_3 + Ca(OH)_2 \rightarrow CaCO_3 + 2Li^+ + 2OH^-$$
$$2LiF + Ca(OH)_2 \rightarrow CaF_2 + 2Li^+ + 2OH^-$$

The extent to which these equations go to completion is not easy to establish. In parallel studies it was found that when LiOH is added directly to the mixing water, a substantial amount of it is taken up by CSH forming in the hydrating cement. A similar effect might be expected here with the converted LiOH. Accordingly, the amount of $Li^+$ remaining in solution in the steady state condition may be substantially less than the total LiOH generated by the above processes.

It has been found that for the case of LiF, at least, some small portion of the added LiF has not been converted to the corresponding hydroxide. Small white crystals can be recovered from the hardened cement paste, which on X-ray diffraction prove to be LiF. They are somewhat coarser than the finely ground LiF added to the mixing water, so some reprecipitation may be involved.

The conclusions drawn from these investigations are that when 1 percent treatment levels of $Li_2CO_3$ or LiF are added to the mixing water (1) the $Li_2CO_3$ added to the mixing water is either directly dissolved or dissolved as the result of spontaneous precipitation of $CaCO_3$ when cement is added; (2) that only a little of the LiF added in the mixing water is directly dissolved, and that most of the remainder is indirectly dissolved as a result of spontaneous

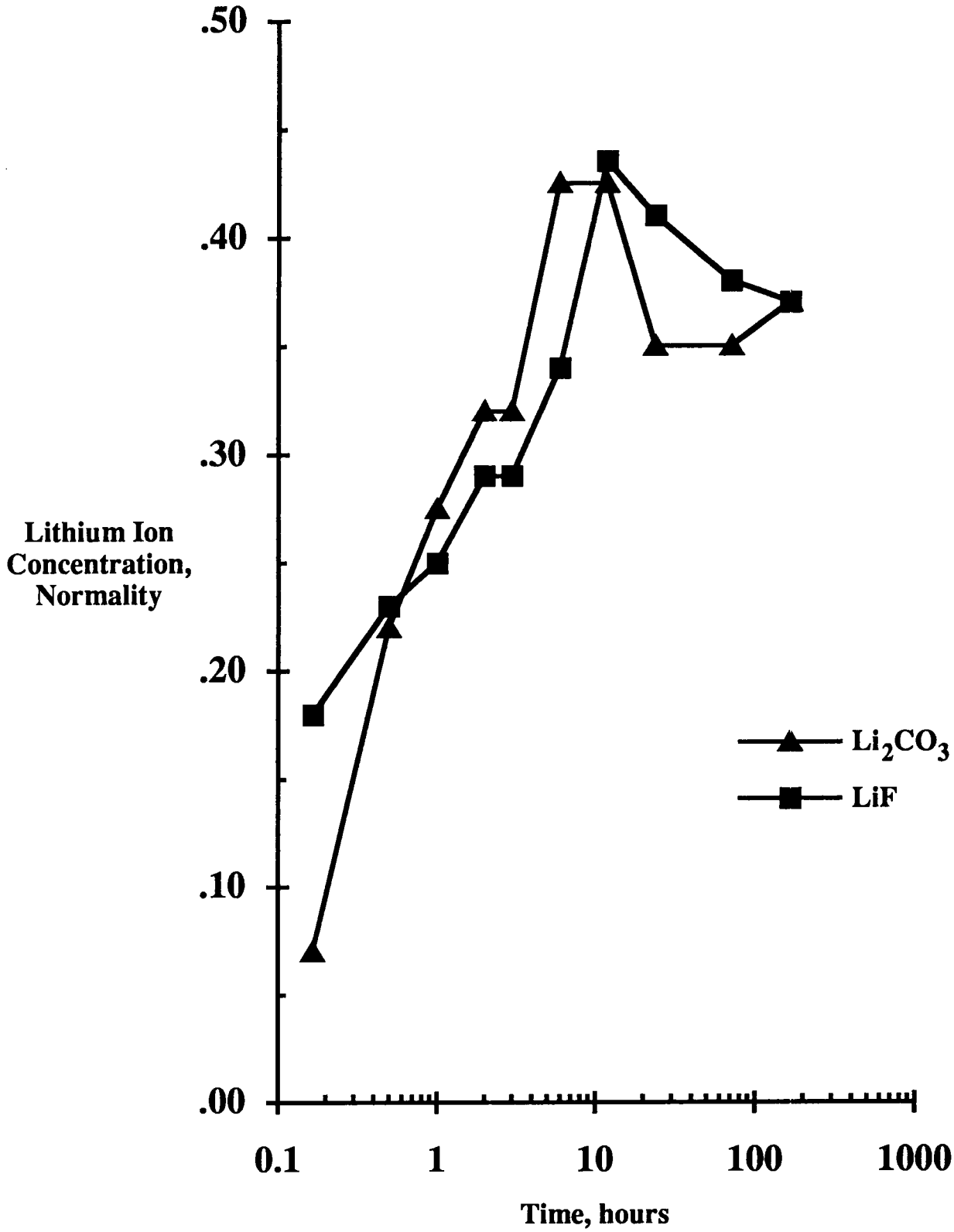


Figure 4.1. Li ion concentrations found in cement paste pore solutions as a function of time.

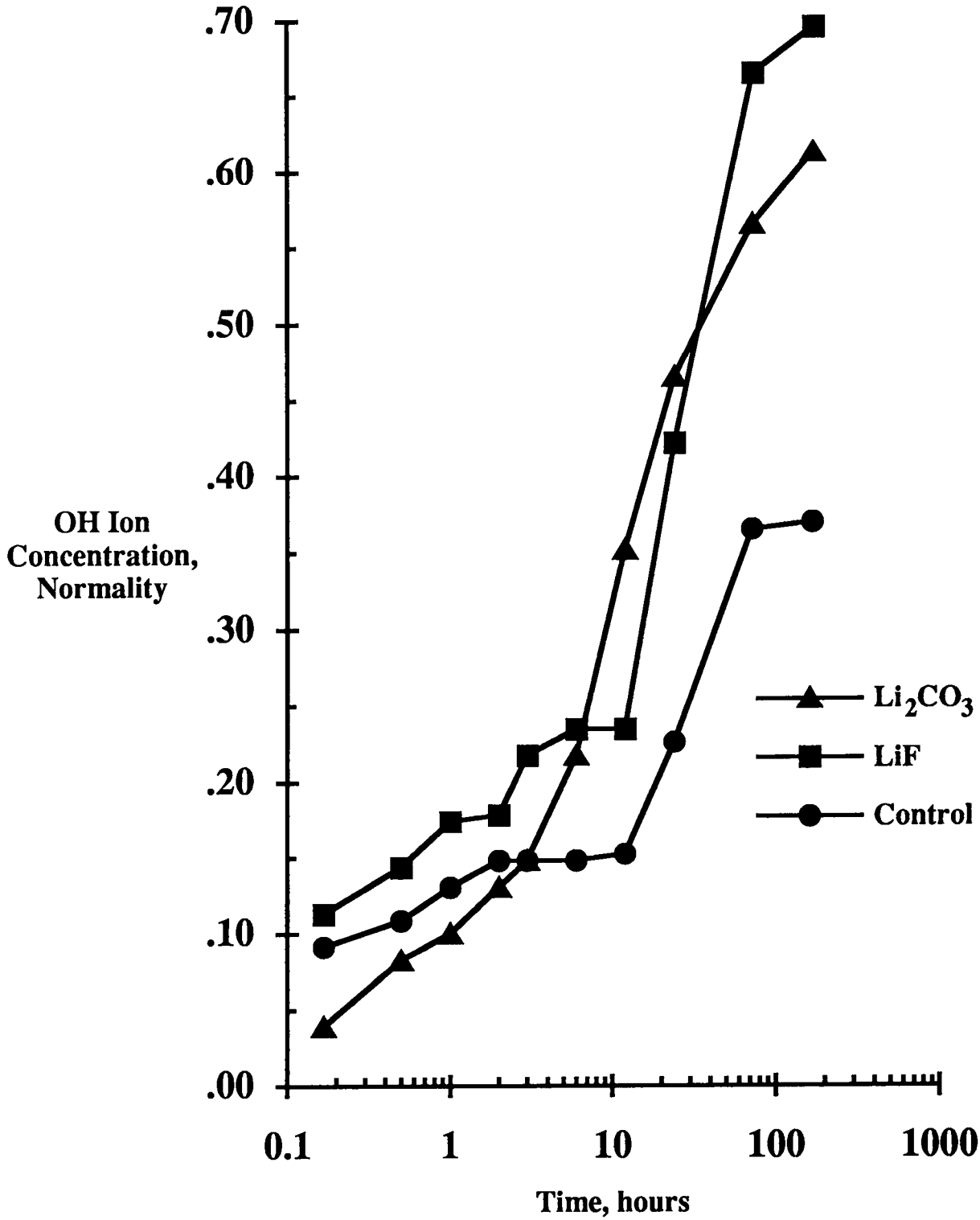


Figure 4.2. OH ion concentrations found in cement paste pore solutions as a function of time: (a) Paste treated with 1 percent $Li_2CO_3$; (b) Paste treated with 1 percent LiF; (c) Control paste without treatment.

precipitation of $CaF_2$. In either case, most of the $Li^+$ ions end up in solution partnered by $OH^-$ ions, and result in substantial increases in the respective $OH^-$ ion concentrations. In effect, most of the added partly soluble lithium salt is converted to fully soluble LiOH.

The addition of lithium salts results in an increased $OH^-$ ion concentration and a substantially higher pH, meaning that the potential for some kind of reaction with ASR-susceptible aggregates is increased -- not decreased. The beneficial effect of the treatment is thus dependent on the specific behavior of dissolved LiOH in solution being different from the behavior of dissolved NaOH or KOH on ASR.

### *4.1.2 LiOH Effects: Background*

Since the influence of lithium salts on the pore solution chemistry (and thus on ASR) was seen to be conditioned by the fact that these salts are quickly converted to lithium hydroxide when incorporated into concrete, it was felt the primary study should be concerned with the chemistry of LiOH in cement systems and in ASR reaction systems. Accordingly, considerable research was undertaken to determine the details of how LiOH interacts in cement paste pore solutions.

### *4.1.3 Removal of LiOH from Solution by Hydrating Cement*

A pore solution separation and analysis procedure similar to that used previously to study $Li_2CO_3$ and LiF effects was used in these studies, except that mortars instead of paste were used, and the dosage rate at which LiOH was added was equivalent to that of 1 percent $Na_2O$ in the cement, rather than 1 percent LiOH by weight of cement. This difference is important: 1 percent $Na_2O$ in the cement, corresponds to only 0.386 percent LiOH by mass of cement. This dosage was selected to facilitate later comparisons of LiOH effects with those of NaOH and KOH, and levels of these alkali hydroxides are keyed to the equivalent percent $Na_2O$ in the cement.

The mortars were prepared at a water-cement ratio of 0.485 using a pure ground calcitic limestone with no reactive aggregate component. The aggregate was graded as specified in ASTM C 227 for mortar bars. The aggregate-to-cement ratio was 2.25, and mixing was carried out using the ASTM C 305 procedure for mortars. LiOH predissolved in the mixing water, like NaOH and KOH (but unlike the lithium salts studied previously), is almost infinitely soluble in water. To eliminate as far as possible any competing effects of alkalies other than LiOH, the cement used was an extremely low alkali white cement, with the equivalent percent $Na_2O$ of only 0.08 percent, mostly as sodium oxide.

After sealed storage at 100 percent RH for periods ranging from 1 to 270 days, pore solutions were expressed by the method described by Barneyback and Diamond (1981) and analyzed by standard methods. At each time, the content of bound water at 212°F (100°C) was determined for each mortar. In these sealed systems changes in ion concentrations reflect changes both in water content (progressively reduced by ongoing cement hydration) and changes due to ions entering or being removed from the aqueous phase. It is possible to eliminate the former effect by calculation, if the bound water content at each stage is established. To do this, the observed pore solution concentrations are mathematically adjusted to constant (i.e. initial) water content (Diamond and Barneyback 1976). Changes in

the adjusted concentrations over time then reflect only changes due to ion entry or removal from the aqueous phase. This was done in the present case, with results for $Li^+$ given in Figure 4.3.

The starting concentration of LiOH in the mixing water was 0.665N. About 40 percent of the $Li^+$ ions were removed from solution by the first day, leaving a concentration of only 0.40N; subsequent uptake reduced the concentration to less than 0.30N. It is inferred from this result that the uptake of LiOH from solution is due to absorption of LiOH by the products of cement hydration. This phenomenon suggests that a substantial portion of the LiOH dosage added to concrete to prevent long-term ASR damage would not be available for that purpose because of earlier uptake by the hydrating cement.

Parallel experiments were carried out with NaOH and with KOH, both added at an equivalent dosage level. There was some uptake of both alkalies, amounting to about 25 percent of the added NaOH and about 20 percent of the added KOH, respectively.

It should be noted that, in all of these experiments, it was found that the uptake of alkali ions from solution was accompanied by uptake of $OH^-$ ions. Indeed, the uptake of $OH^-$ ions in each case actually exceeded that of the cations. Electrical neutrality in these solutions appeared to be preserved by increases in the concentration of $SO_4^{2-}$ ions (from the cement), some of which remained in solution indefinitely. Sulfate ions are usually completely removed from pore solutions as a result of ettringite formation by about the end of the first day's hydration, so this is an unexpected phenomenon.

This finding is of some significance with respect to laboratory studies of ASR. Many researchers routinely build up the alkali concentrations of their reacting mortars or concretes by adding KOH or NaOH to the mixing water. It has not been appreciated that such addition does not increase the $OH^-$ ion concentration proportionally to the dosage of alkali hydroxide added, and may change the long-term sulfate concentration from effectively zero to a substantial level.

### *4.1.4 ASR Reaction with LiOH*

A series of experiments was next carried out to determine whether a mortar with lithium hydroxide as its primary alkali component would enter into any type of ASR reaction with reactive aggregates. Mortars identical to those above were prepared except that they contained an approximately pessimum proportion of alkali-reactive aggregate. One series contained Beltane opal at 4.5 percent by mass of the total aggregate; a second, cristobalite, (calcined flint) was used at 30 percent by mass. Both series had LiOH dosages equivalent to 1 percent $Na_2O$ by mass of cement dissolved in the mixing water.

In Figure 4.4, $Li^+$ concentrations (adjusted for cement-bound water) found in the pore solutions recovered from mortars of both series are plotted along with the previous data for the non-ASR reactive mortar. Mortars containing the reactive aggregates both showed substantially greater removal of $Li^+$ ions from the pore solution over the 270-day test period. This augmented uptake of $Li^+$ is interpreted as evidence of an alkali-silica reaction with lithium, just as augmented uptake of $Na^+$ or $K^+$ ions would be interpreted as evidence of the formation of ASR gel in normal ASR reactions. The Beltane opal is seen to react faster than the cristobalite; it appears to have been fully reacted by 90 days.

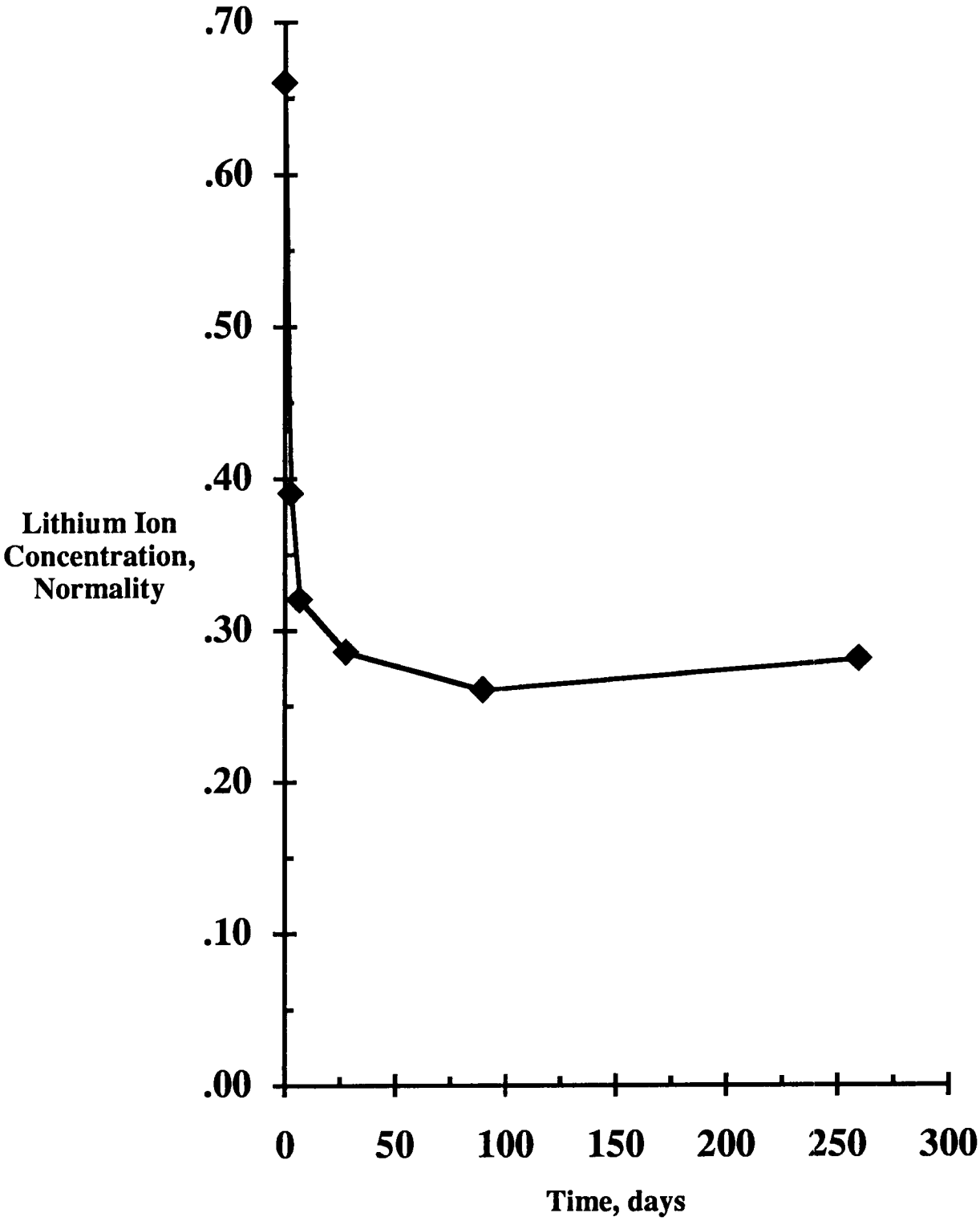


Figure 4.3. Lithium ion concentration (adjusted for cement-bound water) in pore solutions of LiOH-treated non-reacting mortar. Lithium dose level: LiOH equivalent to 1 percent $Na_2O$ in the cement.

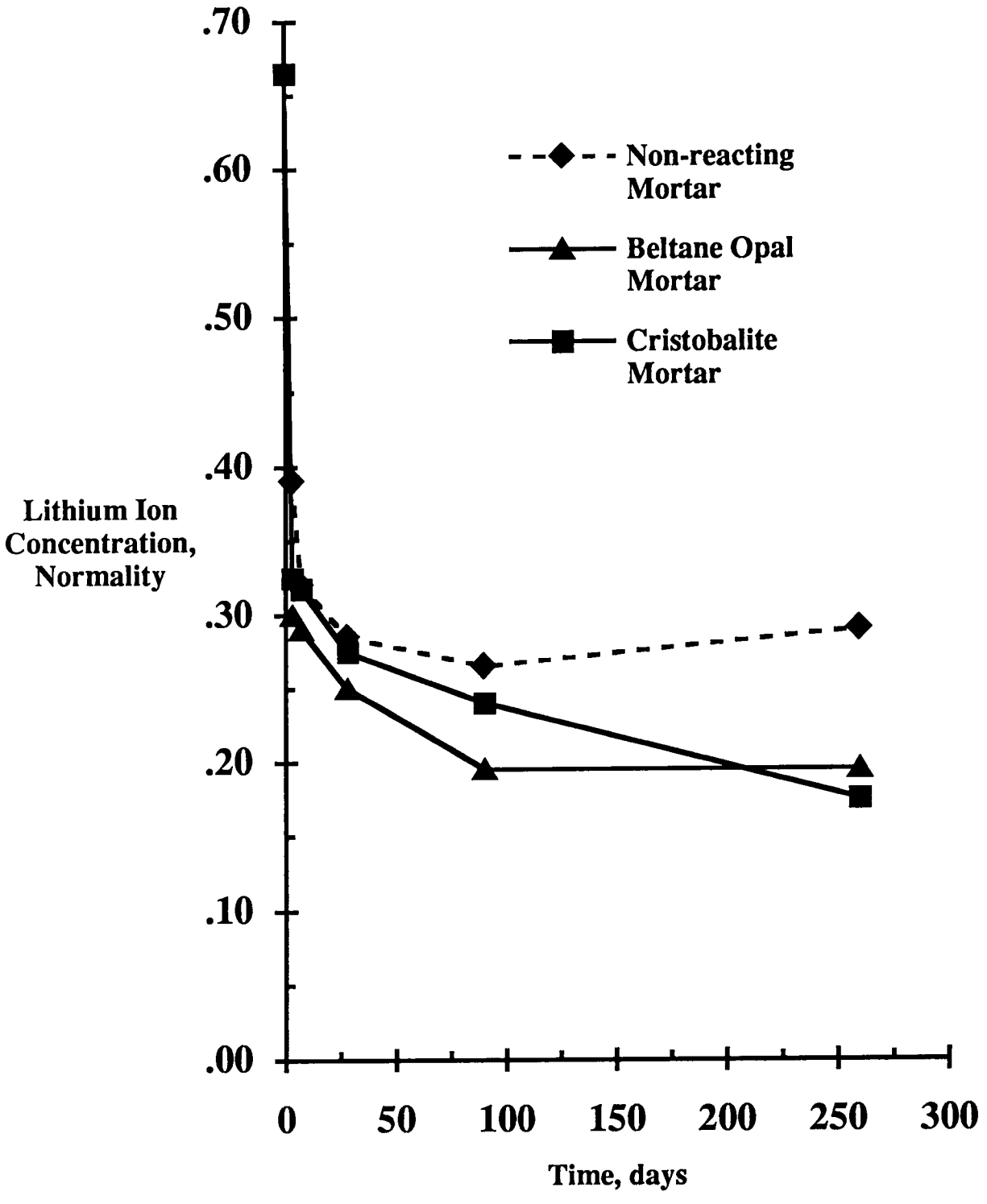


Figure 4.4. Difference in uptake of lithium ions between non-reacting and ASR-reacting mortars as indicated by pore solution lithium ion concentrations (adjusted for cement-bound water). In each case, lithium ion dose level was equivalent to 1 percent $Na_2O$ in the cement.

The fact that an ASR reaction had occurred with LiOH was confirmed by examination of fracture surfaces of the Beltane opal-LiOH mortar in UV light after the uranyl acetate treatment. Definite indication was found of the presence of a gel capable of absorbing uranyl ions and fluorescing.

To assess the relative amount of the ASR gel formed with LiOH compared to what would be formed with NaOH or KOH, parallel experiments were conducted with reactive mortars to which NaOH or KOH had been added to the mixing water at the same 1 percent $Na_2O$ equivalent dosage level. Data for the NaOH bearing mortars are shown in Figure 4.5. The augmented uptake of $Na^+$ found in this NaOH-ASR reaction is much greater than that of $Li^+$ in the LiOH-ASR reactions, as shown in Figure 4.4. The corresponding KOH uptake by the reacting aggregates (not shown) was even greater than the NaOH response. From these data, it is concluded that, while LiOH reacts to form a lithium-bearing ASR gel, the extent of reaction and the amount of gel formed is considerably less than would take place with either KOH or NaOH under the same conditions.

The expansive potential (or lack of it) of such lithium-bearing ASR reaction products has been explored by preparing mortar bars of compositions identical to those cited above and exposing them to the standard ASTM C 227 test conditions of 100 percent RH at 100°F (38°C). Resulting expansion data are shown in Figure 4.6. Unlike the sodium- and potassium-bearing mortars, no significant expansion was found for the lithium-bearing mortars, despite the previously cited evidence that ASR reaction takes place within them. The mortar bars showed no cracks or surface gel deposits, in contrast to the extensive cracking and surface gel deposits observed with the corresponding sodium- and potassium-bearing mortar bars.

It should be pointed out that the expansions recorded here for the sodium- and potassium-bearing mortar bars were much smaller than expected. Details of the exposure as specified at the time the tests were run (ASTM C 227-90) requires that wicking material be maintained at no more than 1 1/4 in. (30 mm) distance from each surface of the mortar bars. Unfortunately, this leads to extensive leaching of alkali hydroxide from the mortar bars, and thus to less expansion than would otherwise take place.

Studies also were carried out of the extent of leaching of the alkali cation from the bars under these conditions. It was found that very extensive KOH and NaOH leaching took place, but the amount of LiOH leached out of the mortars bars was much less.

### *4.1.5 LiOH Effects In Mixed Alkali Hydroxide Systems*

The above results were derived from mortars in which LiOH was added to an almost alkali-free cement. In using lithium treatments to prevent or mitigate ASR, one would naturally expect to use it primarily when high-alkali cements are used. That is, lithium would be considered for use primarily when the cements used generate high concentrations of NaOH or KOH (or both) in the pore solutions. The major question underlying such use is the degree to which the presence of added lithium hydroxide can overcome the expansive tendencies associated with the potassium- and sodium-bearing gel reaction products that normally are produced.

To determine this, mortars were prepared from the previously-used cement but, in each case, a fixed high dosage of NaOH and KOH was added to the mixing water, along with the LiOH

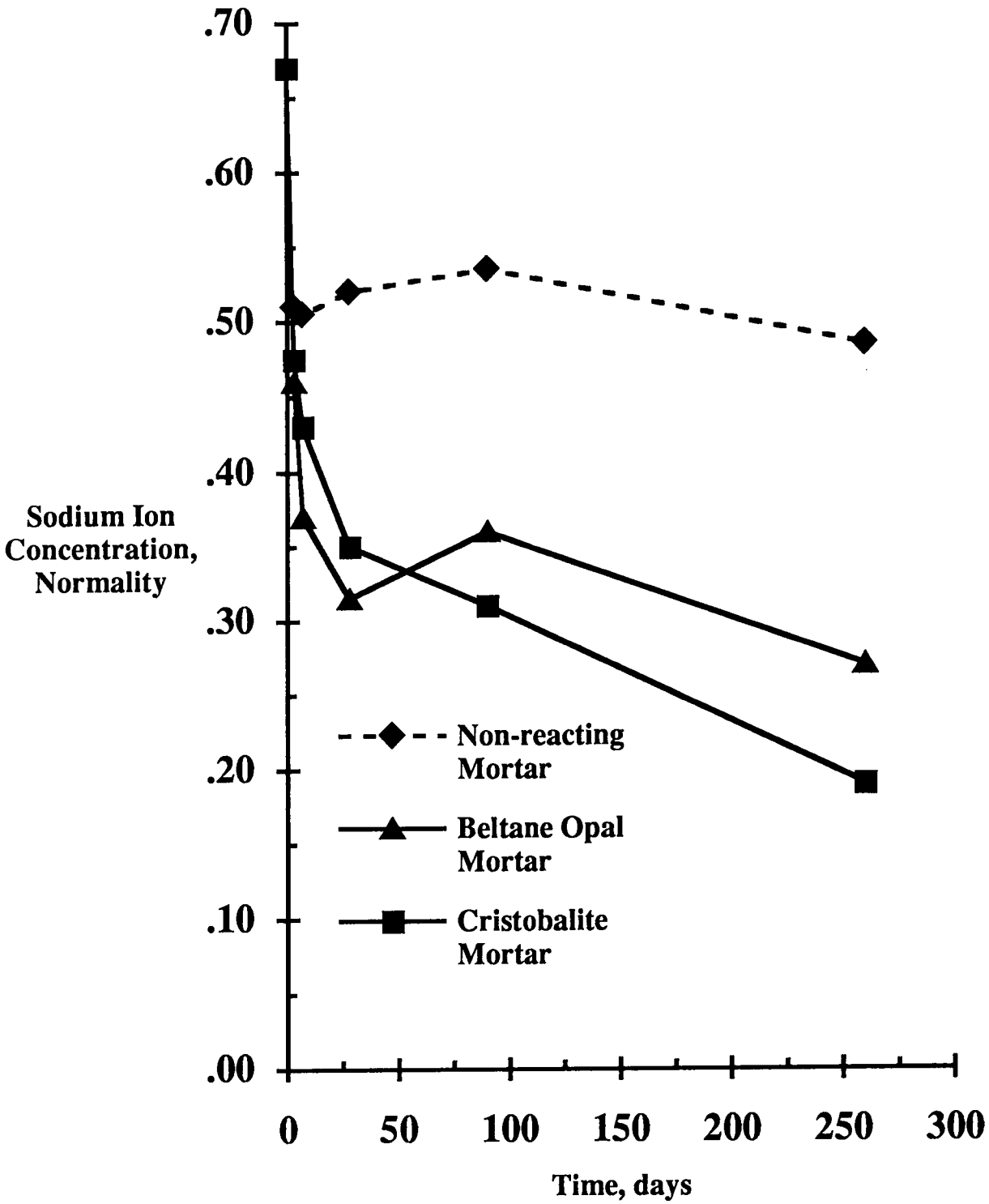


Figure 4.5. Difference in uptake of sodium ions between non-reacting and ASR-reacting mortars as indicated by pore solution sodium ion concentrations (adjusted for cement-bound water). In each case, sodium ion dose level was equivalent to 1 percent $Na_2O$ in the cement.

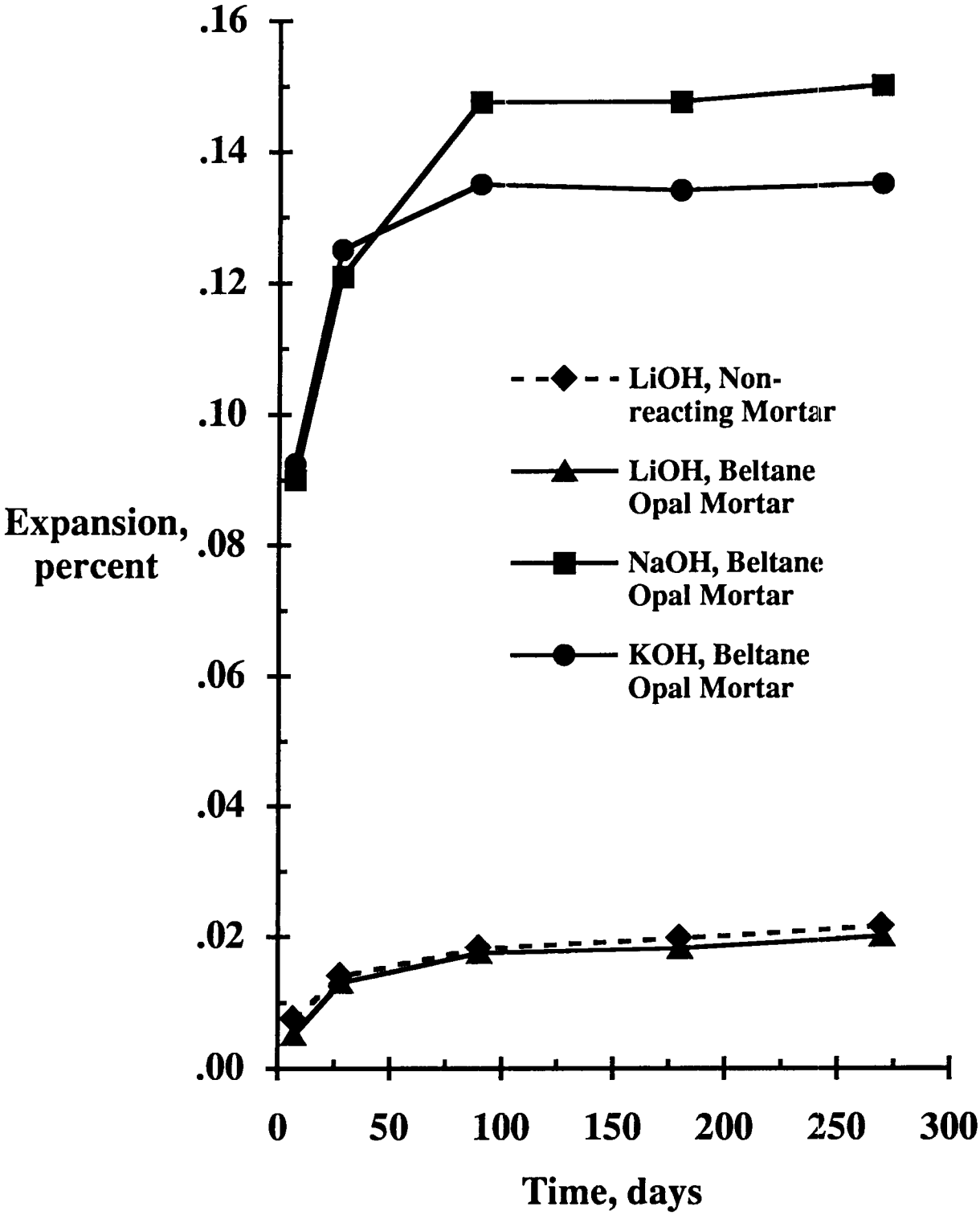


Figure 4.6. Measured expansions for mortar bars as follows: lithium ion treated, no reactive aggregate; lithium ion treated, Beltane opal; sodium ion treated, Beltane opal; and potassium ion treated, Beltane opal.

treatment. In all of the mixtures, NaOH and KOH were each added in amounts equivalent to 0.5 percent $Na_2O$ each in the cement, the combined alkali loading corresponding to an $Na_2O$ equivalent of the cement of 1.0 percent. LiOH was added at three levels: a low dosage level, corresponding to 0.4 percent $Na_2O$ equivalent; an intermediate dosage level, corresponding to 0.8 percent $Na_2O$ equivalent; and a high dosage level, corresponding to 1.2 percent $Na_2O$ equivalent. As before, both non-reacting mortars containing only limestone, and mortars containing pessimum proportions of Beltane opal and of cristobalite were prepared.

It was found that even in the mortars with only innocuous aggregate, a substantial part of the LiOH added was taken up by the hydrating cement as expected, despite the presence of NaOH and KOH. Thus, even in high alkali concretes, it is expected that much of the lithium added will be effectively sequestered by cement hydration products, and not be available to participate in modifying later ASR reactions.

In mortars or concretes containing reactive aggregates, it is expected that ASR gel (formed only after the bulk of cement hydration has been completed) will take up additional lithium over and above that previously removed from solution by the cement itself. This is indeed found as indicated in Figure 4.7. Here, plots are compared of the adjusted $Li^+$ ion concentrations of opal-bearing high-LiOH dosage mortars with those of the corresponding non-reacting mortars. The presence of the Beltane opal causes much greater removal of lithium from solution than takes place in its absence. Results similar to those shown in Figure 4.7 were obtained for the cristobalite-bearing mortars at the same LiOH dosage levels, and also for mortars with both Beltane opal and cristobalite at the lower lithium dosage levels.

The amount of extra lithium shown to be taken up in Figure 4.7 is much greater than that previously shown in Figure 4.4, where only LiOH (and no NaOH or KOH) had been added. This would be expected since, with NaOH and KOH available as well as LiOH, one should expect a considerable increase in the total extent of ASR reaction and gel formation, i.e. an enhanced opportunity for $Li^+$ to be incorporated in ASR gel.

It appears from Figure 4.7 that the enhanced uptake of $Li^+$ ions from this mixed pore solution by Beltane opal occurs at the expense of uptake of alkali ions that would have occurred if no lithium were present. This is confirmed by a comparison of the present data for the extra or augmented uptake of $Na^+$ and of $K^+$ in these lithium-bearing mixed alkali mortars with data for augmented uptake of $Na^+$ and $K^+$ ions in the "pure" NaOH- and KOH-treated mortars described earlier. The implication is that $Li^+$, $Na^+$, and $K^+$ ions are all competing for incorporation in the ASR reaction product being formed in the mixed systems.

It is an over simplification to consider only the content of these three cations as determining the composition of the ASR gel. ASR gels also incorporate significant amounts of calcium and often some aluminum, and are known to vary in composition from place to place within a given concrete. Nevertheless, it is of interest to compare the original proportion of $Li^+$ to the sum of $Li^+ + Na^+ + K^+$ ions added in the mixing water (with this almost alkali-free cement) to the proportion that appears to have been taken up in ASR gel formation. This is taken to provide a crude measure of the proportion of lithium in the ASR gel formed.

At the low dosage level, the data suggest that the proportion of lithium incorporated in the reaction product is only about half the proportion of lithium added. This appears to reflect prior high uptake of lithium by the hydrating cement. That is, when only a little LiOH is added, much of it is picked up by cement hydration before ASR can be significantly

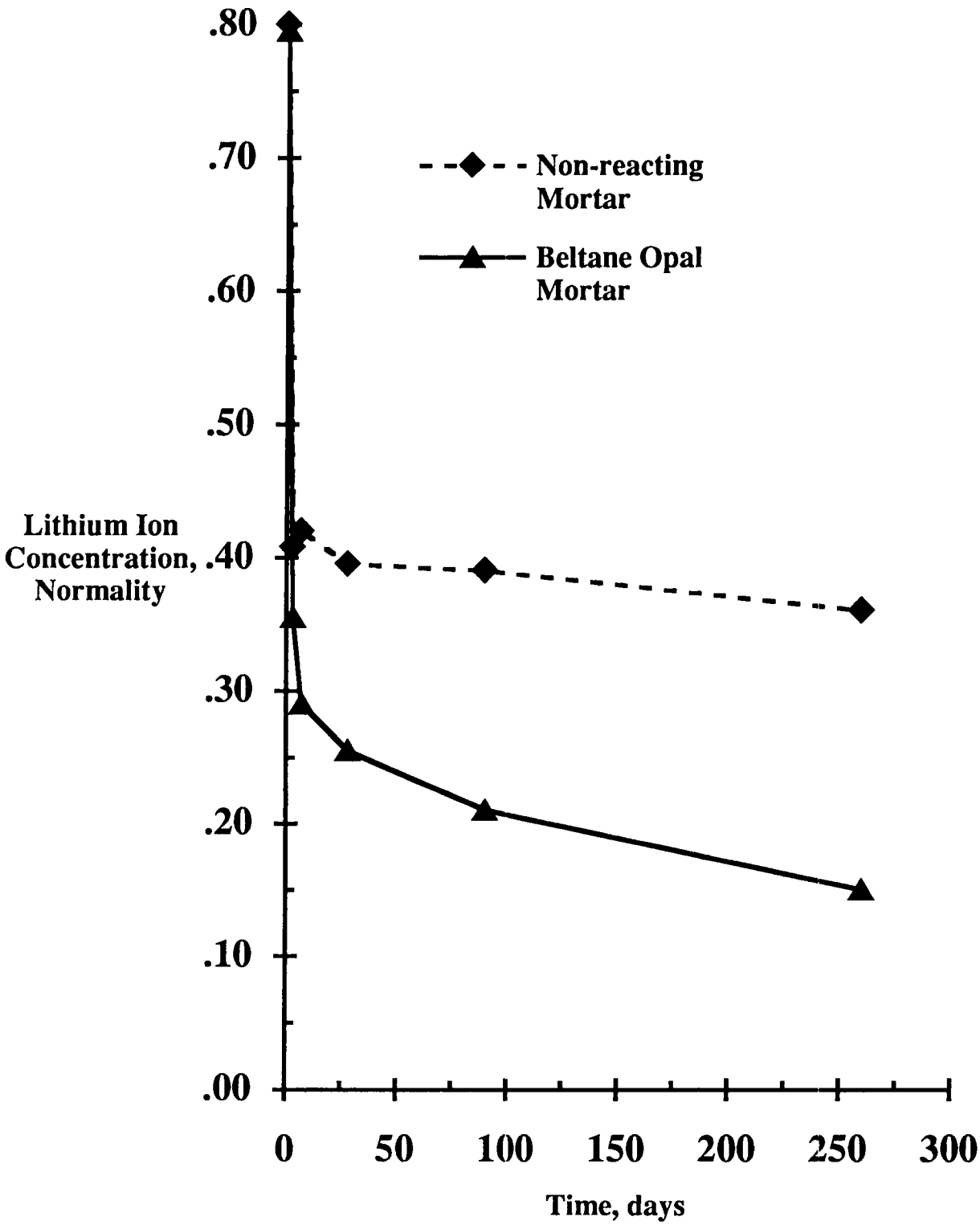


Figure 4.7. Increase in uptake of lithium ions during active ASR in Beltane opal mortar, compared with uptake in non-reacting mortar. Lithium ion concentrations in pore solutions are adjusted for cement-bound water.

established. At the intermediate and high dosage levels, the proportion of lithium apparently incorporated into the ASR product is significantly higher, and nearly reflects the proportion originally added to the mixing water. In general, the proportion of lithium apparently incorporated into the ASR product with Beltane opal-bearing mortars at each LiOH dosage level is similar to that for cristobalite-bearing mortars at the same level.

It should be noted that recourse to this indirect means of assessing the lithium thought to be present in the reaction product gel is necessary because the direct method of energy-dispersive x-ray analysis (EDAX) used normally for such purpose simply does not record the presence of lithium. The very low atomic number of lithium (No. 3) means that the characteristic x-rays produced by electron bombardment of lithium-bearing substances have energies insufficient to penetrate the thin window of the X-ray detector. Indeed nearly all are absorbed within the sample itself.

Thus far, data for the augmented uptake of cations in these mixed alkali mortars have been interpreted from the point of view of assessing the competition among the different alkalies for inclusion in the reaction product gel. From another point of view, the total of such augmented uptake (of $Li^+$, $Na^+$, and $K^+$ ions) in a given case might be used to provide a comparative measure of how much reaction product gel has been formed. It is of interest to determine how much gel has been formed as a function of how much lithium hydroxide was added. It should be recalled that the NaOH and KOH dosage was held constant throughout.

In Figure 4.8, the total augmented uptake of all three ions ($Li^+ + Na^+ + K^+$) is plotted as a function of the starting lithium ion concentration, for both Beltane opal- and cristobalite-bearing mortars exposed for 270 days at 100 percent RH at 100°F (38°C). It is apparent that the greater the starting LiOH dosage, the smaller the combined uptake, i.e. the smaller the amount of gel formed. The trend lines are remarkably similar for the two reactive aggregates, and both are approximately linear. Projections of the trend lines suggest that a starting LiOH ion concentration of about 1.5N might entirely suppress the ASR gel formation. This dosage corresponds to a LiOH treatment level of 1.75 percent by mass of cement. The above data are for uptake representing reactions that had taken place by 270 days. A similar plot for 90 day results gave an entirely similar trend, again projecting to suppression of uptake at a starting $Li^+$ concentration of about 1.5 N.

Since the lithium in these mortars was added as LiOH, and since much of it remained in the solution as dissolved LiOH, it is a necessary consequence that higher lithium dosage levels produce higher $OH^-$ ion concentrations. The actual measured $OH^-$ ion concentrations of the pore solutions at one day for the non-reacting control mortars of this series were 0.46N, 0.54N, and 0.66N for the low, medium, and high lithium dosage levels, respectively. Ordinarily one would expect that the higher the $OH^-$ ion concentration, the greater the extent of ASR reaction. With lithium, the reverse seems to be the case. That is, for a constant dosage of other alkalies, the greater the lithium dosage applied, the less the apparent extent of ASR reaction, in spite of the increased $OH^-$ ion concentration. A high enough dosage of LiOH would apparently suppress the reaction completely.

An indication of the effectiveness (or lack of it) of the different levels of lithium treatments in reducing expansion was obtained in modified ASTM C 227 mortar bar tests, the results of which are plotted in Figure 4.9. These tests were carried out with mortar bars placed in individual plastic sleeves in the 100°F (38°C) exposure cabinet with a small amount of water added before the sleeves were sealed, as described by Hooton and Rogers (5). In Figure 4.9 measured expansions at 270 days are plotted against starting $Li^+$ ion concentration in the mix water.

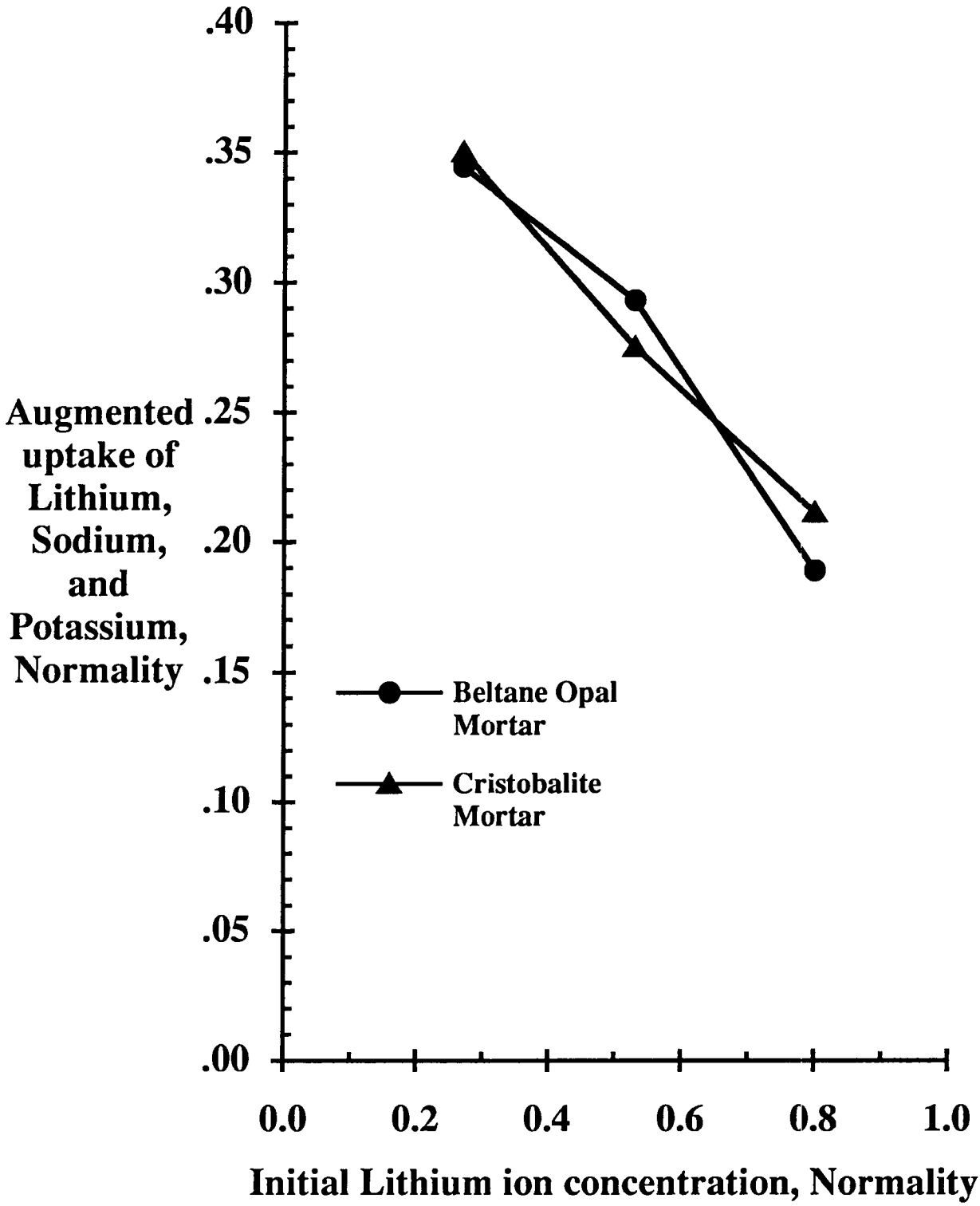


Figure 4.8. Indication of extent of ASR reaction as a function of lithium ion dosage. The indication of reaction is the combined augmented uptake of lithium, sodium, and potassium ions at 270 days.

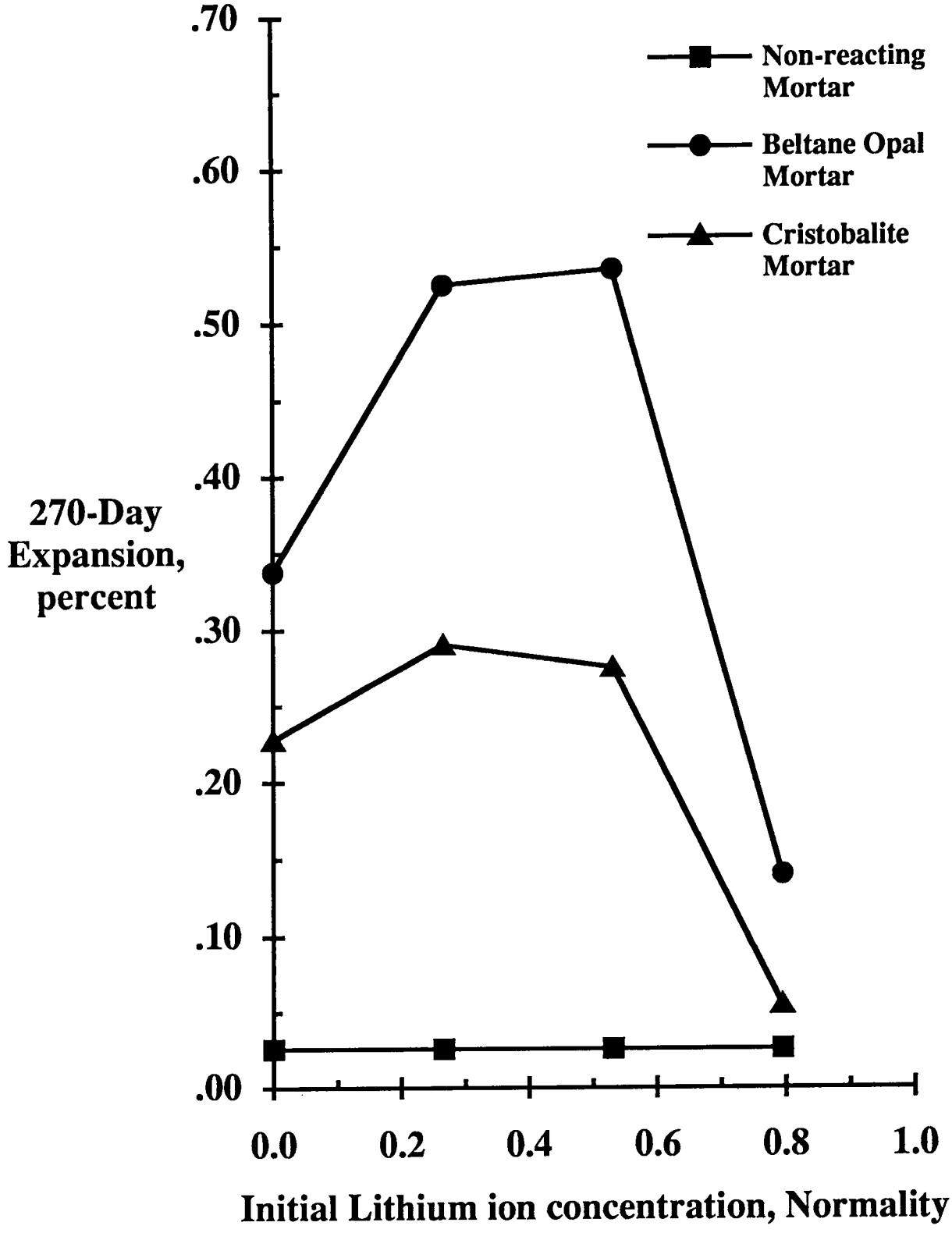


Figure 4.9. Expansions of ASR reacting mortar bars as a function of lithium ion dose levels.

The mortars without reactive aggregate showed small expansions (around 0.02 percent) which were independent of $Li^+$ dosage. Surprisingly, with both Beltane opal and cristobalite, low and intermediate dosage levels of LiOH actually increased the observed expansion. It required the high lithium dose level (equivalent to 1.2 percent $Na_2O$ in the cement) to effectively control expansion, and even here the expansion with Beltane opal was mostly, but not completely eliminated.

Sakaguchi et al. (1989) reported ASR expansion results with LiOH and NaOH added to a normal Portland cement. With their andesite reactive aggregate, high expansion was recorded at a cement alkali level (not counting $Li_2O$) of 1.2 percent $Na_2O$ equivalent. Expansions were eliminated for only those mortars with enough added LiOH to yield Li:Na molar ratios of 0.9 and higher. In the present data, the alkali level (not counting $Li_2O$) is 1 percent $Na_2O$ and it was found that only the high LiOH dosage level, corresponding to a Li-(Na+K) molar ratio of 1.2, was effective. Thus the response observed here is more or less similar to that observed by Sakaguchi et al.

Thus, where added lithium competes with high levels of sodium and potassium for incorporation into ASR products, a high dosage of LiOH needs to be applied, and intermediate levels may possibly exacerbate the situation. In the present studies,the combined sodium plus potassium level was kept constant, so there is no direct evidence whether proportionally higher LiOH dosages are needed for higher alkali cement systems, as implied by the results of Sakaguchi et al. Such a presumption appears likely.

## 4.2 Laboratory Investigation with Commercially Available Aggregates

Prior to this investigation, two series of tests were run in which aggregate AL was used with a portland cement with 1.0 percent as equivalent $Na_2O$ in mortar bars made and tested in accordance with C 227 (Stark 1992). In one series, LiF powder was added to the fresh mixture at rates of 0.25 percent, 0.50 percent, and 1.00 percent by mass of cement. In the other, $Li_2CO_3$ powder was added at the same dosage rates. A control mixture also was made without lithium salt addition. Tests were run for 36 months, with comparator readings being taken at regular intervals.

Results of these tests are given in Table 4.1 and Figures 4.10 and 4.11. These data verify the earlier results of McCoy and Caldwell, and also suggest that a threshold level of lithium ion is needed, above which expansive ASR is effectively suppressed. For LiF, this level was between 0.25 percent and 0.50 percent, probably closer to 0.50 percent by mass of cement. For $Li_2CO_3$, the level was between 0.50 percent and 1.00 percent. These ranges correspond to about 0.10 percent to 0.20 percent lithium ion by mass of cement.

Prior to studies of lithium effects on ASR in Project C 202, it was felt that LiOH might be preferred to LiF or $Li_2CO_3$ because LiOH is highly soluble in water while the latter two salts dissolve appreciably only after contact with the highly alkaline solution in fresh concrete. It was felt that lithium ion could be more uniformly dispersed in large concrete batches if dissolved in the mixing water prior to introduction into the batch. As noted previously, LiF and $Li_2CO_3$ react in concrete also to produce LiOH. Thus, it was believed that advantage could be taken of the greater LiOH solubility to permit better dispersal of lithium ions in fresh concrete.

Table 4.1 Expansions of mortar bars containing LiF or $Li_2CO_3$

| Admixture | | Percent Expansion | | | | | | | | | | | |
|---|---|---|---|---|---|---|---|---|---|---|---|---|---|
| Type | Dosage, percent weight of cement | 14D | 1M | 2M | 3M | 4M | 6M | 9M | 12M | 18M | 24M | 30M | 36M |
| None | — | .007 | .130 | .290 | .388 | .459 | .536 | .600 | .622 | .622 | .627 | .624 | .629 |
| LiF | 0.10 | .003 | .067 | .203 | .305 | .380 | .484 | .588 | .618 | .632 | .628 | .626 | .627 |
| | 0.25 | .007 | .027 | .141 | .250 | .330 | .433 | .544 | .590 | .640 | .677 | .703 | .713 |
| | 0.50 | .002 | .004 | .011 | .016 | .025 | .039 | .054 | .062 | .064 | .062 | .061 | .063 |
| | 1.00 | .003 | .006 | .011 | .011 | .014 | .016 | .016 | .018 | .019 | .017 | .015 | .019 |
| $Li_2CO_3$ | 0.10 | .008 | .087 | .248 | .372 | .442 | .522 | .592 | .613 | .627 | .635 | .642 | .648 |
| | 0.25 | .000 | .033 | .144 | .262 | .344 | .456 | .568 | .605 | .619 | .624 | .627 | .631 |
| | 0.50 | .004 | .010 | .057 | .125 | .186 | .294 | .436 | .497 | .539 | .552 | .566 | .575 |
| | 1.00 | -.001 | .009 | .017 | .018 | .027 | .027 | .035 | .041 | .042 | .043 | .042 | .045 |

Note: 1. All results are the average of four companion specimens.
2. D = day; M = month.

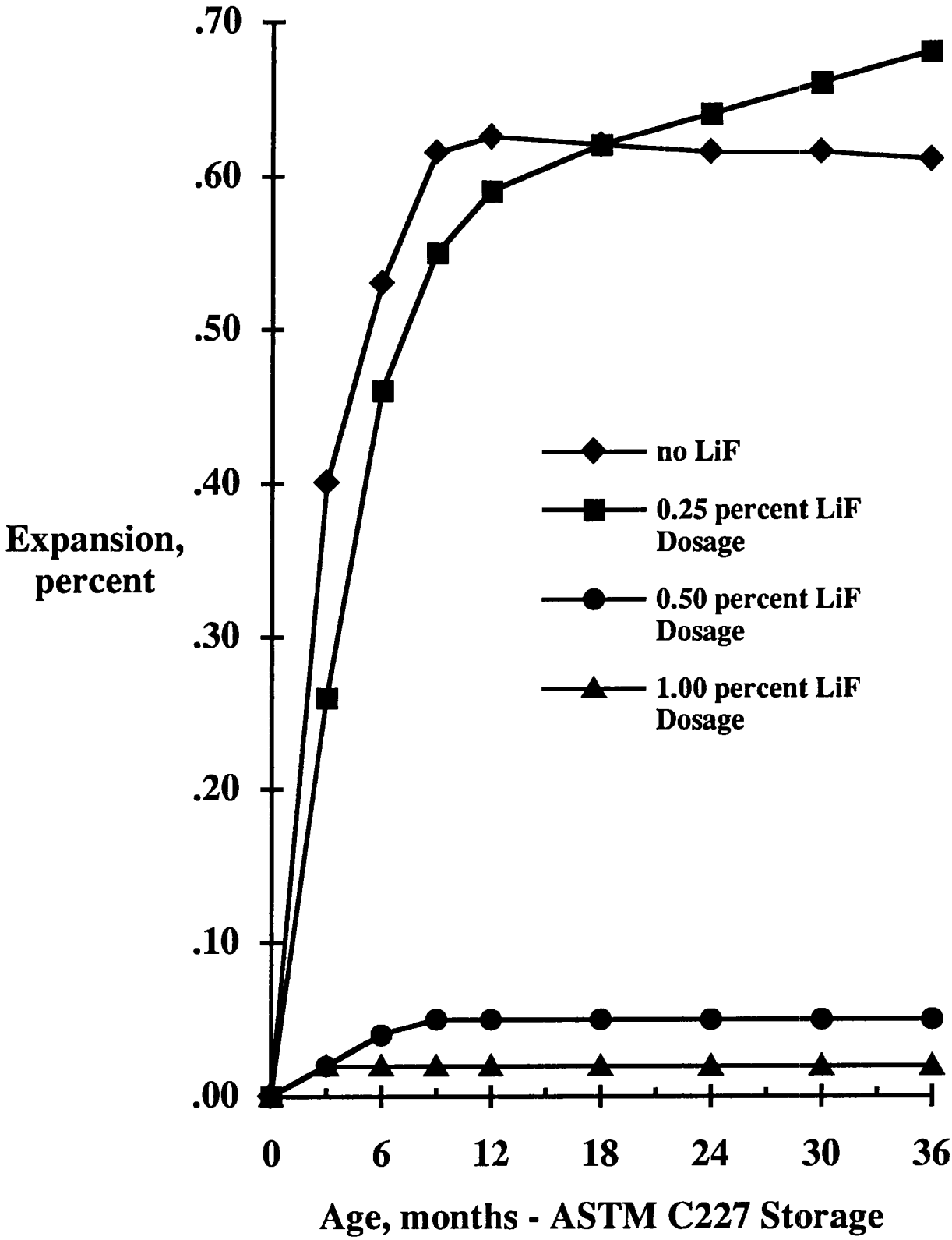


Figure 4.10. Expansion of specimens containing lithium fluoride admixture.

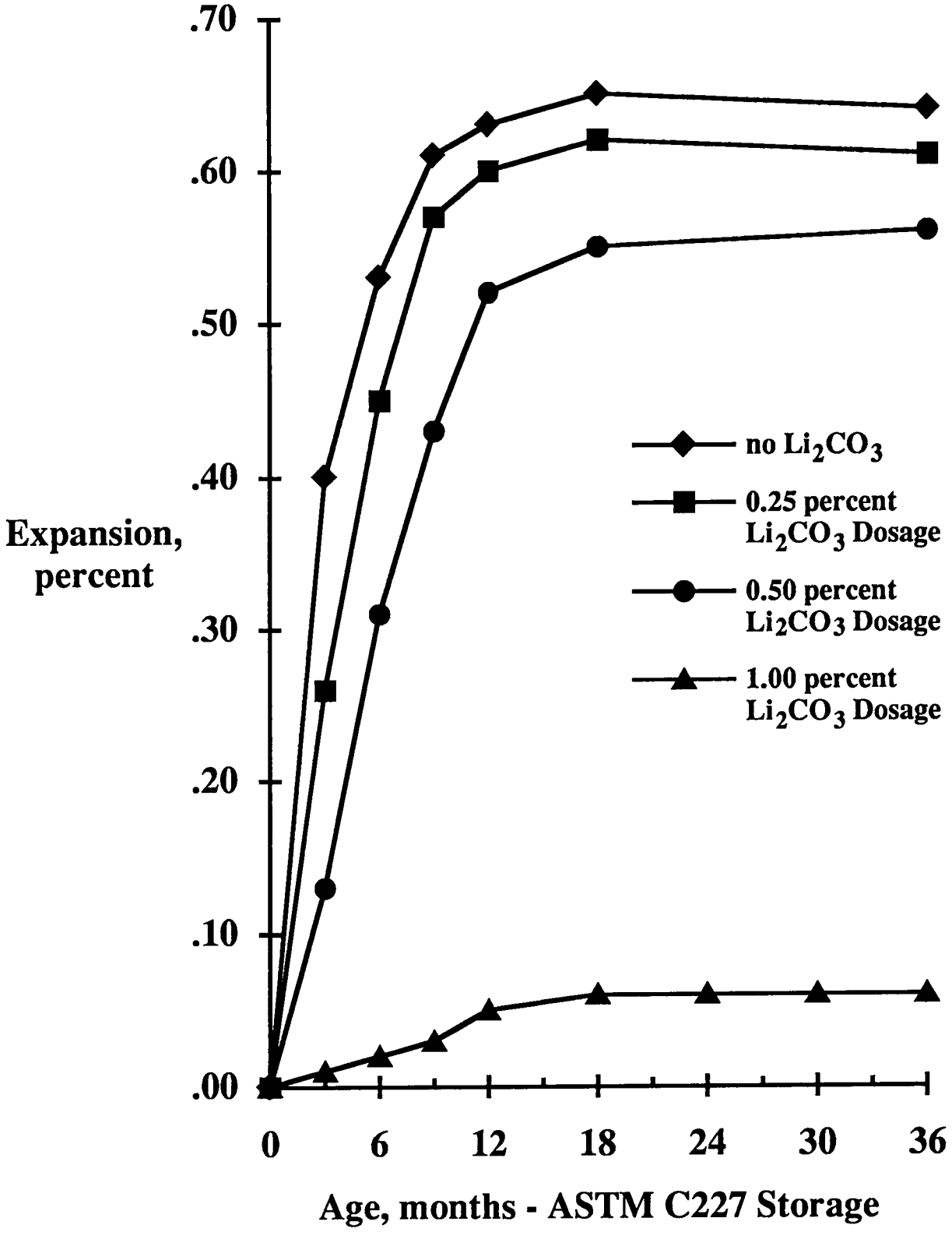


Figure 4.11. Expansion of specimens containing lithium carbonate admixture.

### *4.2.1 Effects of LiOH on Expansive ASR*

To evaluate the effects of LiOH on expansion due to ASR involving commercially available aggregate, mortar bars were made using aggregate AL, which contains highly reactive volcanics, and aggregate PR, which consists of slowly reactive granite gneiss. Cement B (Table 3.2) with 0.18 percent equivalent $Na_2O$ was used in these series. The water-cement ratio was 0.50. After removal from the molds at one day, the specimens were stored in water and brought to 176°F (80°C), for one day. Comparator readings were taken, then the specimens were transferred to the prescribed immersion solution for storage at 176°F (80°C) for 28 days.

In one series of tests with each of these aggregates, 1N NaOH immersion solutions were used, to which was added sufficient $LiOH \cdot H_2O$ (the most stable form as manufactured) to produce concentrations of 0.33N, 0.67N, and 1N LiOH in the 1N NaOH solution. Thus, hydroxyl ion concentration increased progressively from that in the straight 1N NaOH solution up to the concentration to which the equivalent of 1N LiOH was added.

In the second series of tests, hydroxyl ion concentration was maintained at 1N with the addition of NaOH. Then LiOH was substituted for NaOH to maintain that $OH^-$ concentration. Final $Na^+$ to $Li^+$ ratios were 1.0, 1:0.33, 1:0.67, 1:1, and 0:1.

The introduction of lithium ion into the immersion solution rather than into the fresh mortar was done to avoid leaching of lithium into the solution from the test specimens. In this approach, ASR is essentially completely dependent on diffusion of lithium and sodium from solution into the mortar specimens.

Results of these tests are summarized in Table 4.2 and show several meaningful relationships. First, both aggregates AL and PR are highly reactive in 1N NaOH solution with no LiOH addition, as expected. Second, virtually no expansion developed in 1N LiOH solution to an age of 28 days, thus demonstrating that, even at high OH concentration, any ASR product that may have formed is non-expansive. Third, increasing LiOH concentrations in NaOH solutions progressively decreased expansions due to ASR. It appears that regardless of whether OH concentrations are held constant at 1N or range up to 2N, addition of lithium ion or substitution of lithium for sodium are capable of suppressing expansion due to ASR after some threshold ratio of Na:Li is reached.

Relationships among expansions at 14 days (the test period recommended for the rapid immersion method) and the various sodium-lithium hydroxide solutions are better seen in Figures 4.12 and 4.13. In Figure 4.12, sodium-lithium molar ratios at constant 1N $OH^-$ concentration are plotted against percent expansion for five solutions for the two aggregates. For the more highly reactive aggregate AL, expansion in the straight 1N NaOH solution was 0.87 percent. Expansions then dropped rapidly to below the 0.08 percent test criterion when the sodium-lithium molar ratio in the solution reached about 1:0.60. Expansions remained less than the failure criterion with further increase in proportion of lithium. A similar trend developed for the more slowly reacting granite gneiss aggregate PR, with expansions dropping below the test criterion with sodium-lithium ratios of about 1:0.50.

Figure 4.13 presents results for mortar bars immersed in 1N NaOH solutions to which were added sufficient LiOH to produce up to 1N:1N proportions of NaOH and LiOH. Trends similar to those shown in Figure 4.12 are seen in this test series. In this case, with differing OH concentrations, curves for the PR and AL aggregates dropped below the 0.08 percent test

Table 4.2 Effect of LiOH on expansion due to ASR

| Solution | Percent Expansion - Aggregate AL | | | | Percent Expansion - Aggregate PR | | | |
|---|---|---|---|---|---|---|---|---|
| | 7D | 14D | 21D | 28D | 7D | 14D | 21D | 28D |
| 1N NaOH<br>No LiOH | .483 | .867 | >1.00 | >1.00 | .189 | .309 | .385 | .422 |
| 1N LiOH<br>No NaOH | .004 | .000 | .004 | .007 | .002 | -.003 | .001 | .004 |
| 1N OH<br>Na:Li = 1:0.33 | .133 | .325 | .582 | .976 | .055 | .134 | .192 | .240 |
| 1N OH<br>Na:Li = 1:0.67 | .016 | .017 | .025 | .028 | .009 | .008 | .017 | .020 |
| 1N OH<br>Na:Li = 1:1 | .009 | .007 | .015 | .016 | .009 | .004 | .012 | .015 |
| 1N NaOH +<br>0.33N LiOH | .201 | .438 | .766 | >1.00 | .075 | .150 | .207 | .254 |
| 1N NaOH +<br>0.67 LiOH | .086 | .123 | .137 | .177 | .030 | .038 | .042 | .059 |
| 1N NaOH +<br>1N LiOH | .021 | .027 | .042 | .050 | .020 | .018 | .031 | .035 |

Notes: 1. All results are the averages for three companion specimens.
2. D = days.

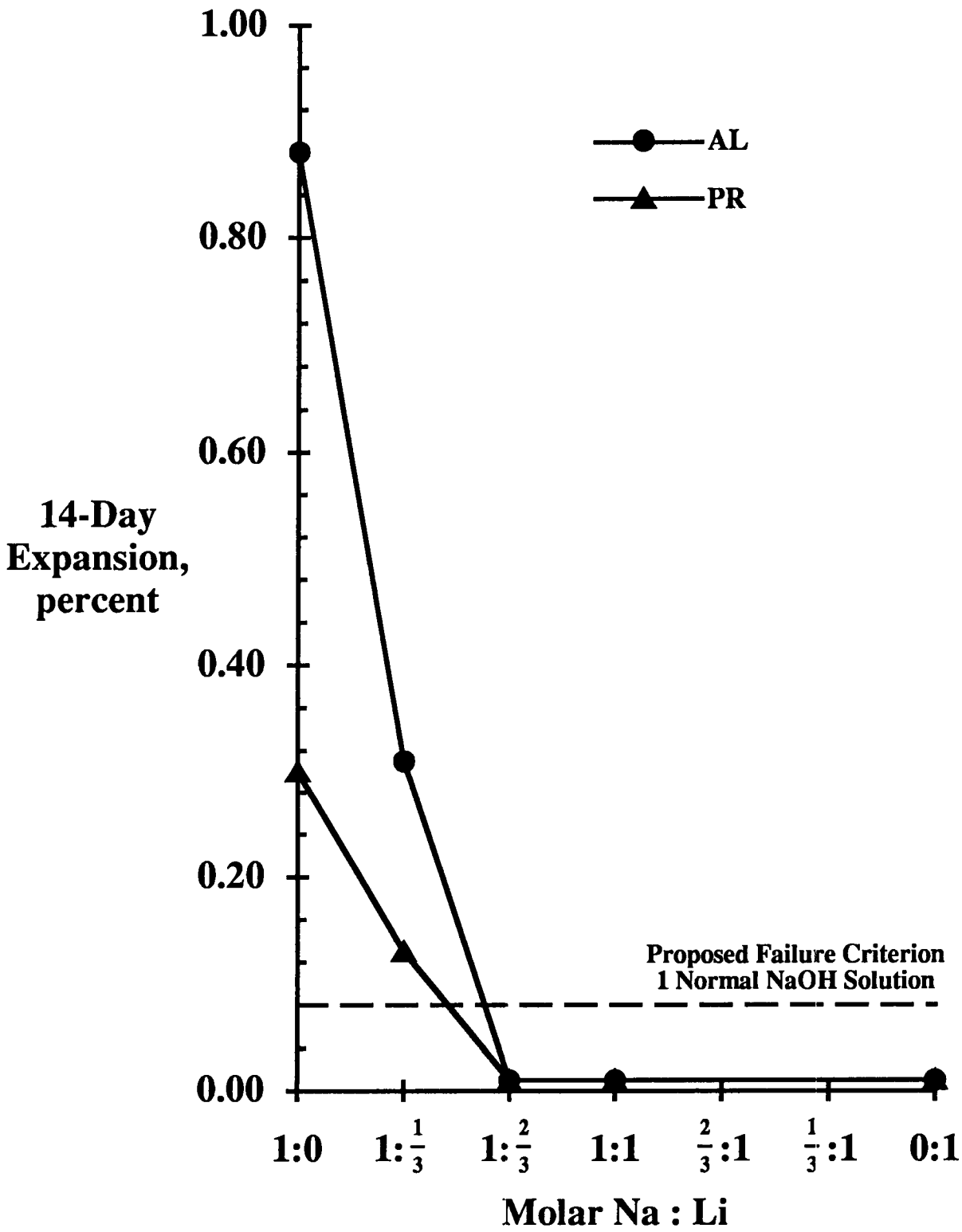


Figure 4.12. Effect on expansion at 14 days of substitution of LiOH for NaOH in solution at constant 1 Normal OH ion concentration.

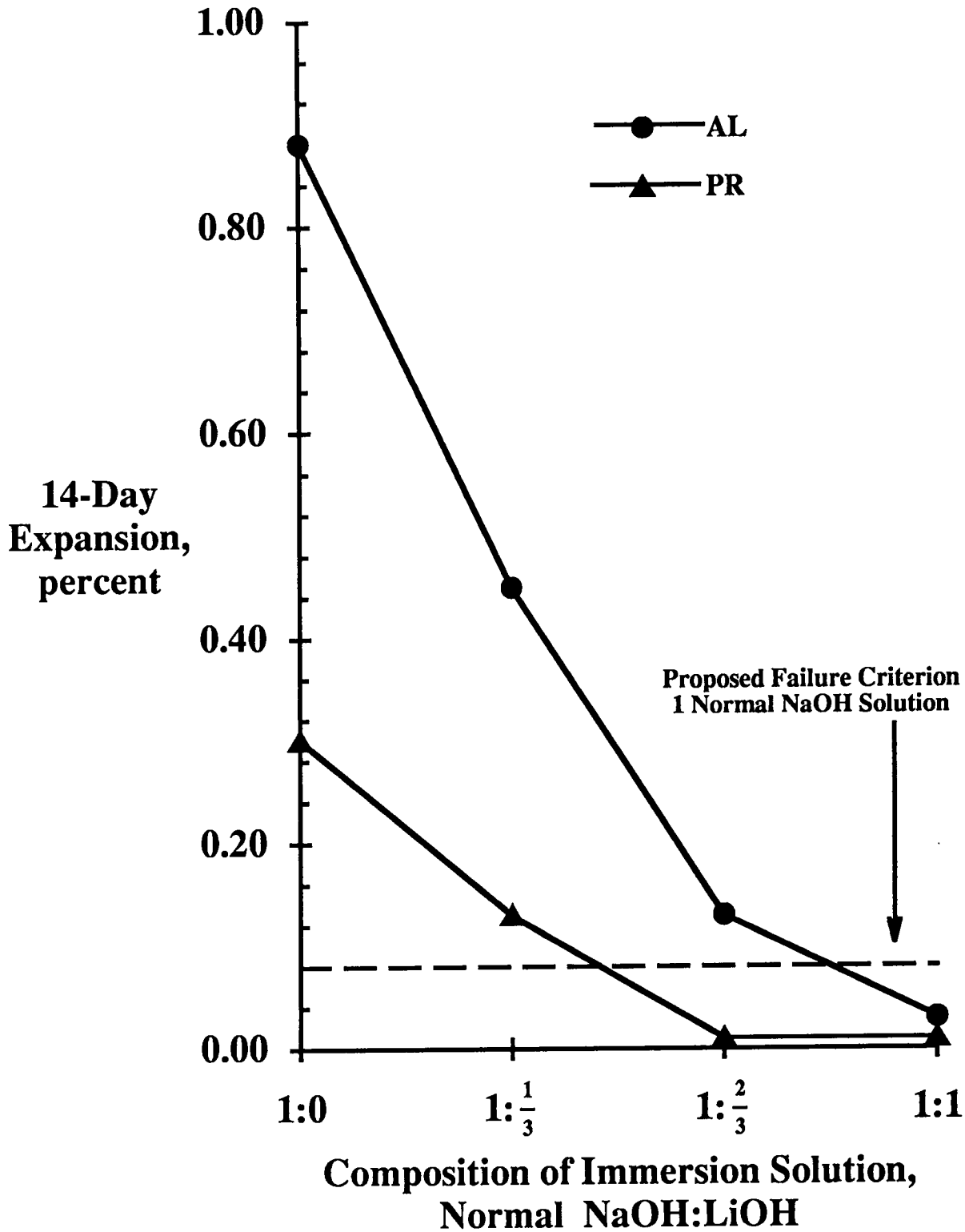


Figure 4.13. Effect on expansion at 14 days of LiOH added to 1 Normal NaOH solutions.

criterion at solution proportions of about 1N NaOH + 0.50N LiOH and 1N NaOH + 0.85N LiOH, respectively. The somewhat greater Li:Na required in the latter series probably is due to the greater hydroxyl ion concentration in the solution.

Besides demonstrating the effectiveness of lithium ion in mitigating expansive ASR, these results suggest that on a threshold concentration ratio of sodium to lithium exists below which the reaction can be brought safely under control. The results further lead to the conclusion that different threshold ratios exist for different cement-aggregate combinations. For example, for highly reactive aggregate AL, the required dosage rate of $LiOH \cdot H_2O$ would be about 1.1 percent by weight of cement with 1.0 percent equivalent $Na_2O$ at a water-cement ratio of 0.50.

It is evident that lithium hydroxide can effectively mitigate expansive ASR when used at required dosages. These dosages would appear to vary with cement alkali level, water-cement ratio, and source of reactive aggregate.

### *4.2.2 Effectiveness of LiOH Used with Fly Ash*

Numerous highway structures exist in the United States where fly ash was incorporated into the concrete structure without regard for possible ASR. Some structures, for example, have been observed where high-lime fly ash was included in the concrete and deleterious ASR developed within the approximate time frame for concrete made with similar cement-aggregate combinations but no fly ash.

The question thus arises whether lithium ion can suppress expansive ASR in cement-fly ash systems. It can be reasoned that cement-fly ash hydration products could complex lithium as they do sodium and potassium, thereby reducing lithium effectiveness while simultaneously intensifying expansive ASR due to greater alkali concentrations in pore solutions.

To investigate this matter, 15 sets of mortar bars were fabricated in which Cement A, with 1.00 percent equivalent $Na_2O$ was combined with Class F fly ash B and highly reactive aggregate AL. LiOH was added to the mixing water in proportions of 0.75 percent, 1.00 percent, 1.50 percent, and 2.00 percent by mass of cement. Control specimens, in which LiOH and fly ash were not included, also were made. Three exposure conditions were included; per C 227 (over water in sealed containers), immersion in 6 percent NaCl solution, and in $CaCl_2$ solution with the same chloride concentration, all at 100°F (38°C). Immersion in NaCl or $CaCl_2$ solutions was intended to simulate the presence of deicer solutions in highway concrete that contains deleteriously reactive aggregates. Immersion in the chloride solutions was begun immediately after removal of specimens from the molds. The rapid immersion test was not used in this series to avoid possible overly rapid expansion, thereforeless chance to distinguish differences among the various storage conditions.

Results for the series are summarized in Table 4.3, where data are grouped for effects of either fly ash or lithium, and for combinations of these two mitigative measures. The data reveal several significant relationships. First, the fly ash, and lithium ion at the rate of 1.0 percent by mass of cement, were both very effective in reducing expansion due to ASR. However, continued minor expansion appeared to develop in the fly ash mixture under C 227 storage after about four months. In contrast, the lithium-bearing mixture showed no such tendency at the later ages.

Table 4.3 Effects of Fly Ash B, LiOH, and storage condition on expansion of mortar bars containing reactive aggregate AL

| Set No. | Fly Ash Percent | LiOH Percent | Exposure | Percent Expansion 1M | 2M | 3M | 4M | 6M | 9M |
|---|---|---|---|---|---|---|---|---|---|
| 1 | 0 | 0 | C 227 | .098 | .272 | .333 | .391 | .456 | .503 |
| 2 | 20 | 0 | C 227 | .008 | .012 | .016 | .029 | .041 | .063 |
| 3 | 0 | 1.0 | C 227 | .012 | .024 | .022 | .029 | .029 | .035 |
| 4 | 0 | 0 | NaCl | .059 | — | — | 1.444 | — | >1.444 |
| 5 | 20 | 0 | NaCl | .010 | .028 | .047 | .066 | .220 | .390 |
| 6 | 20 | 0.75 | C 227 | .005 | .010 | .007 | .014 | .011 | .017 |
| 7 | 20 | .075 | NaCl | .008 | .021 | .019 | .034 | .057 | .102 |
| 8 | 20 | 1.0 | C 227 | .004 | .007 | .007 | .012 | .004 | .010 |
| 9 | 20 | 1.0 | NaCl | .012 | .019 | .016 | .027 | .027 | .045 |
| 10 | 20 | 1.5 | C 227 | .008 | .014 | .007 | .014 | .011 | .016 |
| 11 | 20 | 1.5 | NaCl | .012 | .021 | .017 | .027 | .021 | .030 |
| 12 | 20 | 2.0 | C 227 | .008 | .013 | .009 | .016 | .011 | .021 |
| 13 | 20 | 2.0 | NaCl | .008 | .018 | .014 | .023 | .021 | .028 |
| 14 | 20 | 0 | $CaCl_2$ | .064 | .070 | .103 | .124 | .129 | .132 |
| 15 | 20 | 1.0 | $CaCl_2$ | .015 | .025 | .029 | .037 | .043 | .068 |

Notes: 1. All results are the average for three companion specimens.
2. Fly ash content is expressed as percent weight replacement of cement.
3. Exposure is either ASTM C 227, or immersion in percent NaCl or $CaCl_2$ solution at 100±2°F (38±1°C).
3. M = month.

Storage of companion mixtures in the NaCl solutions revealed pronounced differences in performance. For the mixture with no fly ash or lithium, expansion reached 1.44 percent at four months, after which time the specimens no longer fit in the comparator. This indicates that diffusion of NaCl solution into the specimens can greatly increase expansions related to ASR where, for example, NaCl deicer salts are applied to highway structures. In contrast, immersion in $CaCl_2$ produced expansions of 0.132 percent at 9 months, which further supports the indication that the added sodium ion from the NaCl solution resulted in greatly increased expansions associated with ASR, and that the concrete had some constituent that removed the chloride ion from solution.

Immersion in NaCl solutions of specimens with fly ash but no lithium resulted in reduced expansions compared with those with no fly ash, but expansion levels still reached 0.390 percent at 9 months. This represents expansions that are considered excessive with respect to satisfactory performance in highway concrete exposed to NaCl deicer salts. Companion mixtures immersed in $CaCl_2$ solution produced only 0.132 percent at 9 months. Thus, the data suggest Class F fly ash can greatly reduce expansions associated with ASR but may not reduce them sufficiently to prevent associated distress in field structures.

Results presented in Table 4.3 also reveal that the addition of $LiOH \cdot H_2O$ to the fresh mortars at rates of 1.0 percent, 1.5 percent, or 2.0 percent by mass of cementitious material prevented abnormal expansions associated with ASR, even while immersed in the NaCl solutions, and in the presence of fly ash. Thus, lithium ion in these mixtures appeared not to be complexed by cement-fly ash hydration products to the extent that excessive expansions develop due to ASR.

### *4.2.3 Experimental Pavement*

In view of favorable laboratory test results demonstrating its capability to prevent expansion due to ASR, the New Mexico State Highway and Transportation Department agreed to use LiOH in new highway construction in Albuquerque. Location of the experimental pavement was the approach lanes to a bridge on Lomas Boulevard (State Route 352) over I-40.

Ten test sections, each 40 to 60 ft (12.2 to 18.3 m) long, were included in the experimental pavement. Two local sources of sand and gravel, including AL, were used separately in various test sections. In addition to LiOH, a Class F and a Class C fly ash were used separately with each aggregate at approximately 25 percent mass replacement of cement. A single section made with aggregate AL contained 25 percent mass replacement fly ash consisting of 50 percent Class F (the same source) + 50 percent Class C (different source) ash. $LiOH \cdot H_2O$ was added at the rate of 0.5 percent and 1.0 percent by mass of cement with aggregate AL, but only 1.0 percent by mass of cement with aggregate from the other, nearby source. Control sections also were built in which neither fly ash or LiOH was included. A single source of portland cement with approximately 0.55 percent equivalent $Na_2O$ was used through the project. Installation was carried out in June, 1992.

One concern with using LiOH was its uniform dispersion in the concrete batches in the ready-mix trucks. To maximize uniformity, mixing water was introduced into the trucks the night before placement and the appropriate amount of powdered $LiOH \cdot H_2O$ added to the water. The trucks were batched the next day, driven to the job site and the concrete discharged in the forms 20 to 30 minutes after the beginning of mixing. It was found that the presence of LiOH in the concrete had no discernible effect on slump or air content

compared with the control concrete. Also, joint-sawing could be carried out on the schedule for the control concrete. Overall, no schedule allowances were required in the mixing and placing sequences for the LiOH additions.

Subsequent to placement, unused materials were evaluated in the rapid immersion test method to evaluate the ability of the fly ashes to suppress expansive ASR with aggregates from the two sources used in the experiment pavement. Mortar bars also were made to evaluate the effect of LiOH on ASR, using C 227 storage conditions. The proportions of fly ash and LiOH to cement were the same as those used in the pavement. Cement B, with 0.18 percent equivalent $Na_2O$, was used for rapid immersion tests in 1N NaOH solution.Results for the rapid immersion tests are summarized in Table 4.4. Results for aggregate AL are shown in Figure 4.14. These data indicate that both coarse and fine aggregate from both sources are potentially deleteriously reactive since they all greatly exceed the 0.08 percent test criterion. This confirms previous field performance observations. These results also indicate the use of the Class C fly ash had little beneficial effect on suppressing ASR, whereas the Class F ash reduced expansions below the test criterion. Specimens containing the Class C + Class F mixture produced expansion somewhat greater than the test criterion. Continued monitoring of this experimental pavement over a period of years should validate these test results. Test mixtures containing LiOH admixtures and stored under C 227 conditions are too young to provide meaningful results. Thus, they are not reported here.

## 4.3 Conclusions

This section describes investigations into the use of lithium salts to prevent abnormal expansion due to ASR when used as an admixture to fresh mortar. Reaction chemistry and results for mortar test specimens are reported.

The concept of possibly using lithium salts to mitigate deleterious ASR was initially reported in 1951, but it received almost no attention over the succeeding 40 years. The idea was investigated most thoroughly in this project. The following conclusions are drawn, based on this work.

1) In whatever form lithium salt is added, the lithium salt is converted to LiOH in the pore solution.

2) LiOH itself produces an ASR-type reaction product which appears to be non-expansive. In the presence of sodium and potassium hydroxide in pore solutions, ASR products are formed which incorporate lithium as well as the other alkali cations. The higher the lithium dosage the greater the proportion incorporated in the ASR gel formed.

3) It appears that a molar ratio of sodium to lithium of at least 1.0 to 0.50 to 1.0 to 0.60 is required to prevent expansive ASR, depending on the aggregate.

4) Further tests indicated that LiOH, when used as an admixture with fly ash, could further suppress expansion due to ASR.

Table 4.4 Results of rapid immersion tests on samples of materials used in New Mexico experimental pavement

| Aggregate | Fly Ash | Percent Expansion 3D | 7D | 14D |
|---|---|---|---|---|
| AL - Coarse | None | .330 | .580 | — |
| AL - Fine | None | .245 | .502 | — |
| AL - Fine | Class C | .235 | .405 | — |
| AL - Fine | Class F + C | .023 | .052 | .125 |
| AL - Fine | Class F | .010 | .017 | .045 |
| Alternate-Coarse | None | .347 | .575 | — |
| Alternate-Fine | None | .268 | .511 | — |
| Alternate-Fine | Class C | .213 | .400 | — |
| Alternate-Fine | Class F | .009 | .015 | .055 |

Notes: 1. All results are the averages for three companion mortar bars.
2. Absence of results indicates tests were previously terminated.
3. D = days.

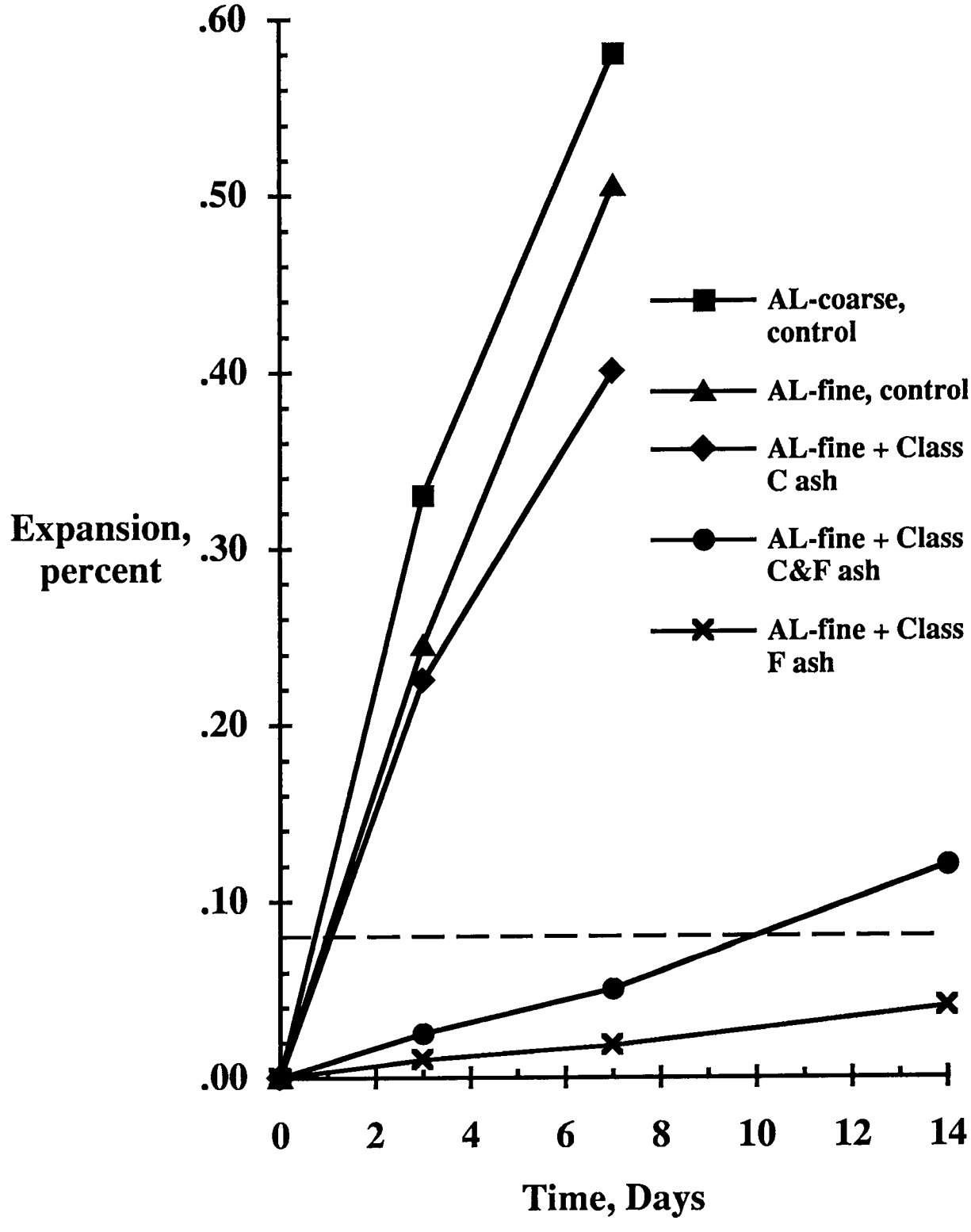


Figure 4.14. Results of rapid immersion tests on samples of aggregate AL and fly ashes used in New Mexico experimental pavement.

5) Lithium hydroxide, when used as an admixture in mortars containing fly ash and stored in NaCl solution (simulated deicer salt applications), effectively reduces expansions due to ASR where companion mixtures made without LiOH showed high expansion levels.

The highly effective nature of lithium in suppressing expansive ASR in the laboratory was applied in pavement test sections in Albuquerque, New Mexico where highly reactive aggregate was used. Comparisons of performance will be monitored in the future. Laboratory results on samples of materials used in the pavement indicate a Class C fly ash replacement for cement will not effectively prevent abnormal expansion due to ASR but that Class F fly ash should prevent such expansion.

# 5.0 Mitigating ASR in Existing Concrete

Numerous highway structures exist in which ASR-related distress has developed, or is likely to develop in the future. Prolonging the service life of these structures thus became of primary significance in this project, and constituted essentially all of the effort expended in Task C.

Various options available to prevent deleterious ASR in new construction appeared also to be possible approaches to mitigating ASR in existing structures. These can be classified into two categories: interference in the mechanism of the reaction, and treatment of symptoms of the reaction. Review of the published literature and consultation among investigators in this project suggested the following possibilities:

Mechanistic interference
1) Treatment with lithium salts
2) Drying
3) Sealants

Treatment of symptoms
1) Restraint
2) Crack filling

Results of investigations into these approaches are described below.

## 5.1 Treatment with Lithium Salts

Investigations described earlier in this report demonstrated the strong capability of adding lithium salts to fresh concrete to prevent abnormal expansion due to ASR. It appeared that treatment with lithium salts, specifically LiOH, might also arrest development of expansive ASR in existing concrete. This would require that lithium ion participate in any further reaction, and also that further expansion of existing ASR gel does not result in continued expansion of the concrete.

Accordingly, laboratory studies were undertaken using mortar bars made with highly reactive aggregate AL and portland cement A with 1.00 percent $Na_2O$ equivalent. These mortar bars were proportioned, made, and cured in accordance with ASTM C 227, then transferred to storage over water in sealed containers held at $100\pm2°F$ ($38\pm1°C$). The plan under this storage was to allow expansions to reach certain levels, remove the mortar bars from storage, apply the intended treatment, than return them to storage. Based on previous testing, it was concluded that this cement-aggregate combination should reach 0.70 percent to 0.90 percent expansion in one year. To evaluate the effectiveness of various treatments in arresting expansive ASR, several sets of four companion mortar bars were removed from

storage when average expansion reached approximately 0.15 percent to 0.20 percent and 0.43 percent to 0.46 percent under C 227 storage conditions. The various treatments were then applied and the specimens returned to C 227 storage and monitored for length change. In some cases, repeating treatments were made when average expansion for control specimens reached about 0.34 percent.

The following test regimes were included in this series. All drying was done at 100°F (38°C), 30 percent RH. Soaking was done at 73°F (23°C).

| No. | Test Regime |
|---|---|
| 1) | Continuous storage over water in sealed containers at 100°F (38°C), per ASTM C 227. |
| 2) | Expansion to 0.19 percent, dry 1 day, soak 2 days in saturated LiOH solution, return to C 227 storage to 0.22 percent expansion, dry 1 day, resoak 2 days in saturated LiOH solution, return to C 227 storage to age 25 months. |
| 3) | Expansion to 0.43 percent, dry 1 day, soak 2 days in saturated LiOH solution, return to C 227 storage to age 25 months. |
| 4) | Expansion to 0.16 percent, dry 1 day, return to C 227 storage to age 90 days, dry 1 day, return to C 227 storage to age 25 months. |
| 5) | Expansion to 0.28 percent, dry 1 day, soak 2 days in saturated $Li_2CO_3$ solution, return to C 227 storage to age 25 months. |
| 6) | Expansion to 0.43 percent, dry 1 day, soak 2 days in saturated LiF solution, return to C 227 storage to age 25 months. |
| 7) | Expansion to 0.43 percent, dry 1 day, soak 2 days in 0.70N NaOH solution, return to C 227 storage to age 25 months. |
| 8) | Expansion to 0.16 percent, soak in water 2 days, return to C 227 storage to 0.23 percent expansion, soak 2 days in water, return to C 227 storage to age 25 months. |

Results for this series are summarized in Table 5.1. These data demonstrate that introduction of LiOH solution into hardened mortar already exhibiting large expansion due to ASR can arrest development of further ASR-induced expansion. This is more clearly seen in Figure 5.1, where mortar bars already exhibiting major expansion due to ASR showed little measurable expansion after treatment. In contrast, the control specimens continued to expand significantly.

Figure 5.2 shows the effect, on subsequent expansion, of introduction of saturated LiOH, $Li_2CO_3$, and LiF solutions. These curves indicate LiOH solutions are more effective in controlling expansive ASR than $Li_2CO_3$ and LiF solutions. The relative effects of these solutions are shown in the following tabulation.

Table 5.1 Results for mortar bars subjected to various treatments during test storage

| No. | Test Regime | Percent Expansion | | | | | | | | | | |
|---|---|---|---|---|---|---|---|---|---|---|---|---|
| | | 32D | Dry 1D | Soak 2D | 56D | 90D | Dry 1D | Soak 2D | 4M | 9M | 15M | 25M |
| 1 | Continuous, C 227 | .194 | — | — | .278 | .335 | — | — | .376 | .596 | .700 | .766 |
| 2 | Soak, Resoak, Sat. LiOH | .188 | .143 | .205 | .211 | .215 | .174 | .223 | .227 | .247 | .241 | .243 |
| 3 | Soak, Sat., LiOH | .182 | — | — | .331 | .434 | .380 | .437 | .446 | .460 | .462 | .465 |
| 4 | Dry, Redry | .205 | .156 | — | .340 | .436 | .380 | — | .498 | .670 | .741 | .767 |
| 5 | Soak, Sat., $Li_2CO_3$ | .190 | — | — | .218 | .276 | .223 | .288 | .296 | .315 | .367 | .385 |
| 6 | Soak, Sat., LiF | .187 | — | — | .236 | .310 | .263 | .328 | .338 | .475 | .557 | .566 |
| 7 | Soak, .70N NaOH | .196 | — | — | .318 | .431 | .377 | .444 | .531 | .904 | .958 | .966 |
| 8 | Soak, Resoak, Water | .142 | .090 | .161 | .173 | .230 | .174 | .248 | .254 | .273 | .354 | .392 |

Notes: 1. Results are the averages of four companion specimens, with the exception of No. 7, which are the results for three specimens.
2. Absence of data indicates measurements were not required by the test regime and were not obtained.
3. D = day; M = month.

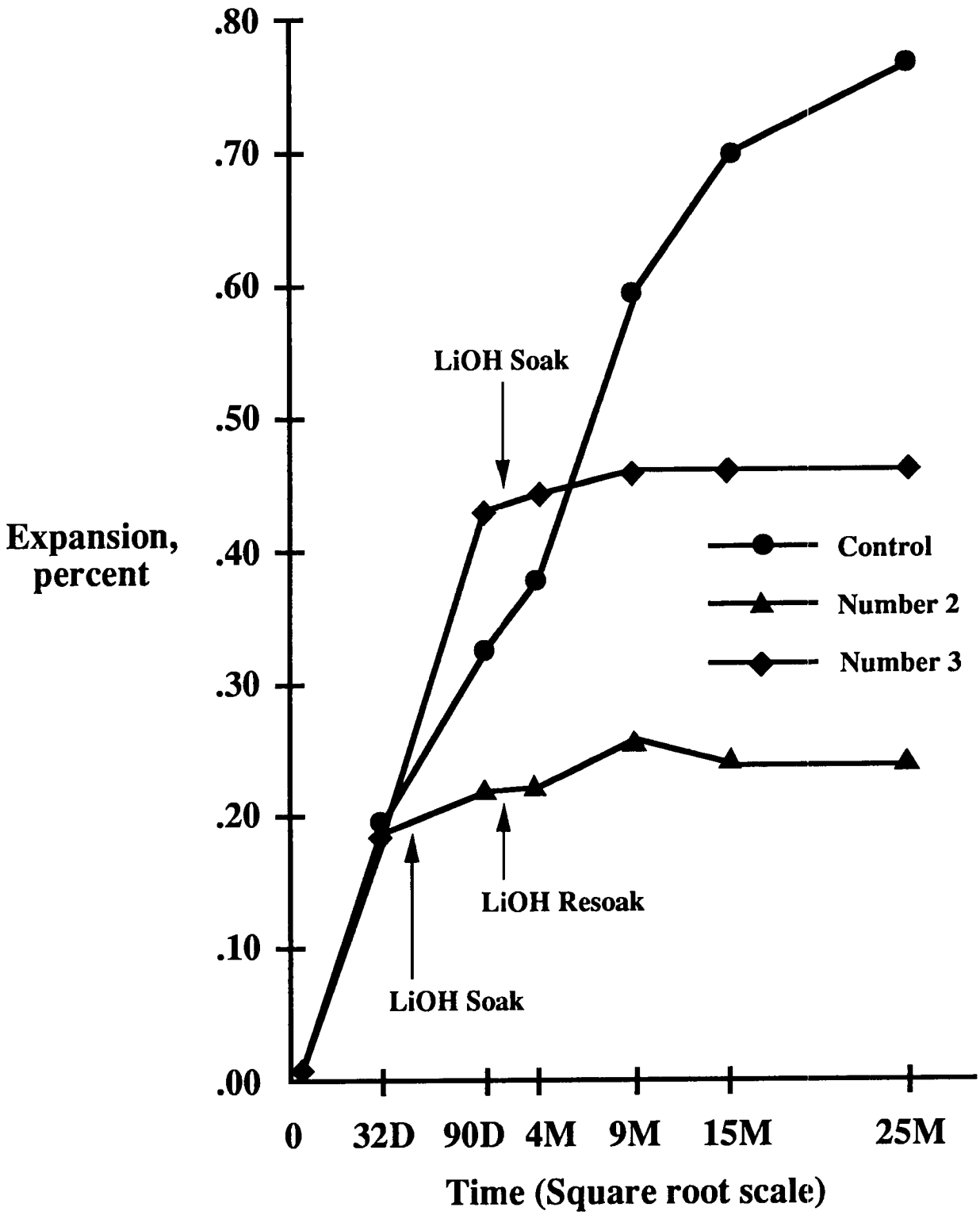


Figure 5.1. Effect of the treatment with LiOH solution on expansion due to ASR.

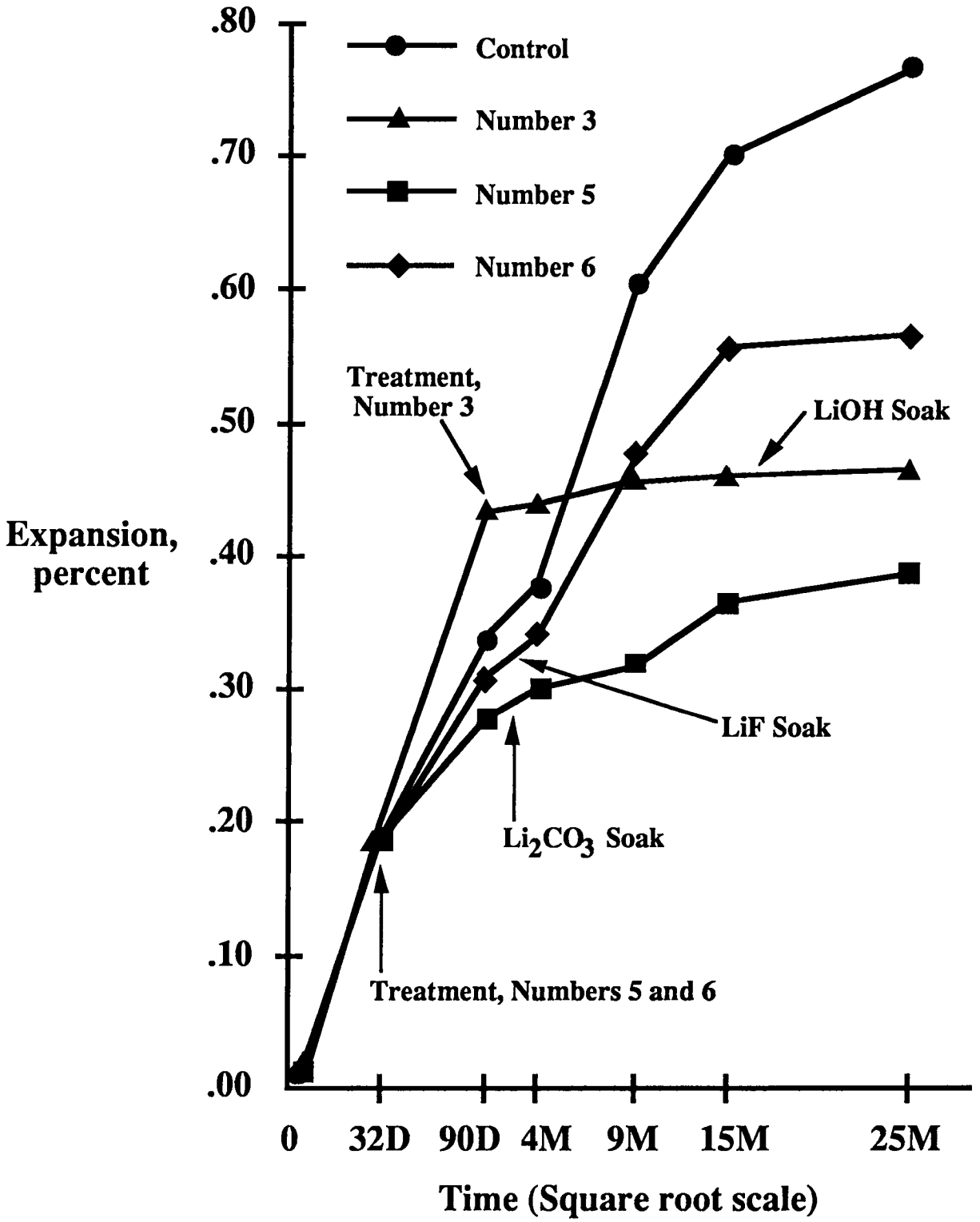


Figure 5.2. Effect of various lithium salt treatments on expansion due to ASR.

| Solution (saturated) | Percent increase in expansion after age at which treatment is applied |
|---|---|
| LiF (No. 6) | 77 |
| $Li_2CO_3$ (No. 5) | 35 |
| LiOH (No. 3) | 6 |
| Control No. 1 (C227) | 129 |

Solution (saturate Data in this table indicate that average expansion of the control (untreated) specimens from the time just prior to treatment of the other specimens (90 days) was more than double (129 percent) the expansion just prior to treatment, while expansions for specimens treated with LiOH solution increased only 6 percent. Intermediate results were obtained for specimens immersed in $Li_2CO_3$ or LiF solution. Differences among the lithium salt treatments undoubtedly reflect differences in solubility of the salts in water, with LiOH being highly soluble. These results also suggest that not only was expansive new reaction controlled by the lithium ion, but also further expansion due to swelling of ASR gel formed prior to treatment. LiOH treatment thus could be an effective means of controlling expansive ASR in highway concrete, provided a means could be devised for the applied solution to penetrate the full depth of highway pavement.

Additional data in this series are plotted in Figure 5.3. Here it is seen, for example, that two separate one-day periods of air-drying at 100°F (38°C) and 30 percent RH had essentially no effect on expansion (No. 4) over the 25-month test period, compared with the control mixture. It could be reasoned that drying might result in less long-term expansion because of additional sorption by cement hydration products of alkali in the more alkaline pore solution. Or, it could be argued that the resulting more highly concentrated alkaline solution would initiate more intense ASR, thereby resulting in greater expansion due to subsequent uptake of moisture by ASR gel after rewetting. Whatever their relative importance, the net result appears to be no measurable effect on expansion at 25 months.

Figure 5.3 also shows the effect of two separate two-day immersions in water immediately following single days of drying (No. 8). Under these conditions, alkali would be expected to leach into the immersion water, thus tending to reduce expansions. This indeed appeared to be the case over a short period of time. However, later expansions (9 to 25 months) appeared to be developing at rates only slightly less than those for the control specimens. If leaching did occur, it had only minor ameliorating effects as expansions of more than 0.15 percentage points developed in this time period.

One other treatment was carried out which resulted in predictable effects. Immersion in 0.70N NaOH solution (No. 7) exacerbated ASR and ultimately produced the greatest expansions at 25 months.

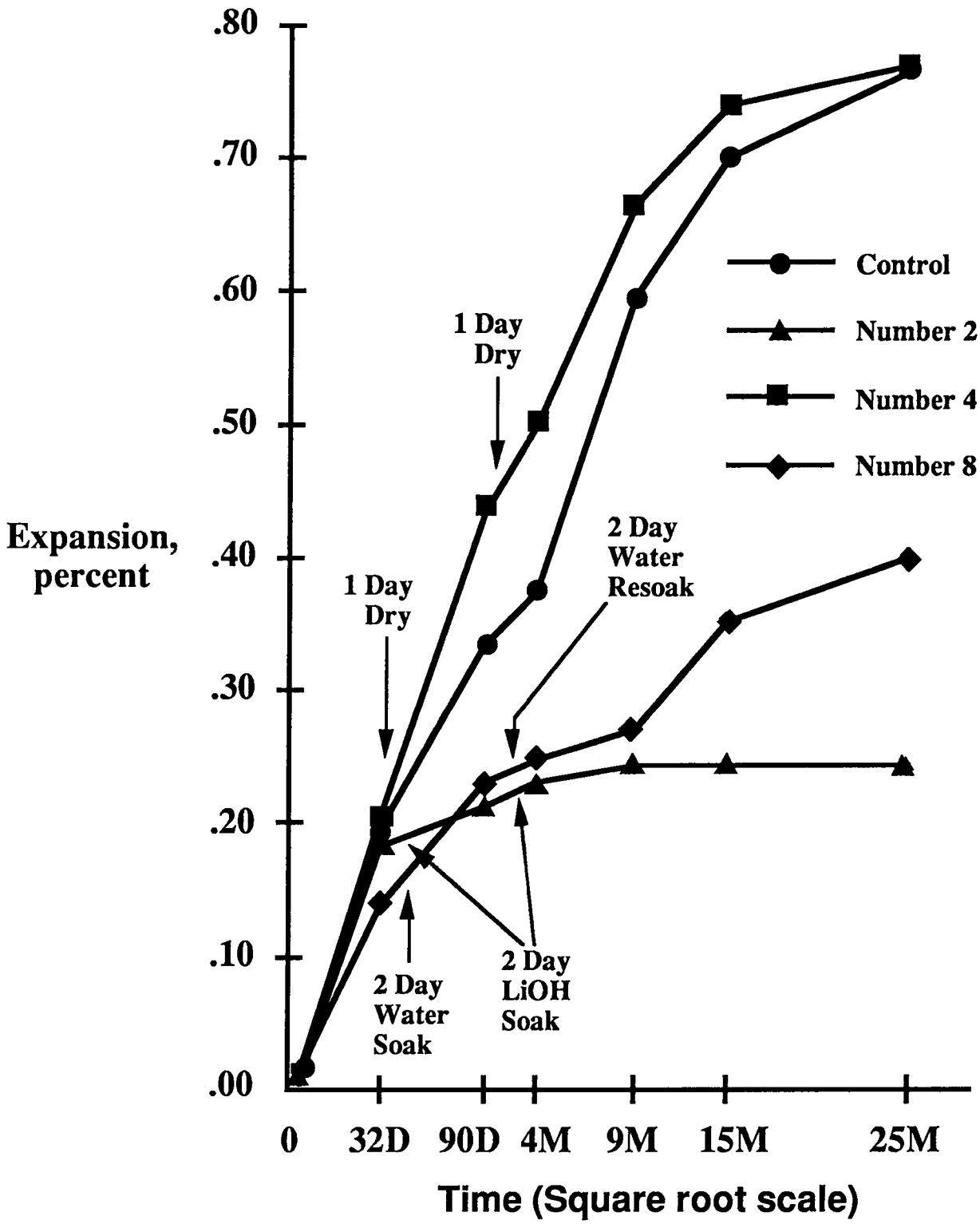


Figure 5.3. Effect of various treatments on expansion of mortar bars.

Based on these results, it was concluded that treatment with LiOH solution was most effective in controlling expansive ASR. This approach was used in sections of I 80 pavement in Nevada, as described in Section 5.5.

## 5.2 Use of Sealants to Mitigate ASR

Reports exist in the published literature in which it was concluded that certain sealants and coatings reduce expansions due to ASR (e.g., Kobayashi, et al. 1989). This reported effect appears to be due primarily to limiting ingress of moisture into the concrete, thereby minimizing swelling of ASR gel.

Laboratory studies on sealants were not conducted in Project C-202, but limited determinations of RH gradients were carried out in field applications in Wyoming where several products, mostly silanes and/or siloxanes, were applied to a bridge deck in the Sun Valley Interchange on I-80 near Cheyenne. Control sections with no treatment were included. Silane applications also were made on I-80 pavement near Cheyenne, which displayed distress due to ASR. RH determinations were made at various depths in the test and control (untreated) sections in June, 1991.

Results of the bridge deck determinations are shown in Figure 5.4. All determinations were made in the gutter area where traffic wear would be at a minimum. Measured bridge deck thickness at these locations was 7 in. (178 mm). Comparison of the test and control sections show little significant difference, with RH values being in the range of 50 percent to 65 percent at mid- and lower depths. The only significant difference lies in two test sections where RH values at 1/2 in. (13 mm) depth range down to 40 to 42 percent. As expected, RH values for a given section are greatest near mid-depth and less near top and bottom surfaces where atmospheric drying can occur most readily. In all sections, however, RH values were below the 80 percent RH threshold level required to sustain expansive ASR. Only two of the four products applied appeared to have had some benefit in the top 1/2 to 1 in. (13 to 25 mm) of deck but no discernible effects at greater depths.

RH determinations in the pavement slabs in I-80 that were treated with silane ranged from 81 percent near the top surfaces to 85 percent to 95 percent in the middle and lower levels. These greater values, compared with those taken in the (nearby) bridge deck a day later reflect the role of subbase moisture in maintaining RH values sufficiently high to support expansive ASR. This is revealed in the presence of surface cracking typical of that associated with ASR.

In summary, the application of the sealants appeared to have little or no meaningful effects in the bridge deck, and they did not reduce RH values in pavement slabs below the threshold level required for expansive ASR.

## 5.3 Crack Filling

One method that has been used to fill cracks in pavement concrete exhibiting distress due to ASR is the application of high molecular weight methacrylate (HMWM) to the wearing surfaces. In this approach, the expectation is for HMWM to penetrate surface cracks sufficiently to strengthen the affected slab, thus extending the service life of the pavement.

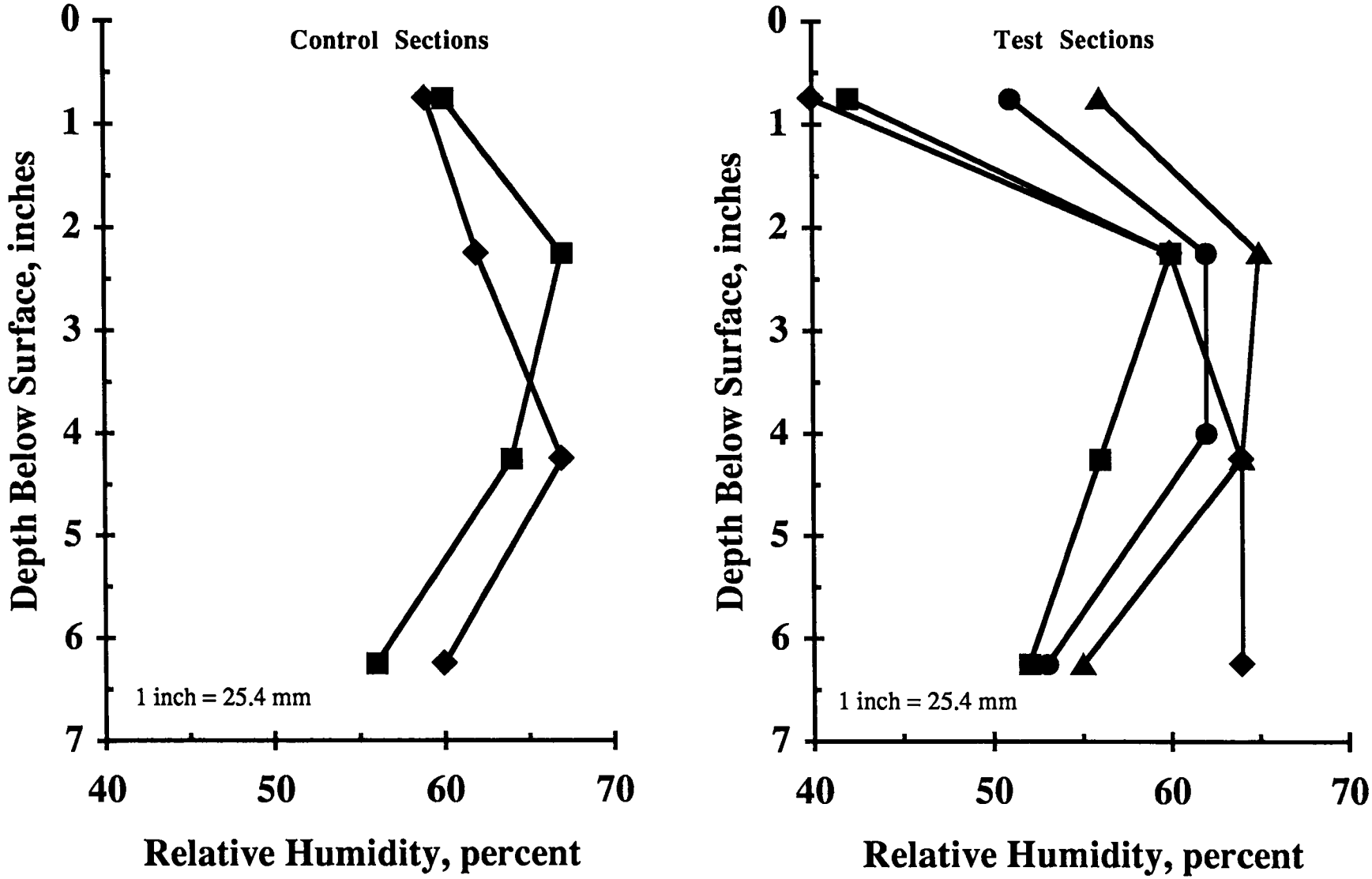


Figure 5.4. Relative humidities of Wyoming bridge deck concrete in control sections and sections with surface sealants.

This method was used in sections of State Route 58 near Boron, California. This is a four-lane divided pavement built in the early 1970s using low-alkali cement and coarse and fine aggregate from source OR, included in project C-202. The time of first appearance of abnormal cracking is not reported. In 1988, HMWM was broomed on to the surface and a sand layer applied to preserve acceptable skid resistance. In 1991, full-depth, 4 in. (102 mm) diameter cores were removed for examination. Measurements on vertical finely-lapped surfaces indicated penetration of HMWM in cracks up to 2 in. (51 mm). This is the approximate maximum depth observed of the surface cracks. Cracks as narrow as approximately 0.002 in. (0.051 mm), or slightly less, were found to be filled with HMWM.

This method appeared to have promise of extending pavement service life, but further field testing appeared to be needed, together with some method of better characterizing performance. This is discussed later.

## 5.4 Drying

It has been recognized for many years that the deleterious effects of ASR in existing concretes can be delayed or mitigated to a considerable extent by drying out the concrete and attempting to prevent its resaturation.

For pavements and highway structural concrete exposed to ambient weather conditions in wet climates, this has not usually been considered a practical solution. These tend to be rewetted or resaturated frequently. Even in dry climates pavements tend not to dry thoroughly but to remain surprisingly wet due to the accumulation of moisture condensing underneath the pavement.

Some benefits have been reported for mostly experimental installations in which vapor-permeable silanes and similar coatings have been applied to highway structures. Such coatings are said to be impermeable to liquid water, but permit water vapor movement. The idea is to permit vapor-phase drying of the protected concrete during dry periods and keep them from getting rewetted during wet periods. For a number of reasons, only partial success is generally achieved.

In considering the mechanism of the benefits derived from such treatments, and from drying of concrete generally, it has usually been assumed that the ASR gel reaction product stops swelling during the period of drying, and that the ASR reaction itself might slow down as the concrete pore solution retreats to the interstices of capillary spaces. For concrete subject to periodic rewetting both of these effects would appear to be temporary and last only until the next wetting episode; on rewetting of the concrete, further swelling of the ASR gel and a resumption of the previous rate of ongoing ASR reaction would be expected.

This presumption has made the deliberate expenditure of funds and the development of technical procedures to dry out ASR-affected highway concrete generally unattractive, since it is almost impossible to guarantee that dried-out pavements and other structures are not eventually resaturated. Even applications of vapor-permeable coatings need to be renewed periodically or they lose their effectiveness.

Surprisingly, it has been determined that some of the effects of drying of concrete tend to be irreversible, or might be beneficial for prolonged periods of time. This determination involves the findings of previously unexpected fixation of a substantial portion of the alkali

hydroxide in the pore solution on drying, in such a way that on resaturation (or even prolonged soaking) it is not returned to solution. This fixed alkali hydroxide is thus unavailable for further ASR, and the rate at which ASR can continue after rewetting is substantially diminished.

Some of the details of the experiments leading to these unexpected findings are provided below.

### *5.4.1 Background*

Experience has shown that concretes from structures that have been allowed to dry out in the normal course of exposure yield, in expression of pore solution, little or no solution. For such concretes attempts were made to bring the water content back up to the saturated surface-dry condition before expressing solution and analyzing it, the presumption being that since the alkali hydroxides are highly soluble, the pore solution concentration should quickly reestablish its original level before the concrete was dried. It was found that, even after allowing for any loss of alkali by leaching in the resaturation process, the alkali hydroxide concentration in the pore fluid of the resaturated concrete was very much lower than it should have been, given the alkali content of the cement thought to have been used. On the other hand, cores taken from field galleries in a dam structure that had apparently been continuously wet showed the expected level of alkali hydroxide concentration in the pore solution. It thus appeared that much or most of the alkali hydroxide from the pore solution had somehow become fixed by drying of the concrete and not returned to the pore solution on rewetting, even though water saturation of the concrete had been obtained.

### *5.4.2 Results of Laboratory Studies*

Laboratory experiments were initiated to investigate the validity of these observations. They have been carried out on laboratory-prepared cement pastes, mortars, and concretes, with basically similar results. Nearly fully hydrated specimens of each kind (2 in. (51 mm) diameter cylinders, suitable for pore solution expression) have been air dried in laboratory air (typical RH close to 50 percent) for periods ranging from several weeks to six months or more, with careful account being kept of the change in mass. Replicate specimens have been analyzed to determine the evaporable and non-evaporable water contents at this point. After the air-drying period, specimens have been subjected to a vacuum saturation procedure derived from the AASHTO T 277-83 method used to saturate concrete samples for the chloride permeability test. Both the gain in water content and the (usually small) amount of alkali hydroxide that leached out of the specimens during vacuum saturation were monitored. After vacuum saturation, the specimens were subject to continuous additional soaking in water for up to several weeks, or to prolonged storage in sealed containers (at the saturated moisture content) for periods up to 13 months. The alkali hydroxide concentrations were determined (a) in companion samples kept continuously sealed and never subjected to air drying, (b) in samples air dried for prolonged periods and then resaturated, and (c) in re-saturated samples exposed to further prolonged wet storage after the resaturation process.

The experiments required a number of corrections and very careful attention to details of handling, which will not be considered here.

In each case it was found that:

1) Sealed (never dried) specimens after vacuum saturation yielded pore solution of the expected concentration of alkali hydroxide, based on the materials used and their proportions including the alkali content of the cement used. The expected alkali concentration includes allowance for the estimated dilution of the pore solution on saturation, the sealed specimens normally being less than fully saturated.

2) Specimens that were air dried and then vacuum re-saturated yielded pore solutions of very much lower alkali hydroxide concentrations than expected, even after accounting for the leaching of alkalis in the re-saturation process. A substantial part of the alkali had been fixed by the air drying process.

3) On subsequent prolonged exposure to wet conditions, there was some recovery toward the expected alkali hydroxide concentration level, but this recovery was only partial and limited in extent.

4) The fixation effect was more pronounced for concrete than for either mortar or cement paste, and generally greater for the $K^+$ ion than for the $Na^+$ ion in a given cement.

5) The $OH^-$ ion concentrations were reduced quantitatively to the same degree as the alkali ion concentrations, confirming that what was being fixed was alkali hydroxide.

Table 5.2 provides data for the pore solutions expressed from (a) a concrete continuously sealed for 7 days, and (b) another specimen similarly sealed, but then allowed to dry out for 15 months, followed by vacuum saturation and further wet sealed storage for 8 days. The alkali hydroxide level after resaturation followed by a post-saturation equilibration period of 8 days in sealed storage was only about a quarter of the normal expected level due to "fixation" of most of the alkali hydroxide.

In experiments in which calcium chloride had been incorporated into the mixing water, it was found that the chloride ions remaining in solution during the normal hydration were not fixed by air drying, but were recovered in concentration equivalent to that in never-dried companion specimens. Thus the fixation effect is confined to alkali hydroxides, and is not general for all substances dissolved in the pore solution.

### *5.4.3 Possible Mechanism of Alkali Fixation*

A number of possible mechanisms for the observed fixation effect were considered, and several exploratory studies were carried out. It appears that the effect somehow involves carbonation, since (a) in a study in which room temperature drying was carried out under nitrogen flow in the absence of carbon dioxide the alkali fixation process was not found to have taken place, and (b) a concrete specimen continuously sealed for a prolonged period, then quickly oven dried at 220°F (105°C) over the course of one day, showed only a modest fixation as compared to a companion specimen slowly air-dried over the same period that its companion had been sealed. The oven drying would have provided only limited opportunity for carbonation.

Table 5.2 Comparison of analytical results of pore solution for Cement B for 0.50 water to cement ratio concrete specimens (a) continuously sealed for 7 days and (b) sealed for 7 days, air dried for 15 months, vacuum saturated, and resealed for 8 days

| Description | | Concentration, N | | |
|---|---|---|---|---|
| | | $Na^+$ | $K^+$ | $\Sigma+$ |
| Expected concentration estimated by applying dilution factor (1.45) to original continuously sealed concentration results | Analysis as determined, diluted to reference SSD state | 0.094 | 0.209 | 0.303 |
| Actual concentrations after saturating formerly air-dried specimen (corrected for leaching) and resealed for 8 days | Analysis as determined | 0.036 | 0.025 | 0.061 |
| | Correction for leaching of alkalies | 0.008 | 0.011 | 0.019 |
| | Net concentration corrected for leaching | 0.044 | 0.036 | 0.080 |
| Percent of expected alkali concentration actually found in pore solution from air dried specimen | | 47% | 21% | 26% |

It should be noted that in no case was the depth of carbonation, as measured with phenolphthalein, complete. Visible carbonation was confined to the external zone of each cylinder, and in some cases to narrow zones around cracks. Nevertheless, some indications of the formation of carbonation products (calcite and vaterite) were found by x-ray diffraction in the central portion of the specimen examined, even though most of the calcium hydroxide here had remained unreacted. Despite extensive efforts to do so, no crystalline compound was detected that could be identified as the repository for the fixed alkali hydroxide.

It thus appears that the mechanism somehow involves carbonation, but the effect extends far beyond the narrow zone of visibly carbonated concrete as detected by the phenolphthalein test.

### *5.4.4 Permanence of the Alkali Fixation Effect*

Studies were carried out to assess the permanence of the alkali fixation effect by monitoring the rate at which fixed alkali could be returned to solution, not within the limited confines of the tight pore structure in concrete, but under conditions of easy access to water. Paste specimens, after air drying, were crushed to sizes between about 0.40 in. (10 mm) and 0.02 in. (0.5 mm). Small amounts were then suspended in glass bottles and mechanically shaken in distilled water for prolonged periods, with the solutions analyzed periodically. Companion studies were carried out with never-dried pastes. Roughly half the total alkali content of both specimens was released quickly (1 day), but subsequent release was very much slower for the air-dried specimen. At about two weeks of shaking the never-dried paste had reached steady state, at which about 80 percent of its total alkali content was in solution. The corresponding amount was only about 55 percent for the previously air-dried sample. The latter continued to progressively release alkali on continuous shaking to 90 days, at which shaking was terminated. However, the slow release of alkalis into the solution continued at a rate that was linear with the square root of time, and had reached about 75 percent of the total by 9 months.

It thus appears that the fixation is not fully permanent, but reversible only very slowly and incompletely, even when the concrete is crushed and shaken in water. This suggests that the benefit obtained by drying with respect to ASR in field concrete should last for a long time and be reversed only under prolonged saturation, and then only in part.

## 5.5 Experimental Pavement

A deflection monitoring program program was initiated in Nevada to evaluate the effectiveness of surface treatments in mitigating the effects of ASR on pavement structural response. The treatments consisted of a LiOH solution, high molecular weight methacrylate resin, poly-siloxane resin sealer (silane), a second silane sealer, and linseed oil. Testing was done by the Nevada DOT using a falling weight deflectometer (FWD) in October 1991 to establish baseline interior and joint deflections A follow-up testing program was done October 1992 to evaluate treatment effects on deflections after one year. Details of the testing program are given in Appendix B.

### *5.5.1 Pavement*

The test section was selected on eastbound Interstate 80 in Humboldt County, Nevada between mile posts 16.45 and 16.80. The section is just east of Winnemucca located in the northwestern part of Nevada. Built in 1981, the pavement design consists of a plain jointed 8 in. (203 mm) thick concrete slab over a 6 in. (152 mm) cement-treated base, and a 3 in. (76 mm) gravel subbase. An asphalt concrete bondbreaker was used between the cement-treated base and gravel subbase. Non-dowelled skewed transverse joints are spaced at 12, 13, 19, and 18 ft (3.65, 3.96, 5.79, and 5.49 m). Concrete shoulders 10 ft (3.05 m) wide are not tied to the mainline pavement.

### *5.5.2 Treatment*

Three different surface treatments were applied to slab surfaces on October 2, 1991. Each treatment was applied to two test sections, consisting of five slabs per section. Surfaces were sandblasted prior to initial treatment application. Treatments were applied to the outside driving lane. The treatments consisted of a LiOH solution, high molecular weight methacrylate resin, and poly-siloxane resin sealer. In addition to the three different treatments, three control sections, also consisting of five slabs per section, were selected. An additional two treatments consisting of a silane surface sealer and linseed oil treatment were applied to separate five slab test sections during the one year follow-up testing program.

$LiOH \cdot H_2O$ powder was dissolved in water at a dosage rate of 64 lbs per 100 gallons of water (76.85 g/L). Dosage was selected for a 1 to 1 equivalent $Na_2O$:LiOH concentration. The solution was mixed approximately 15 hours prior to application to the entire surface and applied with a power sprayer in three applications. A time period between applications allowed for lithium penetration into surface cracks. The residue remaining on the surface after the second application was rinsed off with water the next day. A second treatment was applied but not rinsed off during the one year follow-up testing program.

The methacrylate was a two-component, rapid curing, solvent-free high molecular weight methacrylate resin used for crack repair. The two components were mixed in buckets on site and applied by Nevada DOT personnel. The gravity flow methacrylate was applied by squeegeeing a thin film over the entire surface. The film was allowed to pond over superficial cracks. Within 30 minutes the surface was covered with a light broadcast of dry sand to restore skid resistance. The poly-siloxane resin (silane) was a single-component, colorless liquid formulated to seal cementitious surfaces. The resin produces a water-repellent penetrating sealer which can close the pores of cementitious substrates. Silane was applied by hand sprayers to the entire test section surface. The silane treatment was not applied during the follow-up testing.

An additional two treatments were applied to separate slab sections during the one year follow-up testing program. A second type of silane sealer, manufactured by a different company, and linseed oil were applied. Similar to the initial applications of the other treatment, the surface preparation consisted of a light sandblast to thoroughly clean the surfaces. Silane was applied by the manufacturer's technical representatives. Linseed oil was applied by DOT personnel at the manufacturer's recommended rates. One 5-slab test section per treatment was selected for deflection testing during the follow-up visit.

Test sections were selected within an 82-slab area just east of Winnemucca, Nevada in the eastbound driving lane on I-80. Based on visual inspection of surface cracking the control, lithium, silane, and methacrylate treatments were randomly assigned into five slab sections. One set of treatments at the west end of the test area was located in a less severely distressed (surface) area than the second set of treatments at the east end of the test area. The test layout is shown in Figure 5.5.

### *5.5.3 Test Procedure*

Deflections were acquired by the Nevada DOT using the State FWD. Deflections measured in October 1991 were used as a baseline to evaluate effectiveness of treatments in reducing the rate of structural deterioration due to ASR. Deflections were measured in the slab interior at the center of the slab and at the joint 18 in. (46 mm) from the lane-shoulder longitudinal joint. Deflections at the slab interior along the slab longitudinal centerline axis were measured under the load and at 8, 12, 18, 24, 36, and 60 in. (203, 305, 457, 610, 914, and 1524 mm) away from the load in the direction of traffic. Transverse skewed joint testing was done with the load positioned on the leave slab with the edge of the plate immediately adjacent to the joint. Deflections were measured under the load, 12 in. (305 mm) from the load on the unloaded slab (approach), and on the loaded slab (leave) at 12, 18, 24, 36, and 60 in. (305, 457, 610, 914, and 1524 mm) away from the load in the direction of traffic.

Tests were conducted before treatment application on October 2, 1991. Deflections were also measured in the three control sections and the two methacrylate sections on October 3, 1991, one day after treatment. Tests were done to evaluate deflection repeatability and to evaluate effectiveness of the methacrylate penetrating resin in reducing deflections at one day. Follow-up testing was done on October 7 and 8, 1992, approximately one year after treatment application.

Baseline deflection testing was also conducted at mid-slab 18 in. (46 mm) from the lane-shoulder longitudinal joint. Deflections at the slab edge were measured under the load and at 8, 12, 18, 24, 36, and 60 in. (203, 305, 457, 610, 914, and 1524 mm) away from the load in the direction of traffic.

### *5.5.4 Treatment Analysis*

Normalized deflections (triplicate test average) were adjusted for temperature gradients by multiplying measured deflections by the ratio adjustment factors at each deflection position. Two types of analyses were performed to evaluate the effectiveness of treatments. The first analysis was a paired t-test to statistically evaluate within-treatment differences in deflection magnitudes measured over time. The second type of analysis was an ANOVA (analysis of variance) of the differences in deflections with time to determine if there was a statistical difference between-treatments. If the ANOVA indicated a significant difference in deflections due to different treatments, treatment differences were compared to the replication differences to determine if deflection changes due to treatments are significantly greater than that expected from between-test variability.

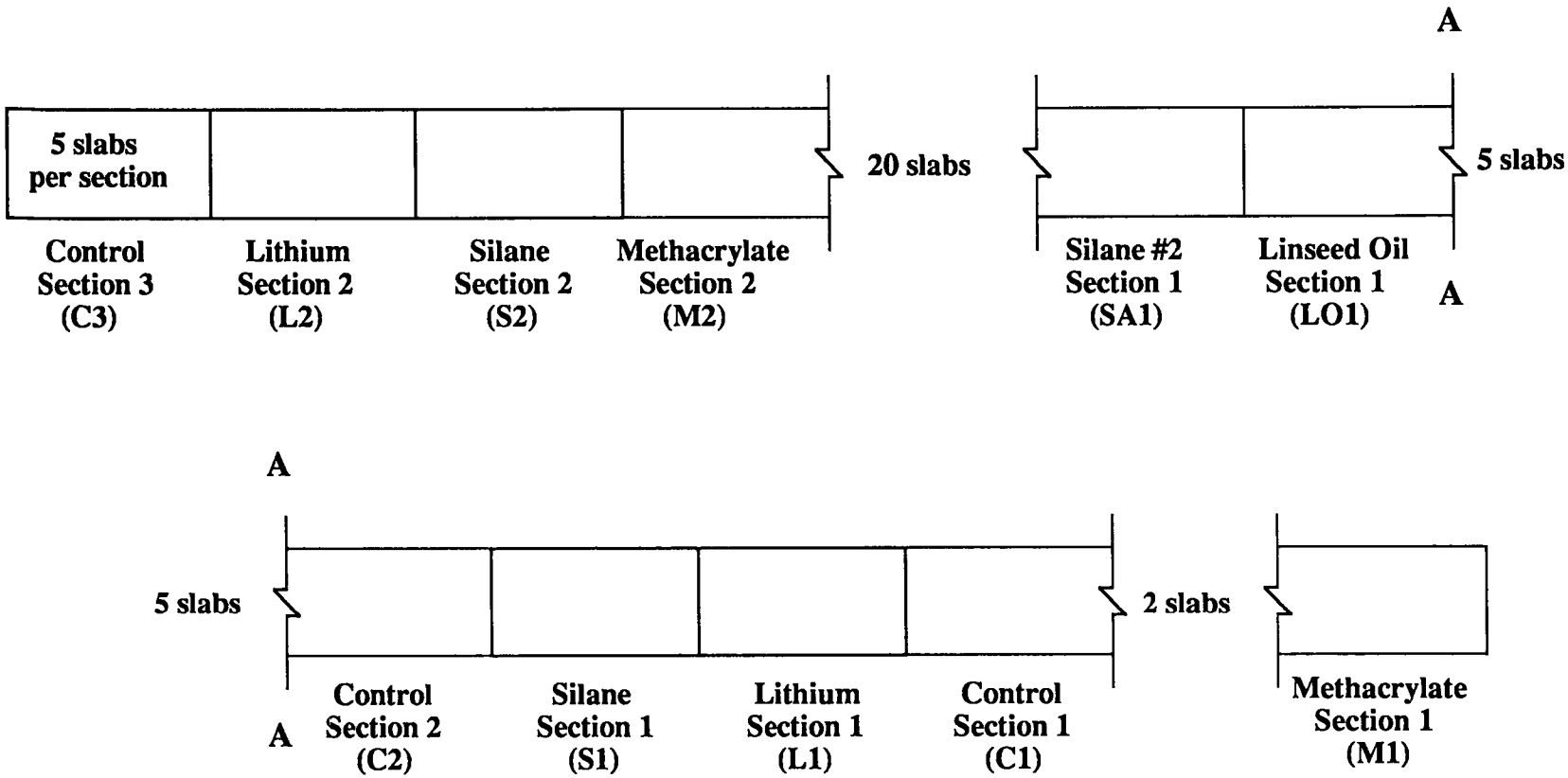


Figure 5.5. Nevada falling weight deflectometer test sections.

The analyses were performed on interior and joint measurements made before treatment and at one year. A similar analysis was made for control and methacrylate data before treatment and one day after treatment to detect any immediate decreases (improvement) in deflections. An analysis was also done for the methacrylate and control sections one day after treatment and at one year to determine if significant differences were measured.

### 5.5.4.1 Effectiveness of Methacrylate Treatment at One Day

The paired t-test analysis indicated that interior and joint deflections significantly decreased after methacrylate application. To evaluate the significance of methacrylate treatment deflection decreases an ANOVA was performed of deflection differences (initial minus after treatment). Significant differences were noted between control sections and methacrylate sections. As listed in Table 5.2, for the maximum interior deflection under the load, the average deflection change at one day was an increase of 0.00017 in. (0.004 mm) for control and a decrease of 0.00036 in. (0.009 mm) for the methacrylate sections.

Significant joint deflection differences were also noted between control sections and methacrylate sections for joint deflections. As listed in Table 5.3, for the maximum joint deflection under the load, the average deflection change at one day was an increase of 0.000038 in. (0.001 mm) for control and a decrease of 0.00596 in. (0.151 mm) for the methacrylate sections.

Since average increases in control section deflections were less than the between-test replicate root mean square, the increase in deflections were determined not statistically different than between-test variability expected due to load positioning, load measurement, and deflection measurement. Assuming that average increases measured at one day in the control sections would be equally reflected in the methacrylate sections, the average deflection decrease (difference between average control increase and methacrylate decrease) at one day due to the methacrylate treatment was 0.00052 in. (0.013 mm) for the maximum interior and 0.0060 in. (0.152 mm) for the maximum joint deflection. Average methacrylate section before treatment deflections were 0.00493 and 0.01365 in. (0.125 and 0.347 mm) for interior and joint deflections, respectively. Deflection decreases after methacrylate averaged 10.6 and 43.9 percent for interior and joint deflections, respectively.

### 5.5.4.2 Effectiveness of Treatments at One Year

The paired t-test analysis indicated that interior deflections in general did not significantly change between initial (before treatment) and one year after treatment applications. This indicates that improvements in the methacrylate sections noted at one day were not measured one year later. To evaluate the significance of treatments on interior deflection changes, an ANOVA was performed of deflection differences (initial minus one year after treatment). As a group, significant differences were not noted between treatment types for all interior deflection positions. Since the ANOVA did not result in any statistical differences and no significant difference between any two treatments were noted, it was concluded that at one year observed changes in interior deflections were not statistically different between treatments.

Table 5.3 Summary of maximum average deflections

| | | Interior Maximum Deflection, 0.001 in. | | | | Joint Maximum Deflection, 0.001 in. | | | |
|---|---|---|---|---|---|---|---|---|---|
| | Treatment | Before Treatment Mean | After Treatment Mean | Mean Difference | Standard Deviation of the Mean Difference | Before Treatment Mean | After Treatment Mean | Mean Difference | Standard Deviation of the Mean Difference |
| Before and One Day After Treatments | Control | 5.281 | 5.449 | -0.167 | 0.151 | 9.777 | 9.816 | -0.038 | 2.307 |
| | Methacrylate | 4.926 | 4.567 | 0.356 | 0.194 | 13.648 | 7.691 | 5.960 | 1.492 |
| Before and One Year After Treatments | Control | 5.281 | 5.317 | 0.036 | 0.625 | 9.777 | 11.917 | 2.140 | 2.154 |
| | Lithium | 5.030 | 4.850 | -0.181 | 0.349 | 10.477 | 13.550 | 3.071 | 2.487 |
| | Silane | 5.178 | 4.887 | -0.290 | 0.548 | 8.812 | 13.284 | 4.471 | 2.086 |
| | Methacrylate | 4.926 | 4.878 | -0.047 | 0.487 | 13.648 | 10.093 | -3.555 | 1.210 |
| One Day and One Year After Treatments | Control | 5.449 | 5.317 | -0.131 | 0.607 | 9.816 | 11.917 | 2.102 | 1.921 |
| | Methacrylate | 4.567 | 4.878 | 0.312 | 0.511 | 7.691 | 10.093 | 2.404 | 1.441 |

Notes: 1. At one day, positive difference if decreasing deflection.
2. At one year, positive difference if increasing deflection.
3. 1 in. = 25.4 mm

The paired t-test analysis indicated that for methacrylate joint deflections, significant decreases in deflections were measured. Significant deflection increases were measured in both silane sections, Control Section 2, and Lithium Section 1. Most other within-treatment changes in deflections were statistically insignificant. The *t*-test analysis indicates that the significant decreases in methacrylate section joint deflections measured one day after treatment are still apparent while other treatment section joint deflections have increased with time. To evaluate the significance of treatments on joint deflection changes, an ANOVA was performed of deflection differences (initial minus one year after treatment). As a group, significant differences were noted between treatment types. Decreases in methacrylate section deflections were significantly different than the increases measured in the control, lithium, and silane sections. Significant increases were also noted between control and silane sections under the load and 12 in. (305 mm) away from the load. This observation was expected since the t-test analysis indicated that significant decreases in the methacrylate treated sections occurred while other section deflections remain unchanged (or increased) between before treatment and one year after treatment deflections.

The ANOVA indicated significant statistical joint deflection decreases at one year in the methacrylate sections. As listed in Table 5.2, the average deflection change was an increase of 0.00214 in. (0.054 mm) for control and a decrease of 0.00356 in. (0.090 mm) for the methacrylate sections.

Since average increases in control section joint deflections were greater than the between-test replicate root mean square, the increase in deflections were assumed statistically different than between-test variability expected due to load positioning, load measurement, and deflection measurement. Assuming that average increases measured at one year in the control section would be equally reflected in the methacrylate sections, the average deflection difference at one year due to the methacrylate treatment was 0.00570 in. (0.145 mm) for the maximum joint deflection. Average methacrylate section before treatment joint deflection was 0.01365 in. (0.347 mm). Joint deflection decrease after methacrylate averaged 41.8 percent.

### 5.5.4.3 Effectiveness of Methacrylate After Treatment and at One Year

The ANOVA of differences between before treatment and one year after treatment indicated significant methacrylate section joint deflection decreases but insignificant changes in interior deflections. The analysis implied that after one year when treated with methacrylate, interior deflection differences were no different than the control sections with no treatment.

The t-test and ANOVA test were done on the one day after and one year after application data to evaluate the effectiveness of methacrylate with age. The interior deflection t-test indicated insignificant changes in deflections. This implies both that the control and methacrylate section interior deflections did not significantly change. Maximum interior deflections and changes between one day and one year after treatment are summarized in Table 5.2.

For joint deflections, the paired t-test indicated that deflections increased in all sections except Control Section 3 and Methacrylate Section 2. Insignificant deflection changes in Control Section 3 were also determined before and one day after application and before and one year after treatment. The paired t-test indicates that joint deflection decreases measured at one day were significantly offset by deflection increases at one year in Methacrylate

Section 1 but not in Section 2. To evaluate the significance of joint deflection increases within Methacrylate Section 1, an ANOVA was conducted on deflection differences one day after and one year after methacrylate application. The ANOVA indicates that the change in joint deflection differences between control and methacrylate sections after methacrylate treatment was not significant. This suggests that the rate of further deterioration resulting in methacrylate application continues at the same rate as the control sections. Any benefits of methacrylate application are after initial application when joint deflection magnitudes are reduced. Maximum joint deflections and changes between one day and one year after treatment are summarized in Table 5.3.

### *5.5.5 Core Test Data*

Deflection testing in 1991 earlier indicated a wide range in deflections which categorically corresponded to severity of surface distress. Higher maximum deflections were noted in areas with more severe ASR surface cracking. To establish that deflection changes could be used as a tool to monitor ASR deterioration progression, material data from cores drilled in each test section were used to calibrate structural deflection response. Cracking throughout the cores was observed just after coring.

Elastic modulus and compressive strength of the concrete were determined for each of the two cores from each test section. Elastic moduli of cores from the west end of the test section were significantly higher than those at the east end. Modulus of elasticity was variable, ranging from 1.44 to 3.93 million psi (9.9 to 27.1 GPa) and averaged 2.87 million psi (19.8 GPa). Compressive strength was slightly higher at the west end than those at the east end. Compressive strength ranged from 4520 to 6480 psi (31.2 to 44.7 MPa) and averaged 5580 psi (38.5 MPa). Compared to non-deteriorated concrete, the compressive strength was relatively higher given the relatively low modulus of elasticity. This indicates that concrete deformations with load are relatively higher but strength is not affected to the same degree when cracking due to ASR is present.

### *5.5.6 Comparison of Measured to Theoretical Deflections*

The finite element computer program ILLI-SLAB was used to compute theoretical deflections using core data material properties (Tabatabai, et al. 1979). Modulus of elasticity and thickness core data were input into the program. Moduli of subgrade reaction, $k$, were back-calculated by matching Slab A maximum deflections measured during the follow-up tests. Cement-treated base moduli of subgrade reaction for the 11 test sections ranged from 350 to 1000 lb/in$^3$ (95 to 271 MPa/m). Average back-calculated $k$-value was 490 lb/in$^3$ (133 MPa/m).

Deflections were computed using an average subgrade support of 500 lb/in$^3$ (136 MPa/m) and thickness of 8.5 in. (216 mm). As shown in Figure 5.6, significant decreases in modulus of elasticity correspond to significant deflection increases. Using Figure 5.6, the relative decrease in elastic modulus with ASR progression can be monitored.

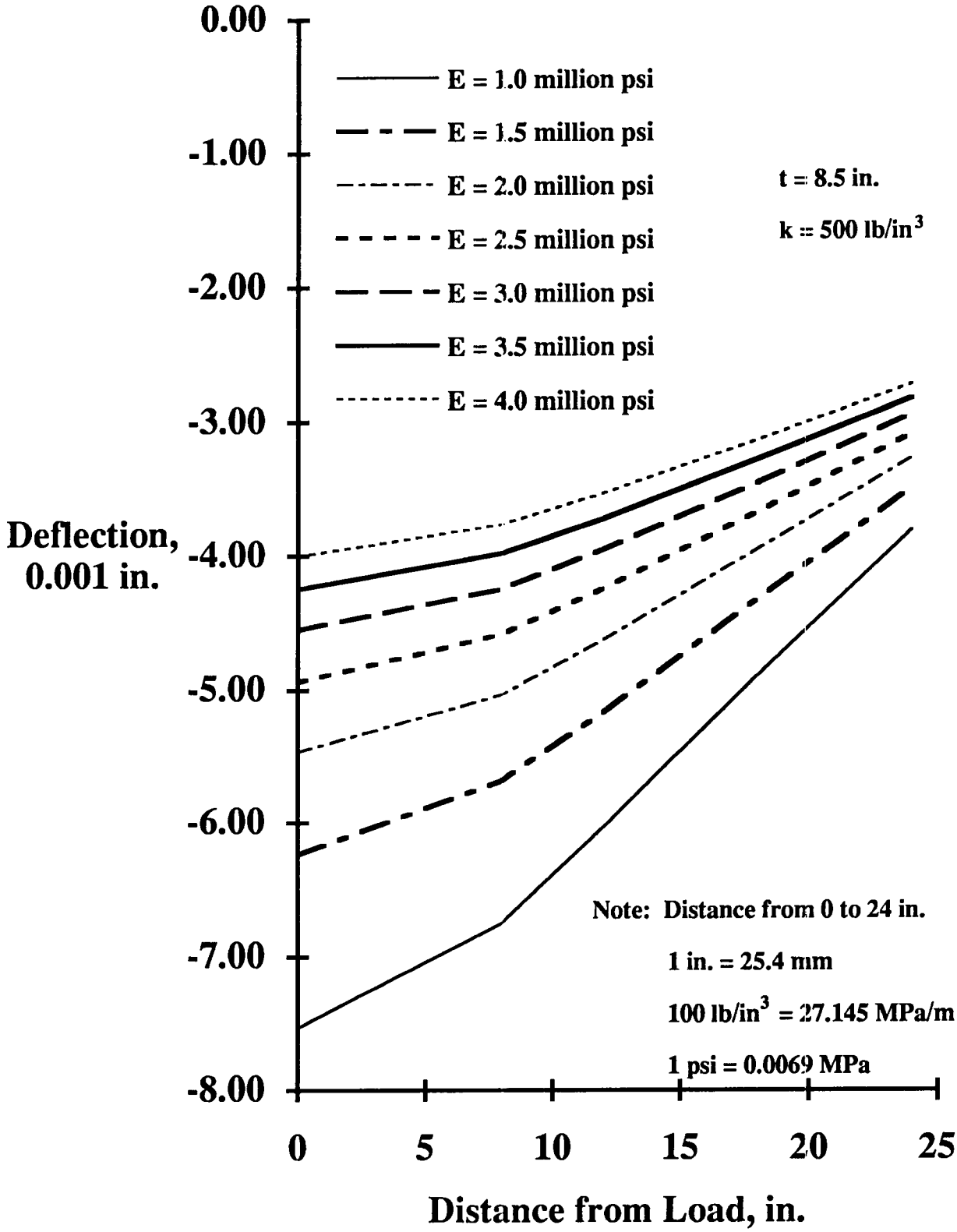


Figure 5.6. Computed deflections with distance from load.

## 5.6 Restraint

A concrete structure affected by expansive ASR may eventually develop cracking which can progress and increase in severity until the structure becomes unserviceable. A volume increase is produced in concrete as ASR develops. If the volume increase were restrained, resultant internal compressive stresses could prevent the onset of severe cracking and thus extend useful life of a structure. Two test programs were conducted to study the relationship between restraint and expansive ASR in concrete.

The first program subjected concrete cylinders to external three-dimensional pressure. Cylinders were made with highly reactive aggregate AL. Cylinders were also made with the same mix design but utilizing innocuous aggregate TH to act as controls. The purpose of this program was to determine basic relationships between ASR expansion, concrete creep and external pressure.

Of major concern is control of damaging ASR expansions in highway pavements. Based on results of the three-dimensional tests, a second testing program was conducted utilizing miniature pavement sections. The miniature pavement sections were subjected to one dimensional restraint. The purpose of this program was to study relationships between ASR development, concrete moisture condition, and imposed restraint on test specimens simulating an actual highway pavement configuration.

The following report sections summarize the three-dimensional and one-dimensional restraint testing programs. Details of these programs are presented in Appendix C.

### *5.6.1 Three-Dimensional Pressure Testing*

Eleven concrete cylinders were cast. Seven cylinders (6 for test and 1 spare) were made with highly reactive aggregate AL from New Mexico. Four cylinders (3 for test and 1 spare) were made with an innocuous dolomite aggregate TH to act as controls. Cylinders were 4 3/4 in. (120 mm) in diameter and 24 in. (610 mm) long.

After curing, the concrete cylinders were placed in steel cylinders and pressurized with water to various test pressures. Prior to pressurization, concrete cylinders were sealed to prevent water migration into the concrete so that any pressure change could be attributed to a true volume change in the concrete cylinder.

The steel cylinders were slightly longer than the test cylinders. Each steel cylinder was equipped with a pressure gage, a quick-disconnect water fitting on the input port through which water could be pumped to increase internal pressure, and a needle valve on the output port through which water could be bled to decrease internal pressure. A graduated tubular metering glass was also fitted to the output port so that volume of water being bled from the cylinder could be measured. After loading and sealing, the steel cylinders were pressurized with water and bled through several cycles to remove entrapped air. A total of nine cylinders was used, six containing reactive aggregate concrete specimens and three containing control specimens. The nine steel cylinders were stored at 100°F (37.8°C) and pressurized to various pressures.

For reactive aggregate specimens held at low pressures, it was necessary to bleed water from the steel cylinders to maintain the low pressure as specimen volume increased due to ASR expansion. Conversely, it was necessary to periodically pump water into steel cylinders containing reactive aggregate specimens held at higher pressures to make up for a net volume loss due to concrete creep deformation exceeding ASR expansion.

The three-dimensional testing program was conducted from June until December, 1989, a time frame of approximately six months.

#### 5.6.1.1 Conclusions

Based on three-dimensional pressure testing of cylinders, for the particular concrete mix used, the pressure at which ASR expansion and concrete volume reduction due to creep achieved a balance was in the range of 200 to 300 psi (1.38 to 2.07 MPa). Considering the highly reactive characteristics of the concrete mix used, it would appear that expansion and therefore serious cracking could be controlled in concrete structures where three-dimensional stress levels no greater 300 psi (2.07 MPa) could be maintained. For example, a cylindrical concrete bridge column would generally have a vertical uniaxial dead load stress greater than 300 psi (2.07 MPa). It would be practical in a cylindrical concrete column constructed with reactive aggregate concrete, to add lateral compressive stress by means of an external wrap of prestressing wire. The column would then be under three-dimension stress and it would be reasonable to expect successful control of damaging expansions and significant extension of useful service life.

### *5.6.2 One-Dimensional Restraint Testing*

The one dimensional restraint testing program is summarized in this report section. Details of the program are presented in Appendix C.

The purpose of the test was to determine if restraint could effectively control expansions and severity of cracking in test specimens affected by expansive ASR and simulating an actual highway pavement configuration. Three-dimensional restraint is not practical in a highway pavement. While two-dimensional restraint, that is, parallel and perpendicular to traffic direction, is feasible, preliminary consideration of schemes to accomplish this in an existing pavement indicated numerous practical problems with this approach. One-dimensional restraint was therefore chosen.

Test specimen configuration was selected to simulate a full size pavement section to eliminate scale effects on behavior. A 9 in. (229 mm) thick section was used. A specimen length four times thickness, 36 in. (916 mm), was chosen. Restraint was applied to expansions in the longitudinal direction. Therefore, specimen width became a less important dimension provided moisture migration was inhibited laterally. With lateral moisture movement inhibited, the test section effectively simulated a longitudinal slice from the inner part of a pavement. A width of two times thickness or 18 in. (458 mm) was selected. The sides of each test section were painted with two coats of heavy-duty epoxy paint to inhibit moisture migration.

One of the unique environmental features of a highway pavement is access to external moisture. Pavements rest on subbases that are damp or saturated, while at the same time they are exposed to dry surface conditions. This environment establishes a vertical moisture gradient through the thickness. Moisture is required for expansive ASR development, while conversely, surface drying accentuates shrinkage and inhibits expansion due to ASR. It was decided to place specimens in an environment that would establish a vertical moisture gradient through the thickness to determine the effect of this realistic field environment on development of cracking. Specimens were constructed on a subbase that was kept continuously moist while the test room itself was maintained at a comparatively dry 25 to 35 percent relative humidity. To accelerate ASR development the test room was maintained at 102°F (38.9°C).

Dictated by environmental and restraint conditions selected, a minimum total of six specimens was required, three constructed using reactive aggregate and three constructed of innocuous aggregate to act as controls. Specimens were grouped as follows:

1. A reactive aggregate and control section to be subjected to one-dimensional restraint and exposed to surface drying.

2. Sections constructed of reactive and innocuous aggregate to be subjected to restraint, but with a sealed surface to inhibit drying to isolate effects of surface drying on restrained concrete.

3. A reactive aggregate and a control section to be exposed to surface drying, but to be unrestrained to isolate effects of restraint.

Test section behavior was monitored by a combination of precision displacement measurement and visual inspection. The same concrete mix used for the three-dimensional pressure specimens was used for the six miniature pavement sections.

### 5.6.2.1 Test Setup

The test setup for miniature pavement sections is shown in Figure 5.7. The four specimens subjected to restraint were placed end-to-end in a loading frame. Hydraulic rams at one end of the frame were used to tension rods extending down both sides of the test sections and terminating in a sliding frame arrangement incorporating high capacity springs and load cells. The springs maintained constant stress in test sections as length changes took place. The load cells were used to monitor the test section stress level. The miniature pavement sections were initially cast in June, 1990 on a subgrade of absorptive 1 in. (25 mm) thick felt. Because of the warm, moist conditions under the miniature sections, both aerobic and anaerobic bacterial action developed in the felt. After attempts at control by chemical treatment proved unsuccessful, it was decided to recast test sections on a granular soil subbase. Test sections were recast in December, 1990 utilizing the same test setup and instrumentation used previously. Sections were monitored until August, 1992, a test period of approximately 21 months.

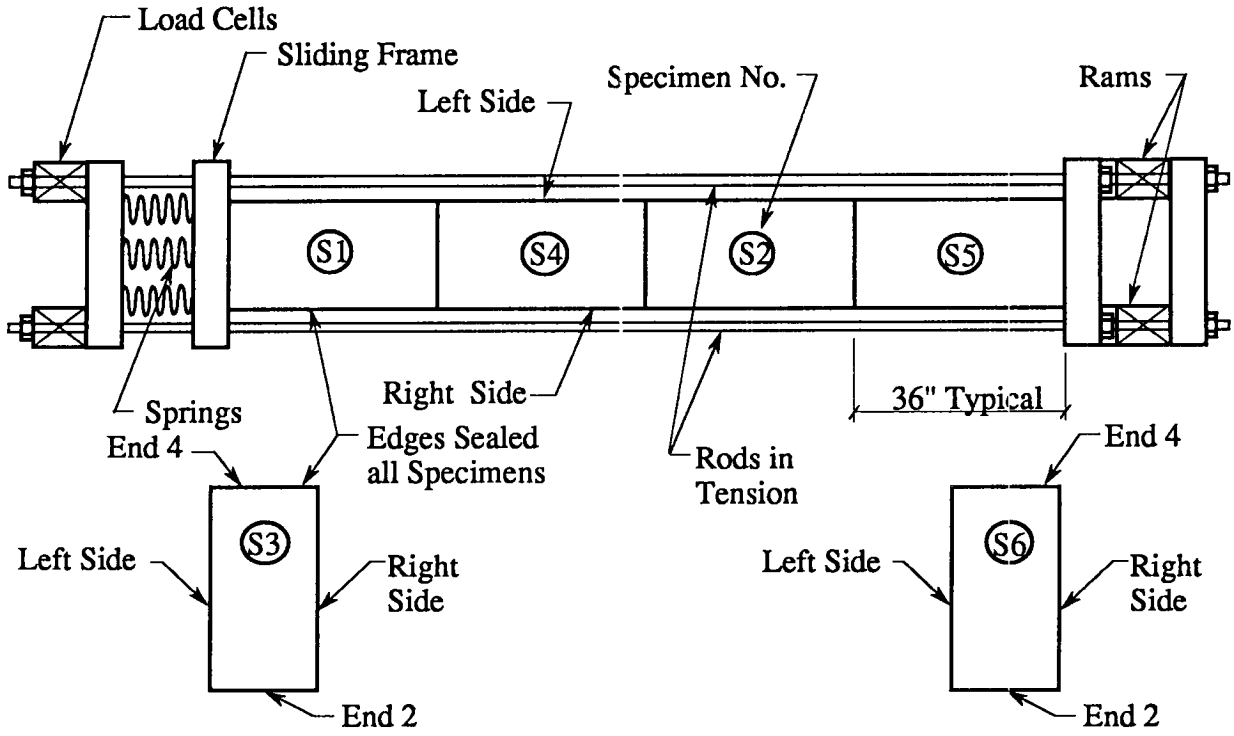


| SPECIMEN NO. | DESCRIPTION |
|---|---|
| S1 | Under Load - Nonreactive Aggregate-Specimen Unsealed (Total Strain Specimen) |
| S4 | Under Load - Reactive Aggregate-Specimen Unsealed (Total Strain Specimen) |
| S2 | Under Load - Reactive Aggregate-Specimen Sealed (Basic Creep Strain Specimen) |
| S5 | Under Load - Nonreactive Aggregate-Specimen Sealed (Basic Creep Strain Specimen) |
| S3 | No Load - Nonreactive Aggregate-Specimen Unsealed (Drying Shrinkage Specimen) |
| S6 | No Load - Reactive Aggregate-Specimen Unsealed (Drying Shrinkage Specimen) |

Note: 1 in. = 25.4 mm

Figure 5.7. Test setup for the miniature pavement sections.

### 5.6.2.2 Conclusions

The following conclusions are based on results of one-dimensional restraint tests of miniature pavement sections affected by expansive ASR. Test results were supplemented by finite element analyses and post-test physical examination of miniature pavement sections.

In unrestrained pavements, supported on a moist subbase, ASR expansion initiates at the bottom where moisture is available for the reaction. Contraction due to drying shrinkage is essentially absent at the bottom due to the moist subbase. If the pavement surface is exposed to a drying atmosphere, ASR development is inhibited in the top 1 to 2 in. (25 to 51 mm) as moisture is not available. The drying atmosphere which inhibits ASR expansion, however, promotes contraction at the top due to drying shrinkage. A strong strain gradient, therefore, exists between the expanding bottom and contracting top. Inevitably, cracking starts in such a pavement. The active expanding ASR sites at the bottom crack the surrounding paste, while the strong strain gradient widens and aggravates surface shrinkage cracking at the top. Horizontal cracks form as the expanding bottom zone and strain gradient split lower sections into layers.

The test results suggest that the rate at which expansion and cracking proceeds in a pavement affected by ASR is strongly influenced by conditions within the pavement at the time of initial ASR development. It is hypothesized that formation of reaction product and subsequent progression of damaging cracking is accelerated when localized sites of ASR, developing on a microscale, become interconnected by microcracking. An appropriate degree of restraint appears to prevent this rapid growth of ASR and cracking. As confirmed by finite element modeling, the restraint need only be one-dimensional, as one-dimensional restraint has a significant three-dimensional effect. Essentially, all zones in all directions surrounding an ASR site, are positively influenced, that is, subjected to some degree of restraint, by application of restraint in only one direction. The key factor, however, is the degree of restraint.

As demonstrated by a test of an unrestrained miniature pavement section, ASR and strain gradient effects, if left unchecked, lead to severe three-dimensional cracking. The tests of restrained pavement sections, however, strongly suggest that a low level of one-dimensional restraint, on the order of tens of psi (several hundreds of kPa), has the positive effect of keeping ASR and microcracking from growing unchecked. Even a small force applied perpendicular to a developing crack will affect its growth, as natural roughness on opposite sides interlocks and inhibits sliding motion. It also appears, however, that moderate to high levels of one-dimensional restraint, equivalent to hundreds of psi (several MPa), may actually aggravate developing conditions within a pavement accelerating expansions and internal cracking.

Because the restrained miniature pavements developed only one surface crack, their external appearance was quite good in comparison with the extensively cracked surface of the unrestrained pavement section. This was in part due to the formation of cracks at the stainless steel bond breaks between sections which controlled surface cracking in sections themselves. More significantly, however, it was due to horizontal cracking and splitting within the cross section which isolated the top from the expanding bottom. As the test progressed, strain data indicated different behavior at the top than at the bottom of restrained pavements, with horizontal cracking strongly suspected as the cause. Post-test examination revealed horizontal cracking and splitting in significant amounts. Horizontal cracking was not as extensive in the pavement that was coated to reduce moisture loss, as the strain

gradient in this section due to surface shrinkage was lower. Horizontal cracking in this pavement, however, was still significant. Regardless of surface condition, horizontal cracking would be particularly detrimental in an actual highway pavement. Live traffic loads would subject such a pavement to excessive live load stress since effective bending cross sections would be reduced. These excessive stresses would aggravate cracking further, eventually rendering the pavement unserviceable.

It is noted, however, that horizontal cracking and splitting in restrained pavement sections took place after restraint stress levels were increased from initial low values. While transverse expansions were taking place in restrained miniature pavements early in the test, the rate of expansion was minor when compared to expansions taking place at equivalent ages in the unrestrained pavement. Clearly, one-dimensional longitudinal restraint had significant positive effect even on transverse and vertical strain.

The fact that damaging cracking due to ASR may be controllable at low restraint levels, however, is not particularly encouraging when considering strategies for preventing growth of cracking in existing highway pavements. The test results suggest that the low level of restraint must be applied early in the life of a pavement, before extensive ASR development. Generally, the true extent of potential for damage in a highway pavement is only evident after initial cracking appears and the diagnosis of ASR is made. Application of restraint would be largely ineffective in these cases. Test data does indicate that application of one-dimensional restraint on the order of hundreds of psi (several MPa), can control expansion in the direction of restraint and significantly reduce the rate of expansion in other directions. Whether the reduction of expansion rate in the other directions would prevent horizontal splitting in lower zones of the pavement is problematical.

## 5.7 Conclusions

Investigations were made into several approaches to prevent future expansion and cracking due to ASR in existing highway concrete. These include application of lithium solutions, restraint, cementing of existing cracks, and drying or limitation on wetting. Thus, attempts were made to interfere with ASR mechanisms and to test symptoms resulting from ASR.

Each of these approaches was investigated either in the laboratory or in the field as well as the laboratory. The following conclusions have been drawn from this work:

1) Application of LiOH solutions are effective in preventing further expansions due to ASR. However, means must be developed to introduce the solution into concrete to achieve acceptable effectiveness. In the field applications, existing cracks transmitted the solution into the concrete. These field applications are presently too recent to judge for effectiveness.

2) Triaxial restraint in the range of 250 to 300 psi (1.73 to 2.07 MPa) can prevent expansion due to ASR. At this restraint level, expansion due to ASR was balanced by creep. This approach would appear feasible for bridge columns, piers, etc.

3) Major uniaxial restraint, such as could exist in pavements or other structures, can prevent ASR-induced expansion in the direction of restraint. However, cracking may be exacerbated parallel to this direction. Intermediate restraint levels, on the order of several hundreds of psi (several MPa) may extend the service life of a pavement affected by ASR, while greater restraint levels may aggravate the situation.

4) Drying is effective in preventing expansion due to ASR, not only by removing moisture otherwise available for absorption by ASR gels, but also by initiating alkali fixation by cement hydration products. However, these phenomena are limited by the slow release of alkali as well as the more rapid availability of moisture upon rewetting. Thus, this approach appears to be temporary but possibly still of some usefulness.

5) Based on FWD determination, sealing of surface cracks due to ASR with high molecular weight methacrylate appears to be beneficial in stiffening the affected pavement. Its effectiveness will depend on penetration of methacrylate into the cracks.

6) Surface sealants that permit diffusion of water vapor into the concrete, such as silane and siloxanes, appear to have little effect on the internal RH of concrete in outdoor exposures. In particular, in highway pavement they would have little beneficial effect due to availability of subbase moisture to the pavement slab.

7) Field installation should be maintained and monitored for performance where mitigative measures in this project have been initiated or contemplated.

# 6.0 Summary

Following is a summary of findings in this investigation:

1. Deleterious ASR is more widespread than earlier thought by state transportation departments in the United States. Much of this stems from lack of familiarization with the symptoms of ASR-associated distress. It is known to occur in states that believe they do not have the problem, or are unsure of its development.

2. Testing and specifications intended to control ASR show wide divergence among the various states. In numerous instances, existing policies almost surely will not prevent deleterious ASR in the respective states.

3. Natural climatic conditions are favorable to the development of deleterious ASR in all states in the United States. Even in hot, arid desert regions, there is sufficient moisture to support expansive ASR, at least on a cyclic basis.

4. Specifications and test procedures rely strongly on ASTM standards such as C 227 and C 289, both of which are too lenient. They generally find as innocuous the slowly reacting aggregates such as some granite gneisses and quartzites. Furthermore, ASTM standards suggest the use of low-alkali cement to preventdeleterious ASR. This is found not always to be effective if certain volcanic materials are present in the aggregate.

5. The rapid immersion test method, originally developed at NBRI in South Africa, is capable of identifying slowly- and rapidly-reacting aggregates with the establishment of an appropriate failure criterion. Testing in this investigation indicates a criterion of 0.080 percent expansion in 14 days of testing, using 1N NaOH solution.

6. By adjusting the concentration of NaOH in the immersion solution, the test appears to be capable of identifying cement alkali levels required to prevent deleterious ASR in highway concrete. A linear regression equation has been developed that relates water-cement ratio and cement alkali level to alkali concentration in the immersion solutions used for testing.

7. The proposed test also appears capable of determining the intrinsic capability, and quantity required, of mineral admixtures to prevent deleterious ASR in highway structures.

8. Extensive testing was done to better define the capability of additions of lithium ion to concrete to prevent deleterious ASR, as first suggested in work published by McCoy and Caldwell in 1951. Investigations of reaction chemistry revealed that lithium ions,

as well as other alkali cations, are components of ASR gel that possesses little or no capacity to swell. For a given level of potassium or sodium in solution, the higher the lithium dosage used, the greater the proportion of lithium that appears to be incorporated into the ASR gel.

9. Rapid immersion test results, in which LiOH was added to the NaOH solution, revealed that Na:Li molar ratios in the range of 1.0:0.75 to 1.0:1.0 were sufficient to prevent excessive expansion due to ASR involving highly reactive volcanic rock aggregate.

10. LiOH additions were found to be effective in suppressing expansive ASR where fly ash is used and where specimens are exposed to NaCl solutions such as encountered with the application of deicer salts.

11. LiOH was added to fresh concrete in an experimental sections of State Route 352 in Albuquerque, New Mexico in June, 1992. Performance comparisons also can be made between control sections with no LiOH or mineral admixtures and sections containing Class F or C fly ashes. Two highly reactive coarse and fine aggregates were used in these concretes. Rapid immersion test results on samples of materials used in these concretes indicate the Class F ash used in the pavement concrete should adequately control ASR while the Class C ash and the Class F + Class C ash, used in a 50:50 proportion, should reduce rate and severity of distress due to ASR but not prevent it.

12. Tests run on mortar bars containing highly reactive aggregate indicate that treatment of the hardened mortars with LiOH solutions after intermediate levels of expansion are reached is effective in suppressing further expansion due to ASR. This suggests that LiOH treatment may be beneficial in reducing expansion due to future ASR in existing highway structures, provided LiOH penetration is obtained.

13. High molecular weight methacrylate surface treatment of ASR-affected pavement near Boron, California revealed that cracks were filled with the methacrylate to depths up to about 2 1/4 in. (57 mm), and that the pavement is performing satisfactorily.

14. RH measurements of pavement and bridge deck concrete with silane/siloxane sealants revealed little or no difference in moisture condition of the concrete, compared with the respective control sections with no treatment.

15. Drying concrete appears not only to remove moisture that might otherwise contribute to swelling of ASR gel, but also to cause alkalies to be complexed by cement hydration products. Both processes are largely reversible, with the latter being so only very slowly. Drying undoubtedly could be effective in controlling expansion due to ASR in a given concrete member, but the procedure would have to be repeated periodically.

16. A section I-80 near Winnemucca, Nevada that displays ASR-induced distress was selected for field evaluation of LiOH, methacrylate, and silane treatments. Initial applications were made in October, 1991. Evaluation was made by falling weight deflectometer measurements with plans to repeat measurements on a yearly basis. A retreatment of LiOH was made after one year. Control sections with no treatment were included for monitoring. Linseed oil and a second silane section were added as experimental sections after one year.

17. FWD measurements appear to be a valid method of monitoring degree of distress induced by ASR. Measurements indicated that high molecular weight methacrylate applied to the surface was effective in reducing wheel path joint deflections. Deflection decreases were still apparent one year after application. No significant differences were measured between control sections and lithium or silane sections.

18. FWD measurements indicated that methacrylate was effective in reducing interior slab deflections one day after application. Reductions were not measured one year after application. Analysis of all treatment data indicates no significant deflection change at slab interior positions between initial baseline tests and tests done one year after applications.

19. Triaxial restraint on the order of 250 to 350 psi (1.7 to 2.4 MPa) appears to be an effective method of preventing excessive expansion where ASR has occurred. Restraint could be a feasible approach to limit expansion in certain concrete members such as bridge columns.

20. Uniaxial restraint, such as encountered in concrete pavement, has a beneficial three-dimensional effect on reducing expansion due to ASR. However, an optimum range of intermediate restraint levels probably exists and probably needs to be present prior to development of expansion due to ASR to have prolonged, sustained, beneficial effect.

# 7.0 Recommendations

Based on findings of this investigation, the following recommendations are made:

1. Personnel in state transportation departments should become more familiar with manifestations of ASR-induced distress in highway structures. A handbook produced in this project should be used to assist in this endeavor.

2. Examination of concrete under UV light, after treatment with uranyl acetate solution, should be incorporated into procedures to identify whether ASR has developed in concrete.

3. The rapid immersion test method should be required in the routine evaluation of aggregates and mineral admixture for use in concrete. Additional research, including evaluation of field performance of highway structures, should be conducted to further substantiate the rapid immersion test criteria suggested for evaluating safe cement alkali levels and pozzolan requirements to avoid deleterious ASR for particular aggregates.

4. Addition of LiOH should be seriously considered as a means of preventing development of deleterious ASR. It does not need to be tested, and it maintains its effectiveness in the presence of fly ashes and deicer salts.

5. Treatment of highway concrete with high molecular weight methacrylate or LiOH should be explored further as a means of extending the serviceability of pavement adversely affected by ASR.

6. Monitoring should continue on new pavement in Albuquerque, New Mexico, to which LiOH was added to fresh concrete, and on the I-80 pavement near Winnemucca, Nevada, to which LiOH and methacrylate treatments were applied.

7. Triaxial restraint of concrete members, such as bridge columns, should be considered as a viable method of controlling expansion due to ASR.

8. Additional investigations should be carried out to monitor field installations initiated under this project, and develop other projects for similar experimental means to inhibit expansions due to ASR.

# Appendix A Identification of ASR

## A.1 Identification of Potential for Expansive ASR

Existing test methods concerned with ASR are designed primarily to determine whether an aggregate or cement-aggregate combination is potentially deleteriously reactive. They generally do not address the issue of what steps are needed to provide for safe use of a particular aggregate, such as maximum acceptable cement alkali level or quantity of a particular pozzolan needed to suppress deleterious ASR. This situation leaves the user in a position of uncertainty regarding materials or specifications to be used in new construction.

Investigations in SHRP C-202, based on previous work carried out at NBRI, were designed to resolve the important question of testing to identify requirements to safely use a particular aggregate, cement, pozzolan, and combinations thereof. Recommended procedures are described below.

## A.2 Determine Potential for Expansive ASR

**Procedure No. 1 Identify Whether Aggregate Is Potentially Deleteriously Reactive**

1) Sieve fine aggregate, or crush and sieve coarse aggregate; wash on appropriate sieve to remove dust and finer particles, oven dry at 210±5°F (105±2°C). Per ASTM C 227, size the dried aggregate, processing sufficient representative material to make three companion mortar bars.

2) Use ASTM C 150 portland cement with an alkali content not exceeding 0.30 percent equivalent $Na_2O$.

3) Make three mortar bars per batch, using the following quantities:

| | |
|---|---|
| Aggregate | 900g |
| Cement | 400g |
| Water | 200g |

Use molds, mix, and cast, per requirements in C 227.

4) Use measuring, storage and test procedures outlined in ASTM P 214 (Vol. 04.02 1991 edition). Specimens are immersed in 1N NaOH solution to age of 14 days.

5) The comparator reading taken after immersion in water for 24±1 hours serves as the reference against which expansions are calculated from subsequent readings taken during the period of immersion in NaOH solution.

6) Take comparator readings at ages of 3, 7, and 14 days storage in NaOH solution. Calculate final expansion as the difference between the reading after one day storage in water and 14 days' storage in NaOH solution.

7) An aggregate should be considered potentially deleteriously reactive if the expansion at 14 days exceeds 0.08 percent. This indicates only that the aggregate is susceptible to deleterious ASR, not that it will be so in all applications. The test result may disagree with field performance because cements with sufficiently low alkali levels may have been used that precluded development of deleterious ASR.

8) If desired, further testing can be done, using this procedure by adjusting NaOH solution concentrations to correspond to cement alkali levels and water-cement ratios intended for possible use in the highway structure.

**Procedure No. 2 Identify Requirements to Safely Use Potentially Deleteriously Reactive Aggregate**

1) Use same steps as outlined in Procedure No. 1 in this Appendix. The only changes will be in the selection of NaOH concentration of the immersion solution. This is based on cement alkali level and water-cement ratio of the highway concrete.

2) Adjustments in NaOH solution concentration are made as follows:

A) Select alkali content (equivalent $Na_2O$) of candidate cement for use in concrete with aggregate to be evaluated. Select projected water-cement ratio of highway concrete. Insert these values into the following equation to determine normality of the immersion solution.

$$\text{Normality} = 0.339 \frac{Na_2O}{w/c} + 0.022 \pm 0.06 \text{ moles/L}$$

Or select values from graph in Figure 3.7.

Example No. 1:

Assume that the cement to be used has an alkali content of 0.60 percent equivalent $Na_2O$, and it is anticipated that a water-cement ratio of approximately 0.45 will be used. Referring to Figure 3.7, it is seen that a 0.55N NaOH immersion solution should be used. From Figure 3.8, it is seen that the failure criterion corresponding to this solution is 0.020 percent. Thus, if expansions using a 0.55N NaOH solution exceed this level, potential exists for expansive ASR in highway concrete using the cement with 0.60 percent alkali.

Example No. 2:

Assume that only cements with alkali contents of 1.0 percent are available and are known to be associated with deleterious ASR using a sample of the aggregate in question. It is decided to use 20 percent weight replacement of the cement by fly ash in a concrete with a 0.40 ratio of water to total cementitious material. Equivalent $Na_2O$ of the cement, plus total equivalent $Na_2O$ in the fly ash is calculated*. Assume 1.5 percent total alkali in the fly ash. This calculates to equivalent $Na_2O$ in the cement fly ash system as follows:

$$(1.0\% \times .80) + (1.5\% \times .20) = 1.10\%$$

Referring to Figure 3.7, this level of alkali corresponds to a 1.01N NaOH immersion solution. Figure 3.8 indicates a test failure criterion of 0.08 percent. In the absence of substantiating data, it is recommended that this criterion be used for solutions of greater normality as well.

Parallel testing, using different solutions, can be done to bracket permissible cement alkali levels or required quantities of mineral admixture if such information is needed.

## A.3 Recognizing ASR in Existing Concrete

One of the major reasons deleterious ASR goes unrecognized as such in highway structures is lack of familiarity, within transportation departments, with symptoms of the reaction. This is particularly true for personnel who routinely inspect highway structures and record the development of abnormal cracking or volume change. Procedures have been described in the "Handbook for the Identification of Alkali-Silica Reactivity in Highway Structures" (Stark 1991a) for this purpose.

Two approaches can be used to characterize the role of ASR in development of distress observed in concrete structures: assessment of crack patterns, and identification of gel products resulting from ASR. Guidance to their use is described below.

Inspection Procedure No. 1

Step 1 - Inspect the structure for pattern or disposition of cracks in structure. Compare with crack patterns shown in handbook to determine if ASR is a possible cause of cracking.

Step 2 - If ASR is a possibility, obtain concrete cores for microscopic examination to confirm the presence of ASR gel and source of microcracks. Core examination can be supplemented by application of uranyl acetate solution to freshly fractured surfaces and viewing in UV light, as described in the handbook. Particular

---

* Total Alkali in the fly ash is believed to be more appropriate than "available" alkali per ASTM C311 as the significance of "available" alkali is not known.

attention should be paid to the presence of fluorescent gel deposits within the periphery of aggregate particles. The UV light procedure should be used as a means of more rapidly identifying locations of possible ASR gel. These locations should then be confirmed by examination of powder mounts in the petrographic microscope.

Inspection Procedure No. 2

Step 1 - Bushhammer a minimum area of 24 sq in. (15.5 x $10^3$ $mm^2$) of exposed (formed or finished) surface to a minimum depth of 1/4 in. (6mm). After rinsing, treat bushhammered area with uranyl acetate solution and view under UV light, using a viewing box to darken the area of the treatment. The presence of fluorescent deposits within the periphery of aggregate particles represents probable development of ASR gel, even in the absence of diagnostic surface cracking.

Step 2 - If such gel deposits are observed, cores should be taken for petrographic examination to confirm ASR as a source of distress. If such deposits are not found, ASR is not a probable source of distress.

# Appendix B Pavement Treatment Experimental Program

## B.1 Experimental Pavement

A field deflection monitoring program was initiated in Nevada to evaluate the effectiveness of surface treatments in mitigating the effects of ASR on pavement structural response. The treatments consisted of a LiOH solution, high molecular weight methacrylate resin, poly-siloxane resin sealer (silane), a second silane sealer, and linseed oil. Testing was done by the Nevada DOT using a falling weight deflectometer (FWD) in October 1991 to establish baseline interior and joint deflections. A follow-up testing program was done October 1992 to evaluate treatment effects on deflections after one year.

### *B.1.1 Pavement*

The selected test section was on eastbound Interstate 80 in Humboldt County, Nevada between mile posts 16.45 and 16.80. The section is just east of Winnemucca located in the northwestern part of Nevada. Built in 1981, the pavement design consists of a plain jointed 8 in. (203 mm) thick concrete slab over a 6 in. (152 mm) cement-treated base, and a 3 in. (76 mm) gravel subbase. An asphalt concrete bondbreaker was used between the cement-treated base and gravel subbase. Non-dowelled skewed transverse joints are spaced at 12, 13, 19, and 18 ft (3.65, 3.96, 5.79, and 5.49 m). Driving and passing lanes are 12 ft (3.65m) wide. Concrete shoulders 10 ft (3.05m) wide are not tied to the mainline pavement.

The 1991 average daily traffic was 5,600 with 6.2 million ESALS (equivalent 18 kip, 8163 kg, single-axle load) in the eastbound lanes. The pavement surface was ground in 1989.

### *B.1.2 Treatment*

Three different surface treatments were applied to slab surfaces on October 2, 1991. Each treatment was applied to two test sections, consisting of five slabs per section. Surfaces were sandblasted prior to initial treatment application. Treatments were applied to the outside driving lane. The treatments consisted of a LiOH solution, high molecular weight methacrylate resin, and poly-siloxane resin sealer. In addition to the three different treatments, three control sections, also consisting of five slabs per section, were selected. An additional two treatments consisting of a silane surface sealer and linseed oil treatment were applied to separate five slab test sections during the one year follow-up testing program. The test sections were opened up to traffic approximately 8 hours after application.

$LiOH \cdot H_2O$ powder was dissolved in water at a rate of 64 lbs per 100 gallons of water (76.85 g/L). Dosage was selected for a 1 to 1 equivalent cement alkali to lithium hydroxide ($Na_2O$:LiOH) concentration. The solution was mixed approximately 15 hours prior to application to the entire surface and applied with a power sprayer in three applications. A time period between applications allowed for lithium penetration into surface cracks. The residue remaining on the surface after the second application was rinsed off with water the next day. A second treatment was applied but not rinsed off during the one year follow-up testing program.

The methacrylate was a two-component, rapid curing, solvent-free high molecular weight methacrylate resin used for crack repair. The two components were mixed in buckets on site and applied by Nevada DOT personnel. The gravity flow methacrylate was applied by squeegeeing a thin film over the entire surface. The film was allowed to pond over superficial cracks. Within 30 minutes the surface was covered with a light broadcast of dry sand to restore skid resistance.

The poly-siloxane resin (silane) was a single-component, colorless liquid formulated to seal cementitious surfaces. The resin produces a water-repellent penetrating sealer which can close the pores of cementitious substrates. Silane was applied by hand sprayers to the entire test section surface. The silane treatment was not applied during the follow-up testing.

An additional two treatments were applied to separate slab sections during the one year follow-up testing program. A second type of silane sealer, manufactured by a different company, and linseed oil were applied. Similar to the initial applications of the other treatments, the surface preparation consisted of a light sandblast to thoroughly clean the surfaces. Silane was applied by manufacturer technical representatives. Linseed oil was applied by DOT personnel at the manufacturer's recommended rates. One 5-slab test section per treatment was selected for deflection testing during the follow-up visit.

Test sections were selected within an 82-slab area just east of Winnemucca, Nevada in the eastbound driving lane on I-80. Based on visual inspection of surface cracking the control, lithium, silane, and methacrylate treatments were randomly assigned into five slab sections. One set of treatments at the west end of the test area was located in a less severely distressed (surface) area than the second set of treatments at the east end of the test area. The test layout is shown in Figure B.1.

### *B.1.3 Test Procedure*

Deflections were acquired by the Nevada DOT using the State FWD. Deflections measured in October 1991 were used as a baseline to evaluate effectiveness of treatments in reducing the rate of structural deterioration due to ASR. It was assumed that progression of ASR would continually decrease the concrete modulus of elasticity. Decreases in elastic modulus could possibly be monitored with falling weight deflectometer deflection measurements. To minimize replication variability attributed to follow-up testing equipment positioning, crosses were ground into the slab using a diamond impregnated cutting wheel mounted on a portable grinder. Theses marks were used to position the falling weight load at each test location. Sections tested during the follow-up program were not ground. Test locations were recorded should additional follow-up testing be done.

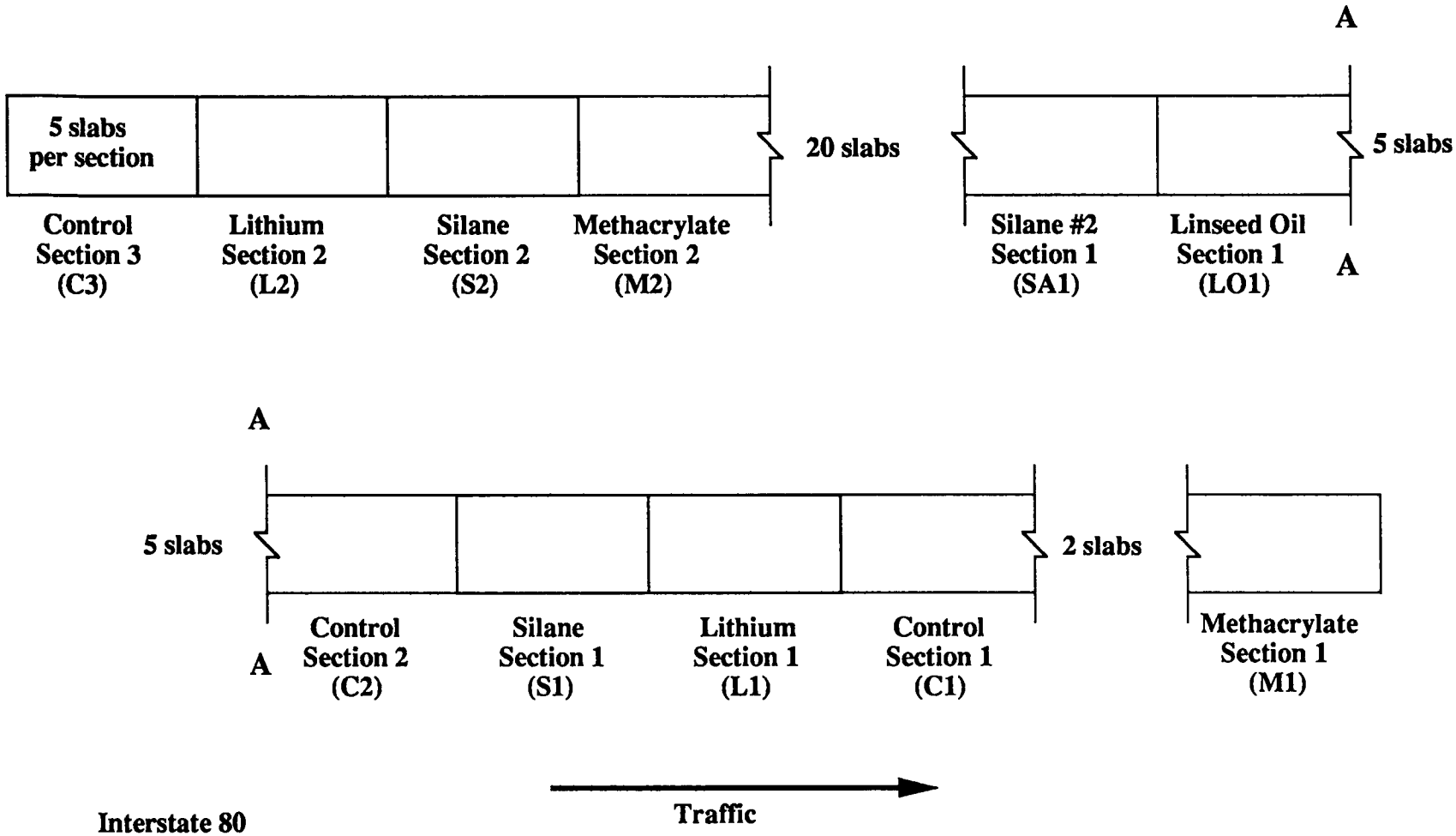


Figure B.1. Nevada falling weight deflectometer test sections.

The falling weight deflectometer was positioned at each slab location and tested. Three drops per test location were done. Deflections and load were measured and recorded for each of the three drops. Nominal load was 9500 lbs (4300 kg). Deflections were measured in the slab interior at the center of the slab and at the joint 18 in. (46 mm) from the lane-shoulder longitudinal joint. Deflections at the slab interior along the slab longitudinal centerline axis were measured under the load and at 8, 12, 18, 24, 36, and 60 in. (203, 305, 457, 610, 914, and 1524 mm) away from the load in the direction of traffic. Loading plate diameter was 11.8 in. (300 mm). Transverse skewed joint testing was done with the load positioned on the leave slab with the edge of the plate immediately adjacent to the joint. Deflections were measured under the load, 12 in. (305 mm) from the load on the unloaded slab (approach), and on the loaded slab (leave) at 12, 18, 24, 36, and 60 in. (305, 457, 610, 914, and 1524 mm) away from the load in the direction of traffic.

Tests were conducted before treatment application on October 2, 1991. Deflections were also measured in the three control sections and the two methacrylate sections one day after treatment on October 3, 1991. Tests were done to evaluate deflection repeatability and to evaluate effectiveness of the methacrylate penetrating resin in reducing deflections at one day. Weather during testing was clear and sunny. Ambient temperatures ranged from approximately 45 to 85°F (7 to 29°C). Follow-up testing was done on October 7 and 8, 1992, approximately one year after treatment application. Weather during testing was also clear and sunny. Ambient temperatures ranged from approximately 45 to 80°F (7 to 27°C). Testing was initiated early in the morning and finished early in the afternoon to allow for traffic control removal before dusk.

Baseline deflection testing was also conducted at mid-slab 18 in. (46 mm) from the lane-shoulder longitudinal joint. Deflections at the slab edge were measured under the load and at 8, 12, 18, 24, 36, and 60 in. (203, 305, 457, 610, 914, and 1524 mm) away from the load in the direction of traffic.

## B.2 Test Data Analysis

Deflection data before treatment, after treatment (one day), and at one year were used to analyze effects of nonlinear response, within-test variability, between-test variability, and effects of temperature on response. Analysis of treatment effects are discussed in the next section.

### *B.2.1 Non-linear Response*

Eight tests were conducted at different loads to evaluate effects of load on deflection magnitudes. By varying the weight drop height, the load magnitude ranged from approximately 7 to 18 kips (3175 to 8163 kg). Four load magnitudes were repeated four times for each of the eight tests. Loads were approximately 7, 10, 13, and 18 kips (3175, 4535, 5895, and 8165 kg). Deflections were measured under the load and at 8, 12, 18, 24, 36, and 60 in. (203, 305, 457, 610, 914, and 1524 mm) away from the load in the direction of traffic.

Plots of deflections with load indicated that slab response was linear from approximately 7 to 12 kips (3175 to 5440 kg). Generally at loads greater than 12 kips (5440 kg) the deflections decreased from linearity. Predicted deflections for one interior test site based on a linear regression through the three lower load deflections are shown in Figure B.2. Deflections are linear with load at loads less than 12.5 kips (5670 kg). Deflections did not intercept zero at zero load indicating a less than perfect linear elastic response. Extrapolated deflections at zero load in Figure B.2 ranged from -0.00029 to -0.00013 in. (-0.007 to -0.003 mm).

To evaluate effects of linearly proportioning deflections with load when load deflection curves do not pass through zero, deflections in Figure B.2 were proportioned to 10 kips (4535 kg) for tests done at 9.2 and 12.5 kips (4170 and 5670 kg). Differences in predicted linear regression deflections (load deflection curve not passing through zero) and proportioned deflections (load deflection curve passing through zero) ranged from 0.1 to 1.2 and averaged 0.6 percent. Tests to evaluate different treatments were conducted at loads ranging from approximately 8.4 to 10.1 kips (3810 to 4580 kg). Load deflection plots indicated that deflections were linear with load up to approximately 12,000 lbs (5440 kg). Since effects of linearly proportioning deflections to 10 kip (4535 kg) loads did not suggest significant errors, the influences of load deflection curves not passing through zero were assumed insignificant.

### *B.2.2 Within-Test Variability*

The falling weight deflectometer equipment was positioned and tested three times within a 30 second period at each test location. Equipment remained stationary between tests. Within-test variability reflects concrete slab deflection differences due to variability in load measurement, linear deflection proportioning to load, and deflection measurement. Since deflections were measured sequentially within seconds, the effects of equipment wear, temperature gradients, moisture gradients, and load positioning on deflection response were not accounted for in the within-test variance analysis.

Repeatability was excellent for all tests. Data measured at slab interior locations in Control Section 2 during the October 1991 tests were evaluated for within-test variance. For the three tests conducted for the five slabs, the within-test deflection (normalized to 10 kips, 4535 kg) coefficient of variation (standard deviation divided by average) ranged from 0.1 to 2.7 and averaged 0.9 percent for all seven deflection positions. Analysis of other sections both at joints and interior also reflect similar low coefficients of variation. Since the normalized deflections have very low coefficients of variation, the average 10 kip normalized deflections were used in the analysis of treatment effectiveness.

### *B.2.3 Temperature Gradient Effects*

Concrete slab temperature differentials can significantly influence slab deflection response. Early in the morning, the near-surface temperatures of the slab can be relatively cooler than near-bottom temperatures, and slab corners and edges can curl upward. Larger joint deflections are measured when slabs are curled up enough to cause a loss of subbase support at corners and edges. Conversely, when testing is done in late afternoon and slab near-surface temperatures are higher than near-bottom temperatures, slab edges and corners curl downward. Slabs with edges and joints curled downward can reduce interior subbase

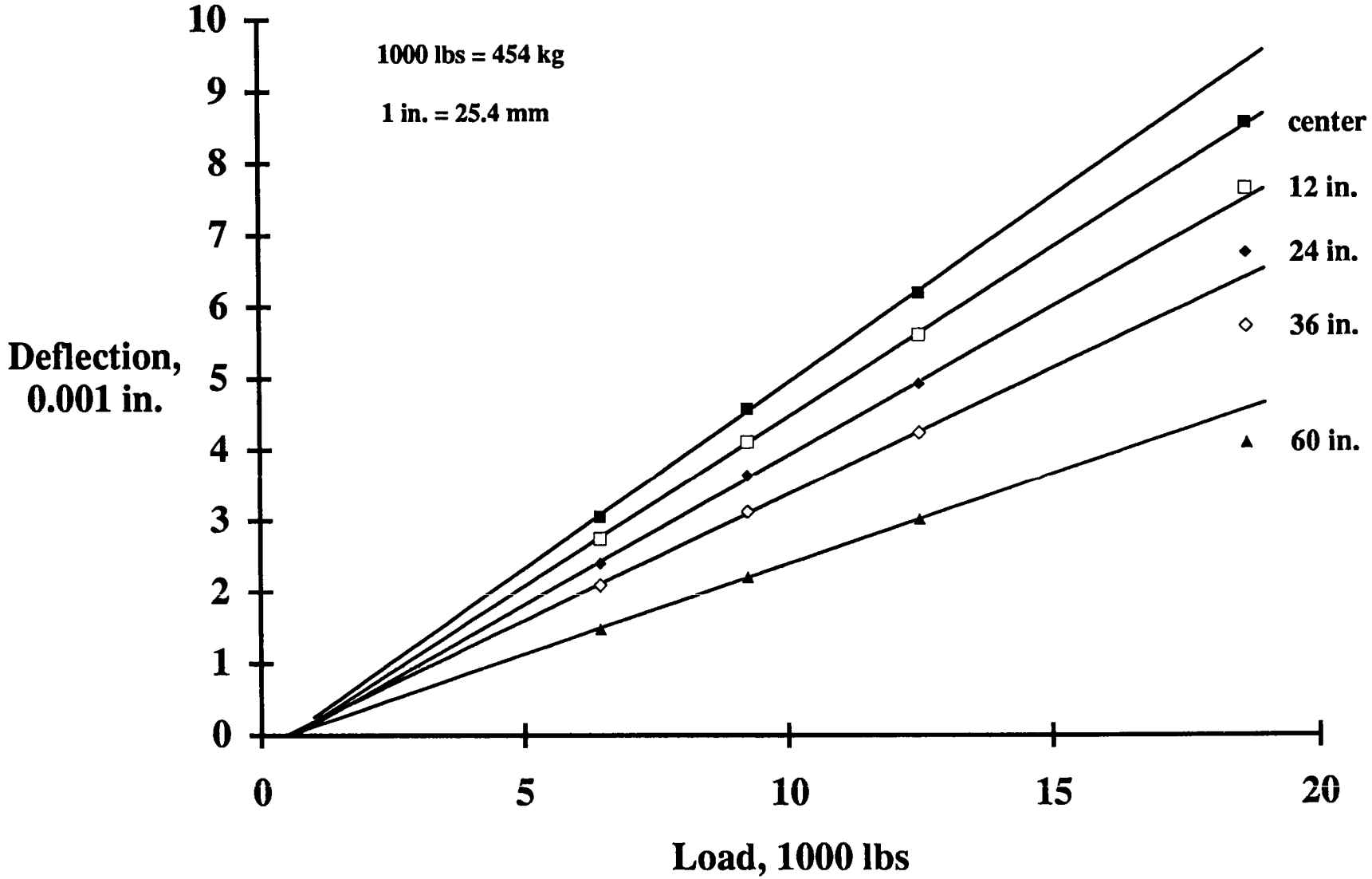


Figure B.2. Nonlinear deflections with load.

support. The degree and extent of slab curling is a function of temperature gradient magnitude and distribution, concrete modulus of elasticity and unit weight, slab dimensions, and transverse and longitudinal joint design. To minimize any seasonal effects of curling temperature distribution and gradient magnitudes, follow-up tests were repeated during the first week of October, approximately one year after initial baseline deflection testing.

In addition to curling due to temperature gradients, vertical slab deformations can also develop with moisture gradients. Commonly, moisture contents near the top surface of the slab are less than moisture contents deep in the slabs, resulting in an upward concave slab deformation. The degree of warping is a function of moisture gradient magnitude and distribution, concrete creep, concrete modulus of elasticity and unit weight, slab dimensions, and transverse and longitudinal joint design. Follow-up tests were conducted during the first week of October to minimize any seasonal effects of warping.

To evaluate effects of temperature on slab deflection response one slab was periodically tested throughout the initial and follow-up testing periods. The slab selected was the fourth slab in Lithium Section 2. Both the center (Slab D) and east joint (Joint D) were tested. Concrete temperature gradient (bottom minus top) was also measured for each test. Temperatures were measured with a probe tip thermocouple on the slab surface and with a thermocouple buried under the outside shoulder edge. To reduce effects of temperature distribution (as opposed to bottom-surface gradient) on deflections, testing was done at approximately the same time of the year. As desired, the temperature gradients with time were not greatly different between the 1991 and 1992 test periods. As shown in Figure B.3, similar gradients with time between 7:00 am and 11:00 am were measured. The gradients during the temperature analysis deflection testing ranged from approximately -20 to 10°F (-11.1 to 5.6°C). Since data did not show any consistent or significant effect of age, the gradient data from both test periods was combined in the analysis.

As the gradient decreased (surface temperatures larger than bottom temperatures), the center deflections slightly increased, reflecting a small loss of center subbase support. As gradients decreased the joint deflections significantly decreased, reflecting increased joint and edge support as the slabs curled downward with increasing surface temperature. The joint deflections with temperature gradient were in opposite directions to that of interior deflections. As expected, the joint deflections are much more sensitive to temperature gradients than are the interior deflections. Measured joint and interior deflection under load with temperature gradients are shown in Figure B.4.

To minimize the effects of temperature gradients during the follow-up testing, testing was scheduled at approximately the same time of the day as the initial tests. Limitations due to surface preparation, treatment application, equipment availability, and traffic control were not conducive to repeated testing at similar temperature gradients. As shown in Figure B.4, the effects of temperature on deflections may mask out any differences in deflections due to treatment types. To account for effects of temperature gradient differences between testing periods, the temperature analysis data was used to adjust measured deflections.

Several assumptions were made when adjusting measured deflections. The first assumption was that the temperature gradient measured at the outside shoulder edge was representative of gradients along the 82 slab test sections. There was no reason to dispute this assumption since there were no changes in pavement design and no shadows cast by vegetation, signing, utility poles, bridge structures, etc. The second assumption was that the temperature distribution through the slab was similar between testing periods (initial and at one year). Ideal testing conditions for deflection monitoring through time would be to test slabs when

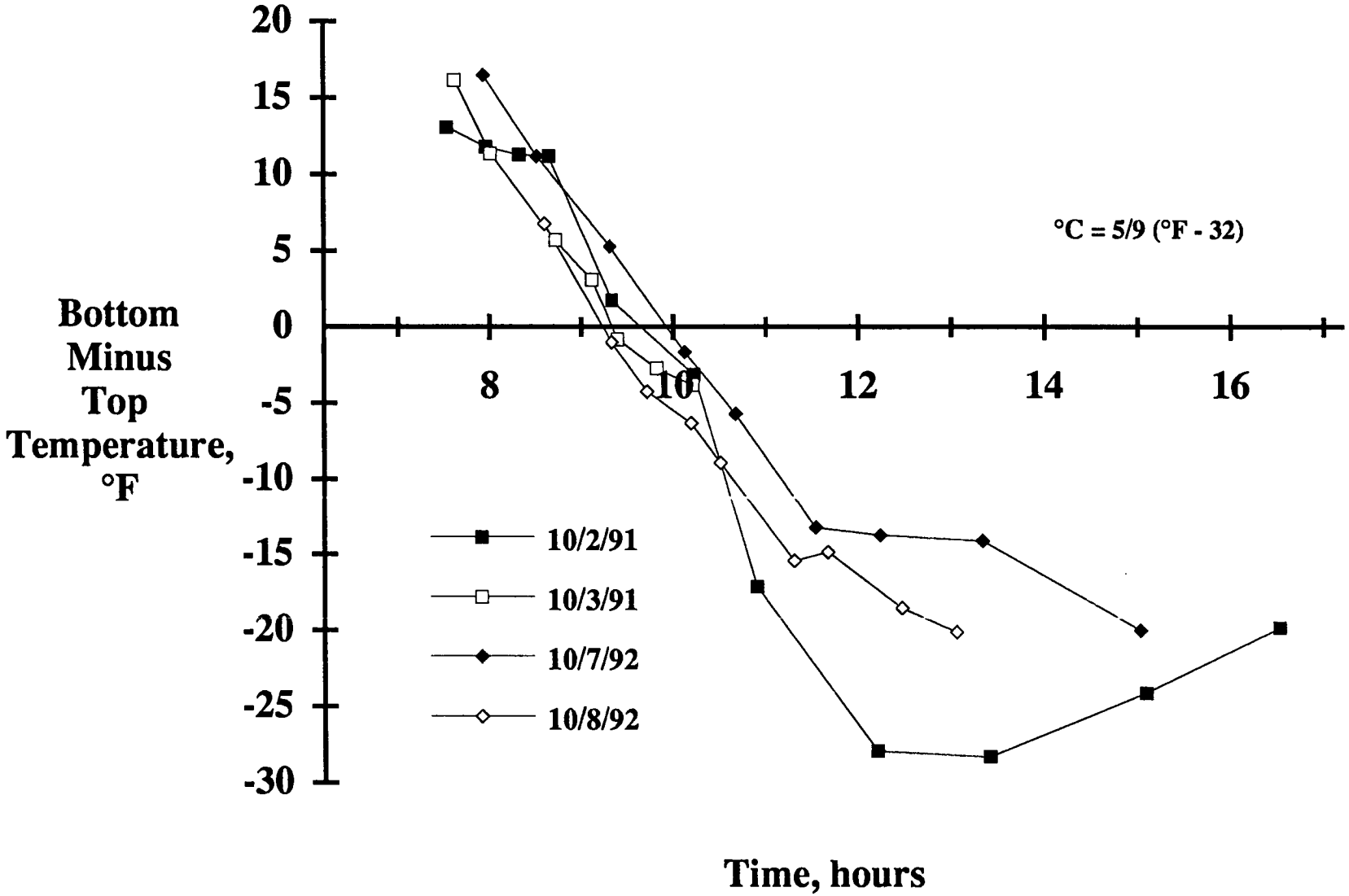


Figure B.3. Concrete temperature gradients.

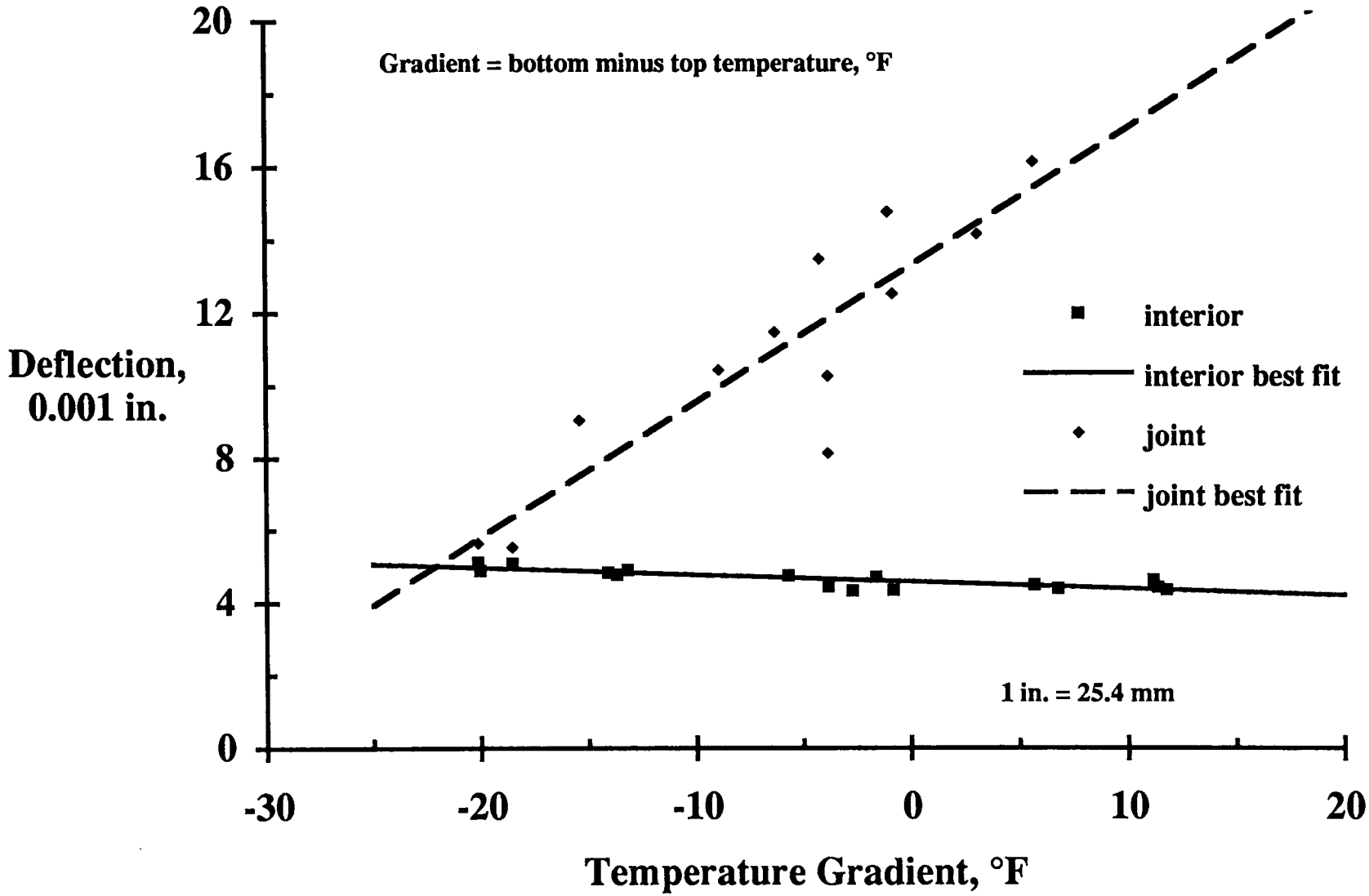


Figure B.4. Maximum interior and joint deflection versus temperature gradient.

there is no change in temperature with depthleading to curling effects on deflections. Since temperature gradients were similar between 1991 and 1992 with time of day, it was assumed that distribution differences were minimal. Another assumption was that the temperature gradient measured at the outside shoulder edge was representative of the slab joint and interior. Since the change in deflections with time was of primary interest, the edge temperature gradient was used only as a calibration method. By calibrating interior and joint deflections to a zero edge temperature gradient, deflections at equal gradients could at least be compared regardless of what the true interior or joint temperature gradient was.

Another assumption was that the effects of temperature on the unloaded slab deflection were similar for all joints. Unloaded slab deflections at non-dowelled joints are a function of aggregate interlock and joint width. As rough edges of joint faces are broken down with traffic and/or joint width increases with temperature drop contraction, the degree of load transfer (unloaded divided by loaded slab deflection) decreases. Changes in aggregate interlock due to slab contraction are a function of temperature change, subbase restraint, and joint spacing. Since joint spacing is variable, this assumption was the weakest of the above assumptions. To minimize effects of joint spacing the 18 ft (5.5 m) long slab was selected for temperature effect testing. This slab was the third longest of four joint spacings.

To adjust deflections for gradient effects it was assumed that the percentage effect on the temperature monitoring slab could be applied to all other slabs. Since deflections throughout the test section were highly variable, a proportional adjustment rather than magnitude adjustment was made to all deflections to account for temperature gradients. Temperature and deflection data from the temperature monitoring slab were used to develop regression equations predicting deflection magnitude for both interior and joint deflections as a function of temperature gradient. For each deflection location, regression prediction equations were developed similar to those plotted in Figure B.4. With the exception of the unloaded slab joint deflection and loaded slab deflection at 60 in. (1524 mm), plots of deflection for other positions were similar to those shown in Figure B.4. These deflections showed a significantly smaller trend with temperature gradient than other deflection positions.

The coefficient of determination for predicting interior deflections (7 positions) with temperature gradient ranged from 0.540 to 0.871 and averaged 0.773. For joint deflection positions excluding the unloaded slab joint deflection and loaded slab deflection at 60 in. (1524 mm), the coefficient of determination ranged from 0.597 to 0.791 and averaged 0.728. The unloaded slab deflection and deflection at 60 in. (1524 mm) had coefficients of determination of 0.266 and 0.135, respectively. The low coefficients of determination indicated that the unloaded slab deflection and deflection at 60 in. (1524 mm) were insensitive to the temperature gradient. Coefficients of determination for interior and joint deflections under load shown in Figure B.4 were 0.676 and 0.791, respectively. Predicted deflections for each deflection location as a function of temperature gradient were generated. Predicted deflections at zero temperature gradient were then divided by predicted deflections at various gradients. Equations were developed to generate the zero gradient adjustment factor (zero gradient deflection / deflection with gradient). When multiplied by measured deflections the zero gradient deflection is determined. Adjustment equations for each interior and joint deflection location are listed in Table B.1.

Table B.1 Deflection temperature adjustment factor equations

| Position | Distance, in. | Slope | Intercept |
|---|---|---|---|
| Interior | 0 | 0.00405 | 1.0013 |
| | 8 | 0.00574 | 1.0027 |
| | 12 | 0.00637 | 1.0034 |
| | 18 | 0.00698 | 1.0040 |
| | 24 | 0.00749 | 1.0047 |
| | 36 | 0.00801 | 1.0054 |
| | 69 | 0.00713 | 1.0042 |
| Joint | -12 | -0.03616 | 0.9983 |
| | 0 | -0.05357 | 0.9910 |
| | 12 | -0.04406 | 0.9956 |
| | 18 | -0.03945 | 0.9973 |
| | 24 | -0.03207 | 0.9993 |
| | 26 | -0.02253 | 1.0006 |
| | 60 | -0.00535 | 1.0002 |

Note: 1 in. = 25.4 mm

### *B.2.4 Replicate Variance*

Control testing (3 sections) done October 2, 1991 (before treatment application) and October 3, 1991 (after treatment application) were used to evaluate test repeatability. Assuming insignificant effects of ASR deterioration within a 24 hour period, differences in replicate test deflections are attributable to equipment wear, equipment positioning, measurement error, and temperature gradient adjustments. Deflections from the 15 interior and 12 joint areas tested in the three control sections were analyzed to determine replication variance. Total load and corresponding deflections were measured for each of the triplicate tests done at each location. Normalized deflections were adjusted for temperature gradients by multiplying measured deflections by the percentage adjustment factors at each deflection position. Gradients at time of each deflection measurement were interpreted from temperature data shown in Figure B.3. Changes in deflections over longer time periods are only significant if they are statistically greater than differences attributed to between-test variability.

Between-test variance (replicate mean square) and standard deviation (replicate root mean square) were computed at each deflection position for both interior and joint deflections. Pooled standard deviations of replicate deflections were computed at each deflection position for interior and joint testing. Joint deflection between-test variability was significantly higher than interior deflections. Differences were attributed to relatively larger deflections at joints. Similarly, the replication standard deviation generally decreased with distance from the load as deflection magnitudes decreased. Replication variance was 0.00046 and 0.00156 in. (0.012 and 0.04 mm) under the load for interior and joint deflections, respectively. The between-test variance analysis is summarized in Table B.2. The analysis for interior and joint replication variance is listed in Tables B.3 and B.4.

## B.3 Treatment Analysis

Measured deflections (normalized to 10 kips, 4535 kg) before treatment, one day after treatment, and one year after treatment are listed in Tables B.5 through B.7 for interior and in Tables B.8 through B.10 for joint deflections. Temperature adjusted deflections are listed in Tables B.11 through B.16. Edge deflections measured only during the follow-up study at one year are listed in Table B.17. Edge load data at midslab 18 in. (457 mm) from the lane-shoulder longitudinal joint are not corrected for temperature gradient effects. Should additional follow-up testing be done, edge deflection temperature gradient effect correction factors would need to be developed. Sections and treatment types are shown in Figure B.1. Within each section slabs are labelled A through E in the direction of the eastbound traffic. Leave side joints are labelled A through D in the direction of traffic.

Normalized deflections (triplicate test average) were adjusted for temperature gradients by multiplying measured deflections by the ratio adjustment factors at each deflection position. Adjustment factors equations are listed in Table B.1. Gradients at time of each deflection measurement were interpreted from temperature data shown in Figure B.3.

Two types of analyses were performed to evaluate the effectiveness of treatments. The first analysis was a paired t-test to statistically evaluate within-treatment differences in deflection magnitudes measured over time. This analysis only evaluates any statistically significant deflection differences within each section or treatment. For example, the t-test for Control Section 3 was used to note any if measured differences in deflection magnitudes between the

Table B.2 Replicate variance summary

| | Interior Deflection Position, in. | | | | | | |
|---|---|---|---|---|---|---|---|
| | 0 | 8 | 12 | 18 | 24 | 36 | 60 |
| Mean difference | 0.35 | 0.29 | 0.25 | 0.22 | 0.18 | 0.15 | 0.09 |
| Replicate mean square | 0.21 | 0.12 | 0.09 | 0.06 | 0.04 | 0.02 | 0.01 |
| Degrees of freedom | 15 | 15 | 15 | 15 | 15 | 15 | 15 |
| Repl. RMS | 0.46 | 0.35 | 0.29 | 0.25 | 0.19 | 0.14 | 0.08 |
| Replicate coefficient of variation, % | 132.8 | 119.6 | 119.0 | 112.7 | 108.0 | 89.7 | 92.5 |

| | Joint Deflection Position, in. | | | | | | |
|---|---|---|---|---|---|---|---|
| | -12 | 0 | 12 | 18 | 24 | 36 | 60 |
| Mean difference | 1.05 | 1.97 | 1.32 | 1.07 | 0.72 | 0.44 | 0.14 |
| Replicate mean square | 0.93 | 2.44 | 1.11 | 0.75 | 0.38 | 0.16 | 0.02 |
| Degrees of freedom | 12 | 12 | 12 | 12 | 12 | 12 | 12 |
| Repl. RMS | 0.97 | 1.56 | 1.05 | 0.86 | 0.62 | 0.40 | 0.13 |
| Replicate coefficient of variation, % | 92.0 | 79.2 | 79.8 | 80.9 | 85.3 | 90.6 | 93.1 |

Notes: 1. Deflections in 0.001 in.
2. 1 in. = 25.4 mm

Table B.3 Between-test interior deflection variance analysis

| Section | Slab | Distance from load, in. -12 | 0 | 12 | 18 | 24 | 36 | 60 |
|---|---|---|---|---|---|---|---|---|
| Control 3 | A | 3.80 | 4.09 | 3.72 | 3.45 | 3.16 | 2.63 | 1.73 |
| | A | 3.95 | 4.26 | 3.78 | 3.54 | 3.23 | 2.68 | 1.74 |
| | s2 | 0.0111 | 0.0141 | 0.0017 | 0.0041 | 0.0026 | 0.0014 | 0.0001 |
| | B | 3.85 | 4.19 | 3.70 | 3.48 | 3.11 | 2.56 | 1.84 |
| | B | 4.10 | 4.38 | 3.91 | 3.67 | 3.32 | 2.83 | 2.13 |
| | s2 | 0.0309 | 0.0185 | 0.0227 | 0.0181 | 0.0207 | 0.0353 | 0.0435 |
| | C | 3.85 | 4.21 | 3.71 | 3.50 | 3.25 | 2.79 | 2.30 |
| | C | 4.03 | 4.35 | 3.86 | 3.62 | 3.33 | 2.91 | 2.43 |
| | s2 | 0.0165 | 0.0097 | 0.0104 | 0.0074 | 0.0031 | 0.0066 | 0.0082 |
| | D | 5.38 | 6.29 | 4.95 | 4.41 | 3.76 | 2.84 | 1.40 |
| | D | 5.52 | 6.55 | 5.08 | 4.54 | 3.89 | 2.96 | 1.44 |
| | s2 | 0.0106 | 0.0353 | 0.0092 | 0.0083 | 0.0084 | 0.0068 | 0.0006 |
| | E | 7.87 | 9.17 | 7.31 | 6.40 | 5.33 | 3.81 | 1.26 |
| | E | 9.61 | 11.56 | 8.77 | 7.63 | 6.22 | 4.32 | 1.26 |
| | s2 | 1.5146 | 2.8663 | 1.0749 | 0.7556 | 0.4017 | 0.1274 | 0.0000 |
| Control 2 | A | 4.33 | 4.83 | 4.15 | 3.78 | 3.36 | 2.66 | 1.62 |
| | A | 4.58 | 5.06 | 4.35 | 4.00 | 3.54 | 2.83 | 1.72 |
| | s2 | 0.0315 | 0.0254 | 0.0206 | 0.0238 | 0.0167 | 0.0138 | 0.0051 |
| | B | 4.47 | 4.97 | 4.28 | 3.99 | 3.57 | 2.90 | 1.76 |
| | B | 4.46 | 4.85 | 4.19 | 3.92 | 3.52 | 2.88 | 1.74 |
| | s2 | 0.0001 | 0.0068 | 0.0044 | 0.0025 | 0.0014 | 0.0001 | 0.0002 |
| | C | 4.69 | 5.03 | 4.54 | 4.29 | 3.89 | 3.20 | 2.02 |
| | C | 4.82 | 5.11 | 4.62 | 4.36 | 3.91 | 3.25 | 2.13 |
| | s2 | 0.0077 | 0.0027 | 0.0026 | 0.0025 | 0.0002 | 0.0010 | 0.0063 |
| | D | 4.33 | 4.75 | 4.21 | 3.95 | 3.59 | 2.97 | 1.95 |
| | D | 4.49 | 4.91 | 4.31 | 4.08 | 3.66 | 3.07 | 2.02 |
| | s2 | 0.0132 | 0.0133 | 0.0049 | 0.0076 | 0.0021 | 0.0045 | 0.0022 |
| | E | 4.34 | 4.47 | 4.15 | 3.81 | 3.36 | 2.69 | 1.60 |
| | E | 4.49 | 4.73 | 4.28 | 3.91 | 3.47 | 2.77 | 1.66 |
| | s2 | 0.0114 | 0.0343 | 0.0077 | 0.0053 | 0.0051 | 0.0032 | 0.0016 |

Table B.3 (continued)

| Section | Slab | Distance from load, in. -12 | 0 | 12 | 18 | 24 | 36 | 60 |
|---|---|---|---|---|---|---|---|---|
| Control 1 | A | 4.30 | 4.53 | 4.14 | 3.89 | 3.54 | 2.95 | 1.86 |
| | A | 4.56 | 4.99 | 4.39 | 4.11 | 3.75 | 3.11 | 1.96 |
| | s2 | 0.0326 | 0.1065 | 0.0312 | 0.0232 | 0.0223 | 0.0128 | 0.0043 |
| | B | 7.49 | 9.55 | 6.98 | 6.22 | 5.38 | 4.18 | 2.38 |
| | B | 7.91 | 9.42 | 7.32 | 6.60 | 5.68 | 4.43 | 2.48 |
| | s2 | 0.0907 | 0.0073 | 0.0554 | 0.0716 | 0.0465 | 0.0309 | 0.0044 |
| | C | 6.14 | 6.49 | 5.87 | 5.43 | 4.90 | 3.95 | 2.37 |
| | C | 6.34 | 6.69 | 6.07 | 5.60 | 5.04 | 4.15 | 2.53 |
| | s2 | 0.0199 | 0.0201 | 0.0196 | 0.0153 | 0.0110 | 0.0201 | 0.0136 |
| | D | 5.26 | 5.57 | 5.09 | 4.79 | 4.31 | 3.50 | 2.11 |
| | D | 5.47 | 5.83 | 5.31 | 4.95 | 4.46 | 3.63 | 2.21 |
| | s2 | 0.0213 | 0.0349 | 0.0245 | 0.0138 | 0.0121 | 0.0088 | 0.0052 |
| | E | 4.60 | 4.95 | 4.44 | 4.12 | 3.73 | 2.97 | 1.62 |
| | E | 4.72 | 5.13 | 4.53 | 4.22 | 3.78 | 3.04 | 1.63 |
| | s2 | 0.0068 | 0.0160 | 0.0040 | 0.0042 | 0.0013 | 0.0024 | 0.0000 |
| | mean difference | 0.29 | 0.35 | 0.25 | 0.22 | 0.18 | 0.15 | 0.09 |
| | Replicate mean square | 0.12 | 0.21 | 0.09 | 0.06 | 0.04 | 0.02 | 0.01 |
| | degrees of freedom | 15 | 15 | 15 | 15 | 15 | 15 | 15 |
| | Replicate RMS | 0.35 | 0.46 | 0.29 | 0.25 | 0.19 | 0.14 | 0.08 |
| | replicate coefficient of variation % | 119.6 | 132.8 | 119.0 | 112.7 | 108.0 | 89.7 | 92.5 |

Notes: 1. Deflections in 0.001 in.
2. 1 in. = 25.4 mm

Table B.4 Between-test joint deflection variance analysis

| Section | Slab | Distance from load, in. -12 | 0 | 12 | 18 | 24 | 36 | 60 |
|---|---|---|---|---|---|---|---|---|
| Control 3 | A | 3.01 | 9.88 | 6.84 | 5.76 | 4.64 | 3.18 | 1.50 |
| | A | 2.97 | 11.71 | 8.20 | 6.90 | 5.53 | 3.73 | 1.75 |
| | s2 | 0.0011 | 1.6734 | 0.9169 | 0.6470 | 0.3960 | 0.1522 | 0.0331 |
| | B | 4.58 | 7.42 | 5.33 | 4.54 | 3.73 | 2.66 | 1.45 |
| | B | 4.70 | 10.54 | 7.48 | 6.32 | 5.08 | 3.51 | 1.81 |
| | s2 | 0.0075 | 4.8607 | 2.3276 | 1.5920 | 0.9211 | 0.3579 | 0.0649 |
| | C | 4.57 | 7.55 | 5.59 | 4.79 | 3.98 | 2.90 | 1.55 |
| | C | 6.49 | 7.78 | 5.80 | 5.01 | 4.18 | 3.06 | 1.66 |
| | s2 | 1.8440 | 0.0273 | 0.0214 | 0.0234 | 0.0199 | 0.0129 | 0.0060 |
| | D | 5.07 | 13.42 | 9.43 | 7.96 | 6.39 | 4.36 | 1.76 |
| | D | 4.72 | 15.78 | 11.51 | 9.94 | 8.12 | 5.67 | 2.04 |
| | s2 | 0.0612 | 2.7903 | 2.1691 | 1.9539 | 1.4890 | 0.8571 | 0.0390 |
| Control 2 | A | 7.36 | 7.62 | 6.44 | 5.96 | 5.28 | 4.29 | 2.61 |
| | A | 7.72 | 8.79 | 7.00 | 6.31 | 5.40 | 4.12 | 2.28 |
| | s2 | 0.0630 | 0.6874 | 0.1573 | 0.0602 | 0.0068 | 0.0141 | 0.0551 |
| | B | 6.81 | 7.17 | 5.96 | 5.44 | 4.78 | 3.78 | 2.22 |
| | B | 7.52 | 8.51 | 6.82 | 6.13 | 5.24 | 3.98 | 2.19 |
| | s2 | 0.2537 | 0.8858 | 0.3701 | 0.2403 | 0.1047 | 0.0209 | 0.0006 |
| | C | 6.94 | 7.52 | 6.17 | 5.61 | 4.92 | 3.86 | 2.28 |
| | C | 7.49 | 8.53 | 6.82 | 6.06 | 5.16 | 3.89 | 2.13 |
| | s2 | 0.1493 | 0.5072 | 0.2085 | 0.1018 | 0.0293 | 0.0005 | 0.0111 |
| | D | 5.35 | 5.96 | 4.79 | 4.36 | 3.83 | 3.05 | 1.91 |
| | D | 5.80 | 6.96 | 5.36 | 4.78 | 4.06 | 3.10 | 1.81 |
| | s2 | 0.1036 | 0.5015 | 0.1591 | 0.0897 | 0.0277 | 0.0015 | 0.0055 |

Table B.4 (continued)

| Section | Slab | Distance from load, in. -12 | 0 | 12 | 18 | 24 | 36 | 60 |
|---|---|---|---|---|---|---|---|---|
| Control 1 | A | 8.07 | 10.27 | 7.80 | 6.81 | 5.52 | 3.95 | 1.98 |
| | A | 6.71 | 7.81 | 6.16 | 5.46 | 4.61 | 3.46 | 1.95 |
| | s2 | 0.9336 | 3.0402 | 1.3436 | 0.9190 | 0.4184 | 0.1223 | 0.0003 |
| | B | 9.18 | 13.78 | 9.92 | 8.41 | 6.69 | 4.47 | 1.94 |
| | B | 7.26 | 10.40 | 7.78 | 6.92 | 6.11 | 4.04 | 2.01 |
| | s2 | 1.8262 | 5.6916 | 2.2782 | 1.1059 | 0.1648 | 0.0912 | 0.0026 |
| | C | 10.11 | 14.32 | 10.51 | 9.01 | 7.15 | 4.86 | 2.12 |
| | C | 8.10 | 12.00 | 8.96 | 7.77 | 6.32 | 4.42 | 2.13 |
| | s2 | 2.0088 | 2.6867 | 1.1936 | 0.7667 | 0.3434 | 0.0944 | 0.0000 |
| | D | 8.97 | 12.42 | 8.84 | 7.48 | 5.86 | 3.85 | 1.64 |
| | D | 6.16 | 8.98 | 6.74 | 5.76 | 4.71 | 3.28 | 1.62 |
| | s2 | 3.9370 | 5.9125 | 2.1934 | 1.4707 | 0.6613 | 0.1657 | 0.0001 |
| mean difference | | 1.05 | 1.97 | 1.32 | 1.07 | 0.72 | 0.44 | 0.14 |
| Replicate mean square | | 0.93 | 2.44 | 1.11 | 0.75 | 0.38 | 0.16 | 0.02 |
| degrees of freedom | | 12 | 12 | 12 | 12 | 12 | 12 | 12 |
| Replicate RMS | | 0.97 | 1.56 | 1.05 | 0.86 | 0.62 | 0.40 | 0.13 |
| replicate coefficient of variation % | | 92.0 | 79.2 | 79.8 | 80.9 | 85.3 | 90.6 | 93.1 |

Notes: 1. Deflections in 0.001 in.
2. 1 in. = 25.4 mm

Table B.5 Measured interior deflections before treatment

| Section | Slab | Time AM | Temperature Gradient °F | Measured Deflection, 0.001 in. 0 | 8 | 12 | 18 | 24 | 36 | 60 |
|---|---|---|---|---|---|---|---|---|---|---|
| Control 3 | A | 7:40 | 12.1 | 3.90 | 3.55 | 3.45 | 3.17 | 2.89 | 2.38 | 1.59 |
| | B | 7:42 | 12.0 | 3.99 | 3.59 | 3.42 | 3.20 | 2.85 | 2.33 | 1.69 |
| | C | 7:44 | 11.9 | 4.01 | 3.59 | 3.44 | 3.22 | 2.97 | 2.54 | 2.12 |
| | D | 7:45 | 11.9 | 5.99 | 5.02 | 4.59 | 4.06 | 3.44 | 2.58 | 1.29 |
| | E | 7:46 | 11.8 | 8.74 | 7.35 | 6.78 | 5.89 | 4.87 | 3.46 | 1.16 |
| Lithium 2 | A | 7:47 | 11.8 | 4.51 | 4.27 | 4.19 | 4.05 | 3.88 | 3.84 | 4.20 |
| | B | 7:49 | 11.7 | 4.75 | 4.15 | 3.93 | 3.64 | 3.26 | 2.67 | 1.68 |
| | C | 7:50 | 11.7 | 4.25 | 3.69 | 3.47 | 3.19 | 2.87 | 2.36 | 1.52 |
| | D | 7:51 | 11.7 | 4.38 | 3.95 | 3.78 | 3.50 | 3.15 | 2.58 | 1.62 |
| | E | 7:57 | 11.6 | 4.64 | 4.22 | 4.07 | 3.88 | 3.61 | 3.19 | 2.76 |
| Silane 2 | A | 7:52 | 11.7 | 4.63 | 4.38 | 4.27 | 4.12 | 3.89 | 3.61 | 3.38 |
| | B | 7:53 | 11.6 | 6.77 | 5.85 | 5.46 | 4.84 | 4.14 | 3.11 | 1.73 |
| | C | 7:54 | 11.6 | 6.02 | 5.05 | 4.68 | 4.10 | 3.48 | 2.58 | 1.35 |
| | D | 7:56 | 11.6 | 3.62 | 3.35 | 3.27 | 3.15 | 2.96 | 2.82 | 2.86 |
| | E | 7:57 | 11.6 | 3.61 | 3.22 | 3.11 | 2.94 | 2.72 | 2.43 | 2.19 |
| Methacrylate 2 | A | 7:58 | 11.5 | 4.33 | 3.76 | 3.53 | 3.15 | 2.72 | 2.10 | 1.27 |
| | B | 7:58 | 11.5 | 3.98 | 3.56 | 3.38 | 3.10 | 2.75 | 2.23 | 1.44 |
| | C | 7:59 | 11.5 | 5.46 | 5.03 | 4.89 | 4.74 | 4.46 | 4.19 | 3.70 |
| | D | 8:00 | 11.5 | 4.47 | 4.16 | 3.99 | 3.75 | 3.48 | 3.00 | 2.41 |
| | E | 8:01 | 11.5 | 4.24 | 3.74 | 3.55 | 3.27 | 2.87 | 2.28 | 1.33 |
| Control 2 | A | 8:03 | 11.4 | 4.61 | 4.05 | 3.85 | 3.49 | 3.08 | 2.42 | 1.50 |
| | B | 8:04 | 11.4 | 4.75 | 4.19 | 3.98 | 3.68 | 3.28 | 2.64 | 1.62 |
| | C | 8:05 | 11.4 | 4.81 | 4.39 | 4.22 | 3.96 | 3.57 | 2.92 | 1.86 |
| | D | 8:06 | 11.3 | 4.53 | 4.06 | 3.91 | 3.65 | 3.30 | 2.71 | 1.80 |
| | E | 8:07 | 11.3 | 4.27 | 4.06 | 3.86 | 3.52 | 3.09 | 2.46 | 1.48 |
| Silane 1 | A | 8:07 | 11.3 | 4.88 | 4.41 | 4.18 | 3.86 | 3.43 | 2.77 | 1.70 |
| | B | 8:08 | 11.3 | 4.73 | 4.32 | 4.17 | 3.89 | 3.50 | 2.84 | 1.79 |
| | C | 8:09 | 11.3 | 4.98 | 4.52 | 4.34 | 4.09 | 3.66 | 3.01 | 1.88 |
| | D | 8:10 | 11.3 | 5.09 | 4.43 | 4.13 | 3.75 | 3.30 | 2.66 | 1.71 |
| | E | 8:11 | 11.3 | 5.10 | 4.53 | 4.28 | 3.93 | 3.54 | 2.89 | 1.83 |

Table B.5 (continued)

| Section | Slab | Time AM | Temperature Gradient °F | Measured Deflection, 0.001 in. 0 | 8 | 12 | 18 | 24 | 36 | 60 |
|---|---|---|---|---|---|---|---|---|---|---|
| Lithium 1 | A | 8:11 | 11.3 | 4.92 | 4.42 | 4.26 | 3.92 | 3.57 | 2.89 | 1.87 |
| | B | 8:12 | 11.3 | 5.12 | 4.75 | 4.57 | 4.28 | 3.85 | 3.19 | 2.06 |
| | C | 8:13 | 11.3 | 5.06 | 4.66 | 4.45 | 4.14 | 3.71 | 3.05 | 2.04 |
| | D | 8:14 | 11.3 | 5.37 | 4.88 | 4.66 | 4.30 | 3.87 | 3.19 | 2.04 |
| | E | 8:14 | 11.3 | 5.00 | 4.64 | 4.47 | 4.20 | 3.82 | 3.22 | 2.13 |
| Control 1 | A | 8:15 | 11.3 | 4.33 | 4.03 | 3.85 | 3.60 | 3.25 | 2.70 | 1.72 |
| | B | 8:16 | 11.3 | 9.12 | 7.01 | 6.49 | 5.74 | 4.94 | 3.82 | 2.20 |
| | C | 8:17 | 11.3 | 6.20 | 5.75 | 5.46 | 5.01 | 4.50 | 3.61 | 2.18 |
| | D | 8:18 | 11.2 | 5.32 | 4.93 | 4.73 | 4.42 | 3.96 | 3.20 | 1.94 |
| | E | 8:18 | 11.2 | 4.73 | 4.31 | 4.13 | 3.81 | 3.42 | 2.71 | 1.49 |
| Methacrylate 1 | A | 8:19 | 11.2 | 4.72 | 3.82 | 3.47 | 3.06 | 2.57 | 1.93 | 1.04 |
| | B | 8:20 | 11.2 | 4.93 | 4.15 | 3.90 | 3.54 | 3.10 | 2.36 | 1.28 |
| | C | 8:21 | 11.2 | 4.79 | 4.31 | 4.12 | 3.81 | 3.42 | 2.78 | 1.59 |
| | D | 8:22 | 11.2 | 5.02 | 4.42 | 4.13 | 3.73 | 3.15 | 2.40 | 1.32 |
| | E | 8:23 | 11.2 | 5.10 | 4.27 | 4.00 | 3.55 | 3.01 | 2.35 | 1.24 |

Notes:
1. Normalized to 10 kips
2. Data measured on 10/2/91
3. 1 in. = 25.4 mm
4. 1°F = 0.556°C

Table B.6 Measured interior deflections one day after treatment

| Section | Slab | Time AM | Temperature Gradient °F | Measured Deflection, 0.001 in. 0 | 8 | 12 | 18 | 24 | 36 | 60 |
|---|---|---|---|---|---|---|---|---|---|---|
| Control 3 | A | 7:48 | 11.6 | 4.06 | 3.70 | 3.51 | 3.27 | 2.96 | 2.44 | 1.60 |
| | B | 7:49 | 11.4 | 4.19 | 3.84 | 3.63 | 3.38 | 3.04 | 2.58 | 1.97 |
| | C | 7:50 | 11.3 | 4.16 | 3.78 | 3.59 | 3.35 | 3.06 | 2.65 | 2.24 |
| | D | 7:51 | 11.1 | 6.26 | 5.18 | 4.73 | 4.20 | 3.58 | 2.70 | 1.33 |
| | E | 7:53 | 10.9 | 11.06 | 9.02 | 8.18 | 7.06 | 5.73 | 3.95 | 1.17 |
| Methacrylate 2 | A | 7:58 | 10.2 | 3.96 | 3.41 | 3.20 | 2.92 | 2.58 | 2.07 | 1.37 |
| | B | 7:59 | 10.0 | 3.92 | 3.50 | 3.34 | 3.09 | 2.79 | 2.32 | 1.53 |
| | C | 8:00 | 9.9 | 5.04 | 4.63 | 4.49 | 4.29 | 3.99 | 3.64 | 3.29 |
| | D | 8:01 | 9.8 | 4.31 | 4.06 | 3.89 | 3.63 | 3.37 | 2.88 | 2.25 |
| | E | 8:03 | 9.5 | 4.03 | 3.66 | 3.48 | 3.21 | 2.85 | 2.30 | 1.33 |
| Control 2 | A | 8:06 | 9.1 | 4.87 | 4.34 | 4.10 | 3.75 | 3.30 | 2.62 | 1.61 |
| | B | 8:08 | 8.8 | 4.68 | 4.23 | 3.95 | 3.67 | 3.29 | 2.68 | 1.63 |
| | C | 8:09 | 8.7 | 4.93 | 4.58 | 4.36 | 4.10 | 3.65 | 3.02 | 2.00 |
| | D | 8:11 | 8.4 | 4.74 | 4.28 | 4.08 | 3.83 | 3.43 | 2.86 | 1.89 |
| | E | 8:12 | 8.3 | 4.57 | 4.27 | 4.05 | 3.68 | 3.25 | 2.59 | 1.56 |
| Control 1 | A | 8:15 | 7.9 | 4.83 | 4.35 | 4.17 | 3.88 | 3.53 | 2.91 | 1.85 |
| | B | 8:16 | 7.7 | 9.13 | 7.56 | 6.95 | 6.24 | 5.35 | 4.15 | 2.34 |
| | C | 8:19 | 7.3 | 6.49 | 6.07 | 5.78 | 5.31 | 4.76 | 3.90 | 2.40 |
| | D | 8:20 | 7.2 | 5.66 | 5.24 | 5.06 | 4.70 | 4.22 | 3.42 | 2.09 |
| | E | 8:23 | 6.8 | 4.99 | 4.53 | 4.33 | 4.01 | 3.58 | 2.86 | 1.55 |
| Methacrylate 1 | A | 8:26 | 6.4 | 4.55 | 3.72 | 3.39 | 3.06 | 2.59 | 1.98 | 1.10 |
| | B | 8:28 | 6.1 | 4.36 | 3.93 | 3.71 | 3.41 | 3.01 | 2.36 | 1.30 |
| | C | 8:29 | 6.0 | 4.62 | 4.18 | 4.02 | 3.76 | 3.35 | 2.75 | 1.56 |
| | D | 8:30 | 5.8 | 4.84 | 4.26 | 3.94 | 3.59 | 3.14 | 2.42 | 1.38 |
| | E | 8:32 | 5.6 | 4.57 | 4.01 | 3.73 | 3.38 | 2.96 | 2.32 | 1.33 |

Notes:
1. Normalized to 10 kips
2. Data measured on 10/3/91
3. 1 in. = 25.4 mm
4. 1°F = 0.556°C

Table B.7 Measured interior deflections one year after treatment

| Section | Slab | Time AM | Temperature Gradient °F | Measured Deflection, 0.001 in. 0 | 8 | 12 | 18 | 24 | 36 | 60 |
|---|---|---|---|---|---|---|---|---|---|---|
| Control 3 | A | 8:15 | 11.8 | 3.75 | 3.53 | 3.35 | 3.13 | 2.88 | 2.46 | 1.68 |
| | B | 9:45 | -0.2 | 4.33 | 3.99 | 3.80 | 3.59 | 3.26 | 2.76 | 1.98 |
| | C | 10:22 | -5.0 | 4.22 | 3.66 | 3.66 | 3.38 | 3.08 | 2.52 | 1.61 |
| | D | 11:16 | -12.6 | 5.23 | 4.46 | 4.14 | 3.72 | 3.26 | 2.57 | 1.59 |
| | E | 12:08 | -13.7 | 4.69 | 4.19 | 3.92 | 3.55 | 3.19 | 2.56 | 1.66 |
| Lithium 2 | A | 8:22 | 10.8 | 4.32 | 4.16 | 4.07 | 3.93 | 3.79 | 3.67 | 3.85 |
| | B | 9:48 | -0.6 | 4.14 | 3.91 | 3.70 | 3.46 | 3.17 | 2.68 | 1.87 |
| | C | 10:25 | -5.3 | 4.37 | 3.81 | 3.57 | 3.30 | 2.96 | 2.45 | 1.62 |
| | D | 11:20 | -13.2 | 4.93 | 4.70 | 4.44 | 4.16 | 3.79 | 3.10 | 1.91 |
| | E | 11:23 | -13.2 | 5.08 | 4.78 | 4.55 | 4.21 | 3.84 | 3.13 | 1.81 |
| Silane 2 | A | 8:24 | 10.6 | 4.26 | 3.96 | 3.81 | 3.53 | 3.22 | 2.66 | 1.81 |
| | B | 9:52 | -1.2 | 5.93 | 5.09 | 4.66 | 4.20 | 3.67 | 2.85 | 1.64 |
| | C | 10:30 | -6.0 | 5.43 | 4.54 | 4.25 | 3.72 | 3.22 | 2.48 | 1.38 |
| | D | 11:26 | -13.3 | 3.97 | 3.75 | 3.61 | 3.43 | 3.18 | 2.73 | 2.02 |
| | E | 11:58 | -13.7 | 4.15 | 3.83 | 3.64 | 3.42 | 3.12 | 2.55 | 1.50 |
| Methacrylate 2 | A | 8:30 | 9.8 | 4.54 | 4.24 | 3.93 | 3.73 | 3.37 | 2.81 | 1.89 |
| | B | 9:59 | -2.1 | 3.75 | 3.42 | 3.23 | 2.96 | 2.68 | 2.25 | 1.50 |
| | C | 10:32 | -6.3 | 5.61 | 5.22 | 5.03 | 4.69 | 4.26 | 3.43 | 1.88 |
| | D | 11:28 | -13.3 | 5.30 | 4.83 | 4.68 | 4.41 | 4.05 | 3.20 | 1.62 |
| | E | 11:54 | -13.6 | 5.57 | 5.35 | 5.11 | 4.78 | 4.36 | 3.56 | 2.39 |
| Silane #2 1 | A | 8:36 | 9.1 | 3.43 | 3.11 | 2.89 | 2.64 | 2.33 | 1.85 | 1.14 |
| | B | 12:18 | -13.8 | 4.43 | 3.89 | 3.61 | 3.30 | 2.96 | 2.35 | 1.35 |
| | C | 12:20 | -13.8 | 3.77 | 3.30 | 3.04 | 2.70 | 2.39 | 1.87 | 1.06 |
| | D | 12:22 | -13.8 | 3.96 | 3.19 | 2.98 | 2.71 | 2.42 | 1.85 | 1.23 |
| | E | 13:05 | -14.1 | 5.66 | 5.34 | 5.09 | 4.74 | 4.29 | 3.42 | 1.64 |
| Linseed Oil 1 | A | 8:39 | 8.7 | 4.85 | 4.15 | 3.95 | 3.56 | 3.13 | 2.41 | 1.42 |
| | B | 10:03 | -2.6 | 3.67 | 3.41 | 3.19 | 2.89 | 2.52 | 1.98 | 1.03 |
| | C | 10:37 | -7.0 | 3.88 | 3.55 | 3.30 | 2.93 | 2.55 | 1.93 | 1.14 |
| | D | 11:33 | -13.4 | 4.07 | 3.69 | 3.45 | 3.12 | 2.74 | 2.13 | 1.25 |
| | E | 12:12 | -13.8 | 6.21 | 5.67 | 5.32 | 4.83 | 4.26 | 3.29 | 1.55 |
| Control 2 | A | 8:41 | 8.5 | 4.93 | 4.45 | 4.19 | 3.82 | 3.45 | 2.76 | 1.67 |
| | B | 10:05 | -2.8 | 4.58 | 4.34 | 4.15 | 3.87 | 3.54 | 2.91 | 1.80 |
| | C | 10:39 | -7.3 | 5.62 | 5.31 | 5.15 | 4.80 | 4.36 | 3.52 | 1.99 |
| | D | 11:35 | -13.4 | 5.62 | 5.28 | 5.09 | 4.74 | 4.31 | 3.49 | 2.00 |
| | E | 12:14 | -13.8 | 4.68 | 4.27 | 4.10 | 3.79 | 3.37 | 2.76 | 1.76 |
| Silane 1 | A | 8:34 | 5.0 | 5.08 | 4.58 | 4.29 | 3.94 | 3.53 | 2.84 | 1.72 |
| | B | 10:08 | -3.2 | 5.34 | 5.03 | 4.75 | 4.47 | 4.03 | 3.28 | 1.89 |
| | C | 10:41 | -7.6 | 5.68 | 5.22 | 4.97 | 4.60 | 4.15 | 3.36 | 1.98 |
| | D | 11:37 | -13.4 | 4.82 | 4.41 | 4.19 | 3.83 | 3.45 | 2.92 | 1.89 |
| | E | 12:54 | -14.0 | 5.25 | 4.77 | 4.51 | 4.14 | 3.75 | 3.09 | 1.98 |

Table B.7 (continued)

| Section | Slab | Time AM | Temperature Gradient °F | Measured Deflection, 0.001 in. 0 | 8 | 12 | 18 | 24 | 36 | 60 |
|---|---|---|---|---|---|---|---|---|---|---|
| Lithium 1 | A | 8:44 | 8.1 | 5.18 | 5.03 | 4.81 | 4.54 | 4.23 | 3.69 | 1.50 |
| | B | 10:10 | -3.5 | 5.37 | 5.05 | 4.81 | 4.49 | 4.07 | 3.36 | 1.74 |
| | C | 11:01 | -10.5 | 4.86 | 4.65 | 4.43 | 4.09 | 3.69 | 3.03 | 2.03 |
| | D | 11:03 | -10.7 | 5.53 | 5.19 | 4.95 | 4.61 | 4.24 | 3.56 | 2.28 |
| | E | 11:05 | -11.0 | 5.70 | 5.38 | 6.32 | 4.88 | 4.42 | 3.59 | 2.27 |
| Control 1 | A | 8:47 | 7.8 | 4.76 | 4.42 | 4.19 | 3.91 | 3.60 | 3.04 | 2.22 |
| | B | 10:12 | -3.7 | 9.11 | 6.58 | 6.05 | 5.38 | 4.72 | 3.74 | 2.17 |
| | C | 10:54 | -9.5 | 6.19 | 5.91 | 5.60 | 5.19 | 4.73 | 3.90 | 2.41 |
| | D | 11:43 | -13.5 | 6.55 | 6.11 | 5.87 | 5.40 | 4.84 | 3.82 | 1.92 |
| | E | 12:56 | -14.0 | 6.50 | 6.24 | 5.96 | 5.62 | 5.07 | 4.07 | 2.11 |
| Methacrylate 1 | A | 11:08 | -11.5 | 4.46 | 3.94 | 3.60 | 3.27 | 2.95 | 2.33 | 1.38 |
| | B | 11:10 | -11.8 | 5.71 | 5.19 | 4.89 | 4.41 | 3.86 | 2.93 | 1.34 |
| | C | 11:13 | -12.2 | 5.43 | 4.99 | 4.76 | 4.32 | 3.90 | 3.09 | 1.61 |
| | D | 10:56 | -9.7 | 5.17 | 4.82 | 4.57 | 4.19 | 3.74 | 3.01 | 1.84 |
| | E | 11:47 | -13.5 | 4.99 | 4.59 | 4.38 | 4.01 | 3.65 | 2.92 | 1.75 |

Notes: 1. Normalized to 10 kips
2. Data measured on 10/7/92
4. 1 in. = 25.4 mm
4. 1°F = 0.556°C

Table B.8 Measured joint deflections before treatment

| Section | Slab | Time AM | Temperature Gradient °F | Measured Deflection, 0.001 in. -12 | 0 | 12 | 18 | 24 | 36 | 60 |
|---|---|---|---|---|---|---|---|---|---|---|
| Control 3 | A | 9:41 | -1.3 | 2.89 | 9.33 | 6.51 | 5.51 | 4.47 | 3.09 | 1.49 |
| | B | 9:43 | -1.4 | 4.36 | 6.95 | 5.03 | 4.31 | 3.56 | 2.58 | 1.44 |
| | C | 9:44 | -1.5 | 4.33 | 7.03 | 5.26 | 4.53 | 3.79 | 2.80 | 1.54 |
| | D | 9:50 | -2.1 | 4.72 | 12.17 | 8.67 | 7.38 | 6.00 | 4.16 | 1.74 |
| Lithium 2 | A | 9:36 | -0.8 | 4.24 | 15.15 | 11.52 | 9.97 | 8.27 | 5.98 | 2.92 |
| | B | 9:51 | -2.2 | 4.68 | 11.25 | 8.38 | 6.95 | 5.73 | 4.49 | 2.35 |
| | C | 10:04 | -4.1 | 5.02 | 7.57 | 5.57 | 4.82 | 3.99 | 2.96 | 1.61 |
| | D | 10:06 | -4.8 | 8.10 | 13.84 | 10.37 | 8.94 | 7.28 | 5.13 | 2.27 |
| Silane 2 | A | 8:45 | 4.2 | 6.34 | 9.56 | 6.92 | 5.97 | 4.99 | 3.67 | 1.73 |
| | B | 8:47 | 4.0 | 6.47 | 7.80 | 5.83 | 5.48 | 4.31 | 3.18 | 1.33 |
| | C | 8:49 | 3.8 | 5.97 | 23.01 | 17.57 | 15.54 | 13.24 | 9.39 | 4.12 |
| | D | 8:52 | 3.4 | 11.23 | 17.34 | 13.01 | 11.30 | 9.22 | 6.23 | 2.70 |
| Methacrylate 2 | A | 12:46 | -28.2 | 4.01 | 4.98 | 3.74 | 3.38 | 2.95 | 2.34 | 1.44 |
| | B | 12:47 | -28.2 | 5.67 | 6.57 | 5.58 | 4.98 | 4.29 | 3.17 | 1.68 |
| | C | 12:48 | -28.2 | 4.18 | 6.75 | 5.20 | 4.43 | 3.72 | 2.63 | 1.45 |
| | D | 12:49 | -28.2 | 4.55 | 5.85 | 4.60 | 3.99 | 3.35 | 2.43 | 1.34 |
| Control 2 | A | 9:03 | 2.9 | 8.25 | 9.15 | 7.44 | 6.77 | 5.84 | 4.59 | 2.65 |
| | B | 9:06 | 2.3 | 7.43 | 8.25 | 6.65 | 5.99 | 5.16 | 3.98 | 2.25 |
| | C | 9:07 | 2.0 | 7.51 | 8.52 | 6.81 | 6.12 | 5.27 | 4.04 | 2.30 |
| | D | 9:09 | 1.7 | 5.71 | 6.62 | 5.21 | 4.69 | 4.05 | 3.17 | 1.93 |
| Silane 1 | A | 9:14 | 1.2 | 5.66 | 7.10 | 5.43 | 4.76 | 4.02 | 2.99 | 1.71 |
| | B | 9:16 | 1.1 | 5.70 | 6.70 | 5.31 | 4.71 | 4.03 | 3.13 | 1.88 |
| | C | 9:18 | 0.9 | 5.77 | 6.86 | 5.44 | 4.83 | 4.15 | 3.16 | 1.84 |
| | D | 9:19 | 0.8 | 5.27 | 5.92 | 4.68 | 4.21 | 3.61 | 2.83 | 1.72 |
| Lithium 1 | A | 9:21 | 0.6 | 5.91 | 7.03 | 5.49 | 4.89 | 4.14 | 3.12 | 1.84 |
| | B | 9:22 | 0.5 | 5.29 | 6.25 | 4.94 | 4.47 | 3.89 | 3.03 | 1.90 |
| | C | 9:23 | 0.4 | 5.54 | 8.35 | 6.53 | 5.78 | 4.98 | 3.91 | 2.32 |
| | D | 9:31 | -0.3 | 5.66 | 8.32 | 6.27 | 5.47 | 4.63 | 3.45 | 1.96 |
| Control 1 | A | 10:29 | -12.7 | 5.54 | 6.15 | 5.02 | 4.55 | 3.93 | 3.07 | 1.85 |
| | B | 10:31 | -13.3 | 6.20 | 8.08 | 6.26 | 5.52 | 4.69 | 3.43 | 1.81 |
| | C | 10:32 | -13.7 | 6.77 | 8.31 | 6.57 | 5.86 | 4.97 | 3.71 | 1.98 |
| | D | 10:42 | -17.1 | 5.55 | 6.51 | 5.05 | 4.47 | 3.79 | 2.78 | 1.50 |
| Methacrylate 1 | A | 10:45 | -17.5 | 4.57 | 5.53 | 4.49 | 4.03 | 3.46 | 2.53 | 1.27 |
| | B | 10:46 | -17.7 | 5.76 | 6.68 | 5.19 | 4.63 | 3.80 | 2.66 | 1.20 |
| | C | 10:48 | -17.9 | 6.16 | 7.28 | 5.95 | 5.29 | 4.51 | 3.26 | 1.46 |
| | D | 10:50 | -18.2 | 5.07 | 5.59 | 4.70 | 4.19 | 3.48 | 2.54 | 1.28 |

Notes:
1. Normalized to 10 kips
2. Data measured on 10/2/91
3. 1 in. = 25.4 mm
4. 1°F = 0.556°C

Table B.9 Measured joint deflections one day after treatment

| Section | Slab | Time AM | Temperature Gradient °F | Measured Deflection, 0.001 in. -12 | 0 | 12 | 18 | 24 | 36 | 60 |
|---|---|---|---|---|---|---|---|---|---|---|
| Control 3 | A | 9:07 | 0.3 | 3.01 | 12.04 | 8.36 | 7.02 | 5.60 | 3.76 | 1.76 |
| | B | 9:10 | -0.3 | 4.65 | 10.44 | 7.41 | 6.26 | 5.03 | 3.48 | 1.80 |
| | C | 9:11 | -0.6 | 6.37 | 7.62 | 5.68 | 4.91 | 4.10 | 3.02 | 1.65 |
| | D | 9:13 | -0.9 | 4.58 | 15.20 | 11.13 | 9.63 | 7.90 | 5.56 | 2.03 |
| Methacrylate 2 | A | 8:53 | 3.3 | 5.12 | 7.56 | 5.49 | 4.82 | 4.09 | 3.07 | 1.79 |
| | B | 8:55 | 3.1 | 7.72 | 10.29 | 8.21 | 7.29 | 6.20 | 4.55 | 2.26 |
| | C | 8:56 | 2.9 | 3.79 | 12.41 | 8.89 | 7.53 | 6.11 | 4.23 | 2.14 |
| | D | 8:57 | 2.6 | 4.66 | 7.90 | 6.37 | 5.71 | 4.89 | 3.71 | 2.08 |
| Control 2 | A | 9:29 | -2.1 | 7.18 | 7.97 | 6.44 | 5.84 | 5.06 | 3.93 | 2.25 |
| | B | 9:31 | -2.2 | 6.97 | 7.65 | 6.23 | 5.65 | 4.89 | 3.79 | 2.16 |
| | C | 9:32 | -2.3 | 6.92 | 7.65 | 6.21 | 5.57 | 4.81 | 3.69 | 2.10 |
| | D | 9:34 | -2.5 | 5.33 | 6.19 | 4.85 | 4.37 | 3.77 | 2.94 | 1.78 |
| Control 1 | A | 9:56 | -3.6 | 5.94 | 6.59 | 5.34 | 4.79 | 4.13 | 3.19 | 1.92 |
| | B | 9:57 | -3.7 | 6.43 | 8.76 | 6.73 | 6.06 | 5.48 | 3.73 | 1.98 |
| | C | 9:59 | -3.8 | 7.15 | 10.07 | 7.72 | 6.78 | 5.65 | 4.08 | 2.09 |
| | D | 10:00 | -3.8 | 5.42 | 7.52 | 5.80 | 5.02 | 4.20 | 3.02 | 1.59 |
| Methacrylate 1 | A | 9:38 | -2.7 | 4.81 | 5.81 | 4.77 | 4.32 | 3.75 | 2.74 | 1.33 |
| | B | 9:40 | -2.8 | 5.89 | 6.60 | 5.29 | 4.66 | 3.92 | 2.76 | 1.27 |
| | C | 9:42 | -2.9 | 6.61 | 7.67 | 6.27 | 5.60 | 4.78 | 3.44 | 1.57 |
| | D | 9:43 | -3.0 | 5.43 | 5.93 | 4.78 | 4.22 | 3.60 | 2.64 | 1.35 |

Notes:
1. Normalized to 10 kips
2. Data measured on 10/3/91
3. 1 in. = 25.4 mm
4. 1°F = 0.556°C

Table B.10 Measured joint deflections one year after treatment

| Section | Slab | Time AM | Temperature Gradient °F | Measured Deflection, 0.001 in. -12 | 0 | 12 | 18 | 24 | 36 | 60 |
|---|---|---|---|---|---|---|---|---|---|---|
| Control 3 | A | 8:42 | 3.6 | 2.60 | 12.11 | 8.29 | 6.85 | 5.57 | 3.72 | 1.75 |
| | B | 9:06 | -0.6 | 2.94 | 13.16 | 9.23 | 7.83 | 6.35 | 4.38 | 2.23 |
| | C | 9:29 | -3.9 | 4.41 | 8.12 | 5.80 | 5.05 | 4.22 | 3.12 | 1.72 |
| | D | 9:58 | -6.2 | 3.70 | 11.54 | 8.12 | 6.80 | 5.56 | 3.68 | 1.29 |
| Lithium 2 | A | 8:44 | 3.3 | 3.93 | 25.16 | 19.62 | 17.30 | 14.92 | 11.17 | 5.47 |
| | B | 9:08 | -1.0 | 2.35 | 16.91 | 8.80 | 10.70 | 8.84 | 6.30 | 3.15 |
| | C | 9:30 | -4.1 | 4.48 | 8.98 | 6.43 | 5.52 | 4.63 | 3.33 | 1.67 |
| | D | 9:59 | -6.3 | 3.22 | 11.49 | 8.27 | 7.05 | 5.84 | 4.11 | 2.02 |
| Silane 2 | A | 9:33 | -4.4 | 3.67 | 9.94 | 7.19 | 6.18 | 5.14 | 3.67 | 1.52 |
| | B | 9:12 | -1.6 | 4.68 | 8.96 | 6.39 | 5.43 | 4.43 | 3.03 | 0.74 |
| | C | 9:35 | -4.5 | 2.30 | 20.91 | 15.91 | 13.80 | 11.52 | 8.13 | 3.41 |
| | D | 10:03 | -6.8 | 4.76 | 15.97 | 11.64 | 9.99 | 8.09 | 5.49 | 2.35 |
| Methacrylate 2 | A | 8:46 | 2.9 | 4.03 | 9.63 | 6.67 | 5.63 | 4.69 | 3.39 | 1.81 |
| | B | 9:36 | -4.6 | 5.33 | 10.77 | 8.13 | 7.04 | 5.89 | 4.20 | 2.10 |
| | C | 9:38 | -4.7 | 3.85 | 8.93 | 6.47 | 5.51 | 4.56 | 3.28 | 1.80 |
| | D | 10:04 | -7.0 | 4.01 | 7.94 | 5.73 | 4.86 | 4.04 | 2.87 | 1.47 |
| Silane #2 1 | A | 8:48 | 2.5 | 5.35 | 10.46 | 7.04 | 5.72 | 4.45 | 2.91 | 1.14 |
| | B | 9:14 | -1.8 | 3.69 | 7.78 | 5.53 | 4.60 | 3.72 | 2.52 | 1.19 |
| | C | 11:03 | -15.0 | 3.17 | 5.26 | 3.68 | 3.15 | 2.62 | 1.92 | 1.06 |
| | D | 11:04 | -15.1 | 3.56 | 4.63 | 3.35 | 2.93 | 2.46 | 1.84 | 1.04 |
| Linseed Oil 1 | A | 8:50 | 2.2 | 4.04 | 12.13 | 8.32 | 6.74 | 5.27 | 3.30 | 1.28 |
| | B | 9:16 | -2.1 | 3.88 | 6.79 | 4.80 | 4.07 | 3.33 | 2.33 | 1.02 |
| | C | 9:45 | -5.3 | 2.42 | 8.17 | 5.57 | 4.55 | 3.54 | 2.34 | 1.12 |
| | D | 10:07 | -7.4 | 3.71 | 5.94 | 4.14 | 3.49 | 2.84 | 1.98 | 1.00 |

Table B.10 (continued)

| Section | Slab | Time AM | Temperature Gradient °F | Measured Deflection, 0.001 in. -12 | 0 | 12 | 18 | 24 | 36 | 60 |
|---|---|---|---|---|---|---|---|---|---|---|
| Control 2 | A | 8:52 | 1.8 | 8.91 | 10.47 | 7.95 | 7.01 | 5.91 | 4.44 | 2.38 |
| | B | 9:19 | -2.5 | 7.94 | 9.15 | 5.93 | 6.15 | 5.26 | 3.95 | 2.16 |
| | C | 9:47 | -5.4 | 5.42 | 9.16 | 6.99 | 6.10 | 5.21 | 3.82 | 2.13 |
| | D | 10:09 | -7.7 | 4.45 | 7.57 | 5.63 | 4.92 | 4.16 | 3.03 | 1.68 |
| Silane 1 | A | 8:53 | 1.7 | 5.80 | 9.63 | 6.99 | 5.89 | 4.84 | 3.46 | 1.81 |
| | B | 9:20 | -2.7 | 5.43 | 8.67 | 6.39 | 5.52 | 4.68 | 3.56 | 2.03 |
| | C | 9:48 | -5.5 | 5.32 | 7.56 | 5.80 | 5.03 | 4.26 | 3.25 | 1.88 |
| | D | 10:11 | -7.9 | 5.66 | 6.22 | 4.92 | 4.40 | 3.75 | 2.94 | 1.69 |
| Lithium 1 | A | 8:59 | 0.6 | 5.98 | 9.22 | 6.82 | 5.91 | 4.90 | 3.52 | 1.97 |
| | B | 9:22 | -2.9 | 5.21 | 7.82 | 5.85 | 5.11 | 4.38 | 3.34 | 1.96 |
| | C | 9:50 | -5.6 | 4.56 | 9.80 | 7.23 | 6.18 | 5.25 | 3.96 | 2.29 |
| | D | 10:12 | -8.1 | 4.74 | 9.53 | 7.08 | 6.11 | 5.19 | 3.84 | 2.16 |
| Control 1 | A | 9:01 | 0.2 | 6.19 | 11.76 | 8.77 | 7.69 | 6.47 | 4.62 | 2.39 |
| | B | 9:24 | -3.2 | 6.63 | 11.24 | 8.64 | 7.58 | 6.50 | 4.86 | 2.40 |
| | C | 9:51 | -5.7 | 5.57 | 12.88 | 9.61 | 8.21 | 6.86 | 4.86 | 2.34 |
| | D | 10:13 | -8.2 | 5.24 | 8.06 | 5.93 | 5.12 | 4.17 | 3.07 | 1.48 |
| Methacrylate 1 | A | 9:02 | 0.1 | 5.36 | 8.35 | 5.55 | 4.72 | 3.90 | 2.69 | 1.25 |
| | B | 9:25 | -3.4 | 7.03 | 8.96 | 6.62 | 5.68 | 4.72 | 3.21 | 1.45 |
| | C | 9:52 | -5.8 | 6.29 | 7.72 | 6.19 | 5.39 | 3.12 | 3.29 | 1.51 |
| | D | 10:15 | -8.5 | 5.34 | 5.98 | 4.78 | 4.26 | 3.61 | 2.69 | 1.32 |

Notes:
1. Normalized to 10 kips
2. Data measured on 10/8/92
3. 1 in. = 25.4 mm
4. 1°F = 0.556°C

Table B.11 Temperature adjusted interior deflections before treatment

| Section | Slab | Time AM | Temperature Gradient °F | Temperature Corrected Deflection, 0.001 in. 0 | 8 | 12 | 18 | 24 | 36 | 60 |
|---|---|---|---|---|---|---|---|---|---|---|
| Control 3 | A | 7:40 | 12.1 | 4.09 | 3.80 | 3.72 | 3.45 | 3.16 | 2.63 | 1.73 |
| | B | 7:42 | 12 | 4.19 | 3.85 | 3.70 | 3.48 | 3.11 | 2.56 | 1.84 |
| | C | 7:44 | 11.9 | 4.21 | 3.85 | 3.71 | 3.50 | 3.25 | 2.79 | 2.30 |
| | D | 7:45 | 11.9 | 6.29 | 5.38 | 4.95 | 4.41 | 3.76 | 2.84 | 1.40 |
| | E | 7:46 | 11.8 | 9.17 | 7.87 | 7.31 | 6.40 | 5.33 | 3.81 | 1.26 |
| Lithium 2 | A | 7:47 | 11.8 | 4.73 | 4.57 | 4.52 | 4.40 | 4.24 | 4.22 | 4.58 |
| | B | 7:49 | 11.7 | 4.98 | 4.45 | 4.24 | 3.95 | 3.56 | 2.94 | 1.83 |
| | C | 7:50 | 11.7 | 4.46 | 3.95 | 3.74 | 3.46 | 3.13 | 2.60 | 1.65 |
| | D | 7:51 | 11.7 | 4.59 | 4.23 | 4.07 | 3.79 | 3.44 | 2.84 | 1.76 |
| | E | 7:57 | 11.6 | 4.86 | 4.51 | 4.38 | 4.21 | 3.94 | 3.50 | 3.00 |
| Silane 2 | A | 7:52 | 11.7 | 4.85 | 4.68 | 4.60 | 4.47 | 4.25 | 3.96 | 3.67 |
| | B | 7:53 | 11.6 | 7.10 | 6.26 | 5.88 | 5.25 | 4.52 | 3.41 | 1.88 |
| | C | 7:54 | 11.6 | 6.31 | 5.40 | 5.05 | 4.45 | 3.80 | 2.84 | 1.47 |
| | D | 7:56 | 11.6 | 3.80 | 3.59 | 3.52 | 3.42 | 3.24 | 3.10 | 3.11 |
| | E | 7:57 | 11.6 | 3.78 | 3.45 | 3.35 | 3.19 | 2.96 | 2.67 | 2.38 |
| Methacrylate 2 | A | 7:58 | 11.5 | 4.54 | 4.01 | 3.80 | 3.41 | 2.97 | 2.31 | 1.38 |
| | B | 7:58 | 11.5 | 4.17 | 3.81 | 3.64 | 3.36 | 3.00 | 2.45 | 1.57 |
| | C | 7:59 | 11.5 | 5.72 | 5.38 | 5.27 | 5.14 | 4.87 | 4.60 | 4.02 |
| | D | 8:00 | 11.5 | 4.68 | 4.45 | 4.29 | 4.07 | 3.79 | 3.29 | 2.61 |
| | E | 8:01 | 11.5 | 4.44 | 4.00 | 3.82 | 3.55 | 3.13 | 2.50 | 1.44 |
| Control 2 | A | 8:03 | 11.4 | 4.83 | 4.33 | 4.15 | 3.78 | 3.36 | 2.66 | 1.62 |
| | B | 8:04 | 11.4 | 4.97 | 4.47 | 4.28 | 3.99 | 3.57 | 2.90 | 1.76 |
| | C | 8:05 | 11.4 | 5.03 | 4.69 | 4.54 | 4.29 | 3.89 | 3.20 | 2.02 |
| | D | 8:06 | 11.3 | 4.75 | 4.33 | 4.21 | 3.95 | 3.59 | 2.97 | 1.95 |
| | E | 8:07 | 11.3 | 4.47 | 4.34 | 4.15 | 3.81 | 3.36 | 2.69 | 1.60 |
| Silane 1 | A | 8:07 | 11.3 | 5.11 | 4.70 | 4.49 | 4.18 | 3.74 | 3.04 | 1.84 |
| | B | 8:08 | 11.3 | 4.95 | 4.61 | 4.48 | 4.21 | 3.82 | 3.11 | 1.94 |
| | C | 8:09 | 11.3 | 5.21 | 4.83 | 4.67 | 4.43 | 3.98 | 3.30 | 2.04 |
| | D | 8:10 | 11.3 | 5.33 | 4.72 | 4.44 | 4.07 | 3.60 | 2.91 | 1.85 |
| | E | 8:11 | 11.3 | 5.34 | 4.84 | 4.60 | 4.26 | 3.86 | 3.16 | 1.99 |

Table B.11 (continued)

| Section | Slab | Time AM | Temperature Gradient °F | Temperature Corrected Deflection, 0.001 in. 0 | 8 | 12 | 18 | 24 | 36 | 60 |
|---|---|---|---|---|---|---|---|---|---|---|
| Lithium 1 | A | 8:11 | 11.3 | 5.16 | 4.72 | 4.58 | 4.25 | 3.88 | 3.17 | 2.03 |
| | B | 8:12 | 11.3 | 5.36 | 5.07 | 4.92 | 4.64 | 4.20 | 3.49 | 2.23 |
| | C | 8:13 | 11.3 | 5.30 | 4.98 | 4.79 | 4.48 | 4.04 | 3.34 | 2.21 |
| | D | 8:14 | 11.3 | 5.63 | 5.21 | 5.01 | 4.66 | 4.22 | 3.50 | 2.22 |
| | E | 8:14 | 11.3 | 5.23 | 4.96 | 4.80 | 4.55 | 4.16 | 3.53 | 2.31 |
| Control 1 | A | 8:15 | 11.3 | 4.53 | 4.30 | 4.14 | 3.89 | 3.54 | 2.95 | 1.86 |
| | B | 8:16 | 11.3 | 9.55 | 7.49 | 6.98 | 6.22 | 5.38 | 4.18 | 2.38 |
| | C | 8:17 | 11.3 | 6.49 | 6.14 | 5.87 | 5.43 | 4.90 | 3.95 | 2.37 |
| | D | 8:18 | 11.2 | 5.57 | 5.26 | 5.09 | 4.79 | 4.31 | 3.50 | 2.11 |
| | E | 8:18 | 11.2 | 4.95 | 4.60 | 4.44 | 4.12 | 3.73 | 2.97 | 1.62 |
| Methacrylate 1 | A | 8:19 | 11.2 | 4.94 | 4.07 | 3.73 | 3.31 | 2.80 | 2.11 | 1.13 |
| | B | 8:20 | 11.2 | 5.16 | 4.43 | 4.20 | 3.84 | 3.37 | 2.59 | 1.39 |
| | C | 8:21 | 11.2 | 5.01 | 4.60 | 4.43 | 4.12 | 3.73 | 3.04 | 1.73 |
| | D | 8:22 | 11.2 | 5.25 | 4.72 | 4.44 | 4.04 | 3.43 | 2.63 | 1.44 |
| | E | 8:23 | 11.2 | 5.33 | 4.55 | 4.30 | 3.84 | 3.28 | 2.57 | 1.35 |

Notes:
1. Normalized to 10 kips
2. Data measured on 10/2/91
3. 1 in. = 25.4 mm
4. 1°F = 0.556°C

Table B.12 Temperature adjusted interior deflections one day after treatment

| Section | Slab | Time AM | Temperature Gradient °F | Temperature Corrected Deflection, 0.001 in. 0 | 8 | 12 | 18 | 24 | 36 | 60 |
|---|---|---|---|---|---|---|---|---|---|---|
| Control 3 | A | 7:48 | 11.6 | 4.26 | 3.95 | 3.78 | 3.54 | 3.23 | 2.68 | 1.74 |
| | B | 7:49 | 11.4 | 4.38 | 4.10 | 3.91 | 3.67 | 3.32 | 2.83 | 2.13 |
| | C | 7:50 | 11.3 | 4.35 | 4.03 | 3.86 | 3.62 | 3.33 | 2.91 | 2.43 |
| | D | 7:51 | 11.1 | 6.55 | 5.52 | 5.08 | 4.54 | 3.89 | 2.96 | 1.44 |
| | E | 7:53 | 10.9 | 11.56 | 9.61 | 8.77 | 7.63 | 6.22 | 4.32 | 1.26 |
| Methacrylate 2 | A | 7:58 | 10.2 | 4.13 | 3.62 | 3.41 | 3.14 | 2.79 | 2.25 | 1.47 |
| | B | 7:59 | 10.0 | 4.09 | 3.71 | 3.57 | 3.32 | 3.02 | 2.52 | 1.64 |
| | C | 8:00 | 9.9 | 5.25 | 4.90 | 4.79 | 4.61 | 4.31 | 3.95 | 3.54 |
| | D | 8:01 | 9.8 | 4.48 | 4.30 | 4.14 | 3.90 | 3.63 | 3.12 | 2.42 |
| | E | 8:03 | 9.5 | 4.19 | 3.87 | 3.70 | 3.43 | 3.07 | 2.49 | 1.42 |
| Control 2 | A | 8:06 | 9.1 | 5.06 | 4.58 | 4.35 | 4.00 | 3.54 | 2.83 | 1.72 |
| | B | 8:08 | 8.8 | 4.85 | 4.46 | 4.19 | 3.92 | 3.52 | 2.88 | 1.74 |
| | C | 8:09 | 8.7 | 5.11 | 4.82 | 4.62 | 4.36 | 3.91 | 3.25 | 2.13 |
| | D | 8:11 | 8.4 | 4.91 | 4.49 | 4.31 | 4.08 | 3.66 | 3.07 | 2.02 |
| | E | 8:12 | 8.3 | 4.73 | 4.49 | 4.28 | 3.91 | 3.47 | 2.77 | 1.66 |
| Control 1 | A | 8:15 | 7.9 | 4.99 | 4.56 | 4.39 | 4.11 | 3.75 | 3.11 | 1.96 |
| | B | 8:16 | 7.7 | 9.42 | 7.91 | 7.32 | 6.60 | 5.68 | 4.43 | 2.48 |
| | C | 8:19 | 7.3 | 6.69 | 6.34 | 6.07 | 5.60 | 5.04 | 4.15 | 2.53 |
| | D | 8:20 | 7.2 | 5.83 | 5.47 | 5.31 | 4.95 | 4.46 | 3.63 | 2.21 |
| | E | 8:23 | 6.8 | 5.13 | 4.72 | 4.53 | 4.22 | 3.78 | 3.04 | 1.63 |
| Methacrylate 1 | A | 8:26 | 6.4 | 4.68 | 3.86 | 3.54 | 3.21 | 2.73 | 2.10 | 1.15 |
| | B | 8:28 | 6.1 | 4.48 | 4.07 | 3.87 | 3.57 | 3.16 | 2.49 | 1.36 |
| | C | 8:29 | 6.0 | 4.74 | 4.33 | 4.19 | 3.93 | 3.52 | 2.90 | 1.63 |
| | D | 8:30 | 5.8 | 4.96 | 4.41 | 4.10 | 3.75 | 3.29 | 2.54 | 1.44 |
| | E | 8:32 | 5.6 | 4.68 | 4.15 | 3.88 | 3.52 | 3.10 | 2.44 | 1.39 |

Notes:
1. Normalized to 10 kips
2. Data measured on 10/3/91
3. 1 in. = 25.4 mm
4. 1°F = 0.556°C

Table B.13 Temperature adjusted interior deflections one year after treatment

| Section | Slab | Time AM | Temperature Gradient °F | Temperature Corrected Deflection, 0.001 in. 0 | 8 | 12 | 18 | 24 | 36 | 60 |
|---|---|---|---|---|---|---|---|---|---|---|
| Control 3 | A | 8:15 | 11.8 | 3.94 | 3.78 | 3.62 | 3.40 | 3.15 | 2.71 | 1.83 |
| | B | 9:45 | -0.2 | 4.34 | 3.99 | 3.81 | 3.60 | 3.27 | 2.78 | 1.99 |
| | C | 10:22 | -5.0 | 4.14 | 3.56 | 3.55 | 3.28 | 2.98 | 2.44 | 1.56 |
| | D | 11:16 | -12.6 | 4.97 | 4.15 | 3.82 | 3.41 | 2.97 | 2.32 | 1.45 |
| | E | 12:08 | -13.7 | 4.44 | 3.88 | 3.59 | 3.23 | 2.87 | 2.29 | 1.51 |
| Lithium 2 | A | 8:22 | 10.8 | 4.52 | 4.43 | 4.36 | 4.24 | 4.12 | 4.01 | 4.17 |
| | B | 9:48 | -0.6 | 4.13 | 3.91 | 3.70 | 3.46 | 3.17 | 2.68 | 1.87 |
| | C | 10:25 | -5.3 | 4.28 | 3.70 | 3.47 | 3.19 | 2.86 | 2.36 | 1.57 |
| | D | 11:20 | -13.2 | 4.67 | 4.35 | 4.08 | 3.79 | 3.44 | 2.79 | 1.74 |
| | E | 11:23 | -13.2 | 4.82 | 4.43 | 4.18 | 3.83 | 3.47 | 2.81 | 1.65 |
| Silane 2 | A | 8:24 | 10.6 | 4.45 | 4.21 | 4.08 | 3.81 | 3.49 | 2.90 | 1.96 |
| | B | 9:52 | -1.2 | 5.91 | 5.06 | 4.64 | 4.18 | 3.66 | 2.84 | 1.63 |
| | C | 10:30 | -6.0 | 5.30 | 4.40 | 4.10 | 3.58 | 3.09 | 2.37 | 1.33 |
| | D | 11:26 | -13.3 | 3.76 | 3.48 | 3.32 | 3.13 | 2.88 | 2.46 | 1.84 |
| | E | 11:58 | -13.7 | 3.93 | 3.54 | 3.34 | 3.11 | 2.82 | 2.28 | 1.36 |
| Methacrylate 2 | A | 8:30 | 9.8 | 4.73 | 4.49 | 4.19 | 4.01 | 3.64 | 3.04 | 2.03 |
| | B | 9:59 | -2.1 | 3.72 | 3.39 | 3.20 | 2.93 | 2.65 | 2.23 | 1.49 |
| | C | 10:32 | -6.3 | 5.47 | 5.04 | 4.84 | 4.51 | 4.08 | 3.28 | 1.80 |
| | D | 11:28 | -13.3 | 5.02 | 4.48 | 4.30 | 4.02 | 3.66 | 2.88 | 1.47 |
| | E | 11:54 | -13.6 | 5.27 | 4.95 | 4.68 | 4.34 | 3.93 | 3.19 | 2.16 |
| Silane #2 1 | A | 8:36 | 9.1 | 3.56 | 3.28 | 3.07 | 2.81 | 2.50 | 1.99 | 1.22 |
| | B | 12:18 | -13.8 | 4.18 | 3.59 | 3.31 | 3.00 | 2.67 | 2.10 | 1.22 |
| | C | 12:20 | -13.8 | 3.57 | 3.04 | 2.78 | 2.45 | 2.15 | 1.68 | 0.96 |
| | D | 12:22 | -13.8 | 3.74 | 2.95 | 2.72 | 2.46 | 2.18 | 1.66 | 1.11 |
| | E | 13:05 | -14.1 | 5.35 | 4.92 | 4.65 | 4.30 | 3.86 | 3.05 | 1.48 |
| Linseed Oil 1 | A | 8:39 | 8.7 | 5.03 | 4.37 | 4.18 | 3.79 | 3.35 | 2.59 | 1.51 |
| | B | 10:03 | -2.6 | 3.64 | 3.37 | 3.15 | 2.85 | 2.48 | 1.95 | 1.02 |
| | C | 10:37 | -7.0 | 3.78 | 3.42 | 3.16 | 2.80 | 2.43 | 1.84 | 1.09 |
| | D | 11:33 | -13.4 | 3.86 | 3.41 | 3.16 | 2.84 | 2.48 | 1.91 | 1.14 |
| | E | 12:12 | -13.8 | 5.88 | 5.24 | 4.87 | 4.38 | 3.84 | 2.95 | 1.40 |
| Control 2 | A | 8:41 | 8.5 | 5.11 | 4.68 | 4.43 | 4.07 | 3.68 | 2.97 | 1.78 |
| | B | 10:05 | -2.8 | 4.53 | 4.29 | 4.09 | 3.81 | 3.48 | 2.86 | 1.77 |
| | C | 10:39 | -7.3 | 5.46 | 5.10 | 4.92 | 4.57 | 4.14 | 3.34 | 1.90 |
| | D | 11:35 | -13.4 | 5.32 | 4.88 | 4.67 | 4.32 | 3.90 | 3.14 | 1.82 |
| | E | 12:14 | -13.8 | 4.42 | 3.95 | 3.75 | 3.44 | 3.04 | 2.47 | 1.59 |
| Silane 1 | A | 8:34 | 5.0 | 5.19 | 4.73 | 4.44 | 4.10 | 3.68 | 2.97 | 1.79 |
| | B | 10:08 | -3.2 | 5.28 | 4.95 | 4.67 | 4.39 | 3.96 | 3.21 | 1.85 |
| | C | 10:41 | -7.6 | 5.52 | 5.01 | 4.75 | 4.38 | 3.93 | 3.18 | 1.89 |
| | D | 11:37 | -13.4 | 4.57 | 4.09 | 3.84 | 3.48 | 3.12 | 2.62 | 1.72 |
| | E | 12:54 | -14.0 | 4.96 | 4.40 | 4.12 | 3.75 | 3.38 | 2.76 | 1.79 |

Table B.13 (continued)

| Section | Slab | Time AM | Temperature Gradient °F | Temperature Corrected Deflection, 0.001 in. 0 | 8 | 12 | 18 | 24 | 36 | 60 |
|---|---|---|---|---|---|---|---|---|---|---|
| Lithium 1 | A | 8:44 | 8.1 | 5.36 | 5.28 | 5.08 | 4.82 | 4.51 | 3.95 | 1.59 |
| | B | 10:10 | -3.5 | 5.30 | 4.97 | 4.72 | 4.40 | 3.98 | 3.29 | 1.70 |
| | C | 11:01 | -10.5 | 4.66 | 4.38 | 4.15 | 3.81 | 3.42 | 2.79 | 1.88 |
| | D | 11:03 | -10.7 | 5.30 | 4.89 | 4.62 | 4.28 | 3.92 | 3.28 | 2.12 |
| | E | 11:05 | -11.0 | 5.45 | 5.06 | 5.90 | 4.53 | 4.08 | 3.29 | 2.10 |
| Control 1 | A | 8:47 | 7.8 | 4.92 | 4.63 | 4.41 | 4.14 | 3.83 | 3.25 | 2.36 |
| | B | 10:12 | -3.7 | 8.99 | 6.46 | 5.93 | 5.27 | 4.61 | 3.65 | 2.12 |
| | C | 10:54 | -9.5 | 5.96 | 5.61 | 5.29 | 4.87 | 4.42 | 3.62 | 2.26 |
| | D | 11:43 | -13.5 | 6.20 | 5.65 | 5.38 | 4.92 | 4.37 | 3.43 | 1.74 |
| | E | 12:56 | -14.0 | 6.14 | 5.76 | 5.45 | 5.10 | 4.56 | 3.64 | 1.91 |
| Methacrylate 1 | A | 11:08 | -11.5 | 4.26 | 3.69 | 3.35 | 3.02 | 2.71 | 2.13 | 1.28 |
| | B | 11:10 | -11.8 | 5.44 | 4.86 | 4.54 | 4.06 | 3.54 | 2.67 | 1.23 |
| | C | 11:13 | -12.2 | 5.17 | 4.65 | 4.41 | 3.97 | 3.57 | 2.80 | 1.48 |
| | D | 10:56 | -9.7 | 4.97 | 4.57 | 4.30 | 3.92 | 3.48 | 2.79 | 1.72 |
| | E | 11:47 | -13.5 | 4.72 | 4.24 | 4.01 | 3.65 | 3.30 | 2.62 | 1.59 |

Notes: 1. Normalized to 10 kips
2. Data measured on 10/7/92
4. 1 in. = 25.4 mm
4. 1°F = 0.556°C

Table B.14 Temperature adjusted joint deflections before treatment

| Section | Slab | Time AM | Temperature Gradient °F | Temperature Corrected Deflection, 0.001 in. -12 | 0 | 12 | 18 | 24 | 36 | 60 |
|---|---|---|---|---|---|---|---|---|---|---|
| Control 3 | A | 9:41 | -1.3 | 3.01 | 9.88 | 6.84 | 5.76 | 4.64 | 3.18 | 1.50 |
| | B | 9:43 | -1.4 | 4.58 | 7.42 | 5.33 | 4.54 | 3.73 | 2.66 | 1.45 |
| | C | 9:44 | -1.5 | 4.57 | 7.55 | 5.59 | 4.79 | 3.98 | 2.90 | 1.55 |
| | D | 9:50 | -2.1 | 5.07 | 13.42 | 9.43 | 7.96 | 6.39 | 4.36 | 1.76 |
| Lithium 2 | A | 9:36 | -0.8 | 4.36 | 15.66 | 11.87 | 10.26 | 8.47 | 6.09 | 2.94 |
| | B | 9:51 | -2.2 | 5.05 | 12.46 | 9.14 | 7.52 | 6.13 | 4.72 | 2.37 |
| | C | 10:04 | -4.1 | 5.76 | 9.18 | 6.56 | 5.59 | 4.52 | 3.23 | 1.65 |
| | D | 10:06 | -4.8 | 9.49 | 17.28 | 12.53 | 10.61 | 8.39 | 5.69 | 2.33 |
| Silane 2 | A | 8:45 | 4.2 | 5.37 | 7.33 | 5.61 | 4.97 | 4.32 | 3.33 | 1.69 |
| | B | 8:47 | 4.0 | 5.54 | 6.07 | 4.79 | 4.61 | 3.76 | 2.90 | 1.31 |
| | C | 8:49 | 3.8 | 5.15 | 18.18 | 14.59 | 13.20 | 11.64 | 8.60 | 4.03 |
| | D | 8:52 | 3.4 | 9.82 | 14.00 | 10.99 | 9.74 | 8.20 | 5.76 | 2.65 |
| Methacrylate 2 | A | 12:46 | -28.2 | 8.09 | 12.45 | 8.37 | 7.13 | 5.61 | 3.83 | 1.65 |
| | B | 12:47 | -28.2 | 11.43 | 16.42 | 12.49 | 10.49 | 8.17 | 5.18 | 1.93 |
| | C | 12:48 | -28.2 | 8.42 | 16.88 | 11.62 | 9.33 | 7.07 | 4.31 | 1.67 |
| | D | 12:49 | -28.2 | 9.18 | 14.63 | 10.29 | 8.41 | 6.37 | 3.97 | 1.54 |
| Control 2 | A | 9:03 | 2.9 | 7.36 | 7.62 | 6.44 | 5.96 | 5.28 | 4.29 | 2.61 |
| | B | 9:06 | 2.3 | 6.81 | 7.17 | 5.96 | 5.44 | 4.78 | 3.78 | 2.22 |
| | C | 9:07 | 2.0 | 6.94 | 7.52 | 6.17 | 5.61 | 4.92 | 3.86 | 2.28 |
| | D | 9:09 | 1.7 | 5.35 | 5.96 | 4.79 | 4.36 | 3.83 | 3.05 | 1.91 |
| Silane 1 | A | 9:14 | 1.2 | 5.39 | 6.56 | 5.11 | 4.51 | 3.86 | 2.91 | 1.70 |
| | B | 9:16 | 1.1 | 5.47 | 6.26 | 5.04 | 4.50 | 3.89 | 3.06 | 1.87 |
| | C | 9:18 | 0.9 | 5.58 | 6.48 | 5.20 | 4.65 | 4.03 | 3.10 | 1.83 |
| | D | 9:19 | 0.8 | 5.11 | 5.61 | 4.50 | 4.07 | 3.51 | 2.78 | 1.72 |
| Lithium 1 | A | 9:21 | 0.6 | 5.77 | 6.74 | 5.32 | 4.77 | 4.06 | 3.08 | 1.83 |
| | B | 9:22 | 0.5 | 5.18 | 6.03 | 4.81 | 4.37 | 3.82 | 2.99 | 1.89 |
| | C | 9:23 | 0.4 | 5.45 | 8.09 | 6.38 | 5.67 | 4.91 | 3.87 | 2.32 |
| | D | 9:31 | -0.3 | 5.72 | 8.39 | 6.33 | 5.53 | 4.67 | 3.48 | 1.97 |
| Control 1 | A | 10:29 | -12.7 | 8.07 | 10.27 | 7.80 | 6.81 | 5.52 | 3.95 | 1.98 |
| | B | 10:31 | -13.3 | 9.18 | 13.78 | 9.92 | 8.41 | 6.69 | 4.47 | 1.94 |
| | C | 10:32 | -13.7 | 10.11 | 14.32 | 10.51 | 9.01 | 7.15 | 4.86 | 2.12 |
| | D | 10:42 | -17.1 | 8.97 | 12.42 | 8.84 | 7.48 | 5.86 | 3.85 | 1.64 |
| Methacrylate 1 | A | 10:45 | -17.5 | 7.45 | 10.67 | 7.93 | 6.80 | 5.39 | 3.53 | 1.39 |
| | B | 10:46 | -17.7 | 9.42 | 12.94 | 9.20 | 7.84 | 5.95 | 3.72 | 1.32 |
| | C | 10:48 | -17.9 | 10.14 | 14.21 | 10.63 | 9.01 | 7.11 | 4.57 | 1.60 |
| | D | 10:50 | -18.2 | 8.41 | 11.00 | 8.46 | 7.19 | 5.50 | 3.59 | 1.41 |

Notes:
1. Normalized to 10 kips
2. Data measured on 10/2/91
3. 1 in. = 25.4 mm
4. 1°F = 0.556°C

Table B.15 Temperature adjusted joint deflections one day after treatment

| Section | Slab | Time AM | Temperature Gradient °F | Temperature Corrected Deflection, 0.001 in. -12 | 0 | 12 | 18 | 24 | 36 | 60 |
|---|---|---|---|---|---|---|---|---|---|---|
| Control 3 | A | 9:07 | 0.3 | 2.97 | 11.71 | 8.20 | 6.90 | 5.53 | 3.73 | 1.75 |
| | B | 9:10 | -0.3 | 4.70 | 10.54 | 7.48 | 6.32 | 5.08 | 3.51 | 1.81 |
| | C | 9:11 | -0.6 | 6.49 | 7.78 | 5.80 | 5.01 | 4.18 | 3.06 | 1.66 |
| | D | 9:13 | -0.9 | 4.72 | 15.78 | 11.51 | 9.94 | 8.12 | 5.67 | 2.04 |
| Methacrylate 2 | A | 8:53 | 3.3 | 4.50 | 6.15 | 4.67 | 4.17 | 3.65 | 2.85 | 1.76 |
| | B | 8:55 | 3.1 | 6.84 | 8.49 | 7.06 | 6.38 | 5.58 | 4.23 | 2.22 |
| | C | 8:56 | 2.9 | 3.39 | 10.39 | 7.73 | 6.66 | 5.54 | 3.96 | 2.11 |
| | D | 8:57 | 2.6 | 4.21 | 6.71 | 5.60 | 5.10 | 4.47 | 3.50 | 2.05 |
| Control 2 | A | 9:29 | -2.1 | 7.72 | 8.79 | 7.00 | 6.31 | 5.40 | 4.12 | 2.28 |
| | B | 9:31 | -2.2 | 7.52 | 8.51 | 6.82 | 6.13 | 5.24 | 3.98 | 2.19 |
| | C | 9:32 | -2.3 | 7.49 | 8.53 | 6.82 | 6.06 | 5.16 | 3.89 | 2.13 |
| | D | 9:34 | -2.5 | 5.80 | 6.96 | 5.36 | 4.78 | 4.06 | 3.10 | 1.81 |
| Control 1 | A | 9:56 | -3.6 | 6.71 | 7.81 | 6.16 | 5.46 | 4.61 | 3.46 | 1.95 |
| | B | 9:57 | -3.7 | 7.26 | 10.40 | 7.78 | 6.92 | 6.11 | 4.04 | 2.01 |
| | C | 9:59 | -3.8 | 8.10 | 12.00 | 8.96 | 7.77 | 6.32 | 4.42 | 2.13 |
| | D | 10:00 | -3.8 | 6.16 | 8.98 | 6.74 | 5.76 | 4.71 | 3.28 | 1.62 |
| Methacrylate 1 | A | 9:38 | -2.7 | 5.28 | 6.61 | 5.32 | 4.77 | 4.07 | 2.91 | 1.35 |
| | B | 9:40 | -2.8 | 6.48 | 7.55 | 5.93 | 5.17 | 4.27 | 2.94 | 1.29 |
| | C | 9:42 | -2.9 | 7.30 | 8.81 | 7.06 | 6.24 | 5.23 | 3.67 | 1.59 |
| | D | 9:43 | -3.0 | 6.00 | 6.82 | 5.38 | 4.71 | 3.94 | 2.82 | 1.37 |

Notes:
1. Normalized to 10 kips
2. Data measured on 10/3/91
3. 1 in. = 25.4 mm
4. 1°F = 0.556°C

Table B.16 Temperature adjusted joint deflections one year after treatment

| Section | Slab | Time AM | Temperature Gradient °F | Temperature Corrected Deflection, 0.001 in. -12 | 0 | 12 | 18 | 24 | 36 | 60 |
|---|---|---|---|---|---|---|---|---|---|---|
| Control 3 | A | 8:42 | 3.6 | 2.26 | 9.66 | 6.94 | 5.86 | 4.92 | 3.42 | 1.72 |
| | B | 9:06 | -0.6 | 3.00 | 13.50 | 9.45 | 8.01 | 6.48 | 4.45 | 2.23 |
| | C | 9:29 | -3.9 | 5.03 | 9.75 | 6.78 | 5.82 | 4.74 | 3.39 | 1.75 |
| | D | 9:58 | -6.2 | 4.52 | 15.28 | 10.31 | 8.45 | 6.67 | 4.20 | 1.33 |
| Lithium 2 | A | 8:44 | 3.3 | 3.47 | 20.55 | 16.72 | 15.03 | 13.36 | 10.36 | 5.38 |
| | B | 9:08 | -1.0 | 2.43 | 17.67 | 9.14 | 11.09 | 9.12 | 6.45 | 3.17 |
| | C | 9:30 | -4.1 | 5.13 | 10.85 | 7.55 | 6.39 | 5.23 | 3.63 | 1.70 |
| | D | 9:59 | -6.3 | 3.95 | 15.27 | 10.53 | 8.78 | 7.01 | 4.69 | 2.09 |
| Silane 2 | A | 9:33 | -4.4 | 4.24 | 12.17 | 8.54 | 7.23 | 5.85 | 4.03 | 1.55 |
| | B | 9:12 | -1.6 | 4.94 | 9.63 | 6.80 | 5.75 | 4.65 | 3.14 | 0.75 |
| | C | 9:35 | -4.5 | 2.67 | 25.77 | 18.99 | 16.21 | 13.18 | 8.95 | 3.49 |
| | D | 10:03 | -6.8 | 5.93 | 21.68 | 15.11 | 12.66 | 9.86 | 6.34 | 2.44 |
| Methacrylate 2 | A | 8:46 | 2.9 | 3.60 | 8.05 | 5.79 | 4.97 | 4.25 | 3.17 | 1.78 |
| | B | 9:36 | -4.6 | 6.21 | 13.32 | 9.73 | 8.29 | 6.75 | 4.64 | 2.15 |
| | C | 9:38 | -4.7 | 4.51 | 11.11 | 7.78 | 6.53 | 5.24 | 3.64 | 1.85 |
| | D | 10:04 | -7.0 | 5.02 | 10.84 | 7.47 | 6.19 | 4.94 | 3.32 | 1.53 |
| Silane #2 1 | A | 8:48 | 2.5 | 4.85 | 8.94 | 6.22 | 5.13 | 4.08 | 2.74 | 1.13 |
| | B | 9:14 | -1.8 | 3.92 | 8.47 | 5.95 | 4.92 | 3.94 | 2.63 | 1.20 |
| | C | 11:03 | -15.0 | 4.89 | 9.44 | 6.10 | 5.01 | 3.88 | 2.57 | 1.14 |
| | D | 11:04 | -15.1 | 5.50 | 8.35 | 5.56 | 4.67 | 3.65 | 2.47 | 1.13 |
| Linseed Oil 1 | A | 8:50 | 2.2 | 3.72 | 10.60 | 7.48 | 6.14 | 4.90 | 3.13 | 1.26 |
| | B | 9:16 | -2.1 | 4.17 | 7.50 | 5.23 | 4.40 | 3.56 | 2.44 | 1.03 |
| | C | 9:45 | -5.3 | 2.87 | 10.39 | 6.83 | 5.48 | 4.13 | 2.62 | 1.15 |
| | D | 10:07 | -7.4 | 4.69 | 8.24 | 5.47 | 4.50 | 3.51 | 2.32 | 1.04 |

Table B.16 (continued)

| Section | Slab | Time AM | Temperature Gradient °F | Temperature Corrected Deflection, 0.001 in. -12 | 0 | 12 | 18 | 24 | 36 | 60 |
|---|---|---|---|---|---|---|---|---|---|---|
| Control 2 | A | 8:52 | 1.8 | 8.31 | 9.35 | 7.27 | 6.48 | 5.55 | 4.25 | 2.36 |
| | B | 9:19 | -2.5 | 8.65 | 10.31 | 6.56 | 6.75 | 5.68 | 4.18 | 2.19 |
| | C | 9:47 | -5.4 | 6.47 | 11.73 | 8.62 | 7.38 | 6.11 | 4.29 | 2.20 |
| | D | 10:09 | -7.7 | 5.67 | 10.61 | 7.51 | 6.39 | 5.18 | 3.55 | 1.75 |
| Silane 1 | A | 8:53 | 1.7 | 5.44 | 8.69 | 6.45 | 5.48 | 4.58 | 3.34 | 1.80 |
| | B | 9:20 | -2.7 | 5.95 | 9.83 | 7.12 | 6.08 | 5.07 | 3.78 | 2.06 |
| | C | 9:48 | -5.5 | 6.36 | 9.71 | 7.17 | 6.10 | 5.01 | 3.66 | 1.94 |
| | D | 10:11 | -7.9 | 7.28 | 8.81 | 6.62 | 5.77 | 4.70 | 3.47 | 1.76 |
| Lithium 1 | A | 8:59 | 0.6 | 5.85 | 8.85 | 6.61 | 5.75 | 4.80 | 3.47 | 1.97 |
| | B | 9:22 | -2.9 | 5.76 | 8.99 | 6.59 | 5.69 | 4.79 | 3.56 | 1.99 |
| | C | 9:50 | -5.6 | 5.48 | 12.67 | 8.99 | 7.53 | 6.20 | 4.46 | 2.36 |
| | D | 10:12 | -8.1 | 6.12 | 13.56 | 9.56 | 8.05 | 6.53 | 4.54 | 2.25 |
| Control 1 | A | 9:01 | 0.2 | 6.12 | 11.50 | 8.63 | 7.60 | 6.42 | 4.60 | 2.39 |
| | B | 9:24 | -3.2 | 7.39 | 13.08 | 9.82 | 8.52 | 7.17 | 5.21 | 2.44 |
| | C | 9:51 | -5.7 | 6.71 | 16.70 | 11.98 | 10.03 | 8.11 | 5.49 | 2.41 |
| | D | 10:13 | -8.2 | 6.79 | 11.53 | 8.05 | 6.76 | 5.27 | 3.63 | 1.54 |
| Methacrylate 1 | A | 9:02 | 0.1 | 5.34 | 8.25 | 5.51 | 4.70 | 3.89 | 2.68 | 1.25 |
| | B | 9:25 | -3.4 | 7.87 | 10.49 | 7.57 | 6.42 | 5.23 | 3.46 | 1.47 |
| | C | 9:52 | -5.8 | 7.59 | 10.04 | 7.74 | 6.60 | 3.70 | 3.72 | 1.56 |
| | D | 10:15 | -8.5 | 6.97 | 8.65 | 6.54 | 5.68 | 4.59 | 3.20 | 1.38 |

Notes: 1. Normalized to 10 kips
2. Data measured on 10/8/92
3. 1 in. = 25.4 mm
4. 1°F = 0.556°C

Table B.17 Measured edge deflections one year after treatment

| Section | Slab | Time AM | Measured Deflection, 0.001 in. 0 | 8 | 12 | 18 | 24 | 36 | 60 |
|---|---|---|---|---|---|---|---|---|---|
| Control 3 | A | 11:19 | 5.27 | 4.96 | 4.66 | 4.27 | 3.83 | 3.00 | 1.71 |
| | B | 11:20 | 6.36 | 6.07 | 5.79 | 5.43 | 4.92 | 4.08 | 2.15 |
| | C | 11:21 | 5.62 | 5.36 | 5.06 | 4.65 | 4.17 | 3.24 | 1.72 |
| | D | 11:22 | 5.67 | 4.94 | 4.60 | 4.11 | 3.56 | 2.80 | 1.67 |
| | E | 11:23 | 5.71 | 5.22 | 4.96 | 4.53 | 4.05 | 3.21 | 1.85 |
| Lithium 2 | A | 11:24 | 5.20 | 5.03 | 4.79 | 4.51 | 4.06 | 3.28 | 1.92 |
| | B | 11:26 | 5.25 | 4.94 | 4.66 | 4.37 | 3.98 | 3.27 | 2.05 |
| | C | 11:28 | 5.68 | 5.16 | 4.85 | 4.42 | 3.97 | 3.16 | 1.91 |
| | D | 11:29 | 5.37 | 5.17 | 4.92 | 4.55 | 4.11 | 3.36 | 2.04 |
| | E | 11:30 | 5.36 | 5.00 | 4.77 | 4.39 | 3.91 | 3.06 | 1.62 |
| Silane 2 | B | 11:32 | 6.06 | 5.21 | 4.80 | 4.22 | 3.66 | 2.80 | 1.59 |
| | C | 11:33 | 7.06 | 5.46 | 4.90 | 4.32 | 3.60 | 2.64 | 1.47 |
| | D | 11:34 | 4.75 | 4.29 | 4.02 | 3.65 | 3.23 | 2.48 | 1.36 |
| | E | 11:35 | 4.40 | 4.03 | 3.78 | 3.46 | 3.10 | 2.42 | 1.35 |
| Methacrylate 2 | A | 11:37 | 5.18 | 4.51 | 4.15 | 3.74 | 3.24 | 2.47 | 1.37 |
| | B | 11:38 | 4.53 | 4.24 | 4.01 | 3.73 | 3.39 | 2.80 | 1.84 |
| | C | 11:38 | 6.41 | 6.03 | 5.82 | 5.42 | 4.77 | 3.83 | 1.65 |
| | D | 11:39 | 5.89 | 5.60 | 5.33 | 5.00 | 4.47 | 3.58 | 1.77 |
| | E | 11:41 | 5.42 | 5.08 | 4.76 | 4.44 | 4.02 | 3.17 | 2.02 |
| Silane #2 1 | B | 11:55 | 4.46 | 4.15 | 3.97 | 3.63 | 3.22 | 2.54 | 1.40 |
| | C | 11:56 | 4.25 | 3.97 | 3.46 | 3.21 | 2.79 | 1.97 | 1.34 |
| | D | 11:57 | 4.44 | 3.73 | 3.30 | 2.90 | 2.54 | 1.85 | 1.27 |
| | E | 11:58 | 4.38 | 4.13 | 3.93 | 3.67 | 3.33 | 2.69 | 1.47 |
| Linseed Oil 1 | B | 11:59 | 5.09 | 4.69 | 4.47 | 4.12 | 3.63 | 2.84 | 1.41 |
| | C | 12:00 | 4.48 | 4.10 | 3.79 | 3.45 | 3.03 | 2.30 | 1.28 |
| | D | 12:01 | 5.43 | 4.81 | 4.31 | 3.94 | 3.36 | 2.47 | 1.31 |
| | E | 12:02 | 5.36 | 5.02 | 4.81 | 4.43 | 3.94 | 3.09 | 1.49 |
| Control 2 | B | 12:04 | 5.78 | 5.34 | 5.10 | 4.72 | 4.31 | 3.52 | 2.08 |
| | C | 12:05 | 6.04 | 5.62 | 5.33 | 4.98 | 4.52 | 3.67 | 2.09 |
| | D | 12:06 | 5.23 | 5.20 | 4.66 | 4.32 | 4.08 | 3.33 | 1.91 |
| | E | 12:07 | 4.73 | 4.40 | 4.18 | 3.84 | 3.46 | 2.78 | 1.71 |
| Silane 1 | B | 12:26 | 5.91 | 5.61 | 5.43 | 5.03 | 4.60 | 3.75 | 2.10 |
| | C | 12:28 | 5.59 | 5.22 | 4.83 | 4.56 | 4.23 | 3.31 | 2.06 |
| | D | 12:29 | 4.97 | 4.49 | 4.24 | 3.90 | 3.53 | 2.93 | 1.94 |
| | E | 12:30 | 5.25 | 4.84 | 4.61 | 4.28 | 3.88 | 3.16 | 2.02 |

Table B.17 (continued)

| Section | Slab | Time AM | Measured Deflection, 0.001 in. 0 | 8 | 12 | 18 | 24 | 36 | 60 |
|---|---|---|---|---|---|---|---|---|---|
| Lithium 1 | A | 12:34 | 6.09 | 5.73 | 5.44 | 5.08 | 4.67 | 3.41 | 1.99 |
| | B | 12:35 | 6.05 | 5.68 | 5.41 | 4.97 | 4.46 | 3.49 | 1.99 |
| | C | 12:39 | 4.95 | 4.81 | 4.30 | 4.13 | 3.88 | 3.17 | 2.22 |
| | D | 12:40 | 5.76 | 5.54 | 5.30 | 4.93 | 4.49 | 3.68 | 2.26 |
| | E | 12:41 | 5.77 | 5.54 | 5.41 | 5.01 | 4.57 | 3.73 | 1.99 |
| Control 1 | A | 12:42 | 5.47 | 5.25 | 5.07 | 4.73 | 4.31 | 3.52 | 2.07 |
| | B | 12:43 | 7.83 | 5.87 | 5.36 | 4.79 | 4.22 | 3.15 | 2.06 |
| | C | 12:44 | 6.36 | 6.00 | 5.80 | 5.32 | 4.77 | 3.89 | 2.32 |
| | D | 12:45 | 5.70 | 5.48 | 5.22 | 4.83 | 4.37 | 3.43 | 1.73 |
| | E | 12:47 | 5.34 | 5.15 | 4.85 | 4.51 | 4.12 | 3.29 | 1.79 |
| Methacrylate 1 | A | 12:09 | 5.11 | 4.08 | 3.75 | 3.31 | 2.83 | 2.10 | 1.04 |
| | B | 12:11 | 6.04 | 5.51 | 5.21 | 4.73 | 4.16 | 3.14 | 1.44 |
| | C | 12:12 | 5.28 | 4.92 | 4.68 | 4.31 | 3.87 | 3.04 | 1.51 |
| | D | 12:13 | 5.75 | 5.26 | 4.90 | 4.40 | 3.90 | 3.03 | 1.75 |
| | E | 12:14 | 5.48 | 4.98 | 4.59 | 4.13 | 3.63 | 2.79 | 1.54 |

Notes:
1. Normalized to 10 kips
2. Data recorded on 10/8/92.
3. 1000 lbs = 6.94 MPa
4. 1 in. = 25.4 mm
5. Data not adjusted for temperature gradient effects.

initial tests and tests done at one year within the control section are significant. The t-test does not compare if any significant differences noted at one year are less than, equal to, or greater than differences noted for other types of treatment sections. The second type of analysis was an ANOVA (analysis of variance) of the differences in deflections with time to determine if there was a statistical difference between-treatments. This analysis was done to evaluate if differences noted in one treatment type are significantly different than differences measured for other types of treatment. Since each slab within each treatment section had initial baseline deflections the ANOVA considered deflection differences to evaluate the effects of treatments.

If the ANOVA indicated a significant difference in deflections due to different treatments, treatment differences were compared to the replication differences to determine if deflection changes due to treatments are significantly greater than that expected from between-test variability. The analyses were performed on interior and joint measurements made before treatment and at one year. A similar analysis was made for control and methacrylate data before treatment and one day after treatment to detect any immediate decreases (improvement) in deflections. An analysis was also done for the methacrylate and control sections one day after treatment and at one year to determine if significant differences were measured.

### *B.3.1 Effectiveness of Methacrylate Treatment at One Day*

The paired t-test analysis indicated that interior and joint deflections significantly decreased after methacrylate application. Statistically significant decreases at the 5 percent significance level were noted within each methacrylate section as well as the combined section. One interior deflection outlier in Control Section 3 Slab E was identified and not included in the analysis. The paired t-test also indicated a significant change in some control section interior deflections. Control section deflection changes were attributed to temperature adjustments. Results of the one day t-tests are summarized in Tables B.18 and B.19 for interior and joint deflections, respectively. Maximum interior and joint deflections measured before and one day after methacrylate treatment are shown in Figures B.5 and B.6, respectively. As shown in the figures, the methacrylate maximum deflections tended to fall below the line of equality (decrease) and control section deflections were scattered around or above the line of equality.

To evaluate the significance of methacrylate treatment deflection decreases, an ANOVA was performed of deflection differences (initial minus after treatment). Significant differences at the 5 percent level of significance were noted between control sections and methacrylate sections for all interior deflection positions. For the maximum interior deflection under the load, the average deflection change at one day was an increase of 0.00017 in. (0.004 mm) for control and a decrease of 0.00036 in. (0.009 mm) for the methacrylate sections.

Significant joint deflection differences at the 5 percent level of significance were also noted between control sections and methacrylate sections for all joint deflection positions except at 60 in. (1524 mm) from the load. For the maximum joint deflection under the load, the average deflection change at one day was an increase of 0.0000348 in. (0.001 mm) for control and a decrease of 0.00596 in. (0.151 mm) for the methacrylate sections.

The F-distribution was used to compare the one day maximum deflection differential standard deviation to the between-test (replicate) standard deviations listed in Table B.2. If significant standard deviation differences do exist, the deflection differentials could result from outlier

Table B.18 Interior deflection within-treatment paired t-test before and one day after methacrylate application

| | distance from load, in. | | | | | | |
|---|---|---|---|---|---|---|---|
| Section | 0 | 8 | 12 | 18 | 24 | 36 | 60 |
| Control 3 | + | + | + | + | + | NS | NS |
| Methacrylate 2 | - | - | - | NS | NS | NS | NS |
| Control 2 | NS | + | NS | NS | NS | NS | + |
| Control 1 | NS | + | + | + | + | + | + |
| Methacrylate 1 | - | - | - | - | - | - | NS |
| All Control | + | + | + | + | + | + | + |
| All Methacrylate | - | - | - | - | - | NS | NS |

Notes:
1. "+" = increase in deflection at 1 day
"-" = decrease in deflection at 1 day
NS = not significant at the 5 percent level of significance
2. Outlier in Control Section 3 Slab D excluded from analysis.
3. 1 in. = 25.4 mm

Table B.19 Joint deflection within-treatment paired t-test before and one day after methacrylate application

| | distance from load, in. | | | | | | |
|---|---|---|---|---|---|---|---|
| **Section** | **-12** | **0** | **12** | **18** | **24** | **36** | **60** |
| Control 3 | NS | NS | + | + | NS | NS | + |
| Methacrylate 2 | - | - | - | - | - | - | + |
| Control 2 | + | + | + | + | + | NS | NS |
| Control 1 | - | - | - | - | - | - | NS |
| Methacrylate 1 | - | - | - | - | - | - | - |
| All Control | NS | NS | NS | NS | NS | NS | NS |
| All Methacrylate | - | - | - | - | - | - | NS |

Notes:
1. "+" = increase in deflection at 1 day
"-" = decrease in deflection at 1 day
NS = not significant at the 5 percent level of significance
2. 1 in. = 25.4 mm

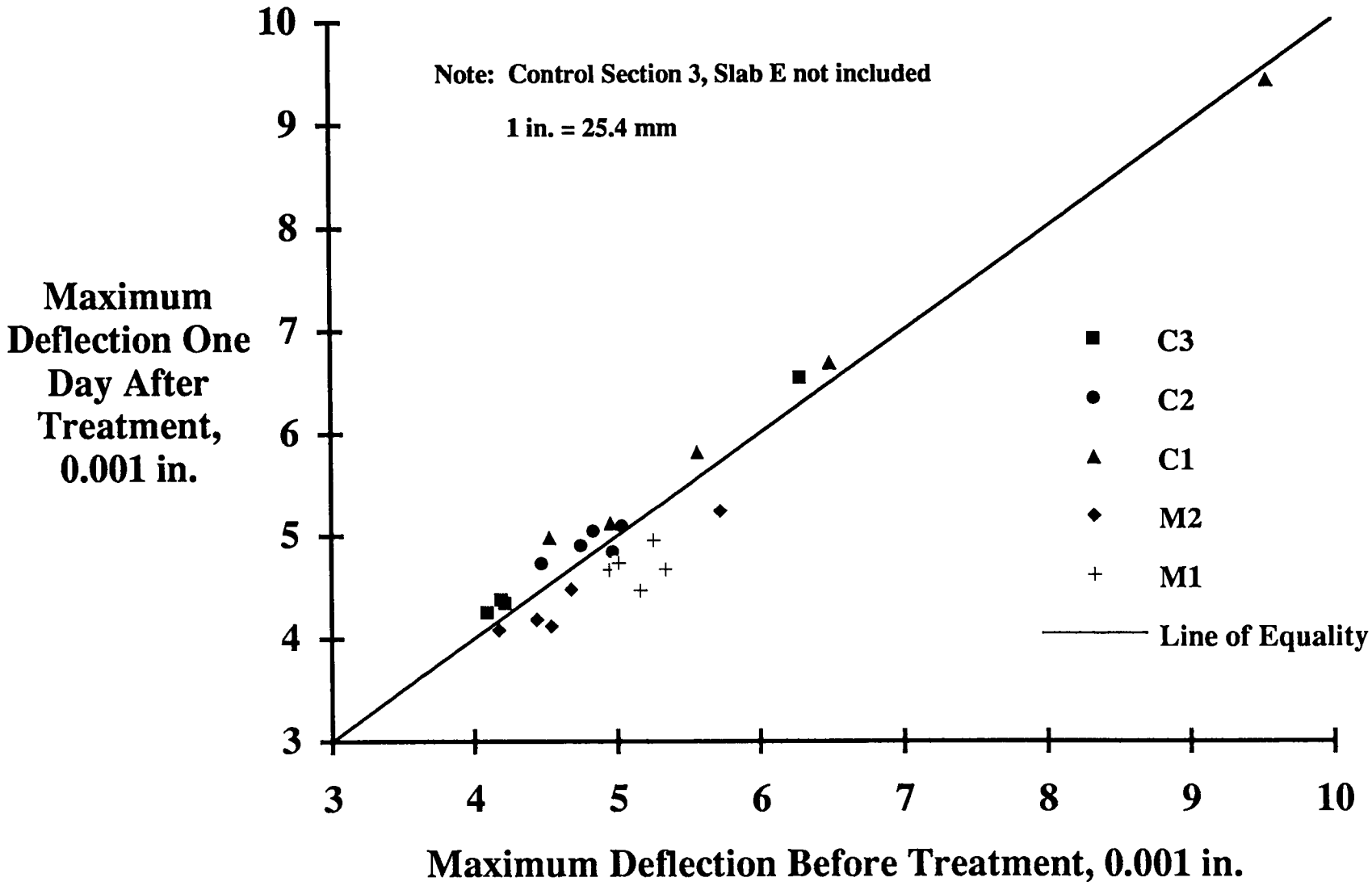


Figure B.5. Comparison of maximum interior deflections before and one day after methacrylate treatment.

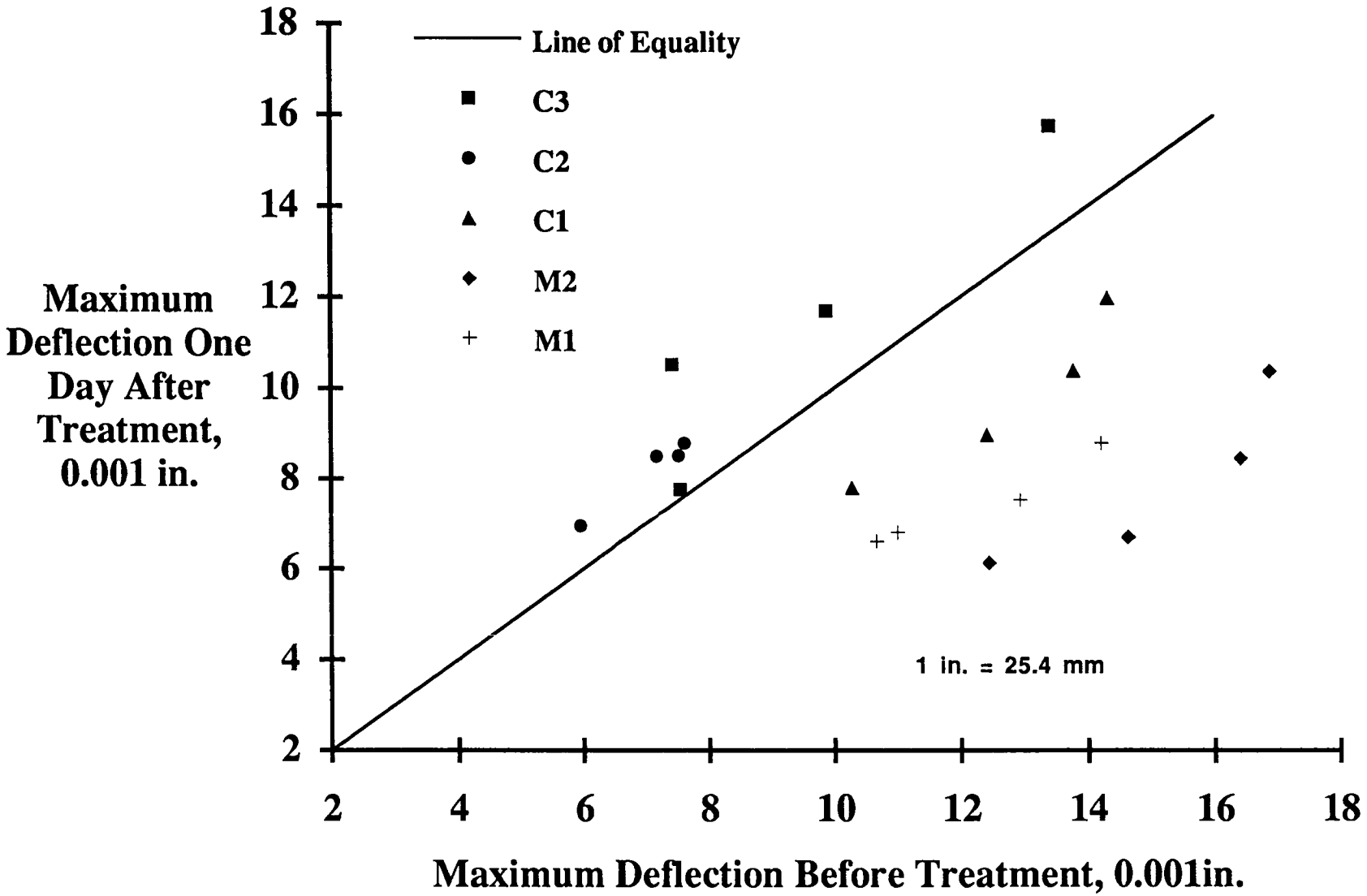


Figure B.6. Comparison of maximum joint deflections before and one day after methacrylate treatment.

data rather than treatment effects. There was no significant difference in the maximum interior and joint deflection standard deviations at the 5 percent level of significance. The ANOVA for all deflection positions is summarized in Tables B.20 and B.21 for interior and joint deflections, respectively.

Since average increases in control section deflections were less than the between-test replicate root mean square listed in Table B.2, the increase in deflections were determined not statistically different than between-test variability expected due to load positioning, load measurement, and deflection measurement. Assuming that average increases measured at one day in the control sections would be equally reflected in the methacrylate sections, the average deflection decrease (difference between average control increase and methacrylate decrease) at one day due to the methacrylate treatment was 0.00053 in. (0.013 mm) for the maximum interior and 0.00600 in. (0.152 mm) for the maximum joint deflection. The average deflections of the methacrylate section before treatment were 0.00493 and 0.01365 in. (0.125 and 0.347 mm) for interior and joint deflections, respectively. Deflection decreases after methacrylate averaged 10.6 and 43.9 percent for interior and joint deflections, respectively. Maximum interior and joint deflections and changes before and after treatment deflection are summarized in Table B.22.

### *B.3.2 Effectiveness of Treatments at One Year*

The paired t-test analysis indicated that interior deflections in general did not significantly change between initial (before treatment) and one year after treatment applications. This indicates that improvements in the methacrylate sections noted at one day were not measured one year later. Statistically significant decreases at the 5 percent significance level were noted within lithium and silane sections only at deflection positions 18 in. (457 mm) or further away from the load. One interior deflection outlier in Control Section 3 Slab E was identified and not included in the analysis. Since no significant changes were noted under the load and at 8 and 12 in. (203 and 305 mm) away from the load, any significant deflection decreases at positions further from the load were attributed to temperature adjustment errors.

To account for effects of joint load transfer efficiency, the free edge deflection, computed as the sum of undowelled loaded and unloaded slab deflection, was also evaluated. For methacrylate joint deflections, significant decreases in deflections at most deflection positions were measured for both the individual and combined sections. Significant deflection increases were measured in both silane sections, Control Section 2, and Lithium Section 1. Most other within-treatment changes in deflections were statistically insignificant. The t-test analysis indicates that the significant decreases in methacrylate section joint deflections measured one day after treatment are still apparent while other treatment section joint deflections have increased with time.

The t-test analysis indicates that interior deflection response did not change. This suggests that any deflection reduction one day after methacrylate treatment was not observed one year later. The joint deflection t-tests indicates that deflection reductions observed at one day after methacrylate application are still apparent at one year. Significant joint deflection decreases, relative to before treatment deflections, still exist one year after treatment. Results of the one year t-tests for interior and joint deflections, respectively, are summarized in Tables B.23 and B.24

Table B.20 Interior differential deflection ANOVA and means table for before and 1 day after methacrylate treatment

| Distance from Load, in. | | Degrees of Freedom | Sum of Square | Mean Square | F-value | P-value | Section | Count | Mean 0.001 in. | Standard Deviation 0.001 in. | Standard Error |
|---|---|---|---|---|---|---|---|---|---|---|---|
| 0 | Section | 1 | 1.596 | 1.596 | 55.178 | <0.0001 | Control | 14 | -0.167 | 0.151 | 0.040 |
| | Residual | 22 | 0.637 | 0.029 | | | Methacrylate | 10 | 0.356 | 0.194 | 0.061 |
| 8 | Section | 1 | 1.269 | 1.269 | 102.978 | <0.0001 | Control | 14 | -0.186 | 0.096 | 0.026 |
| | Residual | 22 | 0.271 | 0.012 | | | Methacrylate | 10 | 0.280 | 0.129 | 0.041 |
| 12 | Section | 1 | 1.033 | 1.033 | 73.172 | <0.0001 | Control | 14 | -0.148 | 0.103 | 0.027 |
| | Residual | 22 | 0.311 | 0.014 | | | Methacrylate | 10 | 0.273 | 0.139 | 0.044 |
| 18 | Section | 1 | 0.814 | 0.814 | 58.812 | <0.0001 | Control | 14 | -0.144 | 0.100 | 0.027 |
| | Residual | 22 | 0.305 | 0.014 | | | Methacrylate | 10 | 0.230 | 0.140 | 0.044 |
| 24 | Section | 1 | 0.505 | 0.505 | 34.891 | <0.0001 | Control | 14 | -0.119 | 0.089 | 0.024 |
| | Residual | 22 | 0.319 | 0.014 | | | Methacrylate | 10 | 0.175 | 0.154 | 0.049 |
| 36 | Section | 1 | 0.376 | 0.376 | 19.173 | 0.0002 | Control | 14 | -0.125 | 0.080 | 0.021 |
| | Residual | 22 | 0.432 | 0.020 | | | Methacrylate | 10 | 0.129 | 0.197 | 0.062 |
| 60 | Section | 1 | 0.131 | 0.131 | 8.676 | 0.0075 | Control | 14 | -0.090 | 0.076 | 0.020 |
| | Residual | 22 | 0.333 | 0.015 | | | Methacrylate | 10 | 0.060 | 0.169 | 0.053 |

Notes: 1. Deflection difference is initial minus 1 day.
2. Does not include outliers in Control Section 3, Slab E
3. 1 in. = 25.4 mm

Table B.21 Joint differential deflection ANOVA and means table for before and 1 day after methacrylate treatment

| Distance from Load, in. | | Degrees of Freedom | Sum of Square | Mean Square | F-value | P-value | Section | Count | Mean 0.001 in. | Standard Deviation 0.001 in. | Standard Error |
|---|---|---|---|---|---|---|---|---|---|---|---|
| 0 | Section | 1 | 172.656 | 172.656 | 41.943 | <0.0001 | Control | 12 | -0.038 | 2.307 | 0.666 |
| | Residual | 18 | 74.096 | 4.116 | | | Methacrylate | 8 | 5.960 | 1.492 | 0.527 |
| 12 | Section | 1 | 49.229 | 49.229 | 29.333 | <0.0001 | Control | 12 | 0.365 | 1.375 | 0.397 |
| Unloaded slab | Residual | 18 | 30.209 | 1.678 | | | Methacrylate | 8 | 3.567 | 1.160 | 0.410 |
| 12 | Section | 1 | 71.750 | 71.750 | 39.953 | <0.0001 | Control | 12 | -0.085 | 1.554 | 0.449 |
| Loaded slab | Residual | 18 | 32.325 | 1.796 | | | Methacrylate | 8 | 3.781 | 0.908 | 0.321 |
| 18 | Section | 1 | 42.566 | 42.566 | 37.295 | <0.0001 | Control | 12 | -0.102 | 1.274 | 0.368 |
| | Residual | 18 | 20.544 | 1.141 | | | Methacrylate | 8 | 2.876 | 0.620 | 0.219 |
| 24 | Section | 1 | 18.221 | 18.221 | 32.971 | <0.0001 | Control | 12 | -0.148 | 0.900 | 0.260 |
| | Residual | 18 | 9.947 | 0.553 | | | Methacrylate | 8 | 1.800 | 0.384 | 0.136 |
| 36 | Section | 1 | 3.169 | 3.169 | 14.042 | 0.0015 | Control | 12 | -0.087 | 0.579 | 0.167 |
| | Residual | 18 | 4.062 | 0.226 | | | Methacrylate | 8 | 0.725 | 0.229 | 0.081 |
| 60 | Section | 1 | 0.066 | 0.066 | 1.529 | 0.2322 | Control | 12 | -0.035 | 0.196 | 0.057 |
| | Residual | 18 | 0.780 | 0.043 | | | Methacrylate | 8 | -0.153 | 0.226 | 0.080 |

Notes: 1. Deflection difference is initial minus 1 day.
2. 1 in. = 25.4 mm

Table B.22 Summary of maximum average deflections

| | | Interior Maximum Deflection, 0.001 in. | | | | Joint Maximum Deflection, 0.001 in. | | | |
|---|---|---|---|---|---|---|---|---|---|
| | Treatment | Before Treatment Mean | After Treatment Mean | Mean Difference | Standard Deviation of the Mean Difference | Before Treatment Mean | After Treatment Mean | Mean Difference | Standard Deviation of the Mean Difference |
| Before and One Day After Treatments | Control | 5.281 | 5.449 | -0.167 | 0.151 | 9.777 | 9.816 | -0.038 | 2.307 |
| | Methacrylate | 4.926 | 4.567 | 0.356 | 0.194 | 13.648 | 7.691 | 5.960 | 1.492 |
| Before and One Year After Treatments | Control | 5.281 | 5.317 | 0.036 | 0.625 | 9.777 | 11.917 | 2.140 | 2.154 |
| | Lithium | 5.030 | 4.850 | -0.181 | 0.349 | 10.477 | 13.550 | 3.071 | 2.487 |
| | Silane | 5.178 | 4.887 | -0.290 | 0.548 | 8.812 | 13.284 | 4.471 | 2.086 |
| | Methacrylate | 4.926 | 4.878 | -0.047 | 0.487 | 13.648 | 10.093 | -3.555 | 1.210 |
| One Day and One Year After Treatments | Control | 5.449 | 5.317 | -0.131 | 0.607 | 9.816 | 11.917 | 2.102 | 1.921 |
| | Methacrylate | 4.567 | 4.878 | 0.312 | 0.511 | 7.691 | 10.093 | 2.404 | 1.441 |

Notes: 1. At one day, positive difference if decreasing deflection.
2. At one year, positive difference if increasing deflection.
3. 1 in. = 25.4 mm

Table B.23 Interior deflection paired t-test before and one year after treatment application

| | distance from load, in. | | | | | | |
|---|---|---|---|---|---|---|---|
| **Section** | **0** | **8** | **12** | **18** | **24** | **36** | **60** |
| Control 3 | NS | NS | NS | NS | NS | NS | NS |
| Lithium 2 | NS | NS | NS | - | - | - | NS |
| Silane 2 | NS | NS | NS | - | - | - | - |
| Methacrylate 2 | NS | NS | NS | NS | NS | NS | NS |
| Control 2 | NS | NS | NS | NS | NS | NS | NS |
| Silane 1 | NS | NS | NS | NS | NS | NS | - |
| Lithium 1 | NS | NS | NS | NS | NS | NS | - |
| Control 1 | NS | NS | NS | NS | NS | NS | NS |
| Methacrylate 1 | NS | NS | NS | NS | NS | NS | NS |
| All Control | NS | NS | NS | NS | NS | NS | NS |
| All Lithium | NS | NS | NS | NS | NS | NS | - |
| All Silane | NS | NS | - | - | - | - | - |
| All Methacrylate | NS | NS | NS | NS | NS | NS | NS |

Notes:
1. "+" = increase in deflection at 1 year
"-" = decrease in deflection at 1 year
NS = not significant at the 5 percent level of significance
2. Outlier in Control Section 3 Slab E excluded from analysis.
3. 1 in. = 25.4 mm

Table B.24 Joint deflection within-treatment paired t-test before and one year after treatment application

| Section | distance from load, in. -12 | 0 | L+U | 12 | 18 | 24 | 36 | 60 |
|---|---|---|---|---|---|---|---|---|
| Control 3 | NS | NS | NS | NS | NS | NS | NS | NS |
| Lithium 2 | NS | NS | NS | NS | NS | NS | NS | NS |
| Silane 2 | NS | + | + | + | + | + | + | - |
| Methacrylate 2 | - | - | - | - | - | - | - | NS |
| Control 2 | NS | + | + | NS | + | + | NS | NS |
| Silane 1 | NS | + | + | + | + | + | + | + |
| Lithium 1 | NS | + | + | + | + | + | + | NS |
| Control 1 | - | NS | - | NS | NS | NS | NS | NS |
| Methacrylate 1 | - | - | - | - | - | NS | - | NS |
| All Control | NS | + | NS | - | + | + | + | NS |
| All Lithium | NS | + | NS | - | + | NS | NS | NS |
| All Silane | NS | + | NS | - | + | NS | + | NS |
| All Methacrylate | - | - | - | - | - | - | - | NS |

Notes:
1. "L+U" = loaded plus unloaded slab edge deflection
2. "+" = increase in deflection at 1 year
   "-" = decrease in deflection at 1 year
   NS = not significant at the 5 percent level of significance
3. 1 in. = 25.4 mm

Maximum interior and joint deflections measured before and one year after treatment are shown in Figures B.7 and B.8, respectively. As shown in the figures, the interior maximum deflections were generally scattered around the line of equality. Joint deflections shown in Figure B.8 also were above (increased with time) or scattered around the line of equality. Methacrylate section joint deflections were significantly below the line of equality (decrease in deflection after application). Some of the lithium and silane treatment section joint deflections were significantly above the line of equality, as determined from the within-treatment t-tests.

To evaluate the significance of treatments on interior deflection changes, an ANOVA was performed of deflection differences (initial minus one year after treatment). As a group, significant differences were not noted between treatment types at the 5 percent level of significance for all interior deflection positions. Fisher's protected least significant difference test was done to analyze effects between any two treatments. Significant decreases in the Silane Section 1 deflections yielded a statistical treatment difference between silane and methacrylate for deflections 24 in. (610 mm) and between silane and control for deflections 36 in. (914 mm) from the load. Since the ANOVA did not result in any statistical differences and no significant difference between any two treatments (excluding effects of silane away from the load) were noted, it was concluded that, at one year, observed changes in interior deflections were not statistically different between treatments.

This result was expected since the interior deflections plotted in Figure B.7 and t-test analysis indicated that no significant changes occurred in the deflections before treatment and one year after treatment. The analysis implied that one year after treatment with methacrylate, interior deflection magnitudes were no different than the control sections with no treatment. The analysis did not conclude that methacrylate section deflections will increase at the same rate as other treatments or no treatments. While the benefits of one-day decreases were not measured at one year for the methacrylate sections, the remaining sections did not indicate significant deflection changes. Long term monitoring is required to evaluate the effectiveness of methacrylate treatments on interior deflections. Effectiveness of methacrylate should be evaluated by comparison with continually deteriorating control sections. Maximum interior deflections and changes before and one year after treatment are summarized in Table B.22. The ANOVA for all interior deflection positions is summarized in Table B.25.

To evaluate the significance of treatments on joint deflection changes, an ANOVA was performed of deflection differences (initial minus one year after treatment). As a group, significant differences were noted between treatment types at the 5 percent level of significance for all joint deflection positions except at 60 in. (1724 mm) away from the load. Fisher's protected least significant difference test was done to analyze effects between any two treatments. Decreases in methacrylate section deflections were significantly different than the increases measured in the control, lithium, and silane sections at all load positions (including the free edge deflection) except at 60 in. (1724 mm) away from the load. Significant differences were also noted between control and silane sections under the load and 12 in. (305 mm) away from the load. This observation was expected since the joint deflections plotted in Figure B.8 and t-test analysis indicated that significant decreases in the methacrylate-treated sections occurred while other section deflections remained unchanged (or increased). Maximum joint deflections and changes before and one year after treatment are summarized in Table B.22. The ANOVA for all joint deflection positions is summarized in Table B.26. The F-distribution was used to compare the one year maximum deflection differential standard deviation to the between-test (replicate) standard deviations listed in Table B.2. If significant standard deviation differences do exist, the deflection differentials

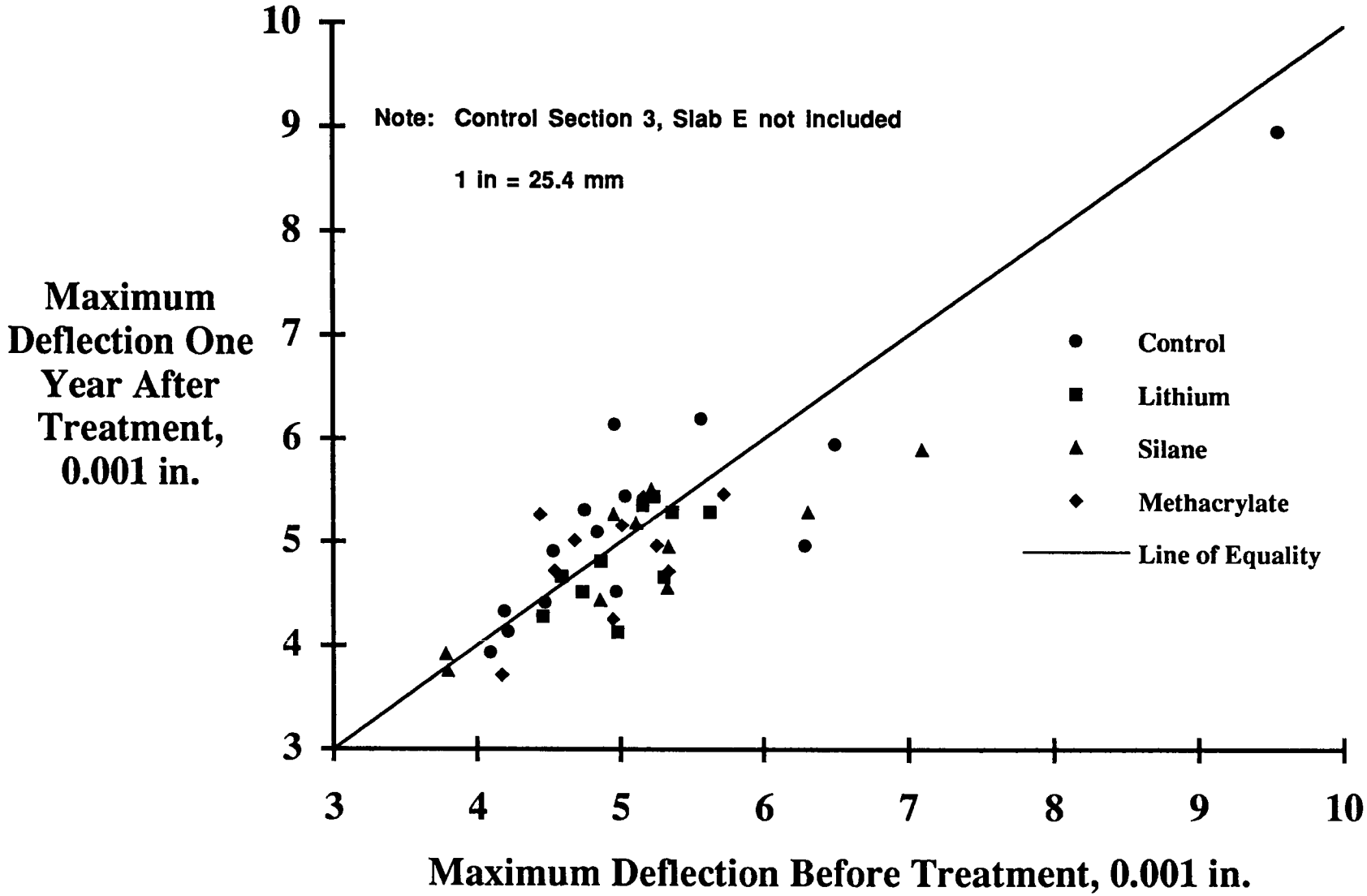


Figure B.7. Comparison of maximum interior deflections before and one year after treatment.

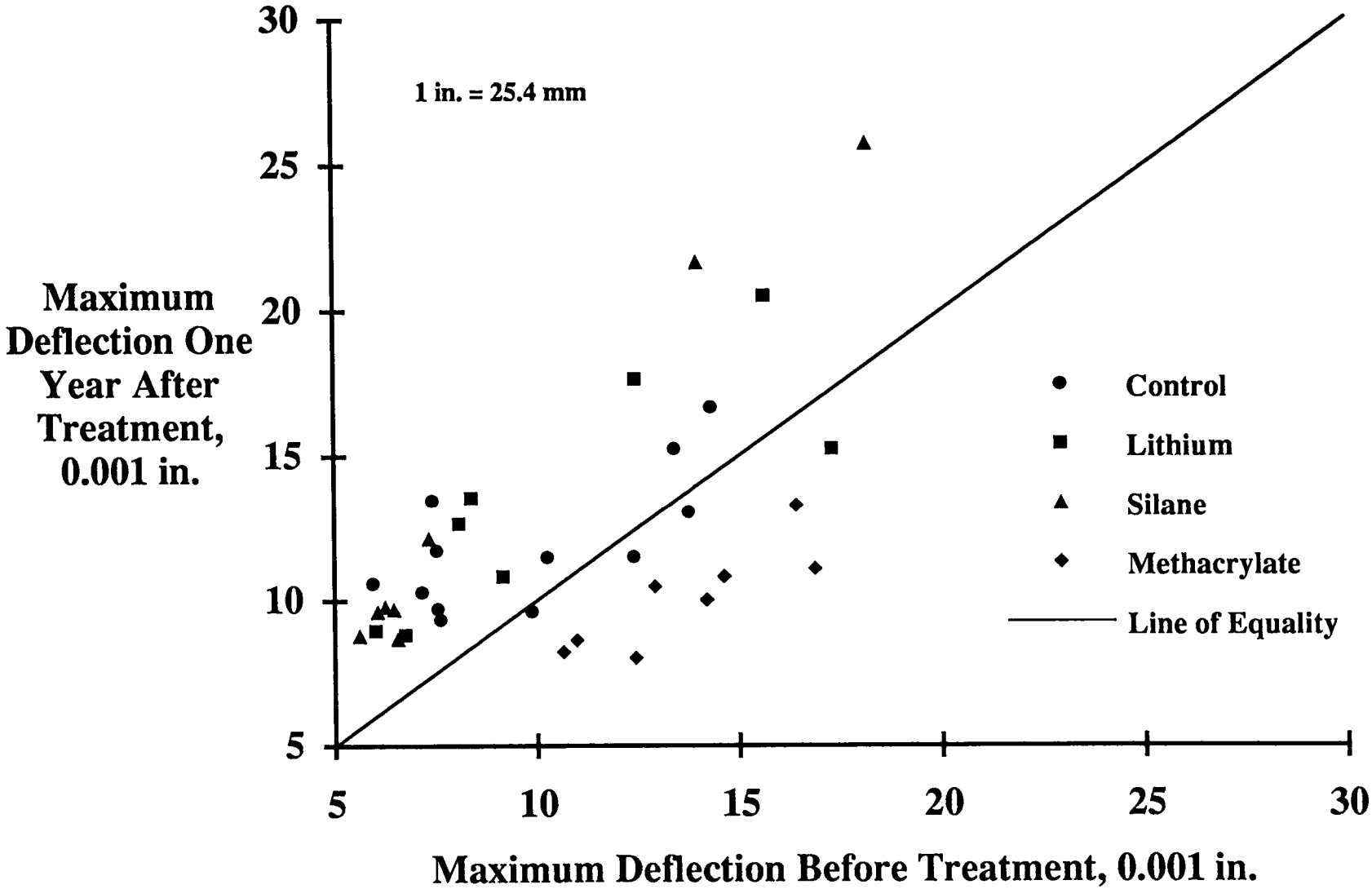


Figure B.8. Comparison of maximum joint deflections before and one year after treatment.

Table B.25 Interior differential deflection ANOVA and means table for before and one year after treatment

| Distance from Load, in. | | Degrees of Freedom | Sum of Square | Mean Square | F-value | P-value | Section | Count | Mean 0.001 in. | Standard Deviation 0.001 in. | Standard Error |
|---|---|---|---|---|---|---|---|---|---|---|---|
| 0 | Treatment | 3 | 0.714 | 0.238 | 0.863 | 0.4680 | Control | 14 | 0.036 | 0.625 | 0.167 |
| | Residual | 40 | 11.020 | 0.275 | | | Lithium | 10 | -0.181 | 0.349 | 0.110 |
| | | | | | | | Silane | 10 | -0.290 | 0.548 | 0.173 |
| | | | | | | | Methacrylate | 10 | -0.047 | 0.487 | 0.154 |
| 8 | Treatment | 3 | 0.765 | 0.255 | 0.960 | 0.4209 | Control | 14 | -0.024 | 0.641 | 0.171 |
| | Residual | 40 | 10.619 | 0.265 | | | Lithium | 10 | -0.126 | 0.340 | 0.108 |
| | | | | | | | Silane | 10 | -0.322 | 0.515 | 0.163 |
| | | | | | | | Methacrylate | 10 | 0.036 | 0.454 | 0.144 |
| 12 | Treatment | 3 | 0.856 | 0.285 | 1.088 | 0.3652 | Control | 14 | -0.056 | 0.589 | 0.157 |
| | Residual | 40 | 10.490 | 0.262 | | | Lithium | 10 | -0.080 | 0.515 | 0.163 |
| | | | | | | | Silane | 10 | -0.378 | 0.468 | 0.148 |
| | | | | | | | Methacrylate | 10 | -0.011 | 0.424 | 0.134 |
| 18 | Treatment | 3 | 0.918 | 0.306 | 1.527 | 0.2222 | Control | 14 | -0.067 | 0.535 | 0.143 |
| | Residual | 40 | 8.011 | 0.200 | | | Lithium | 10 | -0.202 | 0.339 | 0.107 |
| | | | | | | | Silane | 10 | -0.404 | 0.405 | 0.128 |
| | | | | | | | Methacrylate | 10 | -0.024 | 0.444 | 0.141 |
| 24 | Treatment | 3 | 0.978 | 0.326 | 1.957 | 0.1360 | Control | 14 | -0.039 | 0.454 | 0.121 |
| | Residual | 40 | 6.665 | 0.167 | | | Lithium | 10 | -0.184 | 0.341 | 0.108 |
| | | | | | | | Silane | 10 | -0.377 | 0.340 | 0.107 |
| | | | | | | | Methacrylate | 10 | -0.020 | 0.460 | 0.145 |
| 36 | Treatment | 3 | 0.956 | 0.319 | 1.831 | 0.1571 | Control | 14 | -0.015 | 0.346 | 0.093 |
| | Residual | 40 | 6.960 | 0.174 | | | Lithium | 10 | -0.185 | 0.388 | 0.123 |
| | | | | | | | Silane | 10 | -0.391 | 0.330 | 0.104 |
| | | | | | | | Methacrylate | 10 | -0.046 | 0.584 | 0.185 |
| 60 | Treatment | 3 | 1.426 | 0.475 | 1.466 | 0.2383 | Control | 14 | -0.035 | 0.299 | 0.080 |
| | Residual | 40 | 12.974 | 0.324 | | | Lithium | 10 | -0.343 | 0.403 | 0.127 |
| | | | | | | | Silane | 10 | -0.504 | 0.601 | 0.190 |
| | | | | | | | Methacrylate | 10 | -0.180 | 0.888 | 0.281 |

Notes: 1. Deflection difference is 1 year minus initial.
2. Does not include outliers in Control Section 3, Slab E.
3. 1 in. = 25.4 mm

Table B.26 Joint differential deflection ANOVA and means table for before and one year after treatment

| Distance from Load, in. | | Degrees of Freedom | Sum of Square | Mean Square | F-value | P-value | Section | Count | Mean 0.001 in. | Standard Deviation 0.001 in. | Standard Error |
|---|---|---|---|---|---|---|---|---|---|---|---|
| 0 | Treatment | 3 | 299.361 | 99.787 | 23.648 | <.0001 | Control | 12 | 2.140 | 2.154 | 0.622 |
| | Residual | 32 | 135.028 | 4.220 | | | Lithium | 8 | 3.071 | 2.487 | 0.879 |
| | | | | | | | Methacrylate | 8 | -3.555 | 1.210 | 0.428 |
| | | | | | | | Silane | 8 | 4.471 | 2.086 | 0.737 |
| 12 | Treatment | 3 | 36.436 | 12.145 | 4.090 | 0.0145 | Control | 12 | -0.757 | 1.496 | 0.432 |
| Unloaded slab | Residual | 32 | 95.021 | 2.969 | | | Lithium | 8 | -1.073 | 2.070 | 0.732 |
| | | | | | | | Methacrylate | 8 | -3.181 | 1.443 | 0.510 |
| | | | | | | | Silane | 8 | -0.576 | 1.921 | 0.679 |
| 12 | Treatment | 3 | 126.077 | 42.026 | 21.710 | <.0001 | Control | 12 | 1.195 | 1.351 | 0.390 |
| Loaded slab | Residual | 32 | 61.944 | 1.936 | | | Lithium | 8 | 1.592 | 2.078 | 0.735 |
| | | | | | | | Methacrylate | 8 | -2.605 | 0.668 | 0.236 |
| | | | | | | | Silane | 8 | 2.620 | 1.103 | 0.390 |
| 18 | Treatment | 3 | 83.916 | 27.972 | 19.427 | <.0001 | Control | 12 | 0.995 | 1.085 | 0.313 |
| | Residual | 32 | 46.076 | 1.440 | | | Lithium | 8 | 1.750 | 1.983 | 0.701 |
| | | | | | | | Methacrylate | 8 | -2.105 | 0.451 | 0.160 |
| | | | | | | | Silane | 8 | 1.880 | 0.773 | 0.273 |
| 24 | Treatment | 3 | 47.535 | 15.845 | 13.947 | <.0001 | Control | 12 | 0.792 | 0.809 | 0.233 |
| | Residual | 32 | 36.355 | 1.136 | | | Lithium | 8 | 1.509 | 1.838 | 0.650 |
| | | | | | | | Methacrylate | 8 | -1.571 | 0.820 | 0.290 |
| | | | | | | | Silane | 8 | 1.212 | 0.338 | 0.120 |
| 36 | Treatment | 3 | 11.133 | 3.711 | 5.979 | 0.0023 | Control | 12 | 0.456 | 0.527 | 0.152 |
| | Residual | 32 | 19.859 | 0.621 | | | Lithium | 8 | 1.004 | 1.525 | 0.539 |
| | | | | | | | Methacrylate | 8 | -0.606 | 0.206 | 0.073 |
| | | | | | | | Silane | 8 | 0.532 | 0.179 | 0.063 |
| 60 | Treatment | 3 | 1.379 | 0.460 | 2.041 | 0.1279 | Control | 12 | 0.113 | 0.351 | 0.101 |
| | Residual | 32 | 7.206 | 0.225 | | | Lithium | 8 | 0.447 | 0.857 | 0.303 |
| | | | | | | | Methacrylate | 8 | 0.059 | 0.126 | 0.045 |
| | | | | | | | Silane | 8 | -0.127 | 0.292 | 0.103 |

Notes: 1. Deflection difference is 1 year minus initial.
2. Does not include outliers in Control Section 3, Slab E.
3. 1 in. = 25.4 mm

could result from outlier data rather than treatment effects. There was no significant difference in the maximum interior and joint deflection standard deviations.

The ANOVA indicated significant statistical joint deflection decreases at one year in the methacrylate sections. No significant differences were observed between the control and lithium treatments. Significant differences were noted between control and silane sections under the load and 12 in. (305 mm) away from the load. For the maximum joint deflection under the load, the average deflection change was an increase of 0.00214 in. (0.054 mm) for the control and a decrease of 0.00356 in. (0.090 mm) for the methacrylate sections.

Since average increases in control section joint deflections were greater than the between-test replicate root mean square listed in Table B.2, the increase in deflections were assumed to be statistically different than the between-test variability expected due to load positioning, load measurement, and deflection measurement. Assuming that average increases measured at one year in the control section would be equally reflected in the methacrylate sections, the average deflection difference at one year due to the methacrylate treatment was 0.00570 in. (0.145 mm) for the maximum joint deflection. The average joint deflection before methacrylate treatment was 0.01365 in. (0.347 mm). Joint deflection decrease after methacrylate averaged 41.8 percent.

### *B.3.3 Effectiveness of Methacrylate After Treatment and at One Year*

As shown in Table B.22, the average interior deflection of the methacrylate section one day after treatment was 0.00457 in. (0.116 mm) and at one year was 0.00488 in. (0.124 mm). Average joint deflection one day after methacrylate treatment was 0.00769 in. (0.195 mm) and at one year was 0.01009 in. (0.256 mm). The ANOVA of differences between before treatment and one year after treatment indicated significant decreases in the methacrylate section joint deflections but insignificant changes in interior deflections. The analysis implied that one year after treatment with methacrylate, interior deflection differences were no different than the control sections with no treatment.

The t-test and ANOVA test were done on the one day after and one year after application data to evaluate the effectiveness of methacrylate with age. One interior deflection outlier in Control Section 3 Slab E was identified and not included in the analysis. The interior deflection t-test indicated insignificant changes in deflections at the 5 percent significance level at all seven deflection positions. This implies that the control section interior deflections did not significantly change. This is similar to the control section t-test analysis showing no consistent difference between deflections before treatment and one year after treatment.

For joint deflections, the paired t-test indicated that deflections increased in all sections except Control Section 3 and Methacrylate Section 2. Insignificant deflection changes in Control Section 3 were also determined before and one day after application and before and one year after treatment. The paired t-test indicates that joint deflection decreases measured at one day were significantly offset by deflection increases at one year in Methacrylate Section 1 but not in Section 2. The paired t-test analysis for joint deflections at one day and one year after methacrylate application is summarized in Table B.27.

To evaluate the significance of interior deflection changes, an ANOVA was conducted on deflection differences one day after and one year after methacrylate application. No

Table B.27 Joint deflection within-treatment paired t-test at one day and one year after methacrylate application

| | distance from load, in. | | | | | | | |
|---|---|---|---|---|---|---|---|---|
| **Section** | **-12** | **0** | **L+U** | **12** | **18** | **24** | **36** | **60** |
| Control 3 | NS | NS | NS | NS | NS | NS | NS | NS |
| Methacrylate 2 | NS | NS | + | NS | NS | NS | NS | NS |
| Control 2 | NS | + | + | NS | NS | NS | + | NS |
| Control 1 | NS | + | + | + | + | + | + | NS |
| Methacrylate 1 | NS | + | + | NS | NS | NS | NS | NS |
| All Control | NS | + | + | + | + | + | NS | NS |
| All Methacrylate | NS | + | + | + | + | NS | NS | NS |

Notes:
1. "L+U" = loaded plus unloaded slab edge deflection
2. "+" = increase in deflection at 1 year
   "-" = decrease in deflection at 1 year
   NS = not significant at the 5 percent level of significance
3. 1 in. = 25.4 mm

significant difference in interior deflection changes between the methacrylate and control sections at the 5 percent level of significance was determined at all deflection positions except at 8 in. (203 mm) from the load. The ANOVA indicates that the change in interior deflection differences between control and methacrylate sections after methacrylate treatment was not significant except 8 in. (203 mm) from the load. This is expected since the paired t-test before (as well as one day) and one year implied that the control section interior deflections did not significantly change. Maximum interior deflections and changes between one day and one year after treatment are summarized in Table B.22. The ANOVA for interior deflections at one day and one year after methacrylate application is summarized in Table B.28.

To evaluate the significance of joint deflection increases within Methacrylate Section 1 an ANOVA was conducted on deflection differences one day after and one year after methacrylate application. No significant difference in joint deflection changes between the methacrylate and control sections at the 5 percent level of significance was determined at all deflections. The ANOVA indicates that the change in joint deflection differences between control and methacrylate sections after methacrylate treatment was not significant. This suggests that the rate of further deterioration resulting in methacrylate application continues at the same rate as the control sections. Any benefits of methacrylate application are after initial application when deflection magnitudes are reduced. Maximum joint deflections and changes between one day and one year after treatment are summarized in Table B.22. The ANOVA for joint deflections at one day and one year after methacrylate application is summarized in Table B.29.

## B.4 Core Test Data

Deflection testing one year (in 1991) earlier indicated a wide range in deflections which categorically corresponded to severity of surface distress. Higher maximum deflections were noted in areas with more severe ASR surface cracking. To establish that deflection changes could be used as a tool to monitor ASR deterioration progression, material data from cores were used to calibrate structural deflection response. Two cores from Slab A in each test section were drilled during the October 1992 follow-up test program. Cores were taken near slab midlength 18 in. (457 mm) from the longitudinal slab-shoulder joint. Cracking throughout the cores was observed just after coring.

Based on visual inspection of surface cracking within the 82-slab test section, the control, lithium, silane, and methacrylate treatments were randomly assigned as shown in Figure B.1. One set of treatments at the west end of the test area was located in a less severely distressed (surface) area than the second set of treatments at the east end of the test area. Elastic modulus and compressive strength of the concrete were determined for each of the two cores from each test section. As shown in Table B.30, elastic modulus of the sections at the west end of the test section was significantly higher than those at the east end. Modulus of elasticity was variable, ranging from 1.44 to 3.93 million psi (9.9 to 27.1 GPa) and averaged 2.87 million psi (19.8 GPa). Compressive strength was slightly higher at the west end than those at the east end. Compressive strength ranged from 4520 to 6480 psi (31.2 to 44.7 MPa) and averaged 5580 psi (38.5 MPa).

Compared to non-deteriorated concrete, the compressive strength was relatively higher given the relatively low modulus of elasticity. This indicates that concrete deformations with load are relatively higher but strength is not affected to the same degree when cracking due to

Table B.28 Interior differential deflection ANOVA and means table for one day and one year after treatment

| Distance from Load, in. | | Degrees of Freedom | Sum of Square | Mean Square | F-value | P-value | Section | Count | Mean 0.001 in. | Standard Deviation 0.001 in. | Standard Error |
|---|---|---|---|---|---|---|---|---|---|---|---|
| 0 | Section | 1 | 1.143 | 1.143 | 3.522 | 0.0739 | Control | 14 | -0.131 | 0.607 | 0.162 |
| | Residual | 22 | 7.141 | 0.325 | | | Methacrylate | 10 | 0.312 | 0.511 | 0.162 |
| 8 | Section | 1 | 1.589 | 1.589 | 4.514 | 0.0451 | Control | 14 | -0.210 | 0.672 | 0.180 |
| | Residual | 22 | 7.747 | 0.352 | | | Methacrylate | 10 | 0.312 | 0.456 | 0.144 |
| 12 | Section | 1 | 1.270 | 1.270 | 4.209 | 0.0523 | Control | 14 | -0.204 | 0.621 | 0.166 |
| | Residual | 22 | 6.637 | 0.302 | | | Methacrylate | 10 | 0.263 | 0.424 | 0.134 |
| 18 | Section | 1 | 1.020 | 1.020 | 3.798 | 0.0642 | Control | 14 | -0.212 | 0.572 | 0.153 |
| | Residual | 22 | 5.908 | 0.269 | | | Methacrylate | 10 | 0.206 | 0.429 | 0.136 |
| 24 | Section | 1 | 0.735 | 0.735 | 3.502 | 0.0747 | Control | 14 | -0.158 | 0.490 | 0.131 |
| | Residual | 22 | 4.615 | 0.210 | | | Methacrylate | 10 | 0.197 | 0.408 | 0.129 |
| 36 | Section | 1 | 0.292 | 0.292 | 1.790 | 0.1945 | Control | 14 | -0.139 | 0.371 | 0.099 |
| | Residual | 22 | 3.583 | 0.163 | | | Methacrylate | 10 | 0.085 | 0.446 | 0.141 |
| 60 | Section | 1 | 0.00006298 | 0.00006298 | 0.00023 | 0.9881 | Control | 14 | -0.124 | 0.321 | 0.086 |
| | Residual | 22 | 6.127 | 0.278 | | | Methacrylate | 10 | -0.121 | 0.730 | 0.231 |

Notes: 1. Deflection difference is 1 year minus 1 day.
2. Does not include outliers in Control Section 3, Slab E.
3. 1 in. = 25.4 mm

Table B.29 Joint differential deflection ANOVA and means table for one day and one year after treatment

| Distance from Load, in. | | Degrees of Freedom | Sum of Square | Mean Square | F-value | P-value | Section | Count | Mean 0.001 in. | Standard Deviation 0.001 in. | Standard Error |
|---|---|---|---|---|---|---|---|---|---|---|---|
| 0 | Treatment | 1 | 0.436 | 0.436 | 0.142 | 0.7105 | Control | 12 | 2.102 | 1.921 | 0.555 |
| | Residual | 18 | 55.148 | 3.064 | | | Methacrylate | 8 | 2.404 | 1.441 | 0.510 |
| 12 | Treatment | 1 | 2.936 | 2.936 | 3.791 | 0.0673 | Control | 12 | 0.393 | 0.908 | 0.262 |
| Unloaded | Residual | 18 | 13.939 | 0.774 | | | Methacrylate | 8 | -0.389 | 0.834 | 0.295 |
| 12 | Treatment | 1 | 0.021 | 0.021 | 0.014 | 0.9075 | Control | 12 | 1.108 | 1.423 | 0.411 |
| | Residual | 18 | 27.680 | 1.538 | | | Methacrylate | 8 | 1.175 | 0.879 | 0.311 |
| 18 | Treatment | 1 | 0.067 | 0.067 | 0.064 | 0.8029 | Control | 12 | 0.892 | 1.182 | 0.341 |
| | Residual | 18 | 18.726 | 1.040 | | | Methacrylate | 8 | 0.774 | 0.692 | 0.245 |
| 24 | Treatment | 1 | 0.843 | 0.843 | 0.989 | 0.3333 | Control | 12 | 0.647 | 0.952 | 0.275 |
| | Residual | 18 | 15.356 | 0.853 | | | Methacrylate | 8 | 0.227 | 0.876 | 0.310 |
| 36 | Treatment | 1 | 0.300 | 0.300 | 0.799 | 0.3831 | Control | 12 | 0.368 | 0.739 | 0.213 |
| | Residual | 18 | 6.755 | 0.375 | | | Methacrylate | 8 | 0.118 | 0.328 | 0.116 |
| 60 | Treatment | 1 | 0.146 | 0.146 | 1.861 | 0.1893 | Control | 12 | 0.078 | 0.317 | 0.091 |
| | Residual | 18 | 1.415 | 0.079 | | | Methacrylate | 8 | -0.096 | 0.211 | 0.075 |

Notes: 1. Deflection difference is 1 year minus 1 day.
2. 1 in. = 25.4 mm

Table B.30 Core data from October 1992 Nevada follow-up testing

| Section | Length Before Trimming, in. | Average Thickness in. | f'c, psi | Average f'c psi | Modulus of Elasticity, psi | | | |
|---|---|---|---|---|---|---|---|---|
| | | | | | Regression | Average E regression | 40% f'c | Average E 40% f'c |
| C3-1 | 8.5 | | 6,480 | | 3,580,000 | | NA | |
| C3-2 | 8.75 | 8.625 | 5,940 | 6,210 | 3,500,000 | 3,540,000 | 3,390,000 | 3,390,000 |
| L2-1 | 8.5 | | 6,170 | | 3,930,000 | | NA | |
| L2-2 | 8.5 | 8.5 | 5,990 | 6,080 | 3,550,000 | 3,740,000 | 3,470,000 | 3,470,000 |
| S2-1 | 8.25 | | 6,010 | | 3,770,000 | | NA | |
| S2-2 | 8.5 | 8.375 | 5,890 | 5,950 | 3,470,000 | 3,620,000 | NA | NA |
| M2-1 | 8.25 | | 5,370 | | 3,350,000 | | 3,280,000 | |
| M2-2 | 8.25 | 8.25 | 5,420 | 5,395 | 2,700,000 | 3,025,000 | 2,320,000 | 2,800,000 |
| SA-1 | 8.5 | | 5,830 | | 3,860,000 | | 3,800,000 | |
| SA-2 | 8.5 | 8.5 | 5,930 | 5,880 | 3,010,000 | 3,435,000 | 2,830,000 | 3,315,000 |
| LO1-1 | 8.25 | | 5,180 | | 3,000,000 | | NA | |
| LO1-2 | 8.5 | 8.375 | 4,920 | 5,050 | 2,100,000 | 2,550,000 | 1,900,000 | 1,900,000 |
| C2-1 | 9 | | 4,520 | | 1,740,000 | | 1,430,000 | |
| C2-2 | 8.75 | 8.875 | 4,730 | 4,625 | 1,440,000 | 1,590,000 | 1,120,000 | 1,275,000 |
| S1-1 | 9 | | 5,670 | | 2,380,000 | | 2,190,000 | |
| S1-2 | 8.75 | 8.875 | 6,360 | 6,015 | 2,580,000 | 2,480,000 | NA | 2,190,000 |
| L1-2 | 8.5 | | 5,270 | | 3,150,000 | | 2,970,000 | |
| L1-2 | 8.5 | 8.5 | 5,770 | 5,520 | 3,100,000 | 3,125,000 | 2,870,000 | 2,920,000 |
| C1-1 | 8.75 | | 5,770 | | 2,810,000 | | 2,660,000 | |
| C1-2 | 8.5 | 8.625 | 5,830 | 5,800 | 2,950,000 | 2,880,000 | 2,800,000 | 2,730,000 |
| M1-1 | 8.25 | | 4,800 | | 1,460,000 | | NA | |
| M1-2 | 8.25 | 8.25 | 4,940 | 4,870 | 1,760,000 | 1,610,000 | 1,300,000 | 1,300,000 |
| **Minimum** | 8.25 | | 4,520 | | 1,440,000 | 1,590,000 | | |
| **Maximum** | 9 | | 6,480 | | 3,930,000 | 3,740,000 | | |
| **Average** | 8.5 | | 5,580 | | 2,870,000 | 2,870,000 | | |

Notes: 1. 1 in. = 25.4 mm
2. 1,000,000 psi = 6,895 MPa

ASR is present. A relationship between modulus of elasticity and compressive strength (square root) was developed to investigate correlation between strength and modulus. The relationship between modulus of elasticity and compressive strength is relatively poor as shown in Figure B.9 by the scatter of data. Different from non-deteriorated concrete, the constant term in the prediction of elastic modulus equation is significant.

## B.5 Comparison of Measured to Theoretical Deflections

The finite element computer program ILLI-SLAB was used to compute theoretical deflections using core data material properties (Tabatabai, et al 1979). Modulus of elasticity and thickness core data listed in Table B.30 were input into the program. Cores from Slab A within each treatment section at midslab 18 in. from the shoulder joint were drilled during the October 1992 follow-up testing. Moduli of subgrade reaction, *k*, were back-calculated by matching Slab A maximum deflections measured during the follow-up tests. The load was positioned at the interior of a slab 15 ft long by 12 ft wide (4.6 x 3.7 m). Cement-treated base moduli of subgrade reaction for the 11 test sections ranged from 350 to 1000 lb/in$^3$ (95 to 271 MPa/m). This is within the range of subbase support values of 500 to 700 lb/in$^3$ (136 to 190 MPa/m) commonly assumed for cement-treated bases. The high subgrade support value was calculated for Methacrylate Section 1. Cores retrieved in this section were severely deteriorated at the bottom. To match the relatively higher deflections, a higher subbase support value was required to compensate for reduced effective slab thickness. Excluding the modulus of subgrade reaction in Methacrylate Section 1, the average back-calculated k-value was 490 lb/in$^3$ (133 MPa/m).

Plots of calculated versus measured deflections under the load and at 8, 12, 18, and 24 in. (203, 305, 457, and 610 mm) from the load are shown in Figure B.10. Typical measured and calculated deflection basins are shown for Control Sections 1 and 3 in Figure B.11. Modulus of elasticity for Control Sections 3 and 1 were 3.54 million and 2.88 million psi (24,400 and 19,850 MPa), respectively. The figure illustrates that significant deflections are measured with a change in elastic modulus. The 19 percent decrease in modulus of elasticity corresponds to a 25 percent increase in maximum deflection. This indicates that the FWD can be used as a tool to nondestructively measure deflections and evaluate decreases in elastic modulus with time and ASR progression.

Deflections were matched by inputting core moduli and thicknesses of each slab. Since slab support and thickness will vary from slab to slab, deflections were computed using an average subgrade support (excluding high value in Methacrylate Section 1) of 500 lb/in$^3$ (136 MPa/m) and thickness of 8.5 in. (216 mm). As expected the computed deflections using an average subbase support and thickness did not match well with measured deflections. Data was very scattered around the line of equality. The analysis did indicate that the FWD can be used to monitor relative decreases of concrete modulus of elasticity with ASR progression. Using the average subbase support and thickness for the Nevada test site, deflections as a function of modulus of elasticity and distance from load were calculated. As shown in Figure B.12, significant decreases in modulus of elasticity correspond to significant deflection increases. Using Figure B.12, the relative decrease in elastic modulus with ASR progression can be monitored.

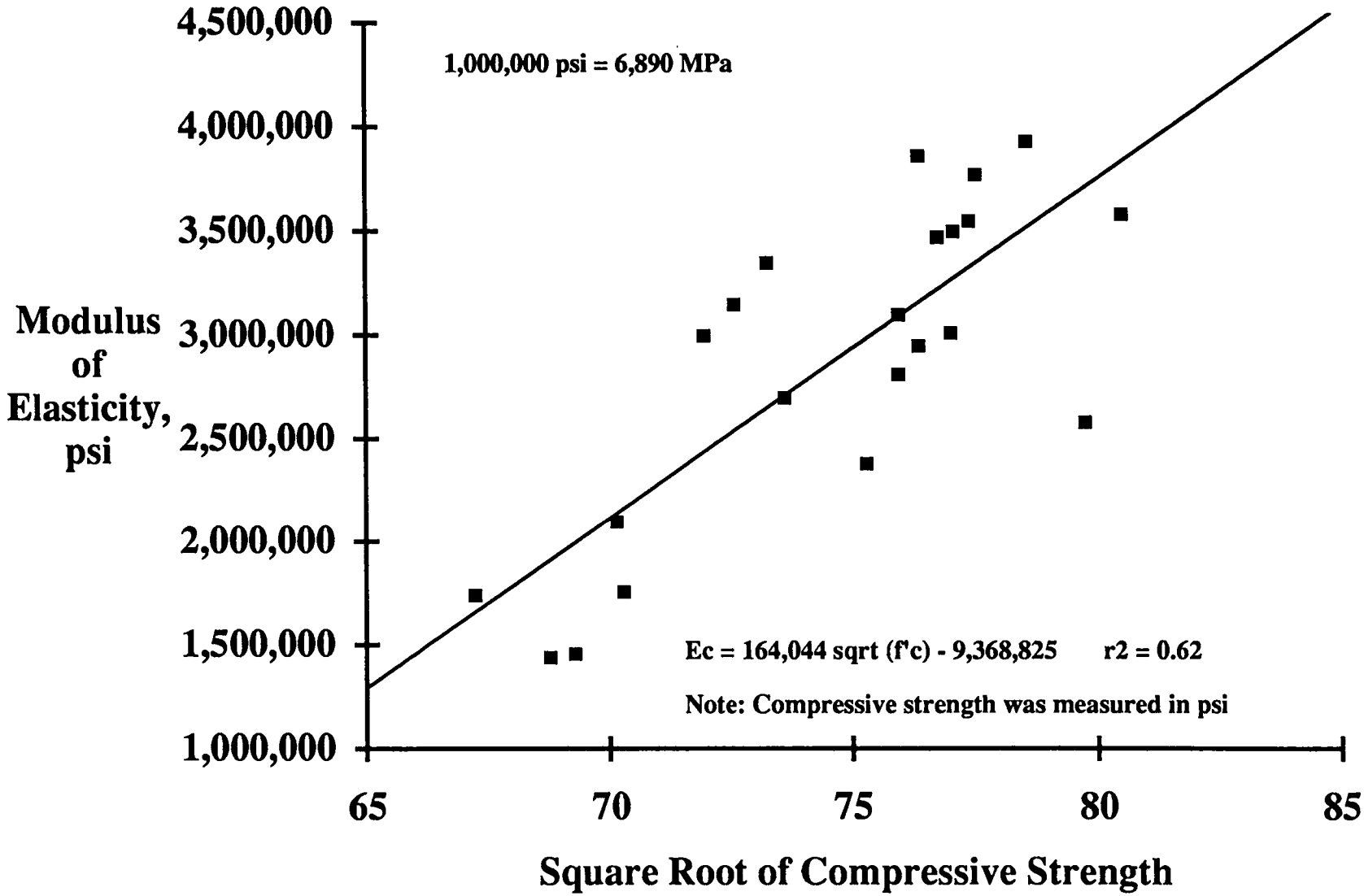


Figure B.9. Core modulus of elasticity versus the square root of the compressive strength.

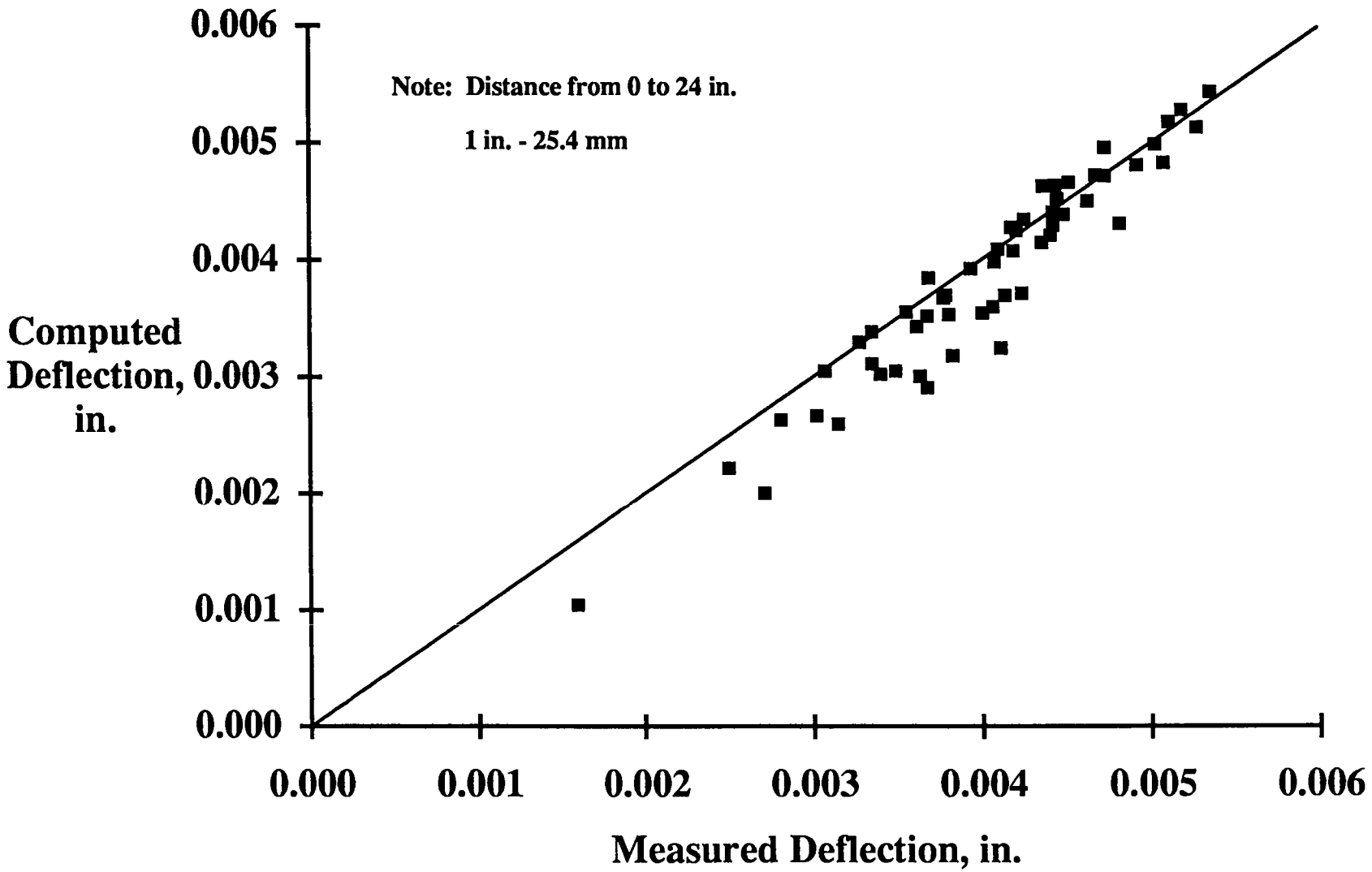


Figure B.10. Comparison of measured and computed deflections using exact $t$ and $k$.

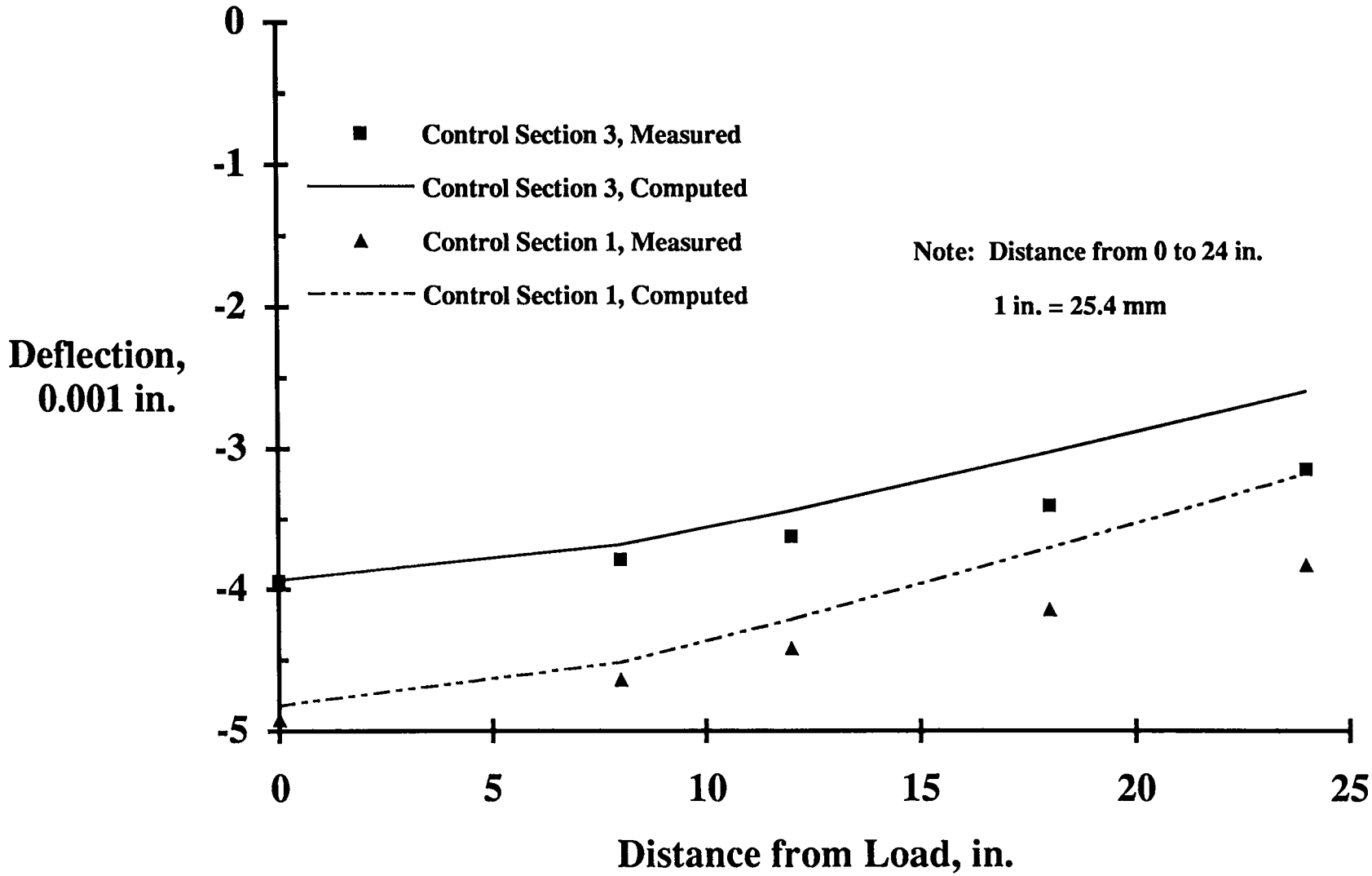


Figure B.11. Measured and computed deflections for slab A in Control Sections 1 and 3.

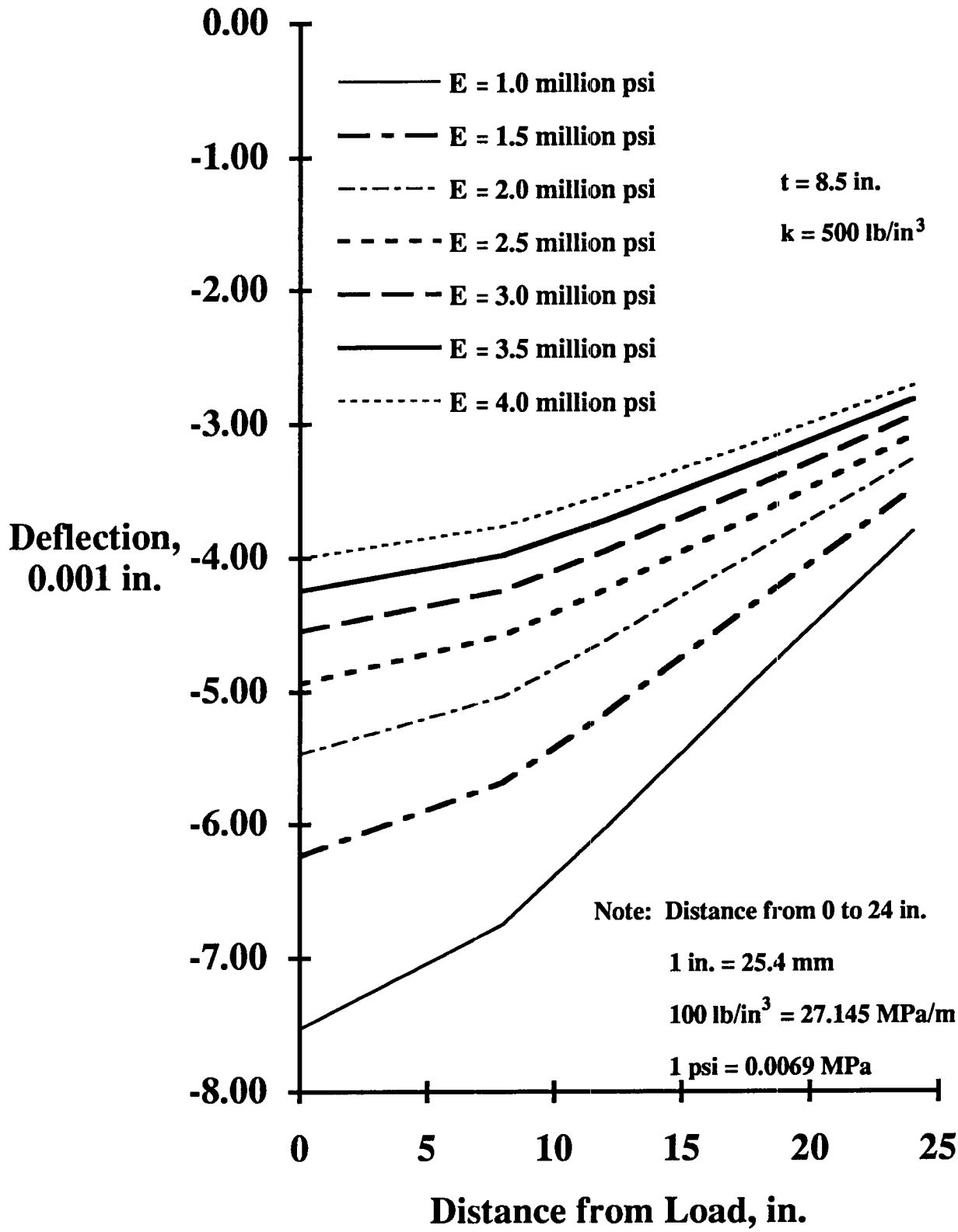


Figure B.12. Computed deflections with distance from load.

## B.6 Conclusions

A deflection monitoring program was initiated in 1991 to evaluate the effectiveness of surface applied treatments in reducing ASR damage on pavement structural response. The FWD was used to nondestructively monitor deflection changes at slab interior and joints. Slabs were treated with lithium hydroxide monohydrate, high molecular weight methacrylate resin, and poly-siloxane resin. In addition to the treated slabs, several control section slabs were tested to compare treatment effectiveness. Baseline testing before treatment, one day after treatment, and approximately one year after treatment was done.

Tests at one day after treatment indicated that both interior and joint deflections decreased in the methacrylate treated sections. Tests indicated that no significant increases in deflections at the slab interior occurred before treatment and at one year. Tests also indicated that at one year, joint deflections were still significantly lower in the methacrylate treated sections. No significant effects of silane and lithium treatments were noted at one year for interior or joint deflections. Test data at one day and one year after treatment did indicate that the deflection differences in methacrylate treated sections with time were statistically equal to control section changes. This suggests that the rate of further deterioration resulting in methacrylate application continues at the same rate as the control sections. Any benefits of methacrylate application are after initial application when deflection magnitudes are reduced.

To evaluate treatment effects, additional testing is highly recommended. Comparison of measured deflections with observed surface distress, core modulus of elasticity, and with calculated deflections indicate that the FWD testing can be used to evaluate relative decreases in concrete modulus of elasticity as ASR deterioration progresses. Long-term monitoring is necessary to evaluate treatment effects. The treatments can not be thoroughly evaluated during a one-year monitoring program. Differences in treatment effects will be more apparent as control section deflections increase with time and ASR progression.

# Appendix C Three-Dimensional and One-Dimensional Restraint Testing

Three-dimensional and one-dimensional testing programs were conducted to investigate relationships between restraint and ASR development. The three-dimensional program consisted of hydrostatic pressure testing of concrete cylinders. Miniature pavement sections were uniaxially restrained in the one-dimensional program. These programs are summarized and conclusions presented in Section 5.6 of this report. The purpose of this appendix is to document details of the testing programs.

## C.1 Three-Dimensional Pressure Testing

Eleven concrete cylinders were cast for the three-dimensional pressure testing program. Seven cylinders (6 for test and 1 spare) were made with highly reactive aggregate AL from New Mexico. Four cylinders (3 for test and 1 spare) were made with an innocuous dolomite aggregate TH to act as controls.

Cylinders were 4 3/4 in. (120 mm) in diameter and 24 in. (610 mm) long. The concrete portion of each cylinder was 22 1/2 in. (570 mm) long with an epoxy cap 3/4 in. (19 mm) long at each end. Cylinders were made by first casting a plug 3/4 in. (19 mm) long in the bottom of a waxed, cardboard tube. When the epoxy had hardened, concrete was cast in the tube, directly on the epoxy plug. The final step in making a specimen was to cast a second 3/4-in. (19 mm) long epoxy plug directly on the hardened concrete in the tube. The epoxy end caps, therefore, were integral with the concrete portion of the cylinder which facilitated sealing. In addition to these cylinders, companion 4 x 8 in. (100 x 200 mm) cylinders were made for strength tests and 3 x 3 x 11 1/4 in. (76 x 76 x 286 mm) prisms were made for length change measurements. Casting of specimens required four concrete batches, two for reactive and two for control specimens. All specimens were cured for 21 days in 1N NaOH solution saturated with $Ca(OH)_2$.

### *C.1.1 Mix Design*

A concrete mix containing 562 lb/yd$^3$ (333 kg/m$^3$) of cement, 1275 lb/yd$^3$ (756 kg/m$^3$) saturated surface dry (SSD) of fine aggregate, 1913 lb/yd$^3$ (1134 kg/m$^3$) SSD of coarse aggregate, and 270 net lb/yd$^3$ (160 kg/m$^3$) of water was used for specimens made with reactive aggregate AL. Cement contained 1.1 percent equivalent $Na_2O$, and both fine and coarse aggregate were natural sand and gravel. Coarse aggregate grading was 420 lb/yd$^3$ (249 kg/m$^3$) of No. 4 to 3/8 in. (4.75 to 9.5 mm), 1149 lb/yd$^3$ (681 kg/m$^3$) of 3/8 in. to 3/4 in. (9.5 to 19 mm), and 344 lb/yd$^3$ (204 kg/m$^3$) of 3/4 in. to 1 in. (19 to 25 mm).

The concrete mix used for control specimens contained the same proportions of cement, coarse aggregate and water as given above for reactive aggregate specimens. Fine aggregate proportion, however, was increased slightly to 1367 lb/yd$^3$ (811 kg/m$^3$) to aid workability since the coarse aggregate used was a crushed dolomite rather than a natural gravel. Fine aggregate used was a natural sand from Elgin, Illinois and is innocuous.

Actual unit weights of reactive and control mixes were 148 lb/ft$^3$ (3.25 kg/m$^3$) and 151 lb/ft$^3$ (3.32 kg/m$^3$), respectively. Both mixes had slumps of 1 to 2 in. (25 to 50 mm) and air contents of 2 to 3 percent. No air-entraining admixture was used.

### *C.1.2 Test Procedure*

After curing, the 24-in. (610 mm) concrete cylinders were placed in steel cylinders and pressurized with water to various test pressures. Prior to pressurization, concrete cylinders were sealed to prevent water migration into the concrete so that any pressure change could be attributed to a true volume change in the concrete cylinder. The final sealing scheme, which evolved from evaluation of several approaches, involved a four-step process. First, the surface of the concrete was wiped with a free flowing cement and sand mortar to fill local surface voids and imperfections. Next, cylinders were painted with two coats of heavy duty epoxy paint. Heat shrink plastic tubing was then slipped over the cylinders and heat shrunk tight in place. The heat shrink tubing extended approximately 1 in. (25 mm) beyond the epoxy plugs on each end of the cylinder so that it folded over the ends of the plugs when shrunk in place. Finally, edges of the shrunk tubing where they folded over epoxy end plugs were sealed with hot wax to the surface of the end plugs. All test specimens were cast June 14, 1989.

The steel cylinders were slightly longer than the test cylinders and had an inside diameter of 5 in. (127 mm). Each steel cylinder was equipped with a pressure gage, a quick-disconnect water fitting on the input port through which water could be pumped to increase internal pressure, and a needle valve on the output port through which water could be bled to decrease internal pressure. A graduated tubular metering glass was also fitted to the output port so that volume of water being bled from the cylinder could be measured. After loading and sealing, the steel cylinders were pressurized with water and bled through several cycles to remove entrapped air. A total of nine cylinders was used, six containing reactive aggregate concrete specimens and three containing control specimens. The nine steel cylinders were then stored at 100°F (37.8°C) on July 13 (at test specimen age of 29 days). In addition, on July 13 companion prisms were stored in sealed containers over water at 100°F (37.8°C).

Compressive strength of three reactive and control cylinders 4 x 8 in. (100 x 200 mm) was also determined at 29 days. Strengths of 5200, 5200 and 5380 psi (35.9, 35.9 and 37.1 MPa), with an average of 5260 psi (36.3 MPa), were obtained for control cylinders. Lower strengths were measured for reactive cylinders, 4130, 4880 and 4900 psi (28.5, 33.7 and 33.8 MPa), with an average of 4640 psi (32.0 MPa).

Over the next 26 days, the basic response and behavior of the pressure cylinder systems were determined and test cylinder sealing was evaluated. Modifications were made as appropriate and three steel cylinders pressurized to a test pressure value on August 7 (at test specimen age of 54 days). Two weeks later after some additional system adjustments, the remaining six steel cylinders were brought to test pressure (at test specimen age of 68 days). Initial test

pressure for each of the nine cylinders is given in Table C.1. As shown in Table C.1, one reactive and one control cylinder were pressurized to 60 psi (0.41 MPa), two reactive and one control cylinder were pressurized to 140 and 240 psi (0.97 and 1.66 MPa), and one reactive cylinder pressurized to 205 psi (1.41 MPa).

### *C.1.3 Test Results*

Figure C.1 shows expansions calculated from comparator readings for prism specimens. Each of the curves of Figure C.1 represent average data for a set of three prisms cast from one of the four concrete batches used for specimen preparation. As indicated by Figure C.1, reactive aggregate prisms expanded substantially, increasing rapidly from the time they were stored at 100°F (37.8°C). Control prisms cast with innocuous aggregate were essentially nonexpansive. As noted on Figure C.1, the pressure cylinder experiment was carried out during the time of steady increase in free expansion of reactive aggregate prisms.

As shown in Table C.1, Cylinders 1, 3 and 5 were pressurized to 240 psi (1.66 MPa) on August 21, 1989. The subsequent pressure-time history for these cylinders is given in Figure C.2. During the monitoring time, pressure in Cylinders 1 and 5 containing reactive aggregate specimens increased rapidly from 240 psi (1.66 MPa) to a range of 260 to 300 psi (1.79 to 2.07 MPa). Pressure fluctuated within this range for the duration of monitoring. Pressure in Cylinder 3 containing an innocuous aggregate specimen dropped steadily from its initial 240 psi (1.66 MPa) pressure as a net volume reduction due to creep deformation progressed in the concrete. As shown in Figure C.2, it was necessary to repressurize Cylinder 3 five times during the monitoring period as volume reduction progressed in the cylinder.

Cylinders 2, 6 and 7 were pressurized to 140 psi (0.97 MPa) on August 21, 1989 (see Table C.1). Subsequent pressure-time history for these cylinders is given in Figure C.3. The pressure scale of Figure C.3 is the same as Figure C.2 for ready comparison. Pressure in Cylinders 2 and 7 containing reactive aggregate specimens initially increased steadily from 140 psi (0.97 MPa) while pressure in Cylinder 6 containing an innocuous aggregate specimen dropped steadily as volume reduction due to creep deformation progressed in the concrete, requiring several repressurizations. At age 98 days, it was decided to increase pressure significantly in one reactive cylinder and the control cylinder to bracket what appeared to be the pressure range where ASR expansion and volume reduction due to concrete creep were in approximate balance. Therefore, pressure in Cylinders 2 and 6 were increased to 360 psi (2.48 MPa) while Cylinder 7 was returned to 140 psi (0.97 MPa) initial pressure level. As shown in Figure C.3, pressure in Cylinder 2 containing reactive aggregate dropped to a level of about 220 psi where ASR expansion and concrete creep appeared to move into approximate balance. Control Cylinder 6 continued to drop in pressure for the remainder of monitoring. Cylinder 7 increased rapidly in pressure to 190 psi (1.31 MPa) and was again returned to 140 psi (0.97 MPa). It again increased in pressure, steadily reaching a steady pressure level of approximately 190 psi (1.31 MPa) at the end of monitoring Figure C.4 shows the pressure-time history for Cylinder 8 containing a reactive aggregate specimen and Cylinder 9 containing an innocuous aggregate specimen. As illustrated in Figure C.4, it was necessary to repeatedly and often reduce pressure in the reactive aggregate cylinder to maintain a pressure level in the range of 60 to 100 psi (0.41 to 0.69 MPa). Conversely it was necessary to increase pressure regularly to maintain pressure in the innocuous aggregate cylinder.

Table C.1 Initial test pressure for each of the cylinders

| Cylinder | Test Specimen Aggregate | Date Pressurized | Test Pressure psi |
|---|---|---|---|
| 1 | Reactive | 8/21 | 240 |
| 2 | Reactive | 8/21 | 140 |
| 3 | Control | 8/21 | 240 |
| 4 | Reactive | 8/7 | 205 |
| 5 | Reactive | 8/21 | 240 |
| 6 | Control | 8/21 | 140 |
| 7 | Reactive | 8/21 | 140 |
| 8 | Reactive | 8/7 | 60 |
| 9 | Control | 8/7 | 60 |

Note: 1 psi = 0.0069 MPa

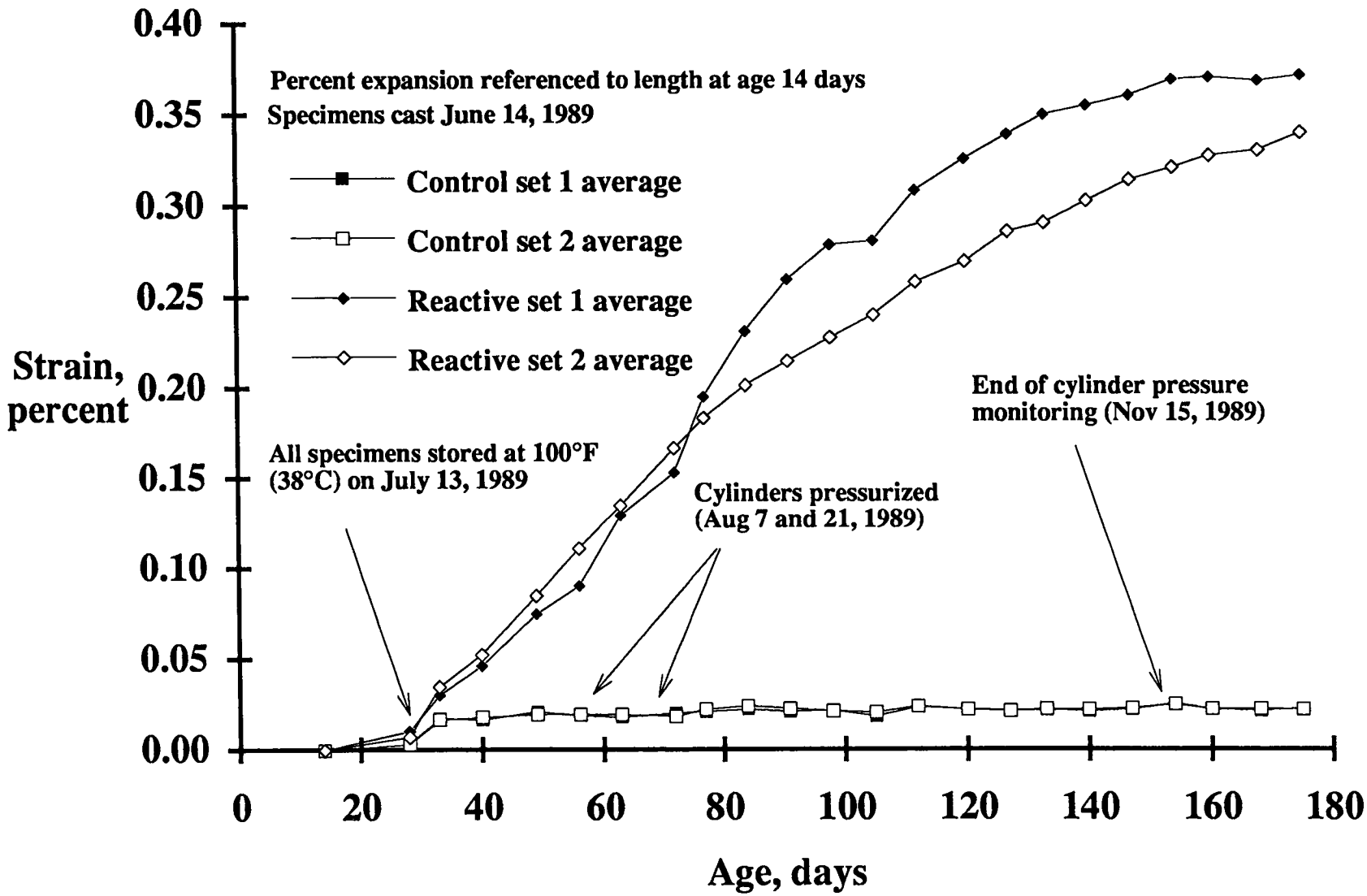


Figure C.1. Prism strain versus time; three dimensional pressure test.

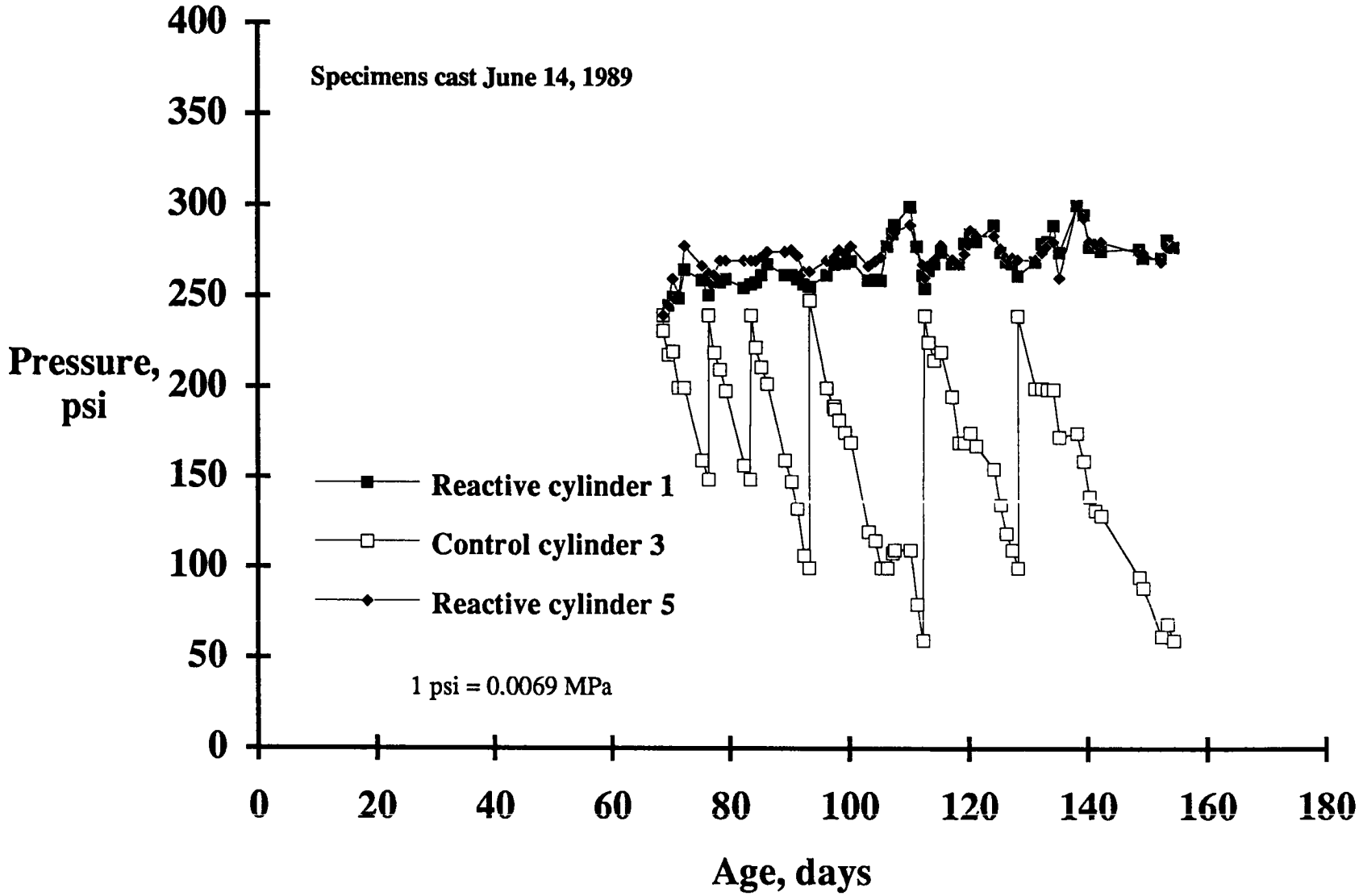


Figure C.2. Pressure versus time for cylinders 1, 3, and 5.

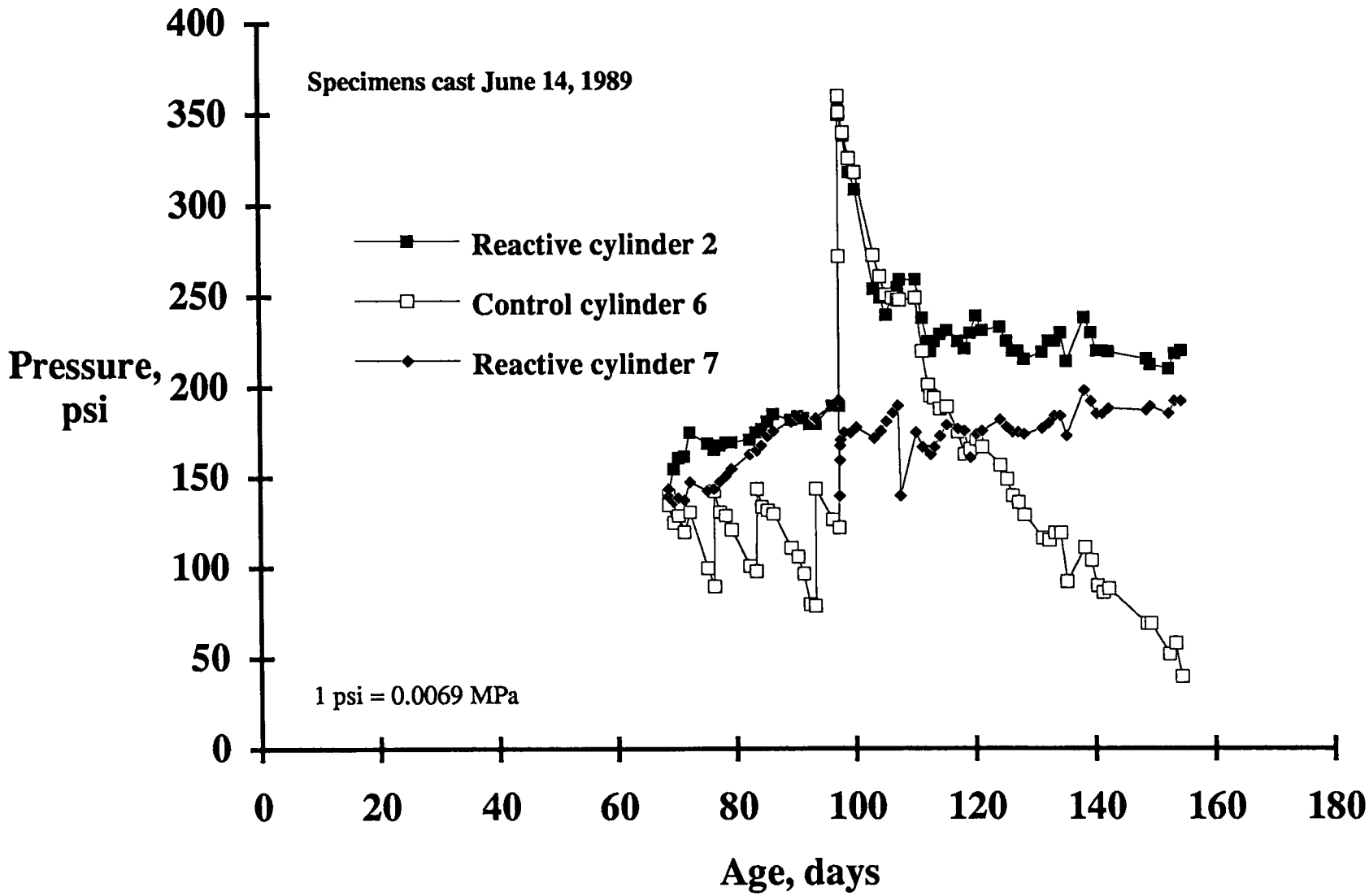


Figure C.3. Pressure versus time for cylinders 2, 6, and 7.

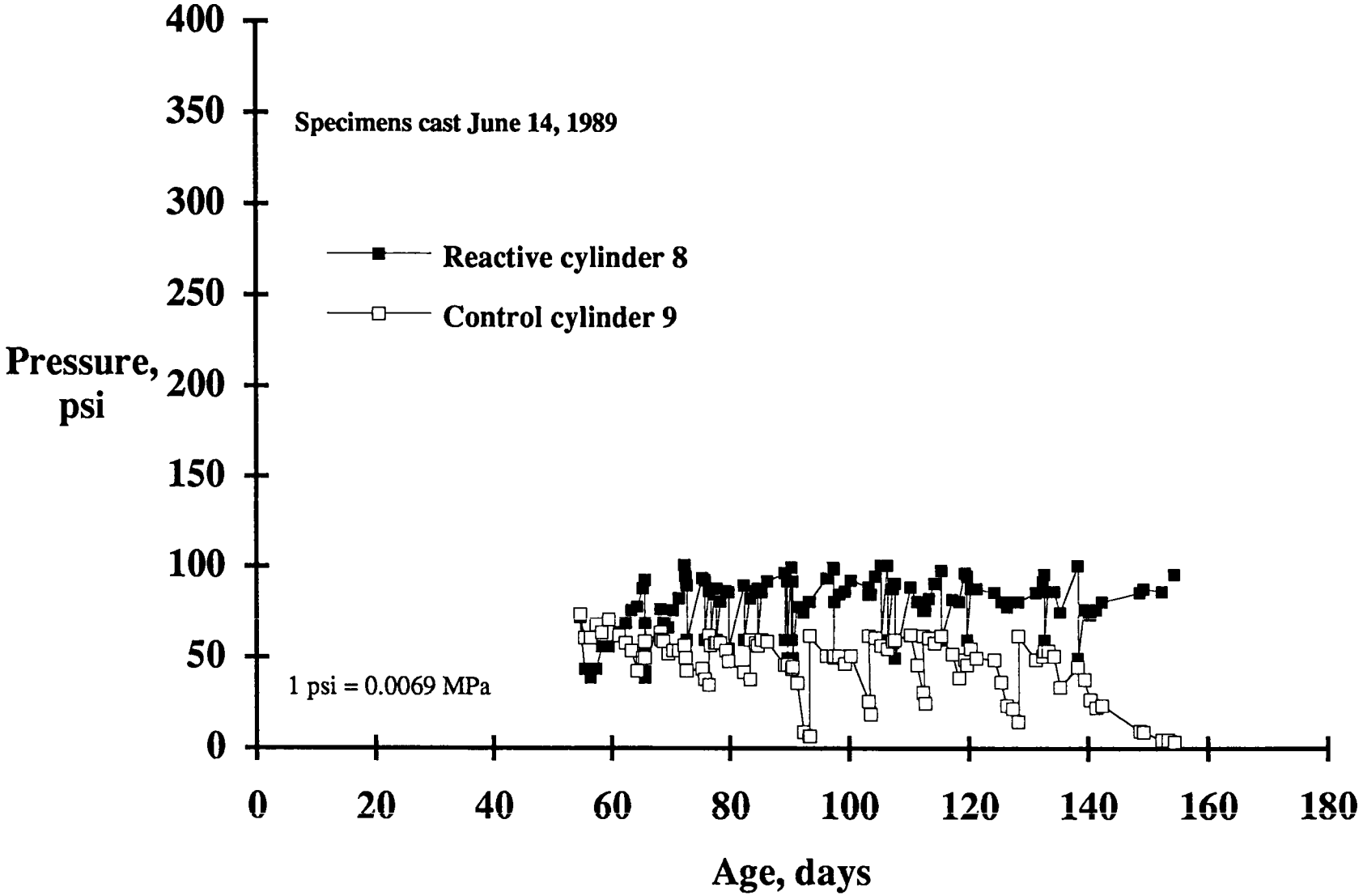


Figure C.4. Pressure versus time for cylinders 8 and 9.

Shown in Figure C.5 is the pressure-time history for Cylinder 4 containing a reactive aggregate specimen. Pressure in this cylinder was initially set at 205 psi (1.41 MPa) and allowed to seek a stabilized pressure level. The pressure in Cylinder 4 increased steadily to approximately 250 psi (1.73 MPa) and held at this level.

### *C.1.4 Conclusions*

Conclusions are presented in Section 5.6.1.1 of this report.

## C.2 One-Dimensional Restraint Testing

The test setup for miniature pavement sections used in the one-dimensional restraint testing program is shown in Figure C.6. The four specimens subjected to restraint were placed end-to-end in a loading frame. Hydraulic rams at one end of the frame were used to tension rods extending down both sides of the test sections and terminating in a sliding frame arrangement incorporating high capacity springs and load cells. The springs maintained constant stress in test sections as length changes took place. The load cells were used to monitor the test section stress level.

Each section was instrumented as shown in Figure C.7. Because of the vertical moisture gradient, and therefore anticipated vertical strain gradient, longitudinal and transverse deformations were measured at three vertical levels, bottom, middle and top. Deformations were also measured in the vertical direction, completing a three-dimensional pattern of deformation monitoring for each test section. Sixteen direct current input, direct current output, linear variable differential transformers (DC DC LVDT) were mounted on each test section.

As illustrated in Figure C.7, Invar rods connected cores of transformers to fixed points on the sections. Deformation was calculated as displacement sensed by the DC DC LVDT divided by the gage length measured from neutral position of the DC DC LVDT to the fixed point termination of the Invar rods. Invar is a material with an essentially zero coefficient of thermal expansion and hence was an ideal material choice for an absolute displacement measurement system to be used in an elevated temperature environment. Since the test was to take place at elevated temperatures for a test period of months, a DC DC LVDT was mounted in the test room independent of test specimens to track stability of the data acquisition system. Also, a DC DC LVDT measurement system was mounted on a 1 in. (25 mm) diameter Invar bar to act as a standard for the experiment.

The resultant total of 98 DC voltage outputs from all DC DC LVDTs were monitored remotely by a digital data acquisition system and stored on computer hard disk for analysis. Room temperature and humidity were monitored by sensors read visually on a regular basis throughout the test.

The miniature pavement sections were initially cast directly on absorptive felt 1 in. (25 mm) thick which extended 4 in. (100 mm) to either side of the test sections. Lengths of standard garden soaker hose were placed on the felt. The felt was kept moist by periodic, timer-controlled waterings through the lengths of soaker hose. The set of pavement sections was cast June 27, 1990. As the test progressed, it became apparent, confirmed by analysis of felt

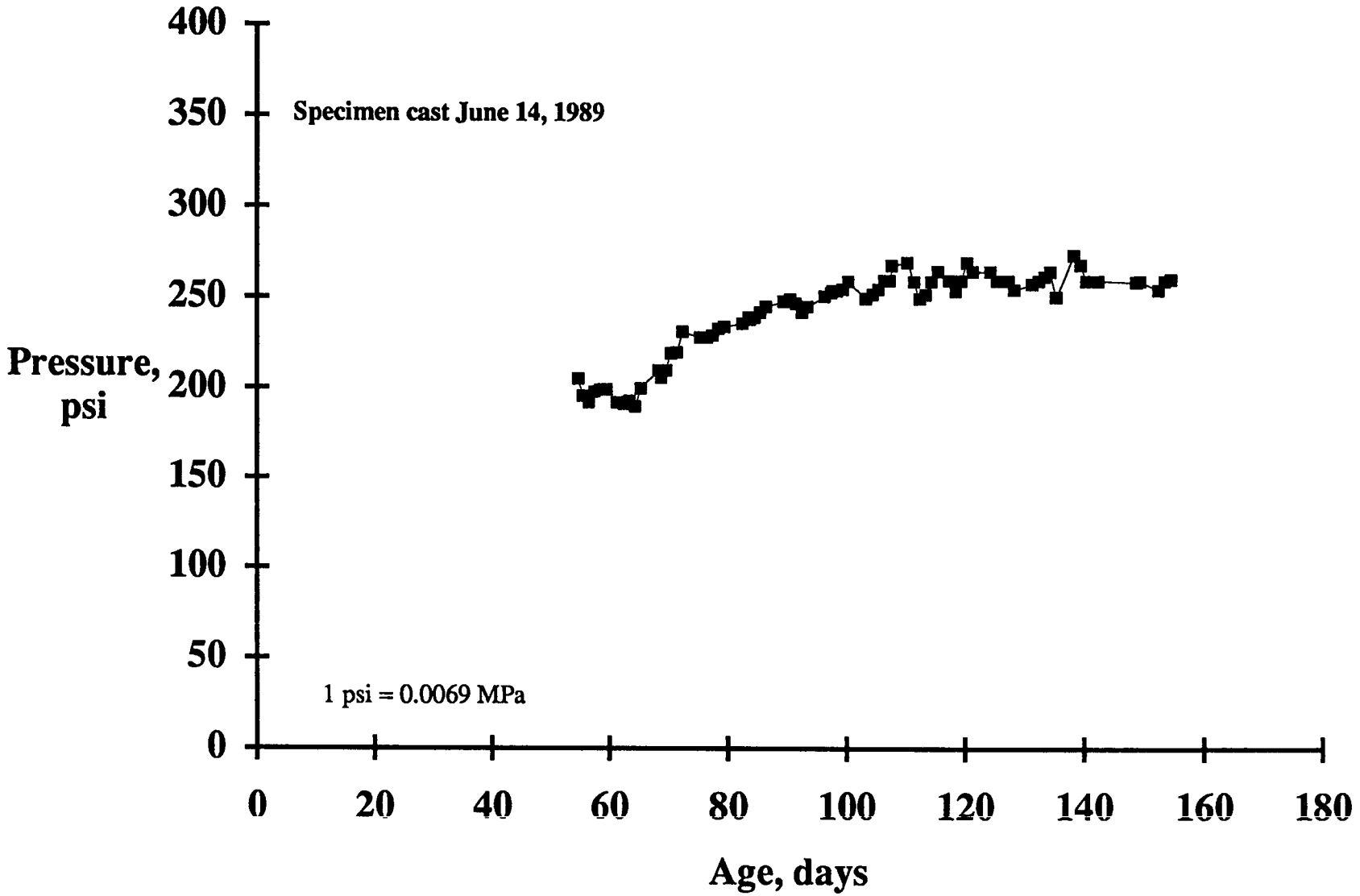


Figure C.5. Pressure versus time for cylinder 4.

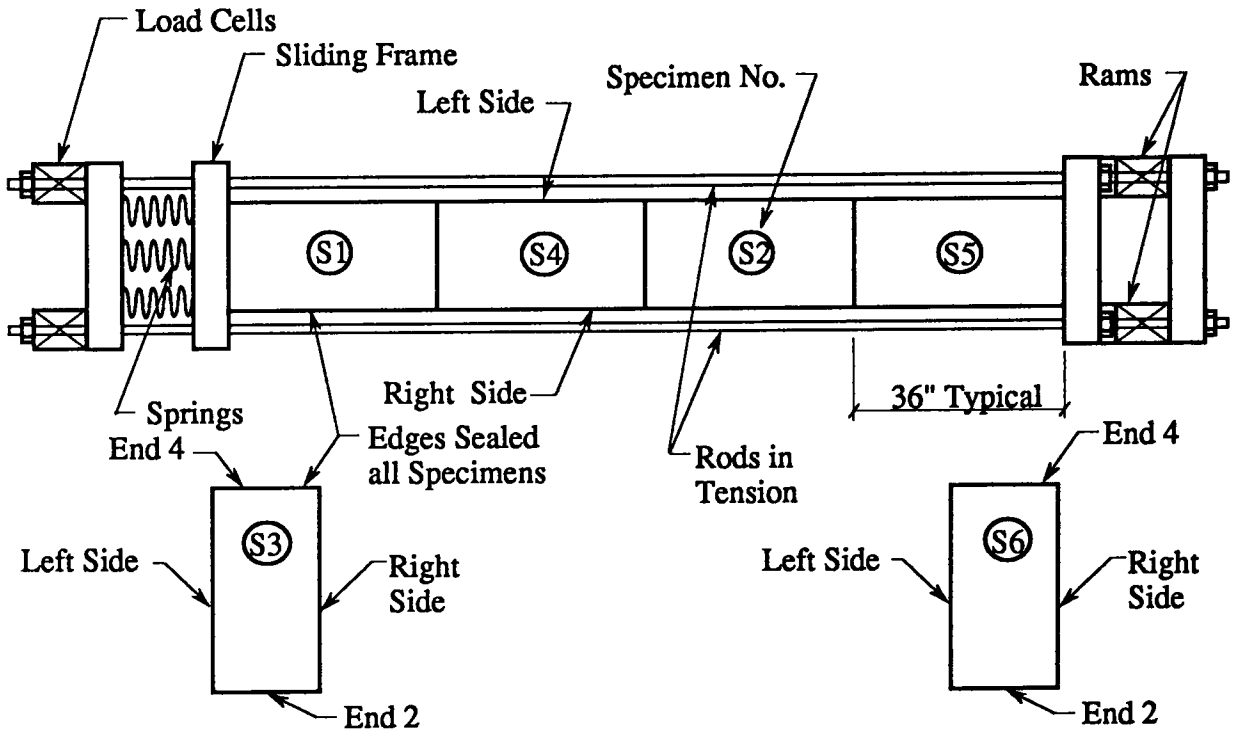


| SPECIMEN NO. | DESCRIPTION |
|---|---|
| S1 | Under Load - Nonreactive Aggregate-Specimen Unsealed (Total Strain Specimen) |
| S4 | Under Load - Reactive Aggregate-Specimen Unsealed (Total Strain Specimen) |
| S2 | Under Load - Reactive Aggregate-Specimen Sealed (Basic Creep Strain Specimen) |
| S5 | Under Load - Nonreactive Aggregate-Specimen Sealed (Basic Creep Strain Specimen) |
| S3 | No Load - Nonreactive Aggregate-Specimen Unsealed (Drying Shrinkage Specimen) |
| S6 | No Load - Reactive Aggregate-Specimen Unsealed (Drying Shrinkage Specimen) |

Note: 1 in. = 25.4 mm

Figure C.6. Test setup for the miniature pavement sections.

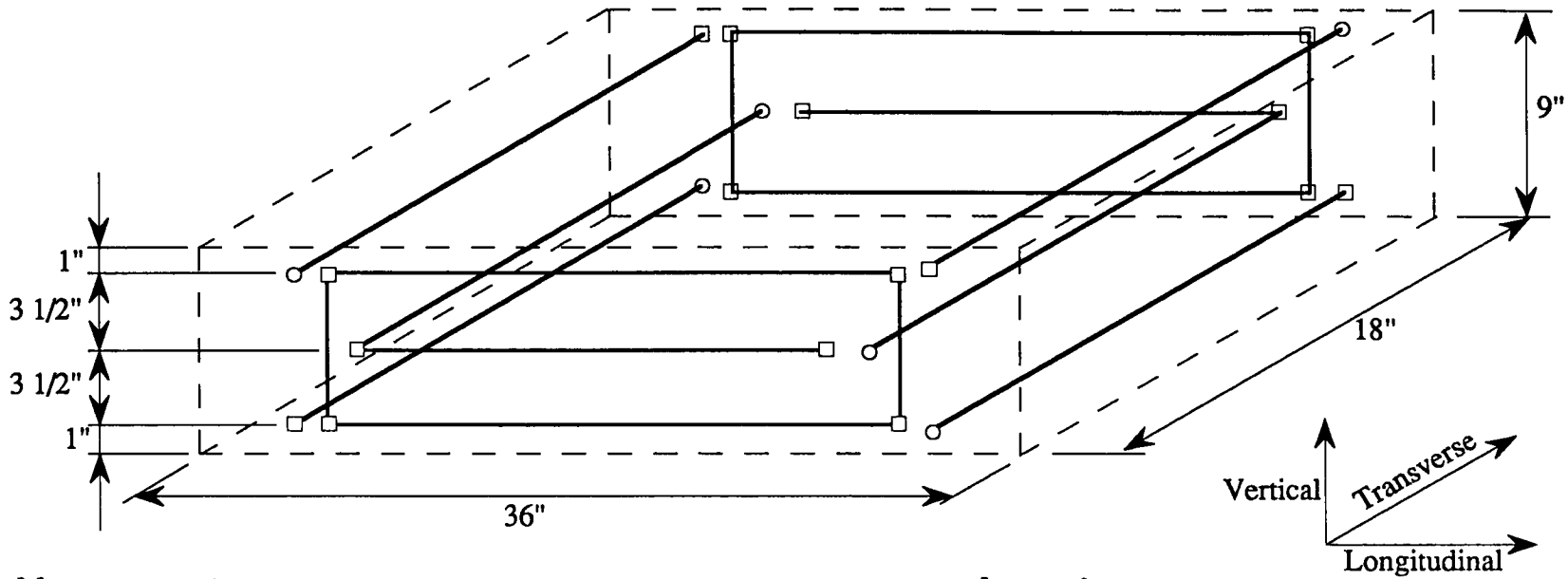


## Measurements

1. 6 Longitudinal: 3 (Top, Middle and Bottom) on both sides.
2. 6 Transverse: 3 (Top, Middle and Bottom) on both ends.
3. 4 Heights: 2 at each end on both sides
4. Longitudinal and height measurements made on outside surface of section.
5. Invar rods for transverse measurements pass through nylon tubes initially cast into section.

## Legend

- — — — Outline of Miniture Pavement Section
- ——— Invar rod - One end connected to DC DC LVDT core. Other end terminates either in a holder of a DC DC LVDT or a plug.
- □ DC DC LVDT in holder fastened to concrete surface.
- o Plug fastened to concrete surface.

Note : 1" = 25.4 mm

Figure C.7. Miniature pavement section instrumentation.

samples, that both aerobic and anaerobic bacterial action was occurring in the felt beneath the concrete. Analysis further indicated that the bacteria developing were harmful to personal health. The combination of temperature, moisture, and darkness under test sections was an ideal environment for growth of bacteria that were assumed to have been present in the felt as purchased. After attempts at control by chemical treatment proved unsuccessful, it was decided to recast test sections on a granular soil subbase. Instruments were removed, the test setup disassembled, a granular soil subbase prepared and test sections recast on December 10, 1990.

In addition to the miniature pavement sections, concrete prisms 3 x 3 x 11 1/4 in. (76 x 76 x 286 mm) were made for determination of length change. The pavement sections and prisms were cured under wet burlap for 8 days. During curing, the sides of all miniature pavement sections were treated with two coats of silane and two coats of heavy duty epoxy paint to inhibit moisture loss through the sides. Also, the tops of Reactive Section 2 and Control Section 5 were treated with the two coats of silane and epoxy to prevent any significant moisture loss from the surface as well as sides of these specimens.

Three sets of concrete prisms, containing three reactive and three control prisms each, were prepared. After curing, one prism set was stored without further conditioning or treatment adjacent to the miniature pavement sections in the test room. These prisms were subject to the same direct drying environment as the tops of the uncoated pavement sections. A second set of prisms was stored in sealed containers over water and, therefore, was in an environment simulating the bottoms of the miniature pavement sections in direct contact with the moist subgrade. A third set of prisms was coated with two coats of silane and epoxy and stored adjacent to the miniature pavement sections in the test room to aid in assessing sealing effectiveness of silane and epoxy treatment.

As was done previously, test sections were cast in an alternate pattern in order of their identification number shown on Figure C.6. Prior to casting Sections S4 and S5, stainless steel shim stock 0.005 in. (0.13 mm) thick was placed against Sections S1 and S2 to act as a bond break to permit independent lateral movement of each specimen. As will be discussed in the next report section, these bond breaks resulted in a loss of contact between specimens at the surface due to surface shrinkage, and therefore a loss at the very top of stress transfer between specimens.

Miniature pavement sections were instrumented, soaker hose and loading hydraulic systems reinstalled. The test room was raised in temperature to 102°F (38.9°C) on January 21, 1991 (at test specimen age of 42 days) and the RH was held at 25 to 35 percent. Later in the day on January 22, 32 hours after the test room was at the elevated temperature, thermal strains in sections were generally constant and stabilized. Therefore, zero strain for all subsequent strain readings was referenced to the absolute strain recorded at that time.

On January 28, the loading frames were tightened against the four restrained sections in order to remove any mechanical looseness from elements of the restraint system. After tightening, residual compressive stress of 15 psi (0.10 MPa) remained in the restrained sections. At the time, this small residual stress was considered insignificant. It was assumed that once ASR developed within the test sections, this low compressive stress would soon be exceeded as expansion started forcing the restrained sections tighter against the loading frames. As will be discussed more fully later, this relatively low stress applied very early in the life of the test section appears to have fundamentally altered the outcome of the experiment.

The test continued until August 20, 1992, at which time the miniature pavement sections and prisms had been at temperature for 577 days.

## *C.2.1 Test Results*

Results are presented in the next five sections. Prism results are given first, followed by performance of the measurement standards used for the miniature pavement specimen test. Behavior of unrestrained miniature pavements is given in the third section. Restrained miniature pavement results are given in the last two sections.

### C.2.1.1 Prisms

Figure C.8 shows the measured length changes for the reactive and control set of prisms stored over water. As indicated by the plots, the reactive set continued to expand rapidly to age 150 days, when the rate of expansion slowed. The control set of prisms expanded significantly less. Note that the reactive prisms expanded to only 20 percent of the value reached by prisms made with the same mix for previously reported three-dimensional pressure tests (Figure C.1). Shown in Figure C.9 are measured weight gain for prisms of Figure C.8 indicating that sufficient moisture was available for expansion to develop due to ASR.

Length and weight changes for prism sets stored in air at 25 to 35 percent RH are given in Figures C.10 and C.11. Note that reactive as well as control prisms stored in this environment, where drying was accelerated, essentially never expanded indicating the importance of adequate moisture for expansion due to ASR to proceed. The weight change plot of Figure C.11 graphically illustrates the rapid drying of these prisms.

Shown in Figure C.12 are measured length changes for coated prism sets stored in air. While these prisms, without a source of moisture, eventually shrank to essentially the same degree as the uncoated prisms, rate of shrinkage was less. Effectiveness of the coating in reducing rate of moisture loss is indicated by comparing weight change with time of the coated prisms (Figure C.13) with weight change of uncoated prisms (Figure C.11). This comparison demonstrates the significant difficulty generally encountered when attempting to seal concrete from moisture loss.

### C.2.1.2 Miniature Pavement Section Standards

Stability of the instrumentation and data acquisition systems used to monitor performance of miniature pavement sections was monitored during the test. Shown in Figure C.14 are results of recorded strain in the Invar standard bar during the test. Zero strain should be indicated, which is essentially the case. The results of the single DC LVDT mounted in the test room is given in Figure C.15. Note the DC LVDT output has been calculated as a strain using the same gage length as the standard bar for ready comparison. As shown in Figures C.14 and C.15, the instrumentation and data acquisition system remained stable throughout the duration of the test.

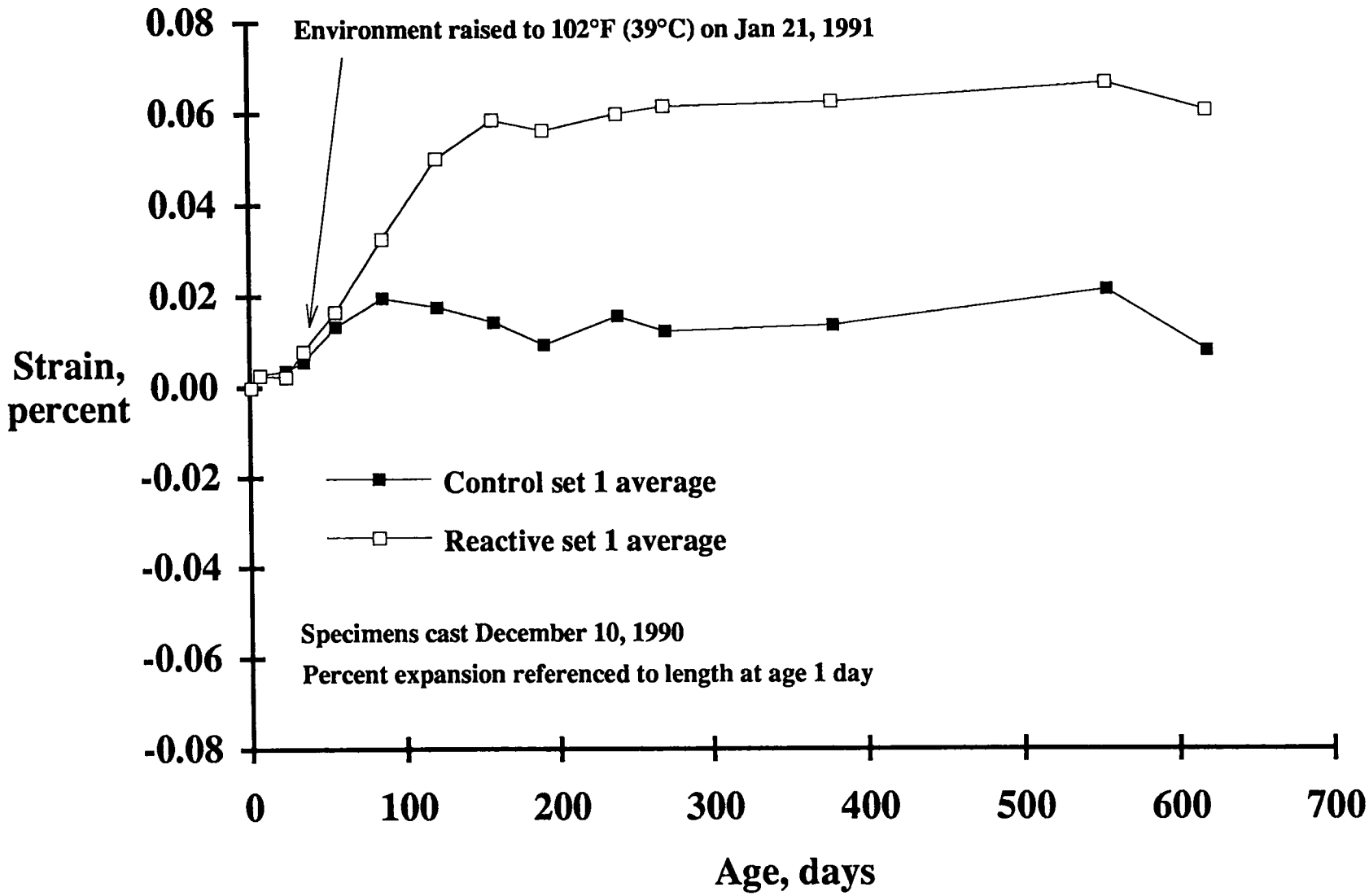


Figure C.8. Prism strain versus time for set 1; one dimensional restraint test.

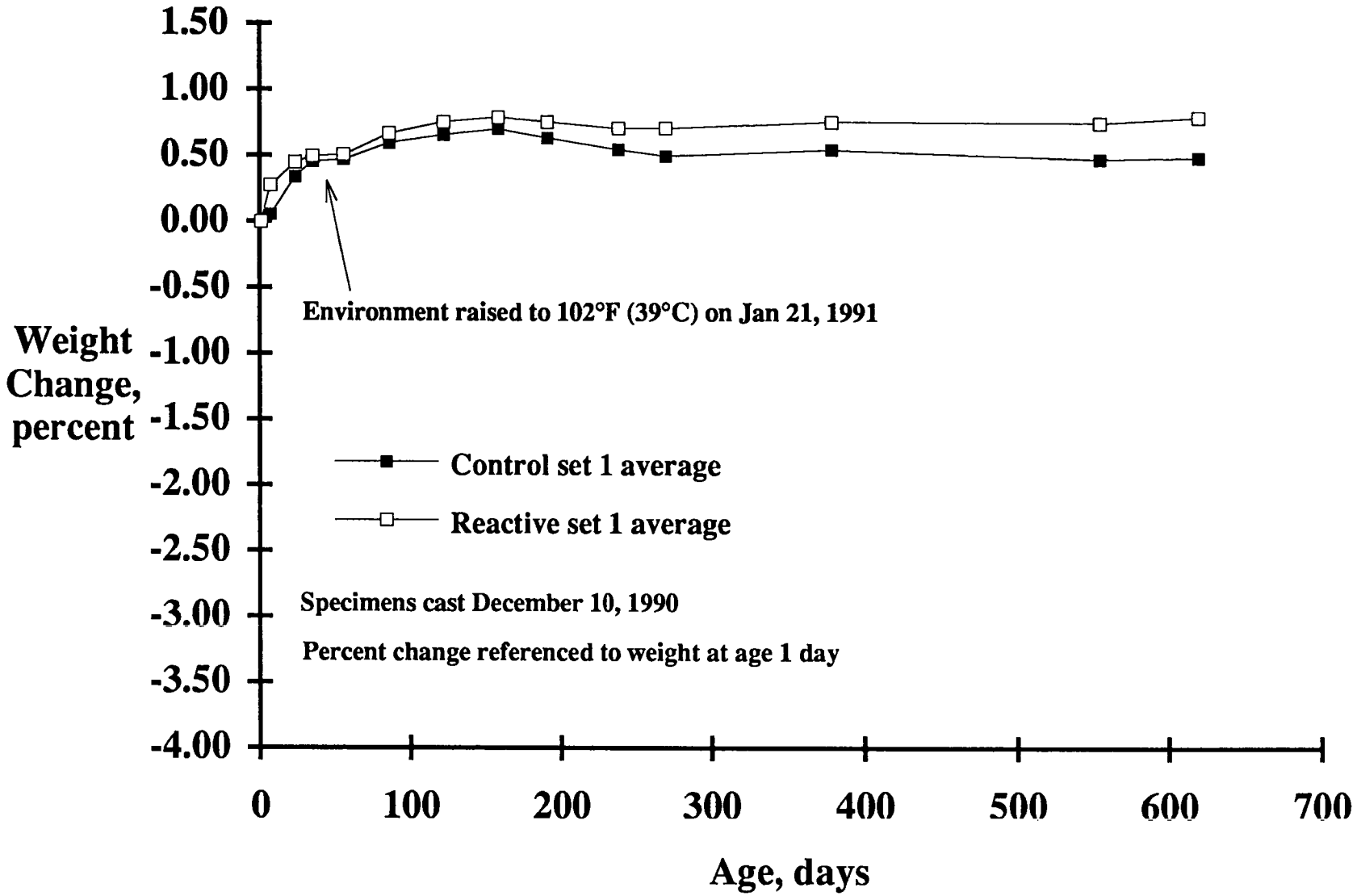


Figure C.9. Prism weight versus time for set 1; one dimensional restraint test.

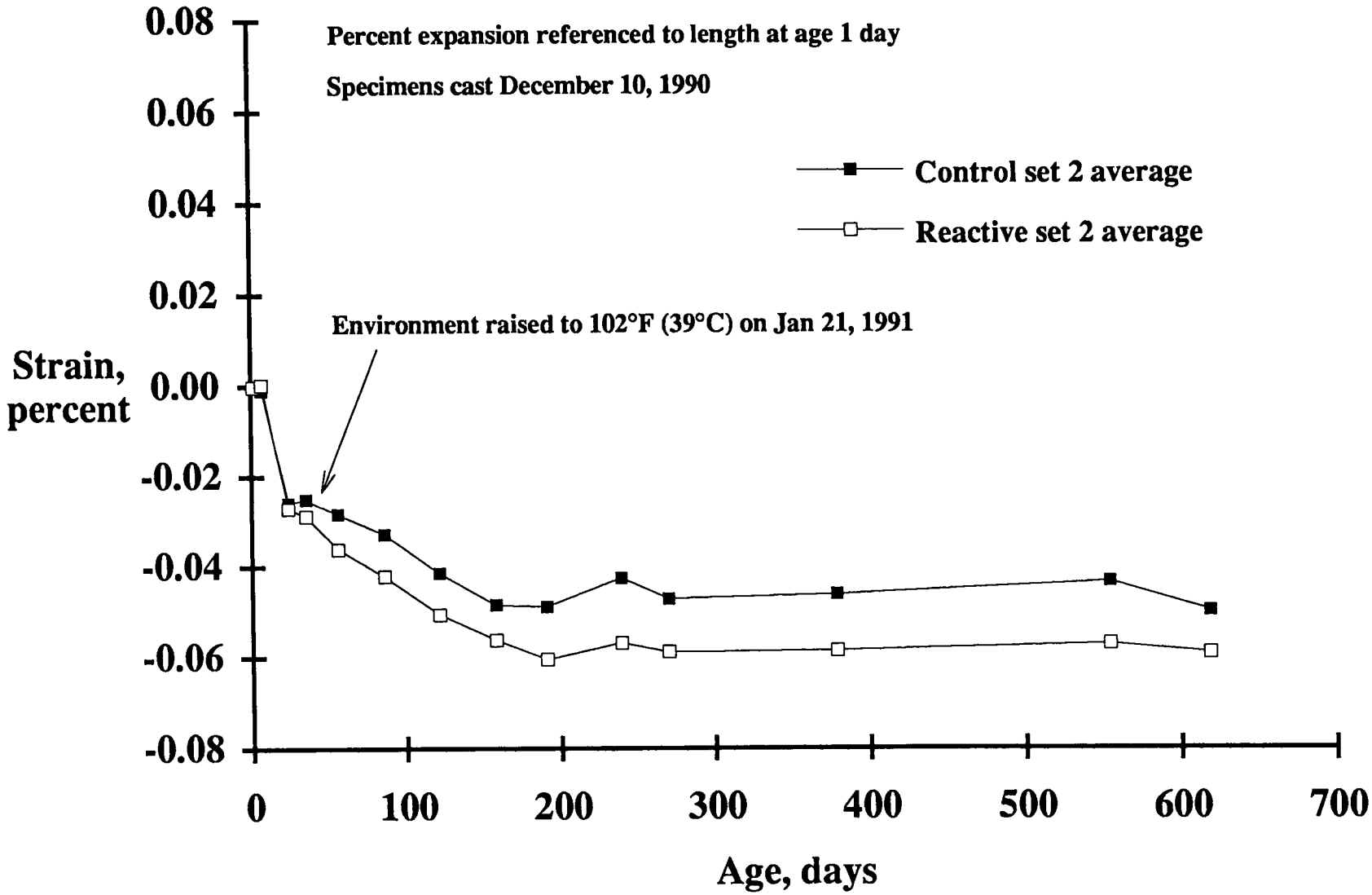


Figure C.10. Prism strain versus time for set 2; one dimensional restraint test.

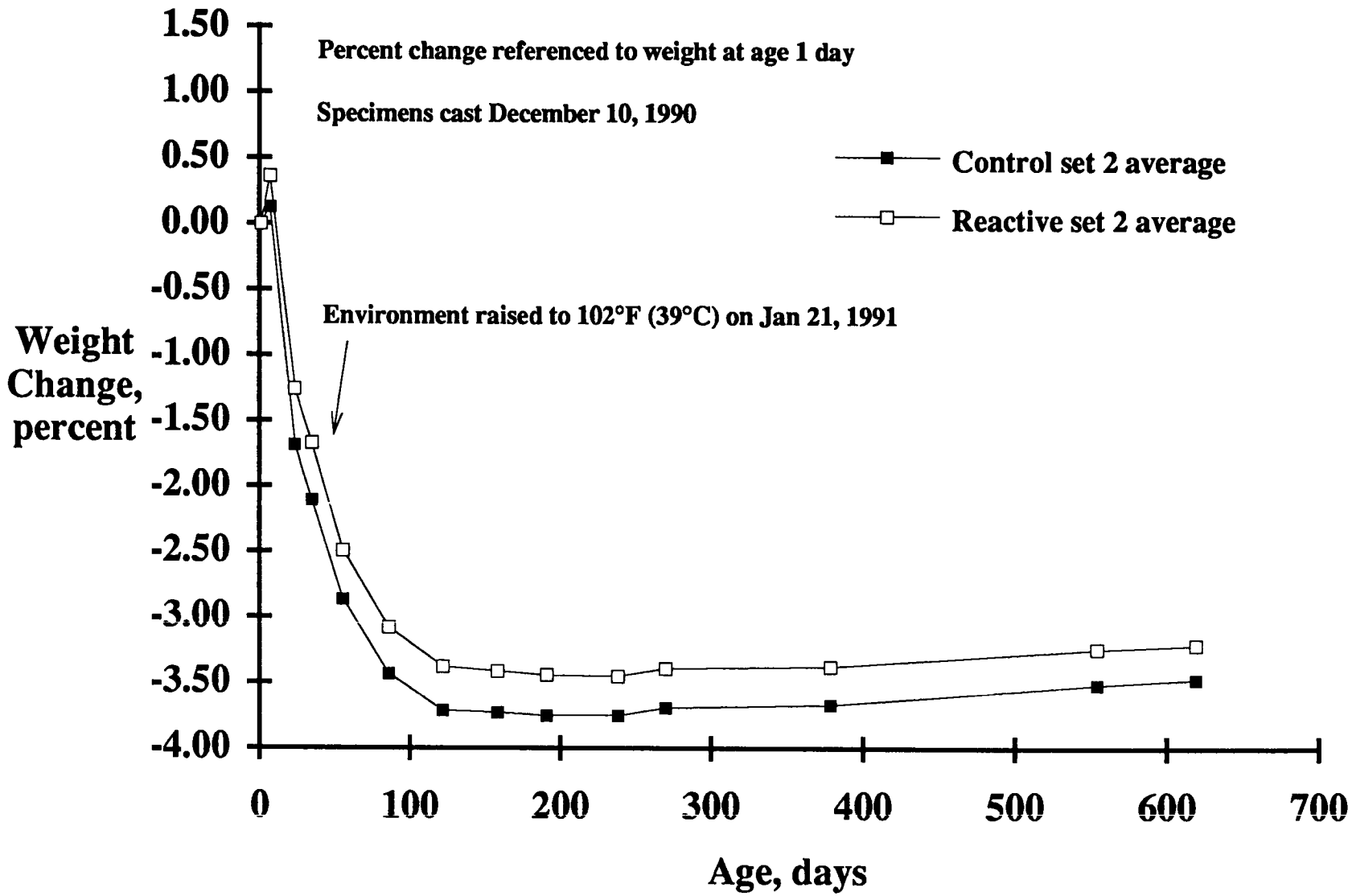


Figure C.11. Prism weight versus time for set 2; one dimensional restraint test.

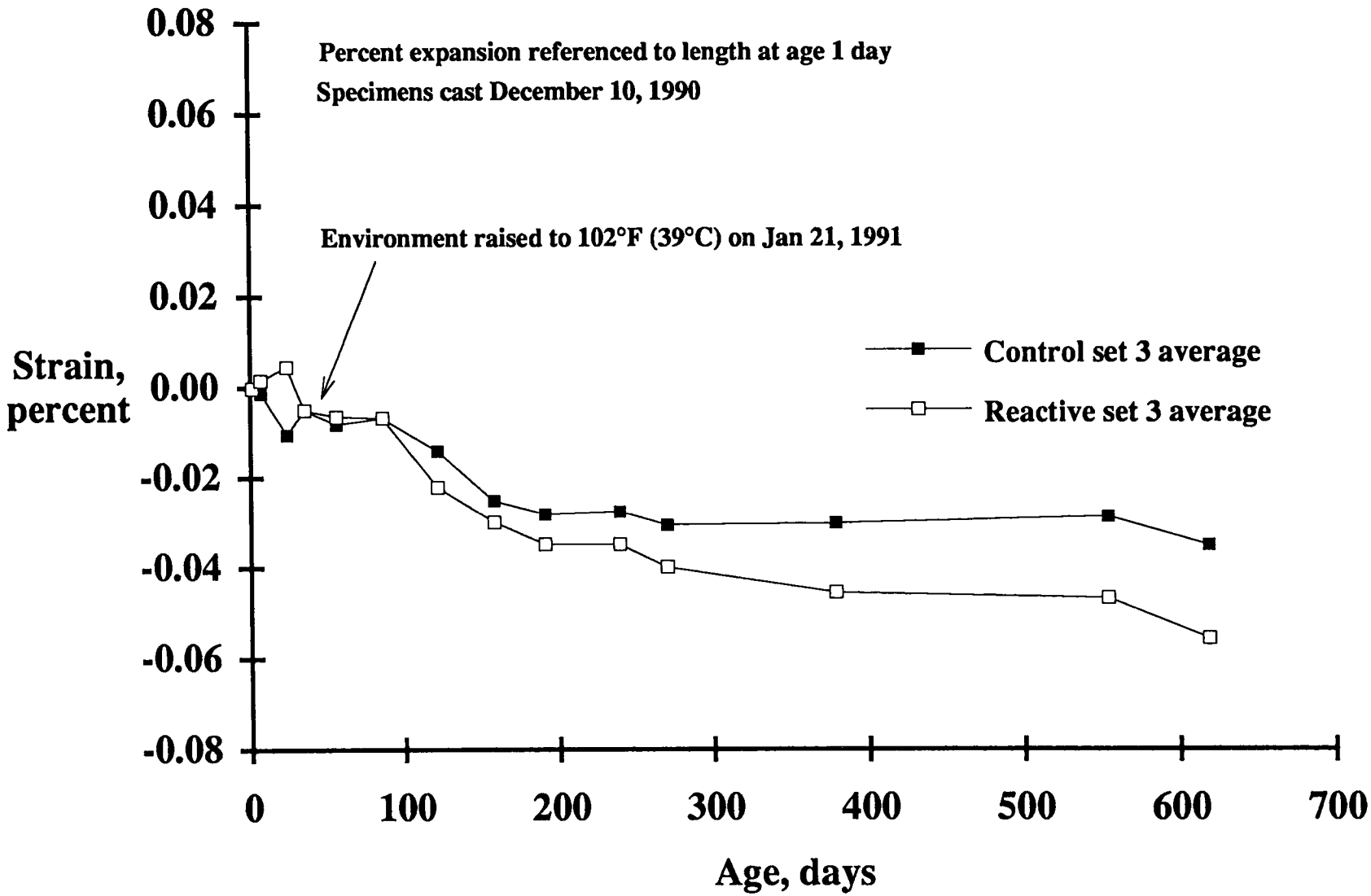


Figure C.12. Prism strain versus time for set 3; one dimensional restraint test.

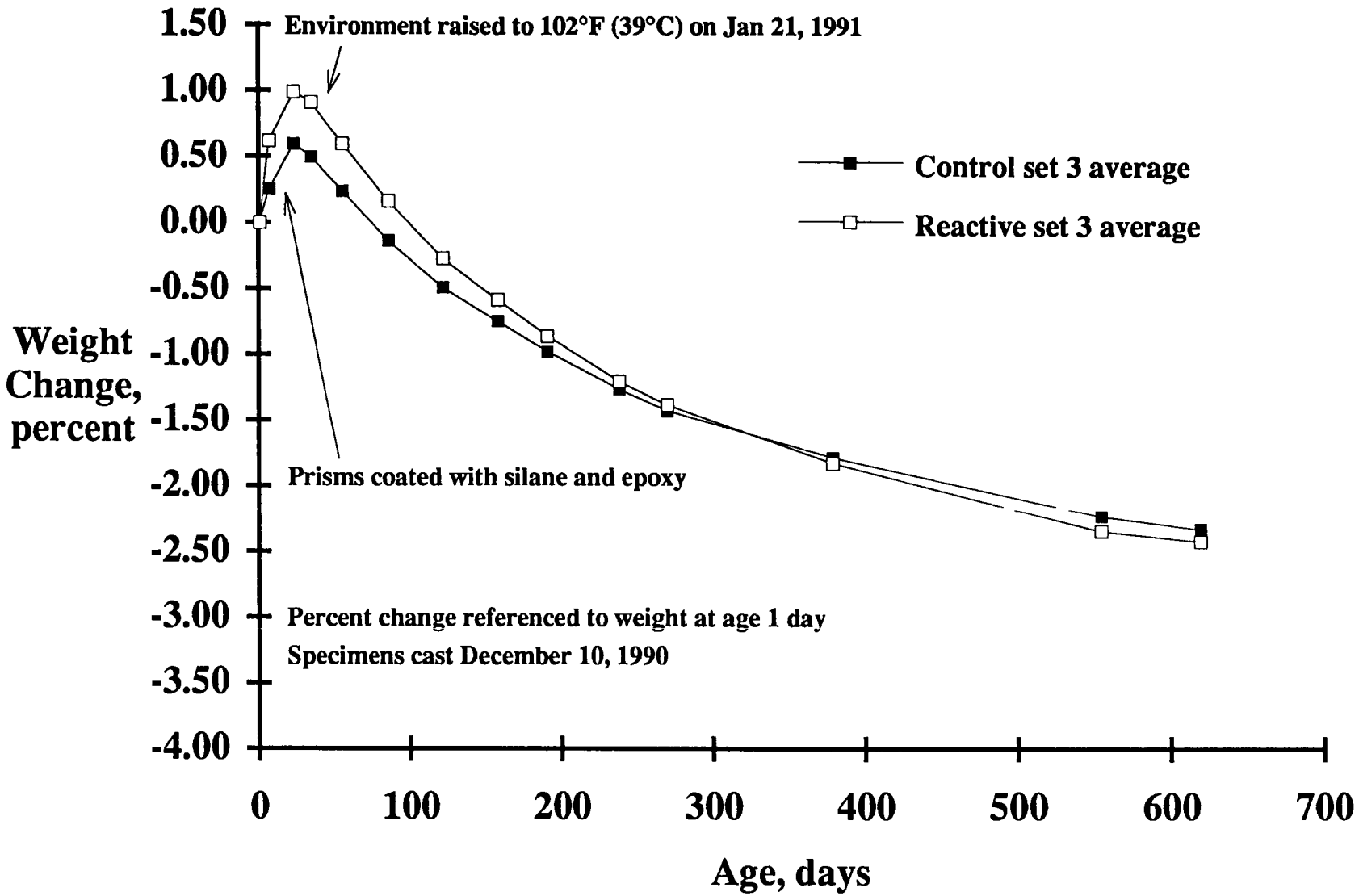


Figure C.13. Prism weight versus time for set 3; one dimensional restraint test.

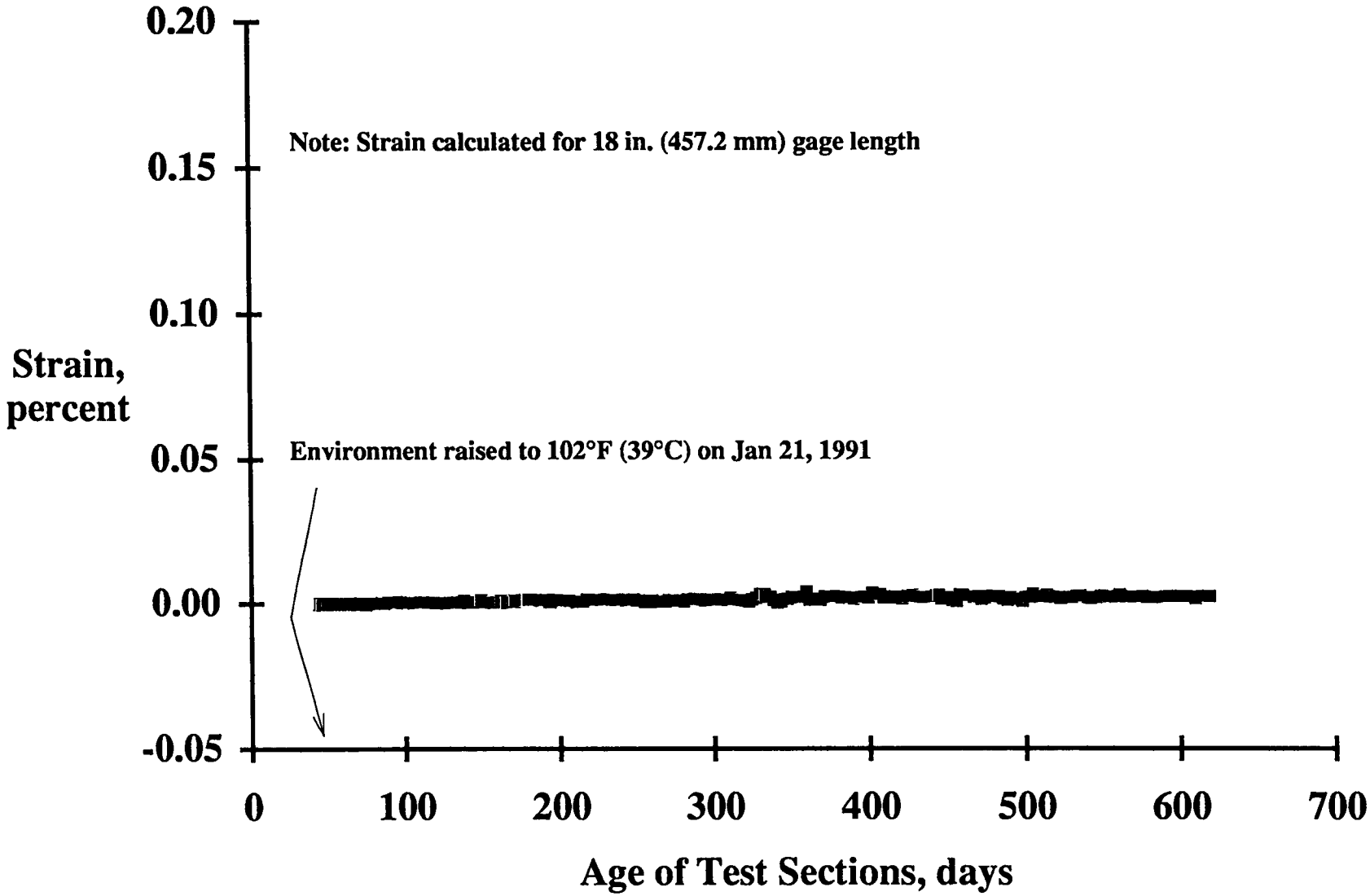


Figure C.14. Strain versus time for the standard bar.

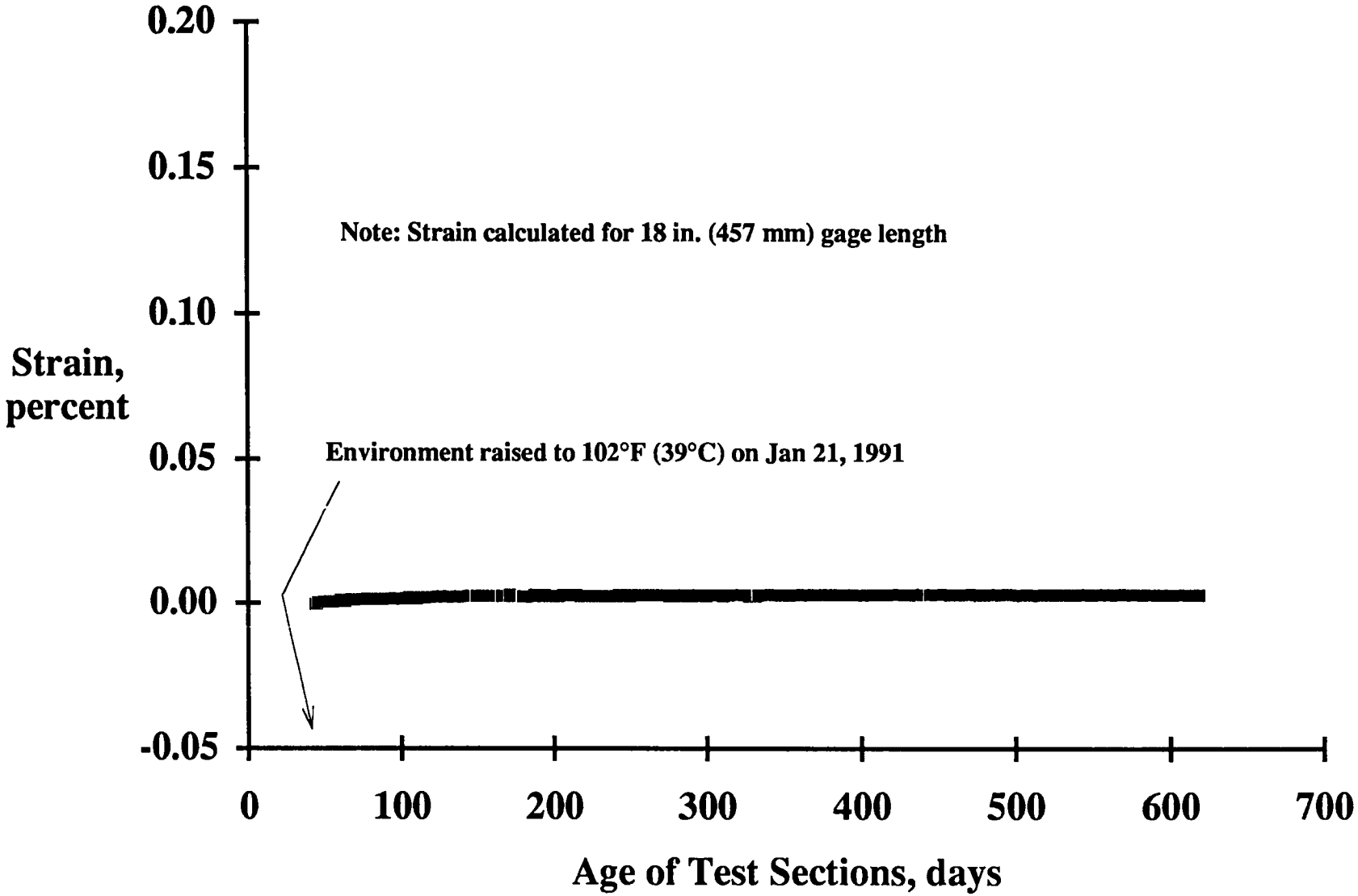


Figure C.15. Strain versus time for the DC DC LVDT standard.

In essentially all instances, behavior of the six miniature pavement sections was symmetric. In presenting section performance, therefore, measurements are averaged. Longitudinal strains on measurements made on each side of sections are averaged to give overall vertical strain behavior of each side. Transverse strains at both ends of sections are averaged to give overall transverse behavior.

### C.2.1.3 Unrestrained Pavement Sections

Figure C.16 shows the average of longitudinal strains measured on both sides of Section S6 which was cast with reactive aggregate. Shown in Figures C.17 and C.18 are averages of transverse strains measured at both ends and vertical strains measured on both sides of Section S6, respectively. Figures C.19, C.20, and C.21 show comparable strains in Section S3 which was cast with innocuous aggregate and acted as a control for Section S6. As would be expected, within each unrestrained section, longitudinal and transverse strains were similar as indicated by comparison of Figures C.16 and C.17 for Section S6 and Figures C.19 and C.20 for Section S3.

Note that in longitudinal (Figure C.19) and transverse (Figure C.20) directions in control Section S3, strains at the bottom that was in direct contact with the moist subbase remained close to zero as shrinkage was not present. Conversely, the surface exposed to the drying test room environment of 25 to 35 percent relative humidity, steadily and continuously contracted due to drying shrinkage. The middle plane of the section contracted an amount equal approximately to the average of top and bottom. Both sides (Figure C.21) contracted vertically as well. The above behavior was as expected.

Comparison of strains in reactive aggregate Section S6 (Figures C.16, C.17, and C.18) with innocuous aggregate Section 3 (Figures C.19, C.20, and C.21) clearly indicates substantial expansion in Section S6, particularly considering that the expanded vertical scale of Figures C.19, C.20, and C.21 has four times the resolution of the vertical scale of Figures C.16, C.17, and C.18.

Early behavior of Section S6 is more clearly illustrated in Figure C.22. The bottom of Section S6 expanded only slightly for the first 30 days of exposure to the 102°F (38.9°C) environment. After 30 days, however, rate of expansion increased substantially. Approximately 30 days later, the first visible cracks in Section S6 were noted. The cracks were vertical on both sides and ends, extending approximately 1 1/2 in. (37 mm) up from the bottom. At about the same time, bottom and middle expansion had grown to the point where they were affecting strains at the top. Contraction at the top due to drying shrinkage was overcome by the influence of expansions below, and top strains went from contraction (negative), through zero, and into expansion (positive). Top surface cracks were initially observed and mapped at age 121 days. Also at this age, small white beads of material were observed on the sides and ends of Section S6. These beads were gel deposits formed as a reaction product of ASR taking place within the section and being forced through the epoxy paint coating sides and ends.

Subsequent crack mapping revealed the following pattern of crack development. Initially, cracking developed randomly over the top surface. New cracks continued to form and existing cracks continued to grow in size until the surface was covered with a pattern of cracks composed of interconnected roughly squares and rectangles, approximately 4 to 6 in. (100 to 150 mm) on a side. Once the interconnected pattern was fully developed no new

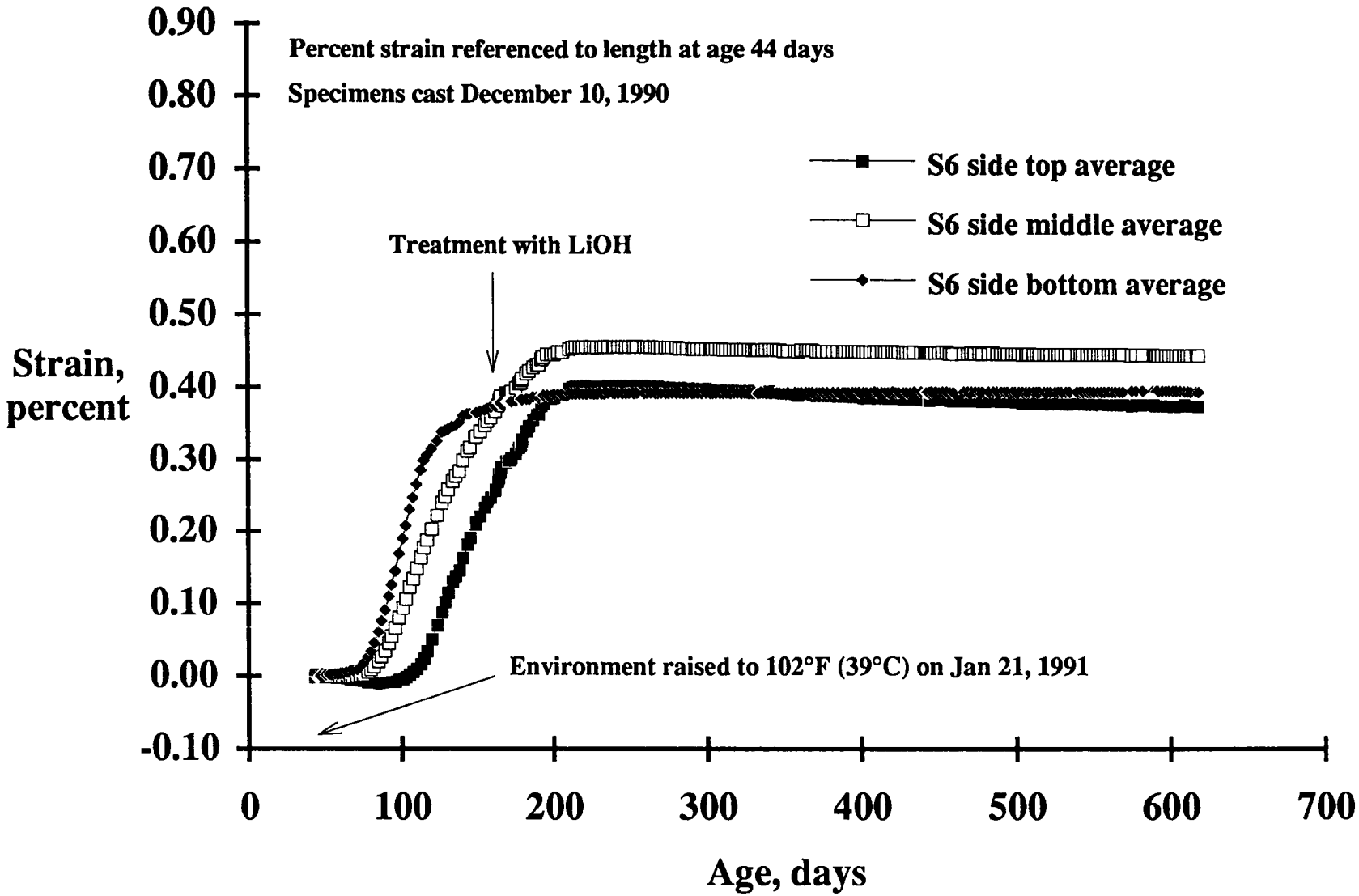


Figure C.16. Longitudinal strain versus time for section S6.

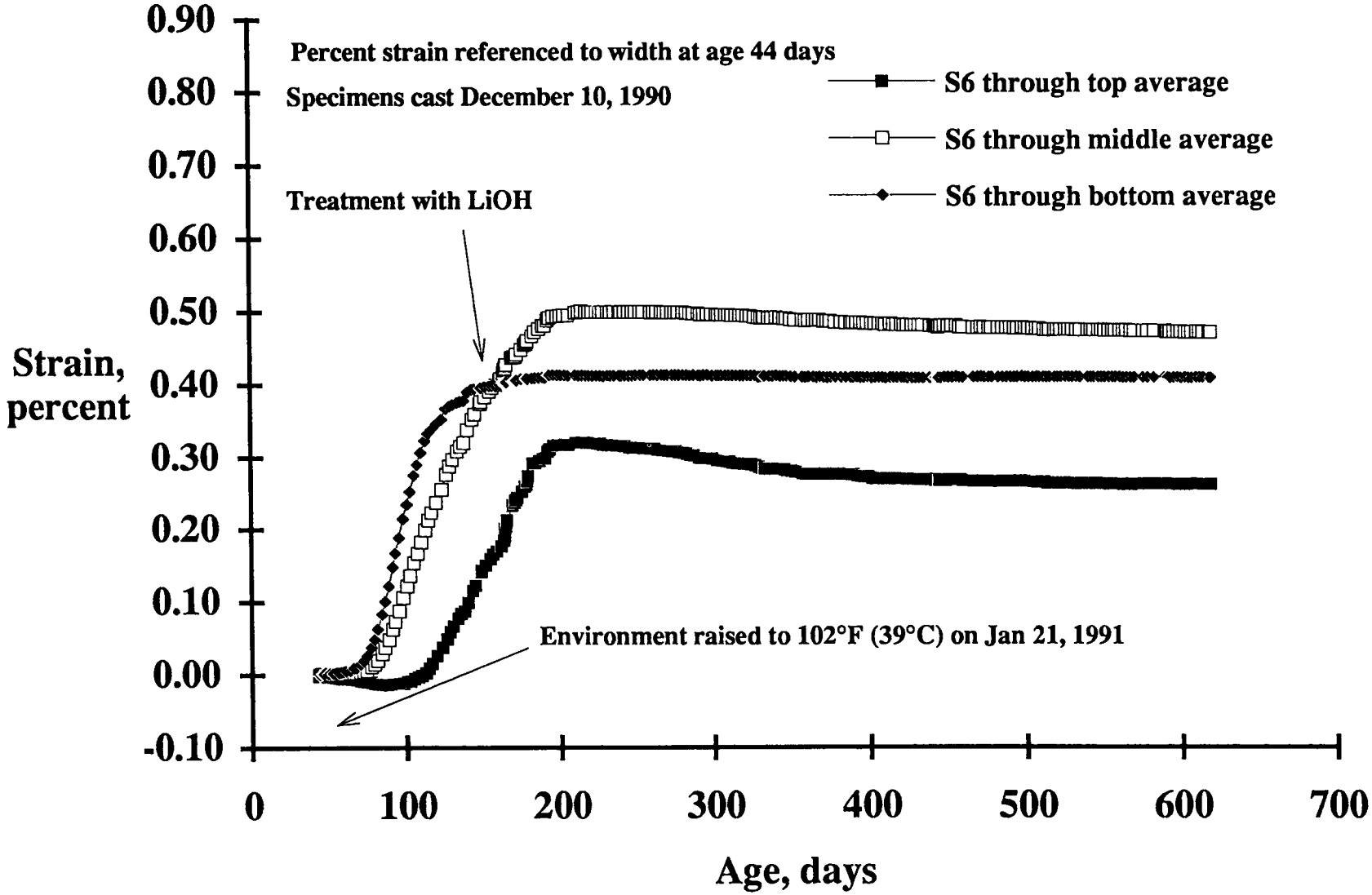


Figure C.17. Transverse strain versus time for section S6.

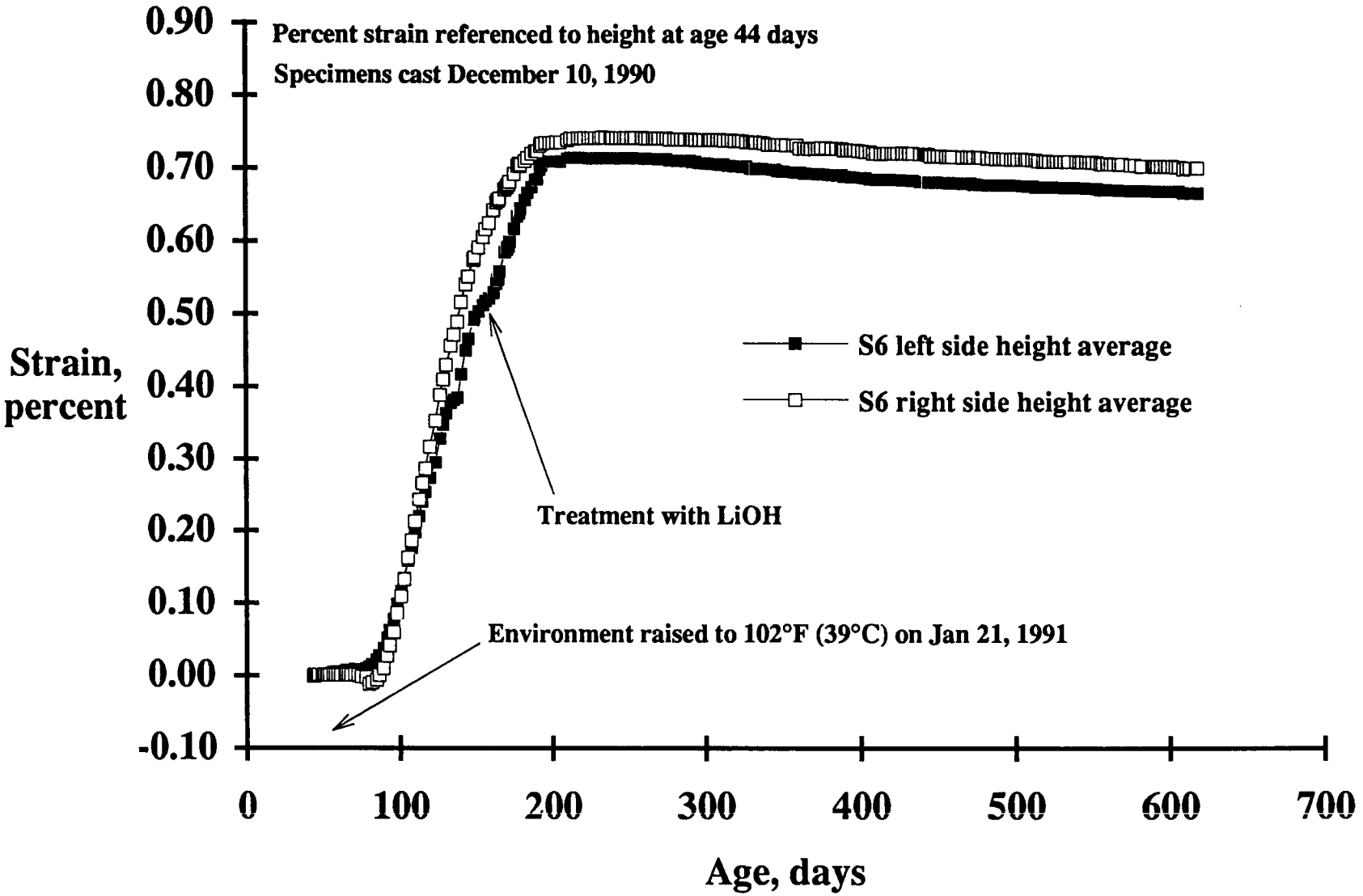


Figure C.18. Vertical strain versus time for section S6.

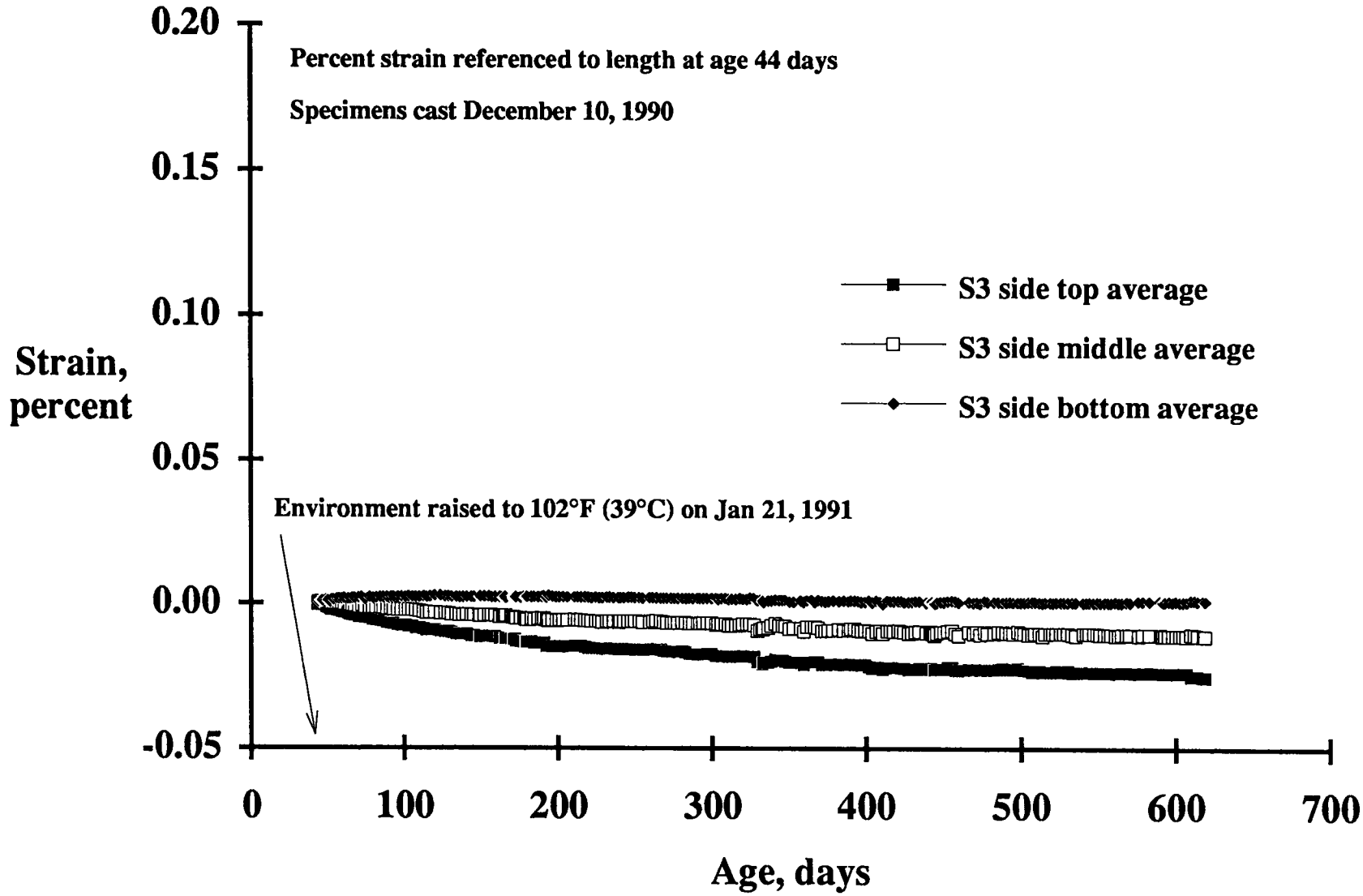


Figure C.19. Longitudinal strain versus time for section S3.

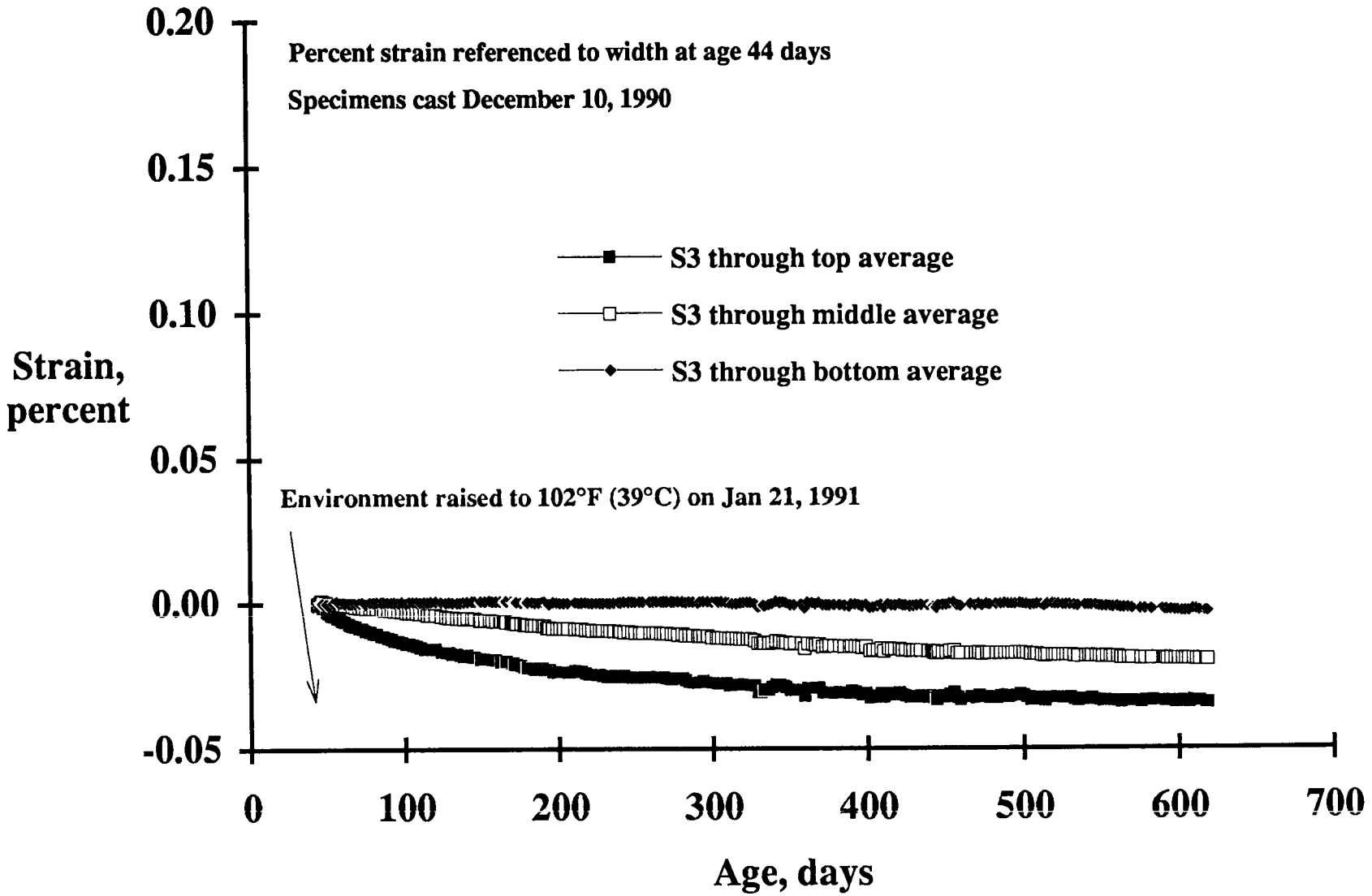


Figure C.20. Transverse strain versus time for section S3.

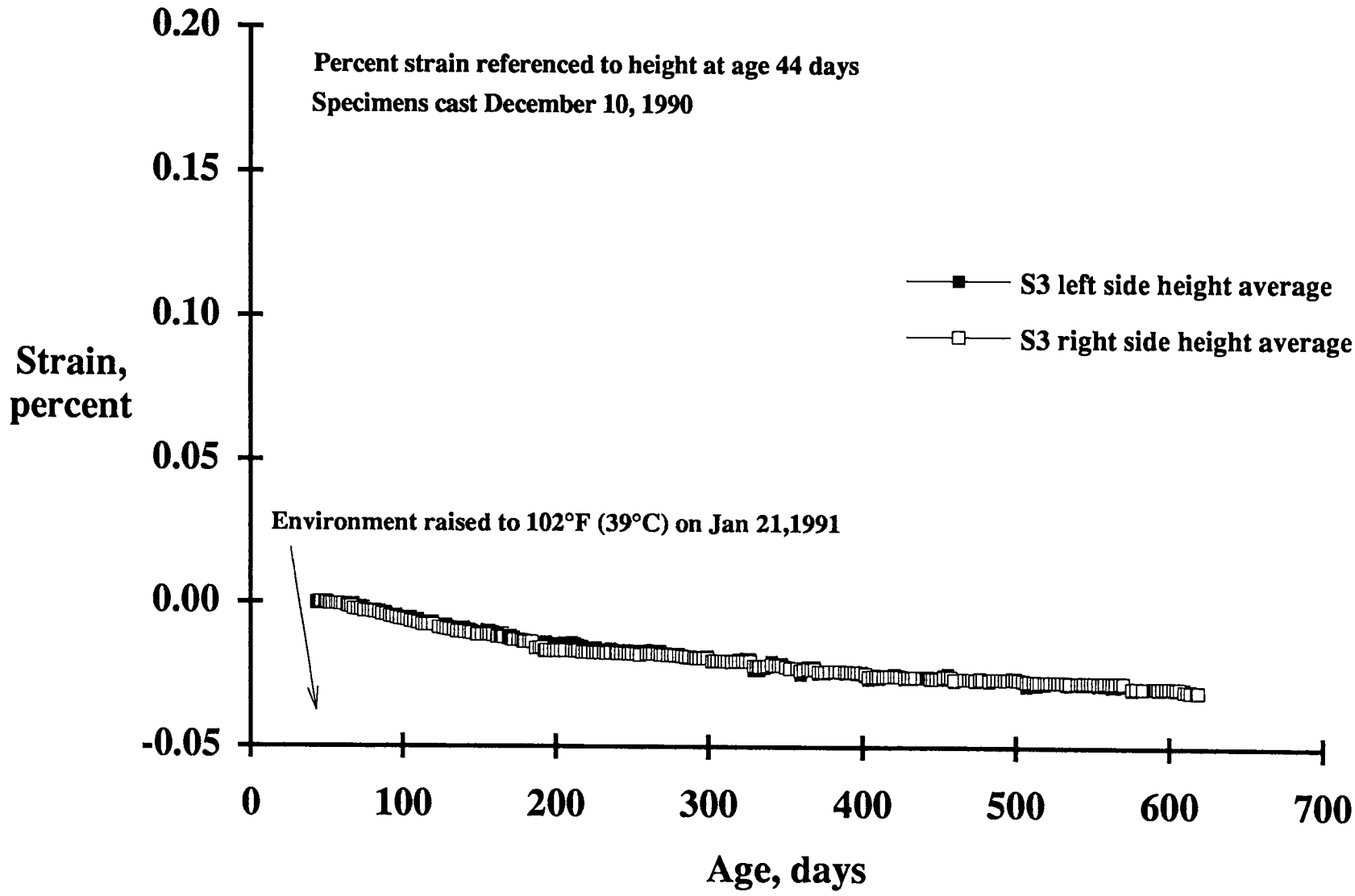


Figure C.21. Vertical strain versus time for section S3.

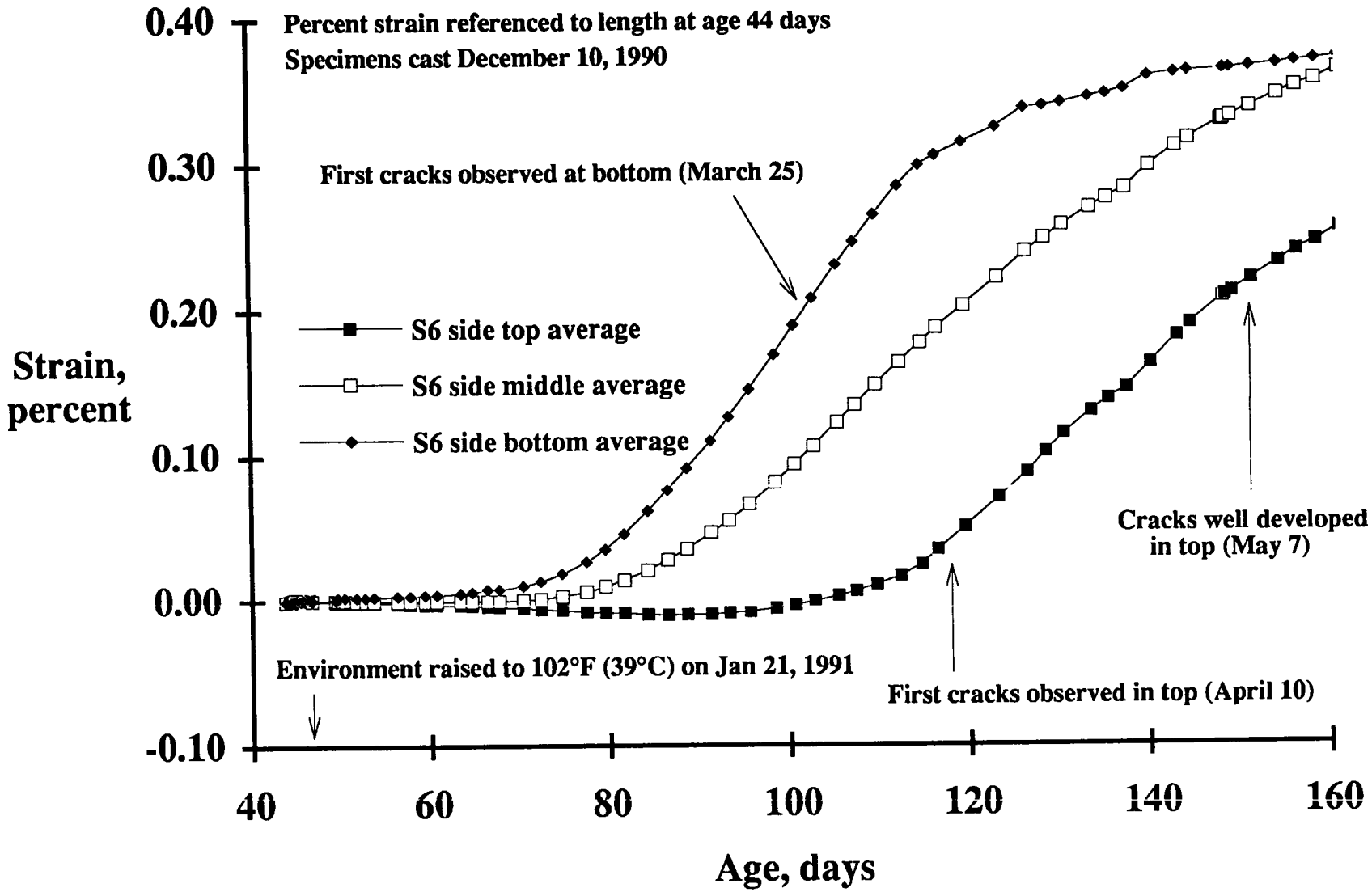


Figure C.22. Longitudinal strain versus time on an expanded scale for section S6.

cracks appeared. Existing cracks simply continued to widen. The pattern was well developed by age 148 days. Accompanying the vertical cracks going downward from the top surface were vertical cracks extending down the sides and ends of Section S6 from the top, together with horizontal cracks at approximately mid-depth extending and progressing from the four corners along the sides and ends. Also, numerous beads of gel reaction product had formed on the sides and ends. The beads were concentrated in the lower 7 in. (175 mm) of the section. No gel beads were present in the upper 2 in. (51 mm).

It is interesting to note as shown in Figure C.16 and C.17 that approximately 100 days after the temperature of Section S6 was raised to 102°F (38.9°C) and 70 days after the onset of rapid expansion at the bottom, the rate of bottom expansion slowed essentially as rapidly as it began.

It is further interesting to note that middle expansions in Section S6 continued after bottom expansions had significantly slowed, actually achieving higher expansive strains than at the bottom. As shown in Figures C.16, C.17 and C.18, all expansions essentially ceased at a specimen age of 200 days, approximately 160 days after the environmental temperature was raised to 102°F (38.9°C). This time frame is consistent with expansive behavior of the prisms stored over water (Figure C.8) and also the prisms cast with the same reactive aggregate mix and monitored during the three-dimensional pressure test reported on earlier (Figure C.1).

By age 148 days cracking in Section 6 was well developed, so it was decided to treat this section with LiOH to determine its effectiveness in countering ASR. A dike was placed around edges of Section S6, the cracks on sides and ends sealed, and at age 148 days the top surface ponded with LiOH solution. After a short time, much of the solution had drained away from the surface through minute cracks in sides and ends that had not been completely sealed. After resealing sides and ends of Section S6, the top surface was reponded with LiOH at age 167 days. This time the surface remained ponded for seven days. Although the top of the section had been covered to prevent evaporation, it appeared from the quantity of crystal residue remaining on surface after liquid was gone, that most of the LiOH solution evaporated rather than having penetrated the section through surface cracks. As indicated by Figures C.16, C.17, and C.18, which show expansions with the perspective of the complete data record, rate of bottom expansion was already reducing significantly by the time LiOH solution was first applied. Although all section expansions did cease during the general time frame of LiOH applications, it is difficult to conclude that they ceased because of LiOH, since prism results indicate that expansions would have ended during this time period with or without LiOH. The results of LiOH application therefore are considered inconclusive.

### C.2.1.4 Restrained Exposed Pavement Sections

Shown in Figure C.23 are averages of recorded longitudinal strain data from both sides of restrained Section S4 cast with reactive aggregate and stored with its top surface exposed to the drying environment of the test room. Transverse strain data for Section S4 are given in Figure C.24. Comparable longitudinal and transverse strain data for control Section S1 are shown in Figures C.25 and C.26, respectively. The five times during duration of the test that longitudinal stress in sections was changed by adjusting loading frame position (Figure C.6) is indicated by vertical steps in the strain plots of Figures C.23 and C.25, the first at about age 150 days, the next two shortly after 300 days, the fourth at about 450 days, and the last at approximately 600 days.

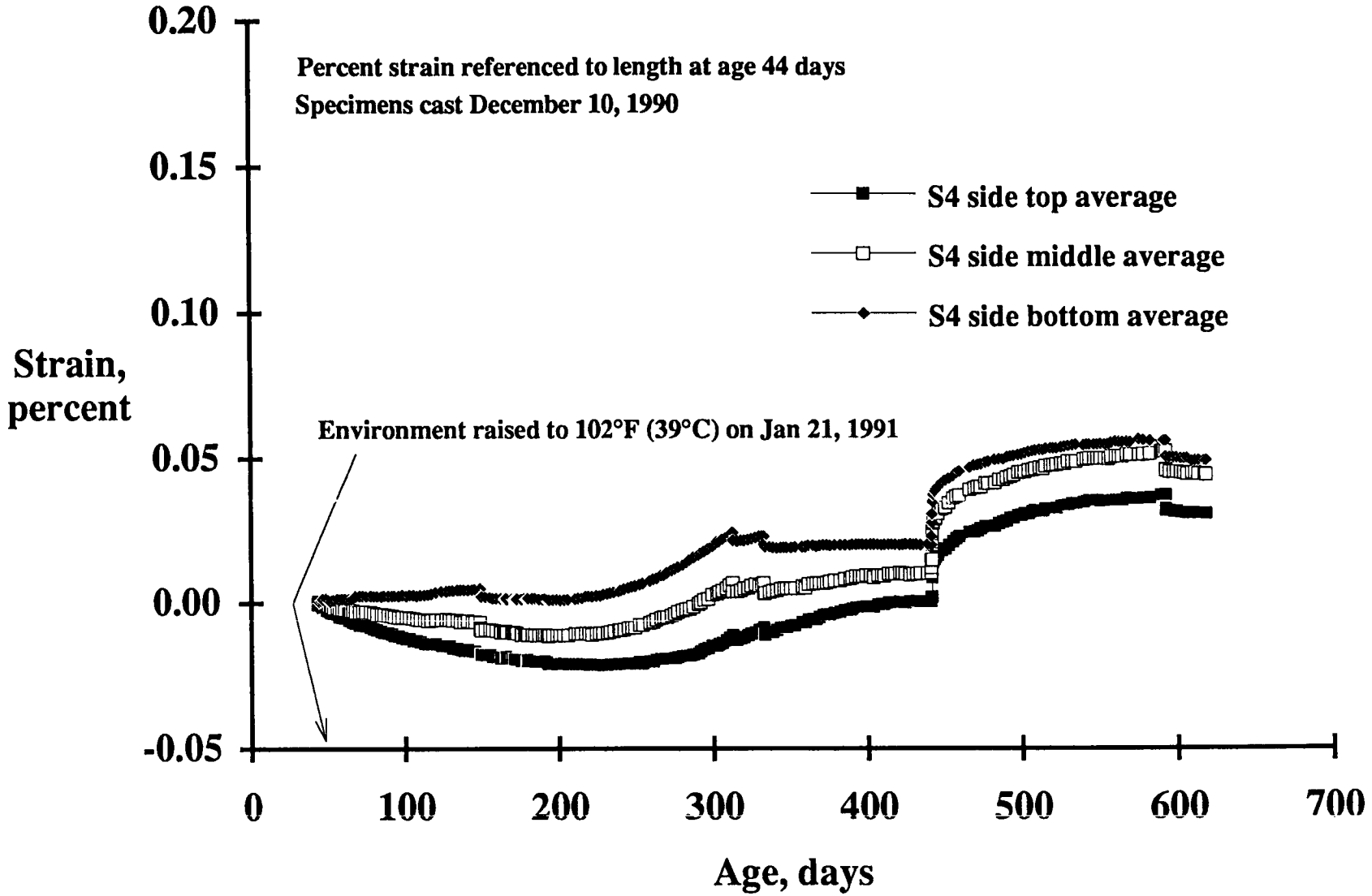


Figure C.23. Longitudinal strain versus time for section S4.

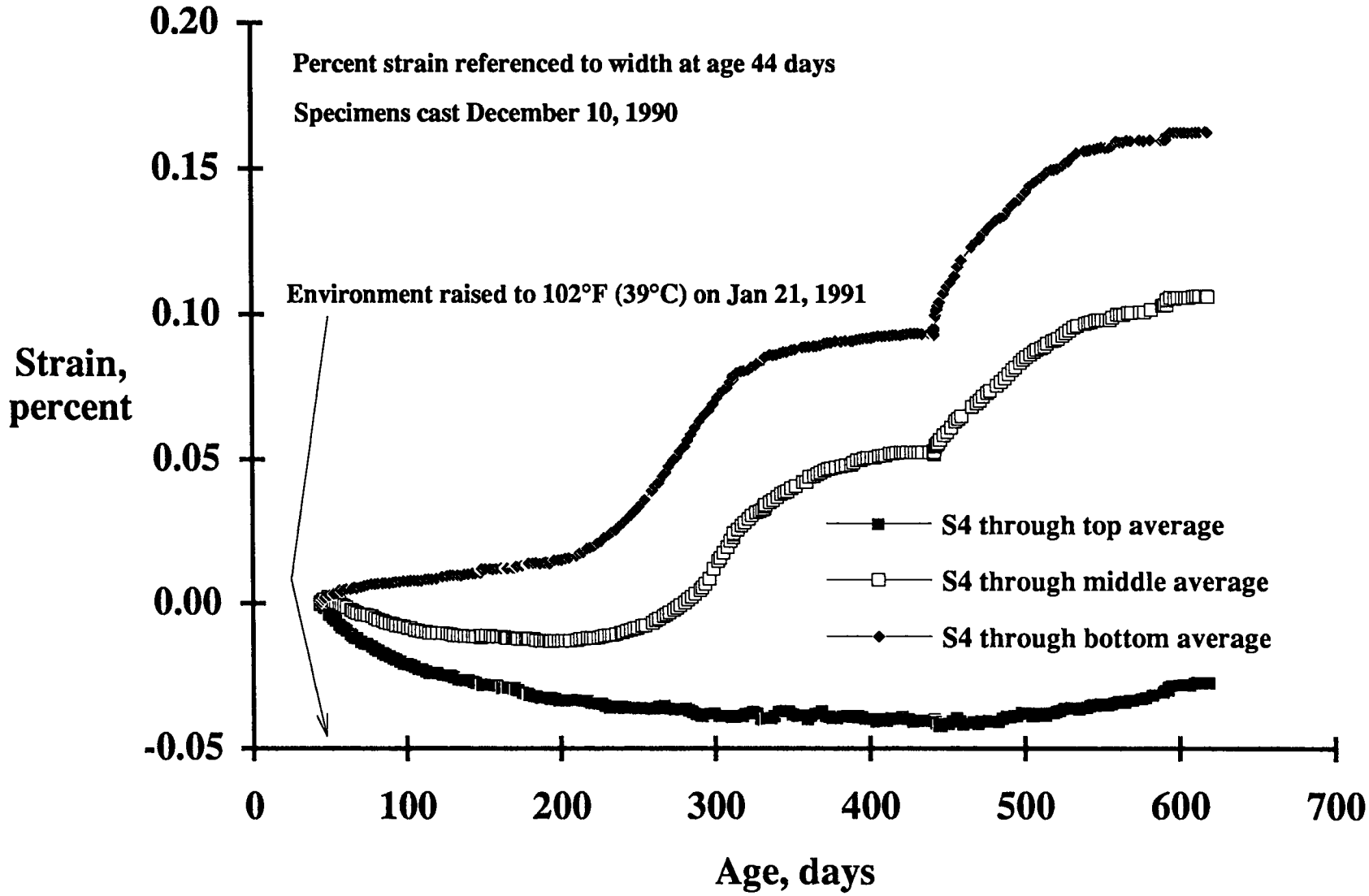


Figure C.24. Transverse strain versus time for section S4.

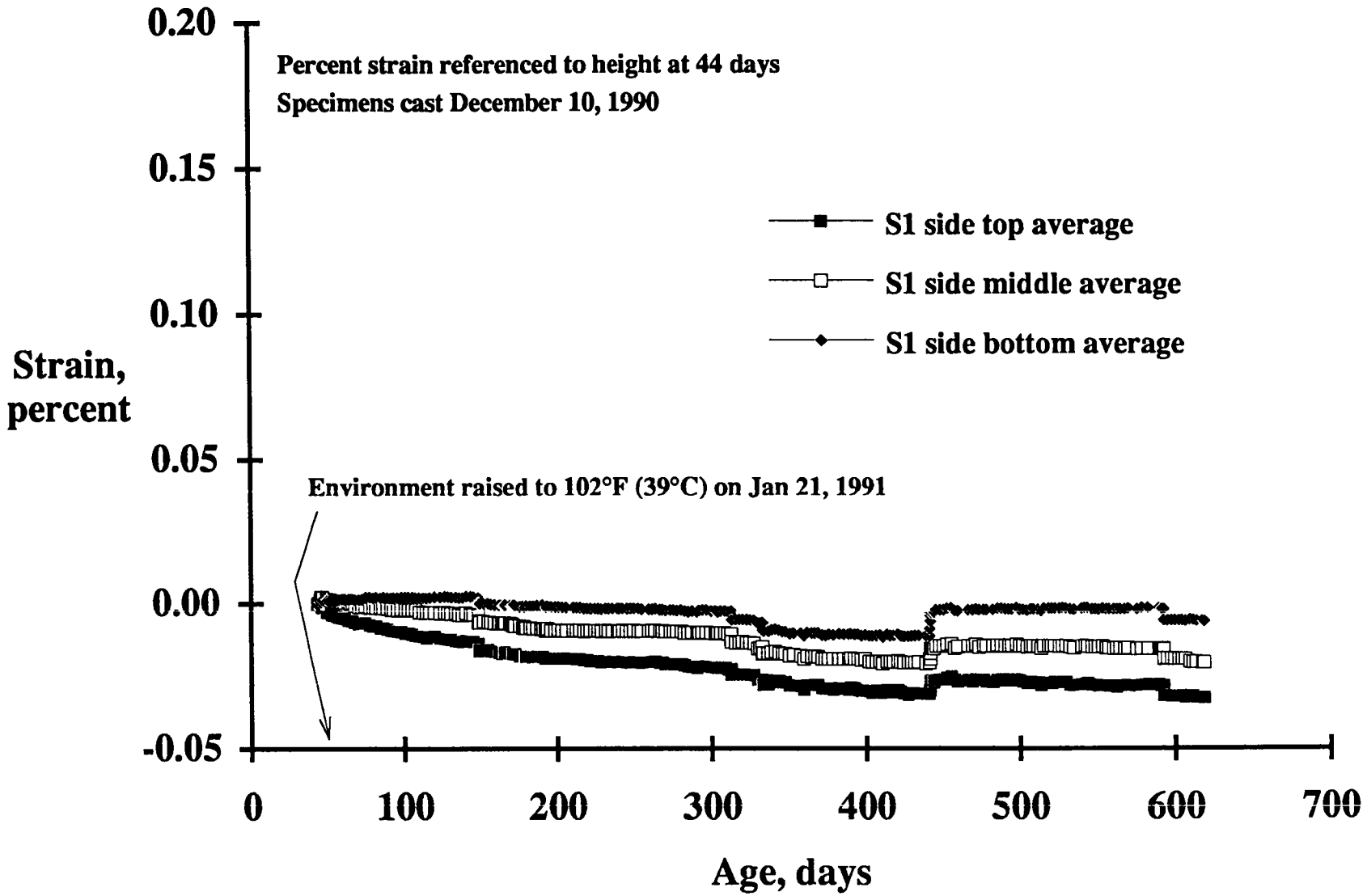


Figure C.25. Longitudinal strain versus time for section S1.

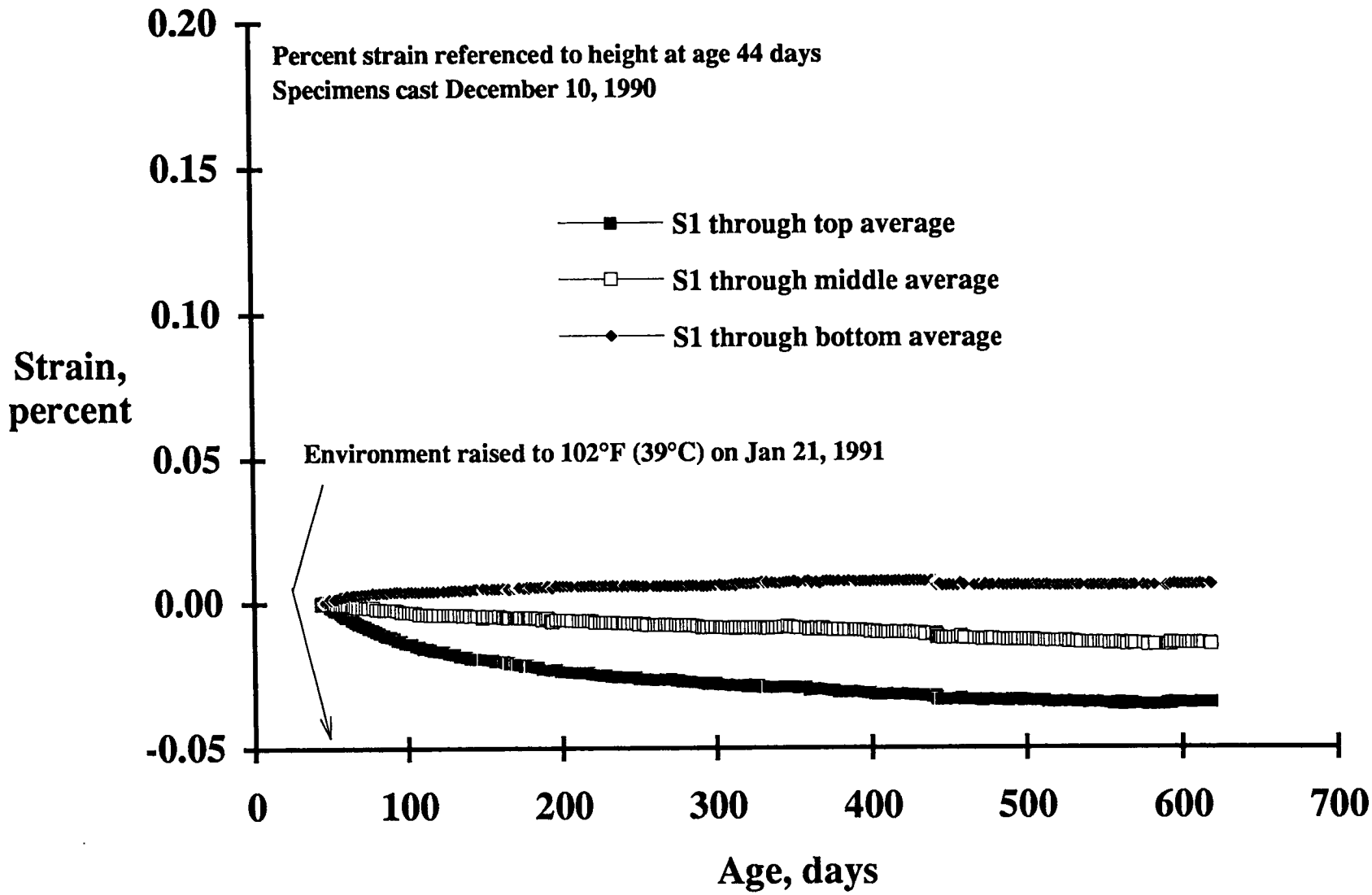


Figure C.26. Transverse strain versus time for section S1.

As shown in Figure C.23, small longitudinal expansion initially took place at the bottom of Section S4 where moisture was continuously available. In the transverse unrestrained direction (Figure C.24), expansion increased at a greater rate. Conversely, the top of Section S4, exposed to drying, contracted at a steady rate in both longitudinal and transverse directions (Figures C.23 and C.24). Initial strain behavior of Section S4 was only slightly different than that of its companion control Section S1.

As shown in Figures C.16, C.17, and C.18, by age 150 days, bottom and middle expansions in reactive, unrestrained Section S6 had reached extreme values in excess of 0.3 percent. Section S6 was extensively cracked as well. At this same age, however, strains in slightly restrained Section S4 were minimal and the section remained visibly uncracked. It was decided to move bottom longitudinal strains closer to zero in Section S4 to insure that the framing system providing restraint was functioning as designed. Loading frames were tightened at section age 148 days until an average longitudinal compressive stress of 150 psi (1.04 MPa) was applied to restrained Sections S1, S4, S2 and S5. The contraction in longitudinal strain due to applied stress is clearly evident in Figures C.23 and C.25. Smaller increase in transverse strain due to Poisson's ratio effects was present, but is not as clearly indicated in Figures C.24 and C.26.

Longitudinal strains in Section S4 (Figure C.23) remained approximately constant, and transverse strains continued to grow at preloading rates (Figure C.24) until approximately age 120 days. At this time, bottom strains began to increase in both longitudinal and transverse directions at a greater rate. In the longitudinal direction, middle and top strains also reversed slope and changed from contraction to expansion. In the transverse direction, middle strains reversed slope, and top strains continued to indicate contraction. These changes in behavior occurred approximately 60 days after the frames were tightened.

Vertical strains in Sections S4 and S1 are given in Figures C.27 and C.28 respectively. As shown in Figure C.27, at approximately age 260 days, vertical strains in reactive Section S4 suddenly began to indicate expansion. By age 300 days, all strains in Section S4, except surface transverse strain (Figure C.24) were clearly indicating expansion, and gel beads were forming on the sides. At age 312 days, loading frames were tightened until average longitudinal compressive stress in restrained sections was increased from 150 to 300 psi (1.04 to 2.07 MPa). As discussed previously, a three-dimensional pressure of 300 psi had been sufficient to balance ASR expansion and creep in concrete cylinders. As shown in Figure C.23, longitudinal strains continued to increase after loading, although at a reduced rate. It is noted that just prior to loading, a single, fine transverse crack across the center of Section S4 appeared. No other cracking was visible.

At age 332 days, average longitudinal compressive stress was increased to 450 psi (3.11 MPa). Longitudinal expansion at the bottom of Section S4 was brought under control by this stress increase.

As indicated by transverse strains plotted in Figure C.24, by age 300 days there was significant difference in transverse strain between the bottom and middle of Section S4 and the top. Also, as shown in Figure C.27, vertical strain was beginning to increase very rapidly by age 300 days. Both longitudinal and vertical strains strongly indicated development of horizontal cracking through Section S4, effectively splitting the comparatively dry, shrinking top of the section, from the moist, expanding bottom where ASR activity was probably greater. Since sides of all miniature pavement sections were painted with two heavy coats of epoxy to minimize moisture loss through the sides, horizontal cracking was not visible at the time. By age 400 days, a horizontal split was clearly evident in Section S4.

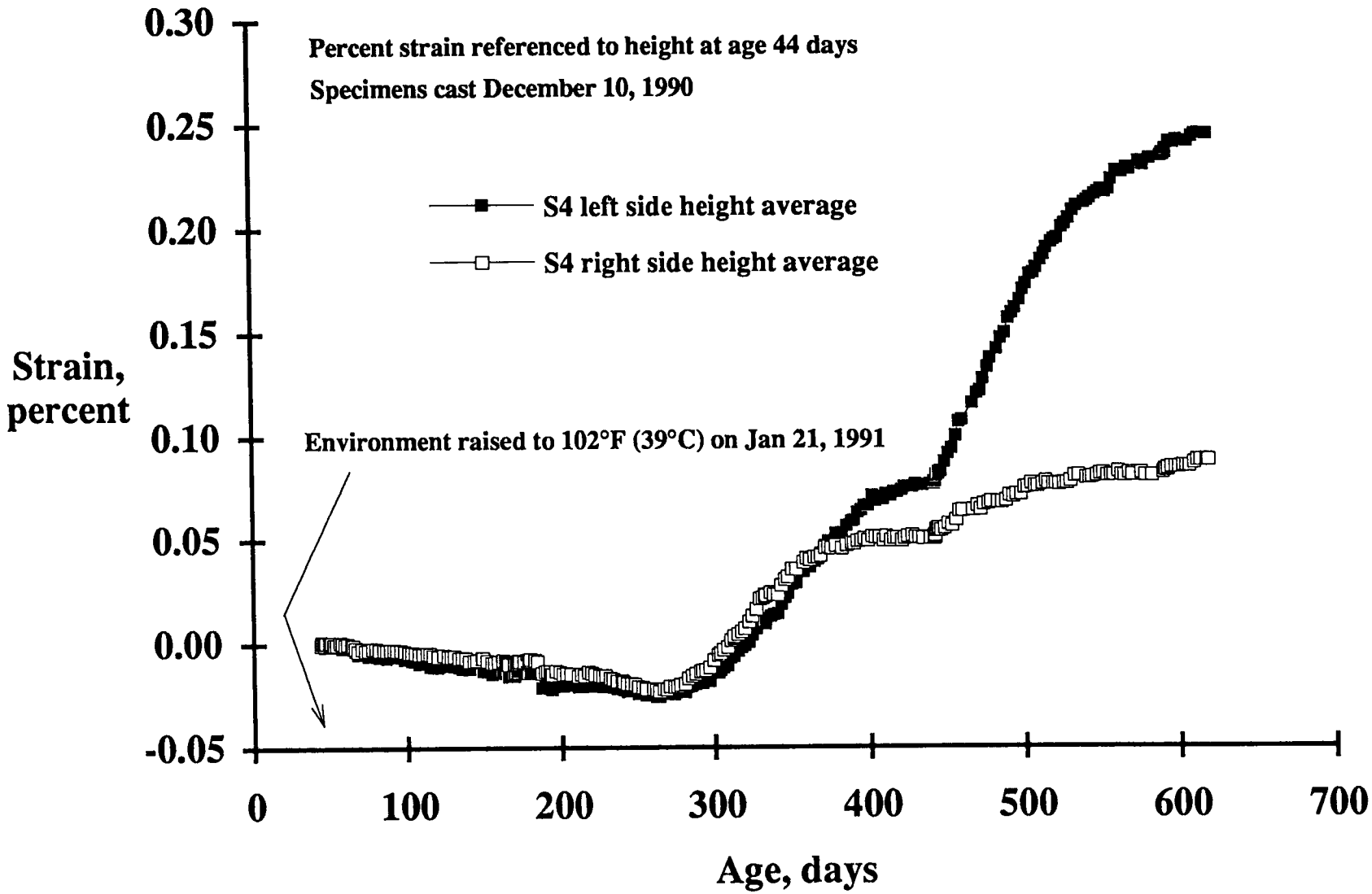


Figure C.27. Vertical strain versus time for section S4.

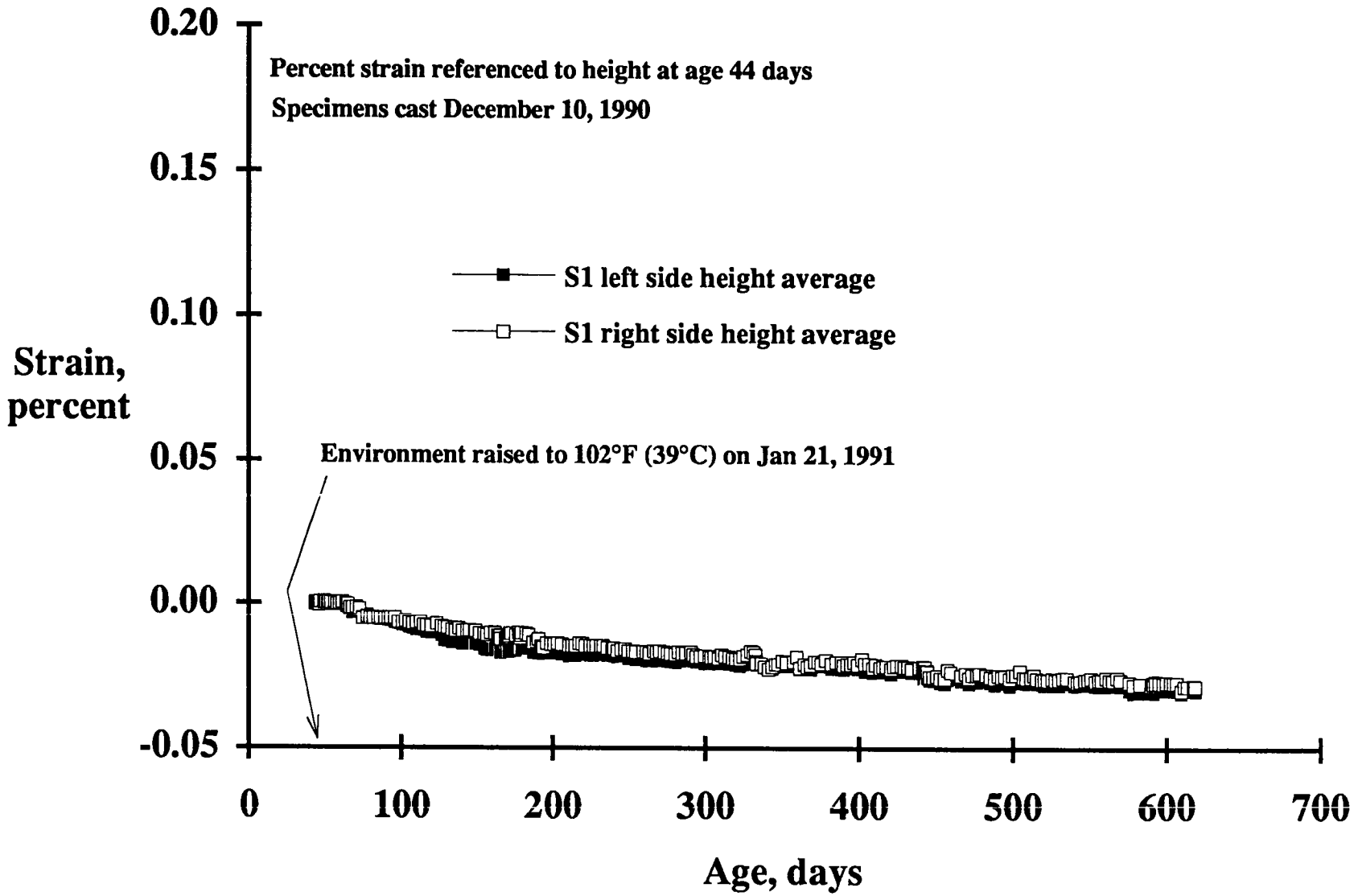


Figure C.28. Vertical strain versus time for section S1.

The split was approximately through the center of the section, that is, 4 to 5 in. (102 to 127 mm) down from the top.

It is significant to note that rate of expansion in both transverse and vertical strains (Figures C.24 and C.27) also was significantly reduced after stress increase.

As shown in Figure C.23, after loading to 450 psi (3.11 MPa) at age 332 days, bottom longitudinal strain leveled off, strain in the middle continued to increase at a reduced rate and the top strain continued to increase at only a slightly reduced rate. One possible explanation for the behavior would be an uneven vertical stress profile through the section, that is, higher development stresses at bottom than at top. Other evidence confirms this behavior. As strain data indicate (Figures C.23 through C.26), tops of Sections S1 and S4 progressively contracted more than the middle and top due to surface drying shrinkage. Because of this surface shrinkage as early as age 100 days, slight separations became evident between the four restrained sections at locations of the three stainless steel bond breaks cast in place to isolate sections from each other.

Shown in Figure C.29 are side strains in Section S4, plotted in a more expanded scale than used in Figure C.23, to more clearly indicate the strain change that took place when restrained sections were loaded to 150 psi (1.04 MPa) at age 148 days. Note that the contraction at the bottom due to the stress increment was noticeably greater than contraction at the top indicating that the rigid loading frames were applying a higher load at the bottom of sections than at the top.

As shown in Figure C.23, after the last frame tightening, longitudinal expansive strain due to ASR remained in balance with contraction due to creep for over 100 days. It was decided, therefore, to significantly reduce longitudinal restraint to determine if expansion would again increase. Loading frames were loosened at age 442 days until average longitudinal stress had dropped to approximately 45 psi (0.31 MPa). The loosening was stopped at this point as the frames were tending to twist unsymmetrically as rebounding slab sections forced them apart. The rebound in longitudinal strain is apparent in Figure C.23.

The rebound longitudinal strain in Sections S4 and S1 is shown in expanded scale in Figures C.30 and C.31, respectively. Note that in both sections the strain increment was larger at the bottom than at the top, indicating again that an uneven vertical stress distribution existed in restrained sections. Note also that rebound strain in Section S4 was about twice that of its companion Section S1 constructed with nonreactive aggregate. Modulus of elasticity of concrete in Section S4 was therefore one-half that of Section S1 at time of unloading, suggesting that ASR in S4 had damaged the concrete internally even though surface cracking was essentially nonexistent.

Note that after substantial reduction in restraint, longitudinal expansions resumed (Figure C.23) and rates of transverse and vertical strain increased significantly (Figures C.24 and C.27) to levels essentially equivalent to levels before the 300 psi (2.07 MPa) stress increase. By age 590 days, however, rates of expansion had reduced substantially.

As a final experiment, loading frames were retightened at age 592 days until an average stress level of 300 psi (2.07 MPa) was applied to restrained sections. Since expansions in Section S4 had slowed considerably prior to retightening frames, this stress level was sufficient to change longitudinal expansion into contraction (Figure C.23) and essentially halt transverse expansion (Figure C.24). The last data point on plots of Figures C.23 through

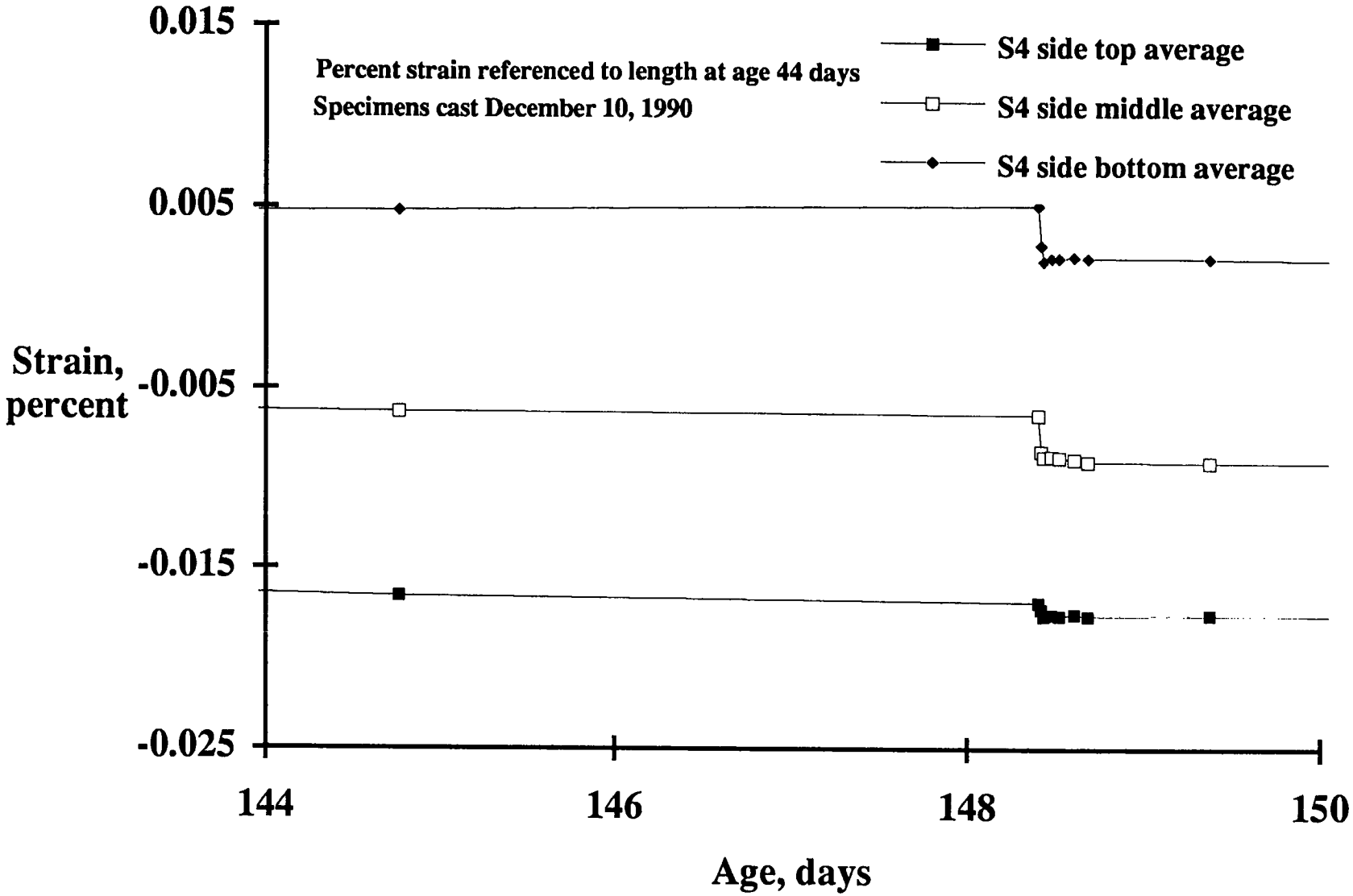


Figure C.29. Longitudinal strain from a 150 psi (1.04 MPa) load increment for section S4.

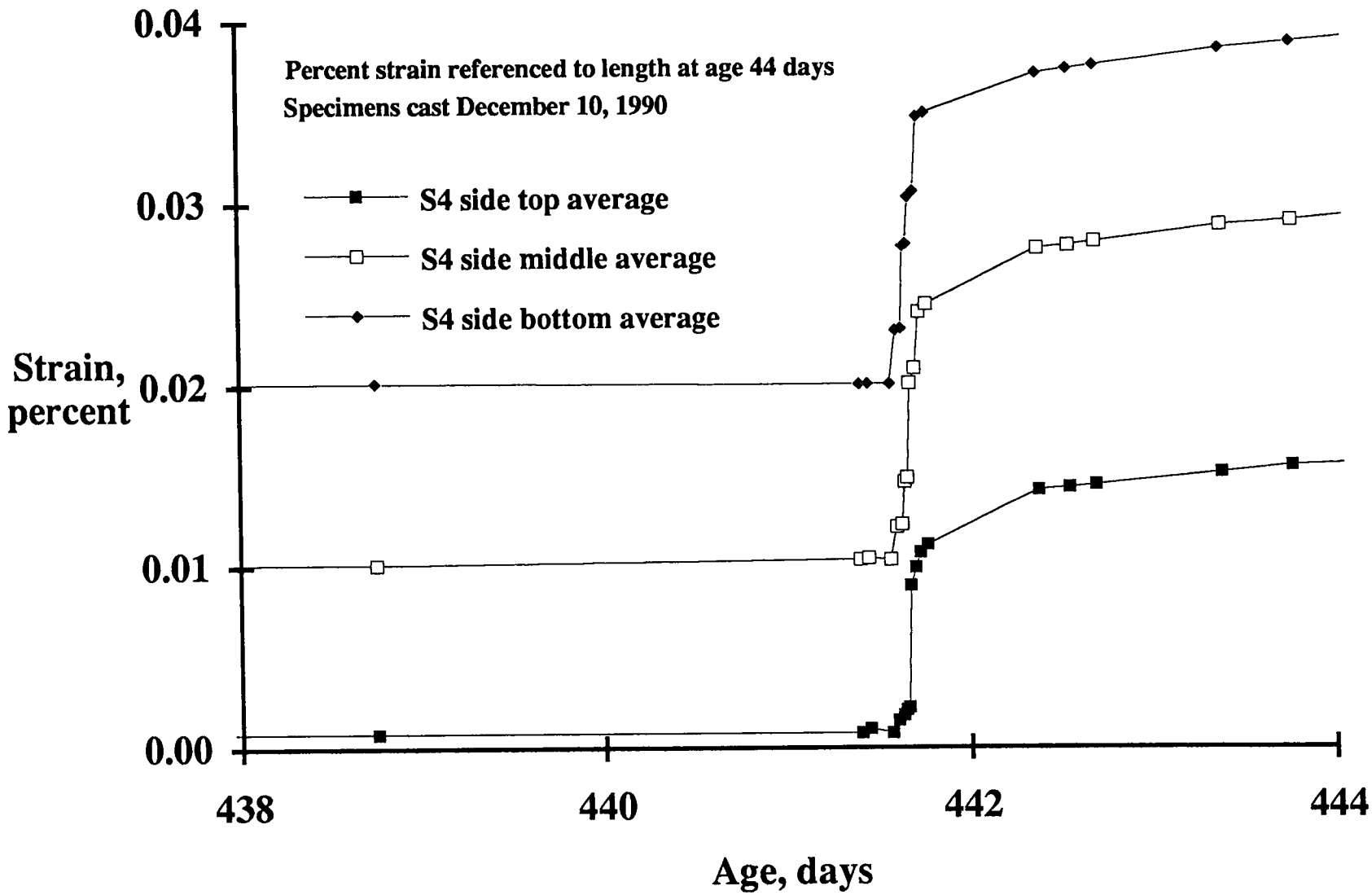


Figure C.30. Longitudinal strain upon unloading for section S4.

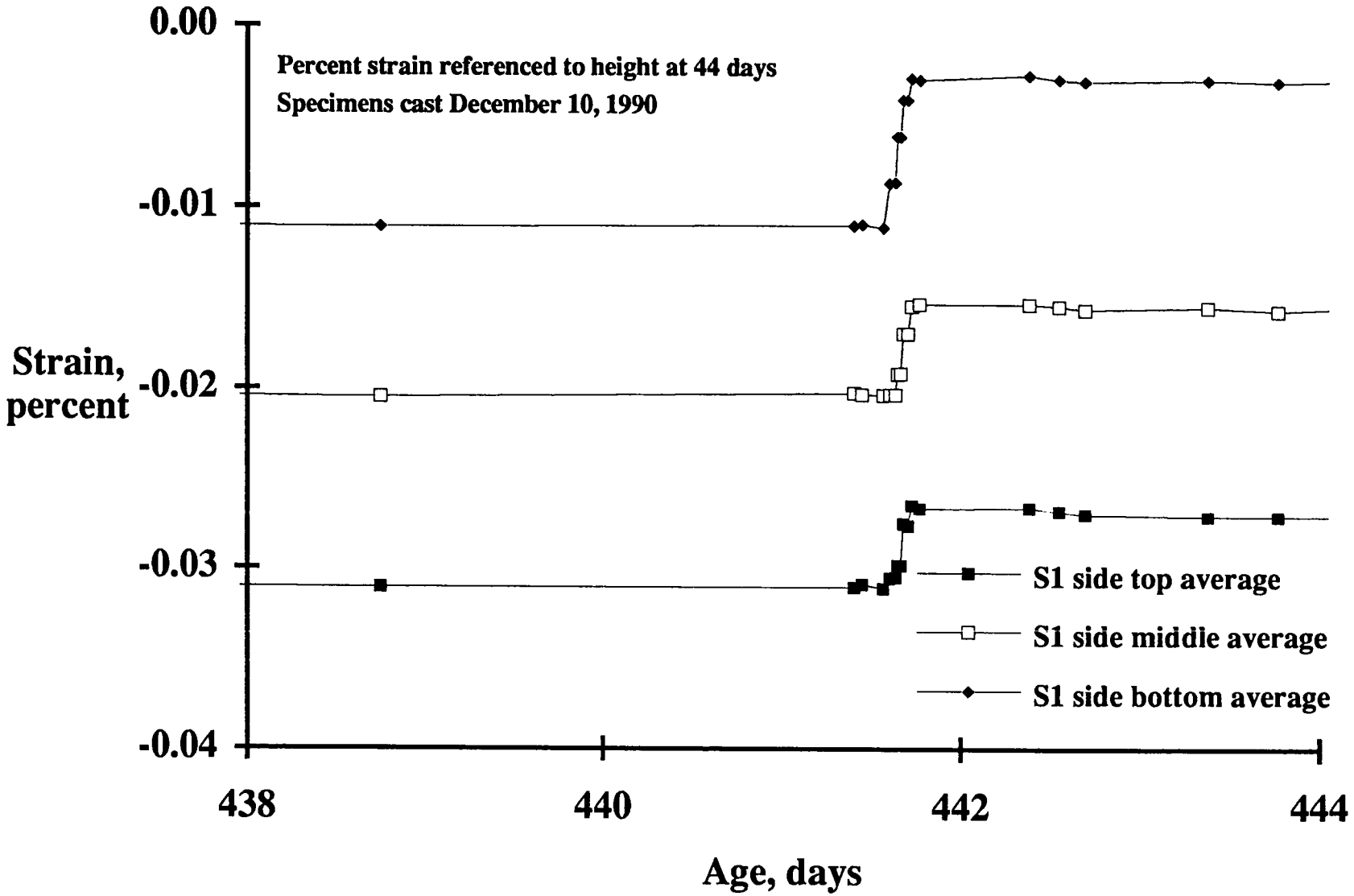


Figure C.31. Longitudinal strain upon unloading for section S1.

C.28 was taken at age 619 days. Temperature in the test room was lowered at age 620 days and the experiment ended.

It is noted that while the sides of Section S4 were covered with numerous gel beads, no beads existed in the upper 2 in. (51 mm).

### C.2.1.5 Restrained Covered Pavement Sections

Shown in Figures C.32, C.33, and C.34 are longitudinal, transverse and vertical strains, respectively, in Section S2 cast with reactive aggregate and coated on all exposed surfaces to reduce moisture loss. Figures C.35, C.36, and C.37 give longitudinal,transverse and vertical strains, respectively, in Section S5. Top surfaces of Sections S5 and S2 were treated with two coats of silane followed by two coats of clear polyurethane rather than opaque epoxy paint so that it would be possible to readily detect surface cracks. As shown in Figures C.32, C.33, C.34, and C.35, initially, surfaces of these specimens contracted due to drying almost as rapidly as uncovered Sections S4 and S1 (Figures C.23 through C.26). The surface coatings were obviously not effective in reducing moisture loss. At age 87 days, therefore, Sections S2 and S5 were covered with rubber sheet stock, tightly taped down around all edges. The sudden slope change in the curves indicating contraction at the tops of Sections S2 and S4 at 87 days indicates the improvement in moisture retention afforded by addition of rubber sheet stock. The rubber was removed periodically to permit visual observation of section surfaces.

As shown in Figure C.33, transverse strain at bottom of Section S2 grew steadily from the start of data recording. Rate of growth in transverse strain increased at approximately age 260 days, about 50 days after the sudden growth rate change experienced by restrained Section S4 (Figure C.23). As illustrated in Figures C.32 and C.34, longitudinal and vertical strains remained under control well beyond age 260 days. Growth rate in both longitudinal and transverse strain increased dramatically at age 442 days when the 450 psi (3.11 MPa) level of imposed longitudinal restraint was reduced to 45 psi (0.31 MPa).

Also, rate of vertical strain at one corner of Section S2 increased significantly at restraint release as shown in Figure C.34. Because vertical strain at diagonally opposite corners of Section S2 behaved differently, all four measured vertical strains are shown in Figure C.34 rather than average strains on each side. In Figure C.34, the legend note "S2 left side S4 end" means strain measured on the left side, on the section end closest to adjacent Section S4.

As shown in Figure C.34, at approximately age 480 days, vertical strain suddenly increased at the diagonally opposite corner to the corner where vertical strain first increased. By age 500 days, horizontal cracks on the sides of Section S2, about at the middle and starting at these opposite corners, were clearly visible reflected through the epoxy paint. Cracks extended only part way down each side , not reaching opposite ends, as also evident from the curves of Figure C.34 where vertical strain rates at two of the corners remained constant and unaffected.

Note that the reapplication of 300 psi (2.07 MPa) longitudinal stress at age 592 days brought longitudinal strain under control (Figure C.32) and significantly reduced rates of both transverse and vertical strains. No top surface cracking was evident in Section S2.

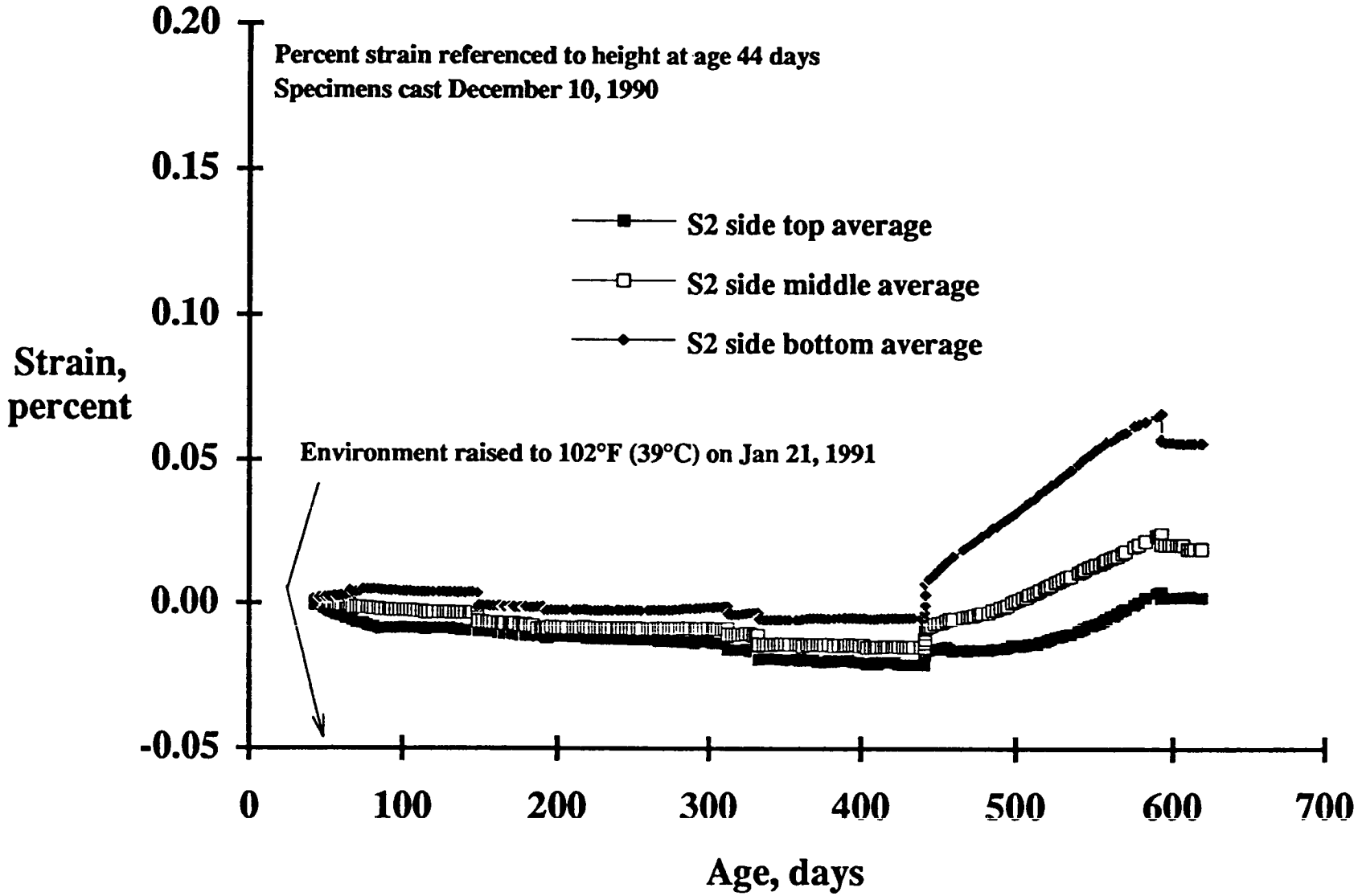


Figure C.32. Longitudinal strain versus time for section S2.

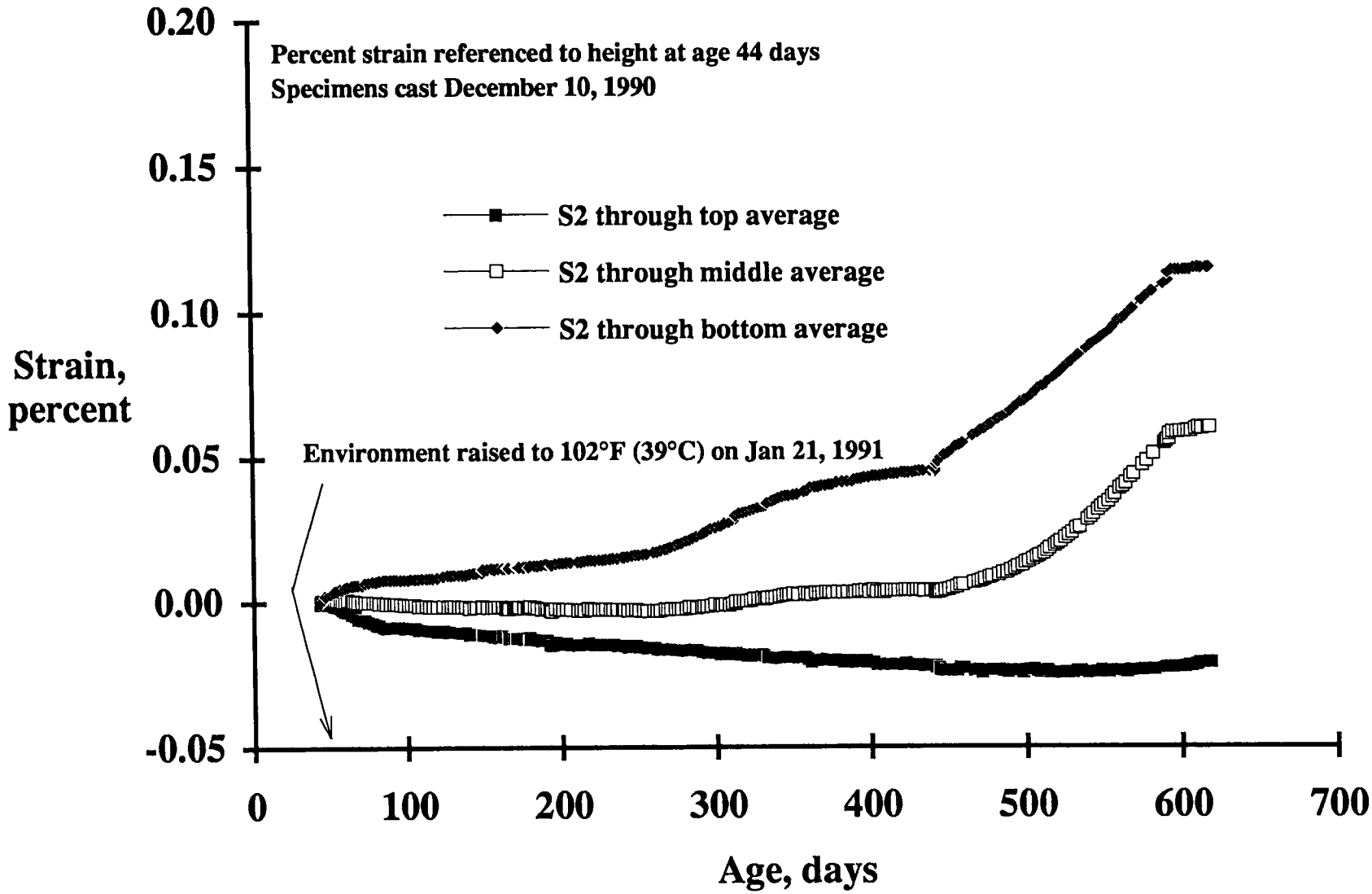


Figure C.33. Transverse strain versus time for section S2.

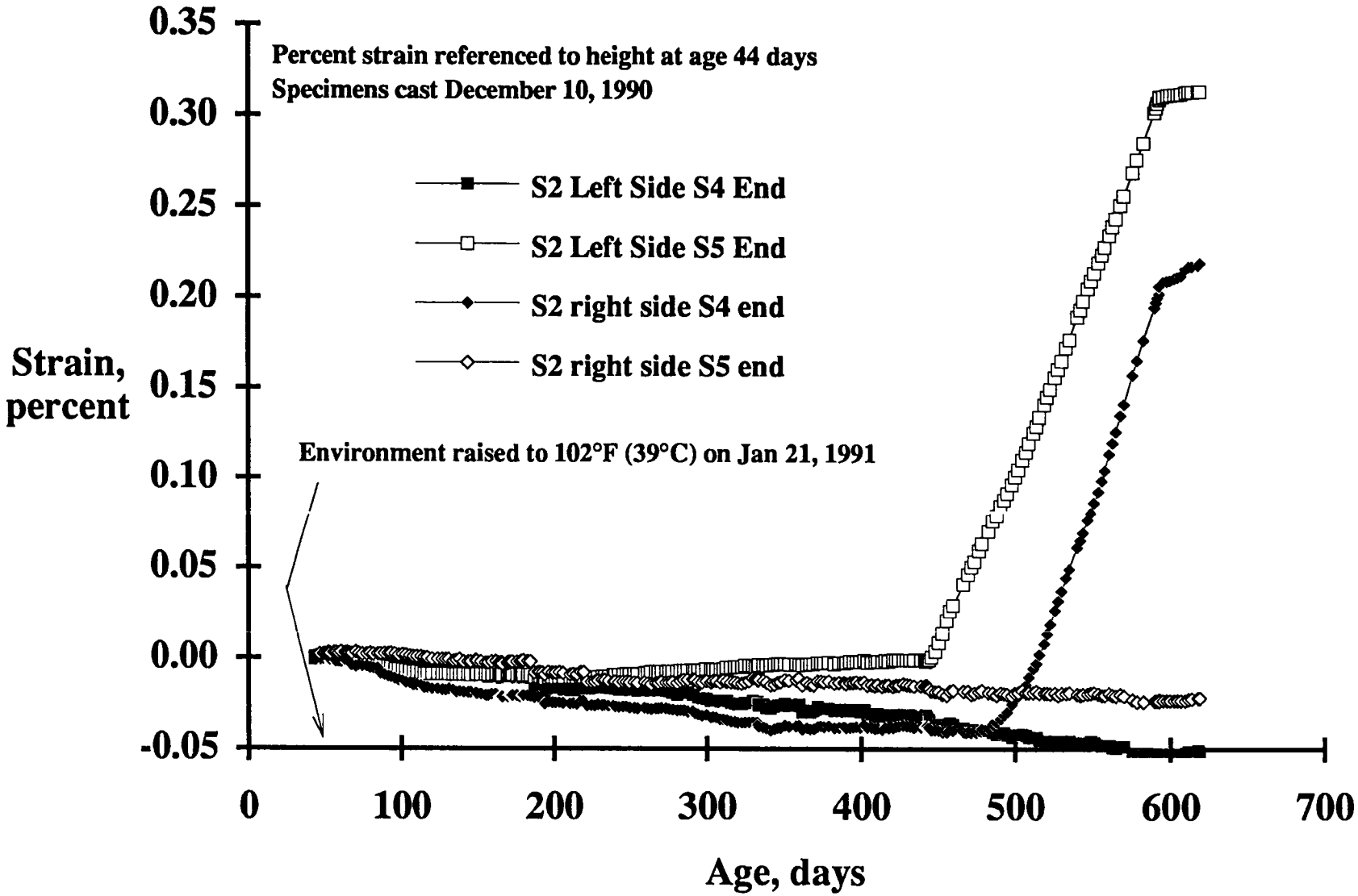


Figure C.34. Vertical strain versus time for section S2.

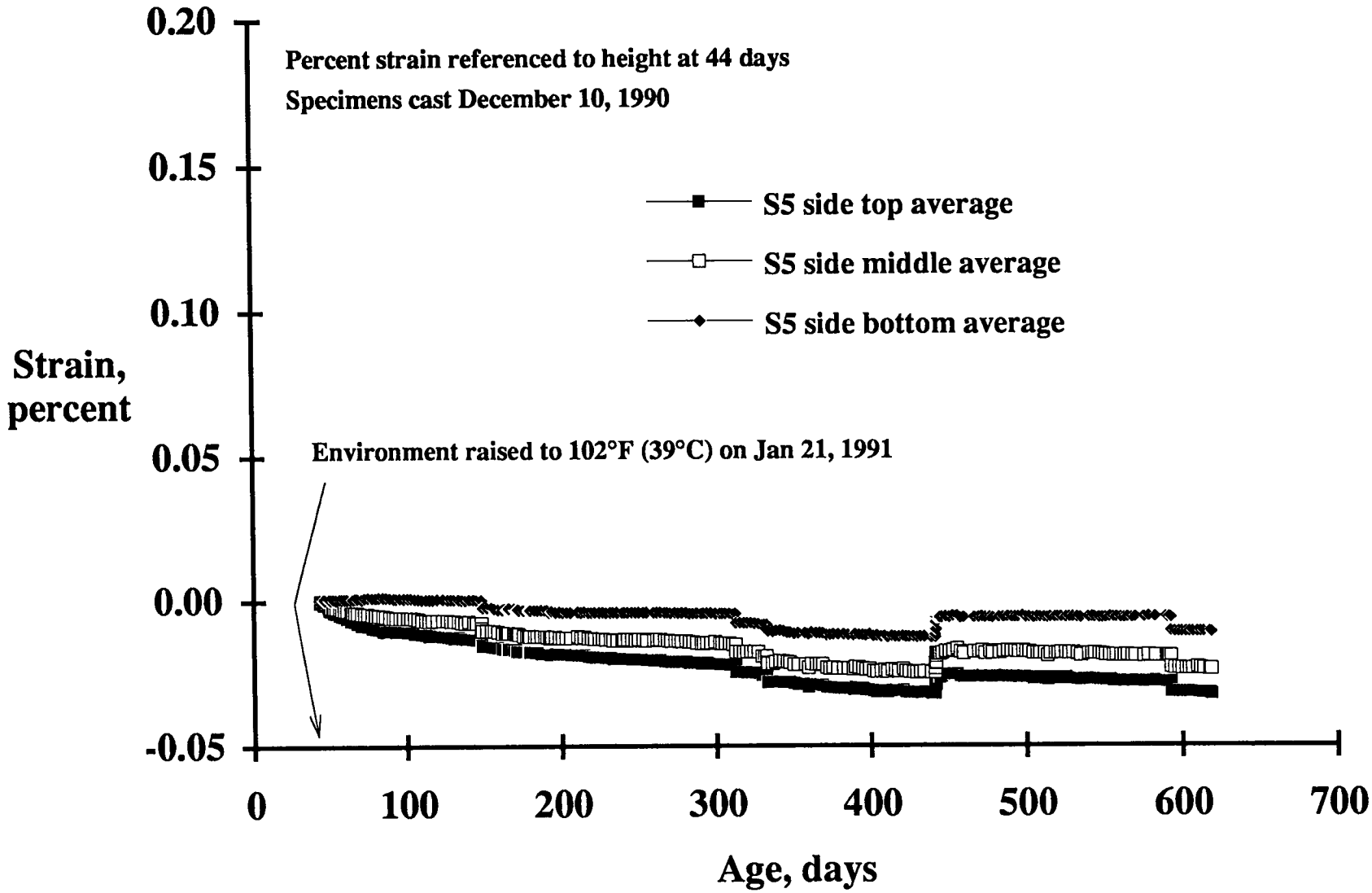


Figure C.35. Longitudinal strain versus time for section S5.

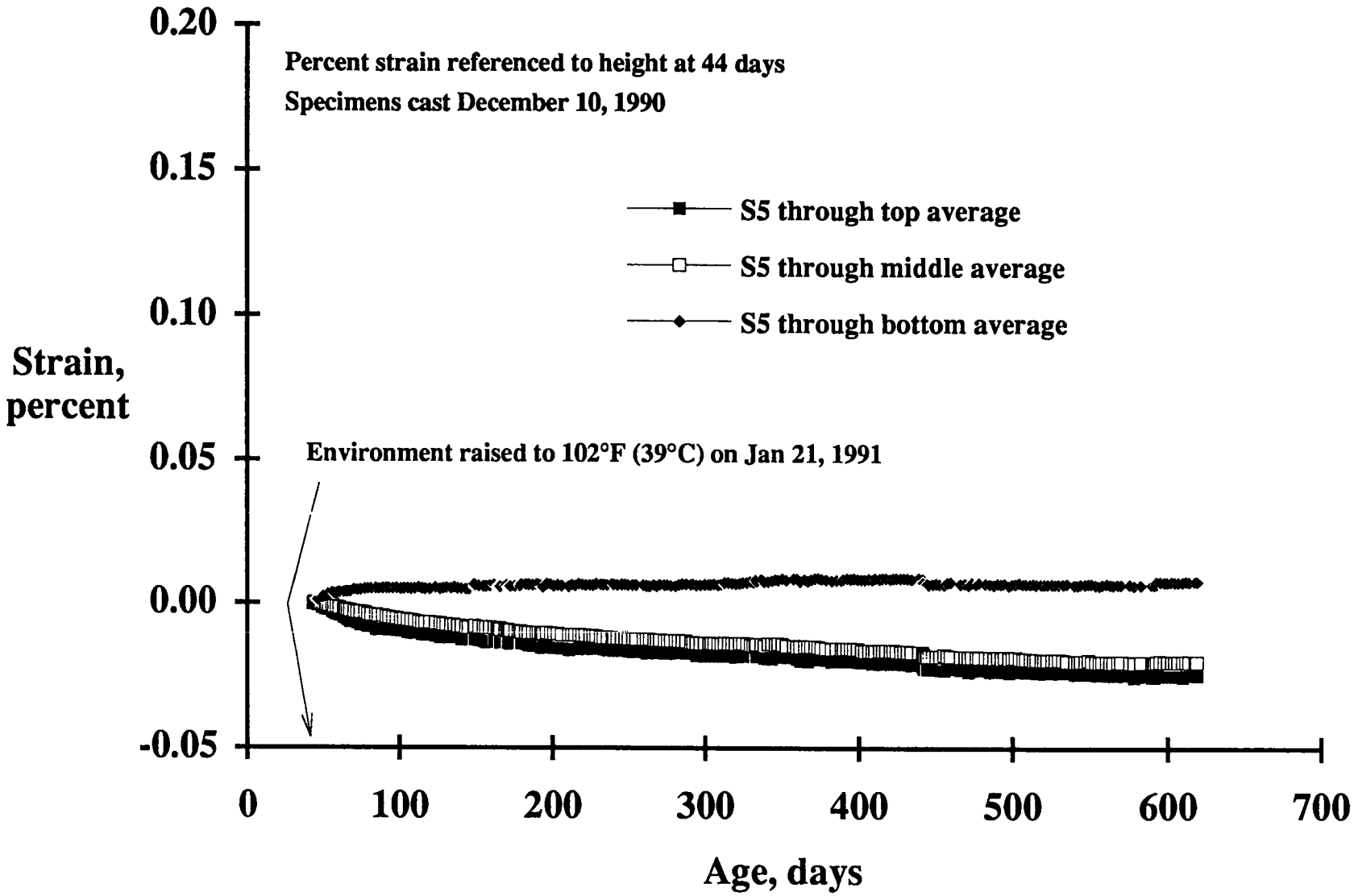


Figure C.36. Transverse strain versus time for section S5.

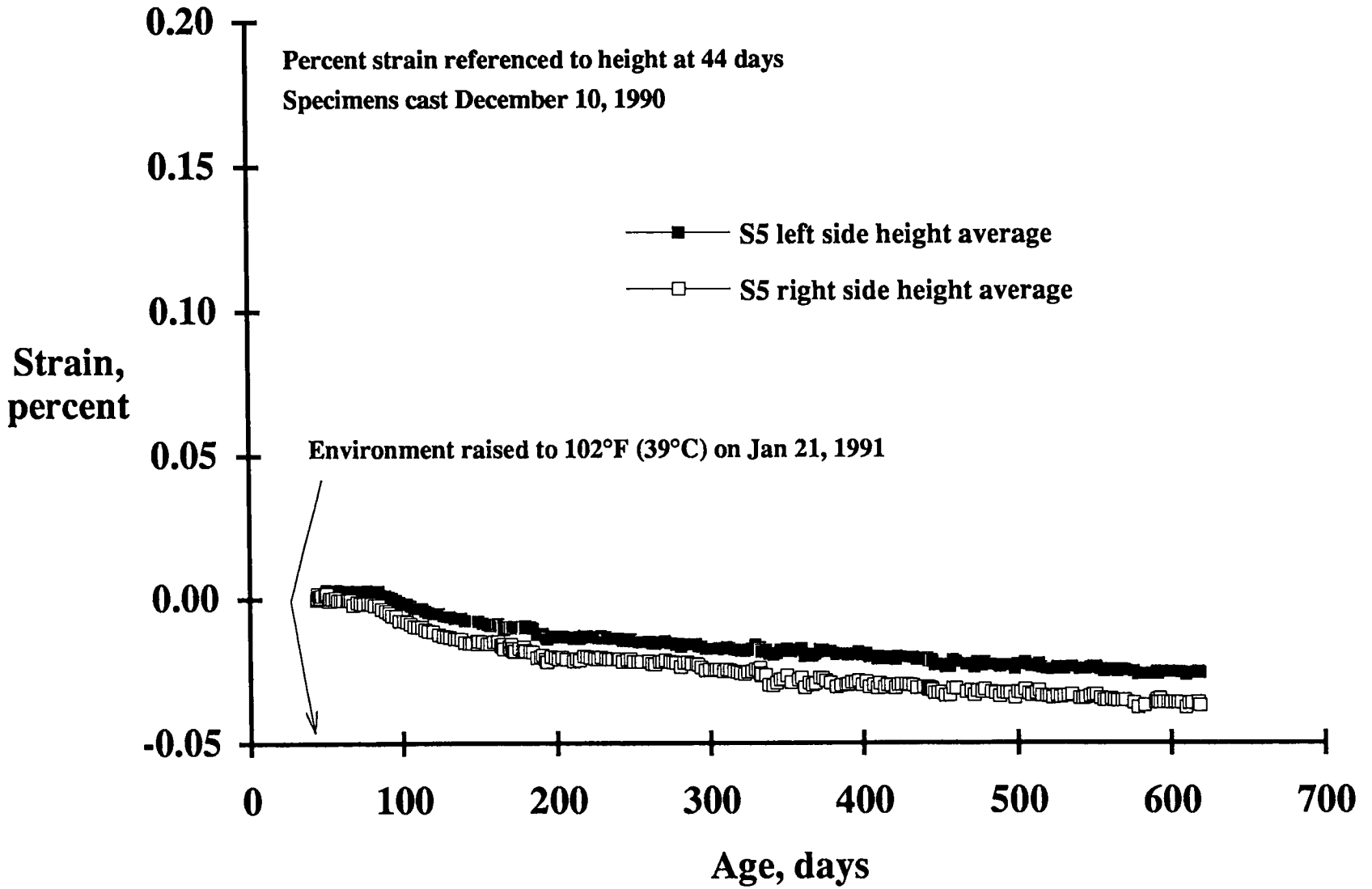


Figure C.37. Vertical strain versus time for section S5.

ASR gel beads were also present on the sides of Section S2, but none were found in the upper 2 in. (51 mm).

As indicated by Figures C.35, C.36, and C.37, strain performance of Control Section S5 was unremarkable and consistent with Control Section S3 (Figures C.19, C.20, and C.21) and Control Section S1 (Figures C.25, C.26, and C.27).

### *C.2.2 Finite Element Modeling*

One of the principal findings of the miniature pavement section tests is that application of restraint in one direction not only affects expansions in that direction, but in the other two mutually perpendicular directions as well. As the test progressed, it was decided to formulate a finite element, digital computer model to better understand this phenomenon. A two-dimensional model was formulated.

Stress distribution in a heterogeneous material like concrete is affected by differences in modulus of elasticity between constituents. In concrete, the principal constituents with different elastic moduli are aggregate and cement paste. Single, two-dimensional aggregate shapes, circular and oblong, were modeled in a solid matrix of cement paste. The two-dimensional model was subjected to uniaxial stress. Ratios of elastic moduli of aggregate to paste of 1.5, 2.0, and 2.5 were used. These ratios correspond to aggregate with moduli of elasticity in the range of 2.3 to 5.0 million psi (16 to 35 GPa) used with cement paste with elastic moduli of 1.5 to 2.0 million psi (10 to 14 GPa).

As expected, an applied uniaxial compressive stress produced zones of tensile stress adjacent to the modeled aggregate particle. The higher the modulus ratio of aggregate to paste, the higher the tensile stress. Absolute values of tensile stresses within these zones, however, were less than 10 percent of the applied compressive stress, and areas within the zones where tensile stress exceeded 5 percent of compressive stress were very small. This was the case for both circular and oblong two-dimensional aggregate particles.

### *C.2.3 Post-test Examination of Miniature Pavements*

At completion of the test, miniature pavements constructed with reactive aggregate were cross- sectioned for examination. To reveal extent of longitudinal and horizontal cracking, pavement Sections S2, S4 and S6 were cut in half transversely. A transverse slice 1 in. (25 mm) thick was then removed from one of the halves . Resultant dimensions of the slice were 1 x 9 (pavement height) x 18 (pavement width) in. (25 x 229 x 458 mm). To reveal the extent of transverse cracking in Section S4, one of the halves of this section was again cut in half longitudinally. A longitudinal slice 1 in. (25 mm) thick was removed from one of the resultant quarter sections. Dimensions of the longitudinal slice were 1 x 9 x 17 in. (25 x 229 x 432 mm).

Section S6, which had been tested unrestrained, was extensively cracked. Surface cracking on the top and sides that had been mapped during the test extended a maximum of 1 1/2 in. (37 mm) into the cross section. Three longitudinal cracks extended approximately 1 1/2 in. (37 mm) into the cross section from the bottom surface. Horizontal cracks radiating from

these three cracks formed an almost continuous horizontal crack across the cross section approximately 1 1/2 in. (37mm) up from the bottom. In addition, a number of other horizontal cracks were present and many randomly oriented, interconnected cracks extended over most of the cross section.

The transverse cross section of restrained pavement S4 revealed two substantial longitudinal cracks penetrating approximately 2 in. (51 mm) into the cross section from the bottom surface. Also, the lower 5 to 6 in. (125 to 150 mm) of the section contained numerous horizontal cracks extending almost the full width of the pavement. The longitudinal cross section of pavement S4 revealed the same extensive horizontal cracks present in the transverse cross section. No transverse cracks were present, however, demonstrating the effectiveness of the longitudinal restraint imposed during the test in controlling transverse cracking. The upper 3 in. (77 mm) of the cross section was crack-free.

The transverse cross section of restrained pavement S2 revealed a similar cracking pattern as restrained pavement S4, but at a reduced severity. Only one 1 1/2 in. (37 mm) crack extended into the cross section from the bottom and the network of horizontal cracks extended only 3 to 4 in. (75 to 100 mm) up from the bottom. The upper 5 to 6 in. (125 to 150 mm) of cross section was essentially crack free.

These crack patterns are similar to those commonly observed in concrete pavement showing distress due to ASR. Longitudinal (uniaxial) restraint of sufficient magnitude forces the resulting major cracks to orient primarily longitudinally and horizontally. In joint areas, the crack pattern in upper levels of the pavement slab may assume a more random orientation due to the presence of the sawed joint, which serves as a relief mechanism to the uniaxial restraint that exists below the joint. Observations in this experiment offer strong support for the above interpretation of cracking observed in pavement concrete.

Results in this experiment also indicate that uniaxial restraint delays the generation of major cracks due to ASR, thereby extending the service life of the concrete. However, it is probable that such restraint can not prevent such cracks indefinitely, unless the cause of cracking (ASR in this case) is diminished. It may be that some particular intermediate uniaxial restraint force may be optimum for extending surface life. This undoubtedly would vary from structure to structure.

### *C.2.4 Conclusions*

Conclusions are presented in Section 5.6.2.2 of this report.

# References


Barneyback, R. S., Jr. and S. Diamond. 1981. Expression and analysis of pore fluids from hardened cement pastes and mortars. *Cement and Concrete Research.* Vol. 11: 279-285.

Davies, G. and R. E. Oberholster. 1987. Use of the NBRI accelerated test to evaluate the effectiveness of mineral admixtures in preventing alkali-silica reaction. *Cement and Concrete Research.* Vol. 17: 97-107.

Diamond, S. and R. S. Barneyback. 1976. A prospective measure for the extent of alkali silica reaction. *Proceedings, 3rd international conference, alkali aggregate reaction,* London: 149-161.

Diamond, S. 1989. ASR-another look at mechanisms. *Proceedings, 8th international conference on alkali-aggregate reaction.* Kyoto, Japan: 83-94.

Diamond, Sidney. 1992. Alkali-aggregate reactions in concrete: an annotated bibliography 1939-1991. Washington, D.C.: National Research Council, Strategic Highway Research Program, SHRP-C/UWP-92-601: 470.

*Handbook of Chemistry and Physics.* 1987-88: B-101.

Helmuth, Richard. 1993. Alkali-silica reactivity: an overview of research. Washington D.C.: National Research Council, Strategic Highway Research Program. SHRP-C-342: 116.

Kobayashi, S., K. Kirimura, K. Kuboyama, and T. Kojima. 1989. Evaluation of surface treatment effect for preventing excessive expansion due to alkali-silica reactivity. *Proceedings 8th international conference on alkali-aggregate reaction*: 821-826.

McCoy. W.J. and A.G. Caldwell. 1951. New approach to inhibiting alkali-aggregate expansion. *Journal of the American Concrete Institute.* Vol. 22: 693-706.

Natesaiyer, K. and K.C. Hover. 1988. In situ identification of ASR products in concrete. *Cement and Concrete Research.* Vol. 18. May 1988; 455-463.

Oberholster, R.E. and G. Davies. 1986. An accelerated method for testing the potential alkali reactivity of siliceous aggregates. *Cement and Concrete Research.* Vol. 16: 181-186.

Sakaguchi, Y., M. Takamura, A. Kitagawa, T. Hori, F. Tomosawa, and M. Abe. 1989. The inhibiting effect of lithium compounds on alkali-silica reaction. *Proceedings, 8th international conference, alkali aggregate reaction.* Kyoto, Japan: 229-234.

Stanton, T.E. 1940. Expansion of concrete through reaction between cement and aggregate. *Proceedings of the American Society of Civil Engineers.* 66: 1781-1811.

Stark, David. 1991a. Handbook for the identification of alkali-silica reactivity in highway structures. Washington, D.C.: National Research Council, Strategic Highway Research Program, SHRP-C-315: 48.

Stark, D. 1991b. The moisture condition of field concrete exhibiting alkali-silica reactivity. *ACI SP-126 Durability of concrete.* Second international conference, Detroit, Michigan: American Concrete Institute: 973-987.

Stark, David C. 1992. Lithium salt admixtures--an alternative method to prevent expansive alkali-silica reactivity. *Proceedings, 9th international conference on alkali-aggregate reaction in concrete:* 1017-1025.

Stark, David C. 1993. Internal report, Portland Cement Association

Tabatabai, A.M., E.J. Barenberg, and R.E. Smith. 1979. Longitudinal joint systems in slip-formed rigid pavements. *Vol. II. Analysis of load transfer systems for concrete pavement.* Washington, D.C.: U.S. Department of Transportation, Federal Aviation Administration. Report No. FAA-RD-79-4, II.

## Concrete and Structures Advisory Committee

James J. Murphy, *Chairman*
*Transportation Research Board*

Howard H. Newlon, Jr., *Vice Chairman*
*Virginia Transportation Research Council (retired)*

Charles J. Arnold
*Michigan Department of Transportation*

Donald E. Beuerlein
*Koss Construction Co.*

Bernard C. Brown
*Iowa Department of Transportation*

Richard D. Gaynor
*National Aggregates Association/National Ready Mixed Concrete Association*

Robert J. Girard
*Missouri Highway and Transportation Department*

David L. Gress
*University of New Hampshire*

Gary Lee Hoffman
*Pennsylvania Department of Transportation*

Brian B. Hope
*Queens University*

Carl E. Locke, Jr.
*University of Kansas*

Clellon L. Loveall
*Tennessee Department of Transportation*

David G. Manning
*Ontario Ministry of Transportation*

Robert G. Packard
*Portland Cement Association*

James E. Roberts
*California Department of Transportation*

John M. Scanlon, Jr.
*Wiss Janney Elstner Associates*

Charles F. Scholer
*Purdue University*

Lawrence L. Smith
*Florida Department of Transportation*

John R. Strada
*Washington Department of Transportation (retired)*

**Liaisons**

Theodore R. Ferragut
*Federal Highway Administration*

Crawford F. Jencks
*Transportation Research Board*

Bryant Mather
*USAE Waterways Experiment Station*

Thomas J. Pasko, Jr.
*Federal Highway Administration*

John L. Rice
*Federal Aviation Administration*

Suneel Vanikar
*Federal Highway Administration*

*11/19/92*

## Expert Task Group

Paul Klieger, *Chairman*
*Consultant*

Stephen Forster
*Federal Highway Administration*

James G. Gehler
*Illinois Department of Transportation*

Vernon J. Marks
*Iowa Department of Transportation*

Bryant Mather
*USAE Waterways Experiment Station*

Richard Meininger
*National Aggregates Association/National Ready Mix Concrete Association*

Larry R. Roberts
*W.R. Grace and Company*

James H. Stokes
*New Mexico State Highway Department*

James Woodstrom
*Consultant*

*3/10/93*